IN-SOIL STRENGTH AND BEHAVIOUR OF GEOSYNTHETIC REINFORCEMENTS

by

Tolga Yardımcı

B.S., Civil Engineering, Çukurova University, 2009

M.S., Civil Engineering, Boğaziçi University, 2013

Submitted to the Institute for Graduate Studies in
Science and Engineering in partial fulfillment of
the requirements for the degree of
Doctor of Philosophy

Graduate Program in Civil Engineering

Boğaziçi University

2022

ACKNOWLEDGEMENTS

I would like to express my heartfelt gratitude to Prof. Fazlı Erol Güler for his continuous support, precious guidance and encouragement. Without his endless patience this study would not be completed. I would also thank to Assoc. Prof. Burak Tanyu for his valuable suggestions throughout the preparation of this thesis.

I am particularly grateful to the members of my thesis committee, Assoc. Prof. Özer Çinicioğlu, Prof. Fazlı Erol Güler, Assoc. Prof. Murat Hamderi, Assist. Prof. İrem Zeynep Yıldırım and Prof. Ayşe Edinçliler who devoted their invaluable time for reading and commenting on my thesis.

I wish to acknowledge the help provided by my friends in the civil engineering department. I would also like to extend my thanks to the technicians of the Karl Terzaghi Soil Mechanics Laboratory, Belgin Özgül and Kadir Gündoğdu for their help.

Many heartfelt thanks to Tolga Tonguç Değer from İstanbul Teknik and Ethem Yıldırım from Dört-E for their help in developing the apparatus and providing me with the required materials. I also appreciate the help of Ayşe Aydın.

This thesis has been supported by Boğaziçi University Scientific Research Project with the project code 18A04D4.

I would like to thank TÜBİTAK BİDEB (The Scientific and Technological Research Council of Turkey) for their support during my graduate study with the national scholarship program for Ph.D. students (2211-E, 2013/2).

ABSTRACT

IN-SOIL STRENGTH AND BEHAVIOUR OF GEOSYNTHETIC REINFORCEMENTS

In this study, in-soil tensile strength and behaviour of various geosynthetic reinforcements is investigated with the help of custom designed and developed in-soil tensile test apparatus in the laboratory. The proposed apparatus, which can simulate the site conditions, is considered an alternative to wide width tensile test apparatus. Displacement controlled in-air and in-soil tensile tests were conducted to investigate the influence of soil type, normal stress and presence of the passive reinforcement (reinforcement located above and below the test reinforcement) on the tensile strength and behaviour of various geosynthetics. Three geosynthetics (nonwoven geotextile, woven geotextile and geogrid) and two soil types (Well Graded Sand and Well Graded Gravel with Sand) are used in the study. Normal stress used in the study ranges from 25 to 75 kPa. A constant strain rate of 2% strain/min was applied in all tests. All geosynthetics tested in soil under normal stress were found to have an improvement in tensile load-strain behaviour. The increase in the stiffness was formulated to quantify the improvement in the behaviour and to reduce carrying out further tests. Gravel was found more effective on influencing the behaviour when compared to the sand. In sand, using passive reinforcements obviously decreases the tensile load-strain behaviour of the geosynthetics while it has various effects in gravel.

ÖZET

GEOSENTETİK DONATILARIN GÖMÜLÜ HALDEKİ DAYANIMI VE DAVRANIŞI

Bu çalışmada çeşitli geosentetik donatıların gömülü haldeki dayanımı ve davranışı özel tasarlanan ve geliştirilen bir gömülü donatı çekme makinesiyle laboratuvarda incelenmiştir. Önerilen makine saha koşullarını taklit edebilmekte ve yaygın (wide-width) donatı çekme makinesine alternatif olarak düşünülmektedir. Hava ve zemin ortamında gerçekleştirilen deplasman kontrollü çekme deneyleri sayesinde zemin tipi, normal gerilme ve pasif donati (test donatısının üstüne ve altına yerleştirilen donatı) varlığının donatı çekme dayanımına ve davranışına etkisi incelenmiştir. Deneylerde üç tip geosentetik (örgüsüz geotekstil, örgülü geotekstil ve geogrid) ve iki tip zemin (İyi Derecelenmiş Kum ve İyi Derecelenmiş Çakıl, Kumlu) kullanılmıştır. Çalışmada kullanılan normal gerilmeler 25-75 kPa skalasında değişmektedir. Deney boyunca sabit kalacak şekilde dakikada yüzde 2 birim uzama (%2 birim uzama/dakika) uygulanmıştır. Çalışmada kullanılan tüm geosentetiklerin gömülü halde ve normal gerilme altında çekme-uzama davranışında iyileşme olduğu gözlenmiştir. Sekant modülündeki artış ölçülebilir olması ve ilerde daha az deney gereksinimi duyulması için formüle edilmiştir. Çakılın, geosentetik davranışını etkilemede kumdan daha etkili olduğu bulunmuştur. Kum ortamında pasif donatı kullanımı geosentetik cekme davranışını açıkça olumsuz etkilerken çakıl ortamında farklı etkileri olabildiği görülmüştür.

TABLE OF CONTENTS

ACKNOWLEDGEMENTS iii
ABSTRACT iv
ÖZET v
LIST OF FIGURES ix
LIST OF TABLES xxxii
LIST OF SYMBOLS xxxiv
LIST OF ACRONYMS/ABBREVIATIONS xxxvi
1. INTRODUCTION 1
2. LITERATURE REVIEW 5
2.1. Introduction 5
2.2. Previous Studies 6
2.3. Evaluation of Previous Studies 64
3. METHODOLOGY 69
3.1. In-Soil Wide Width Test Apparatus 70
3.1.1. Test Box 70
3.1.2. Clamps 74
3.1.3. Control Panel 77
3.1.4. Measuring Devices 79
3.1.5. Vertical Load Frame 81
3.2. Materials 81
3.2.1. Soil 81
3.2.1.1. Gradation Curve and Soil Classification 82
3.2.1.2. Particle Shape 85
3.2.1.3. Index Properties of Sand 87
3.2.1.4. Placing the Sand and Gravel to the Test Box 89
3.2.2. Geosynthetics 92
3.2.2.1. Nonwoven Geotextile 92
3.2.2.2. Woven Geotextile 93

3.2.2.3. Geogrid 94
3.3. Test Procedure 95
3.4. Test Program 103
4. TEST RESULTS AND EVALUATION 106
4.1. Introduction 106
4.2. In-Air (Unconfined) Load-Extension Tests 109
4.2.1. Nonwoven Geotextile 109
4.2.2. Woven Geotextile 111
4.2.3. Geogrid 113
4.3. Single-Layer Tests in Sand 115
4.3.1. Friction Between Sand and Clamp (Clamp Pull-Out Tests) . . . 115
4.3.2. Behaviour of (Single-Layer) Nonwoven Geotextile Confined in Sand 121
4.3.3. Behaviour of (Single-Layer) Woven Geotextile Confined in Sand 128
4.3.4. Behaviour of (Single-Layer) Geogrid Confined in Sand 134
4.4. Single-Layer Tests in Gravel 140
4.4.1. Friction Between Gravel and Clamp (Clamp Pull-Out Tests) . . 140
4.4.2. Behaviour of (Single-Layer) Nonwoven Geotextile Confined in Gravel 144
4.4.3. Behaviour of (Single-Layer) Woven Geotextile Confined in Gravel 151
4.4.4. Behaviour of (Single-Layer) Geogrid Confined in Gravel 156
4.5. Effect of Soil Type on Single-Layer Tests 162
4.6. Multi-Layer Tests in Sand 165
4.6.1. Friction Between Sand and Clamp (Clamp Pull-Out Tests), Multi-Layer Test 166
4.6.2. Behaviour of (Multi-Layer) Nonwoven Geotextile Confined in Sand 169
4.6.3. Behaviour of (Multi-Layer) Woven Geotextile Confined in Sand 174
4.6.4. Behaviour of (Multi-Layer) Geogrid Confined in Sand 178
4.7. Multi-Layer Tests in Gravel 183
4.7.1. Friction Between Gravel and Clamp (Clamp Pull-Out Tests), Multi-Layer Test 183

4.7.2. Behaviour of (Multi-Layer) Nonwoven Geotextile Confined in Gravel 189
4.7.3. Behaviour of (Multi-Layer) Woven Geotextile Confined in Gravel 193
4.7.4. Behaviour of (Multi-Layer) Geogrid Confined in Gravel 197
5. CONCLUSION 203
REFERENCES 209
APPENDIX A: RAW RESULTS OF THE TESTS 214
APPENDIX B: EVALUATION OF STIFFNESS INCREASE IN FINITE ELEMENT ANALYSES 237

LIST OF FIGURES

Figure 1.1. In-soil wide width test apparatus. 2

Figure 1.2. Schematic view of the segmental test box and in-soil test types (measures are in mm). 3

Figure 2.1. Change of ultimate tensile strength, strain at failure and tensile load at 10% strain with gauge length (Specimen width: 200 mm) (Shrestha and Bell, 1982). 8

Figure 2.2. Load at 10% strain vs. Aspect ratio (Shrestha and Bell, 1982). . . 9

Figure 2.3. In-isolation and in-soil test methods (McGown and Andrawes, 1982). 9

Figure 2.4. Uniformity of compression in different soils (McGown and Andrawes, 1982). 10

Figure 2.5. Influence of width to length ratio of test specimens on the load-extension behaviour of a geotextile (McGown and Andrawes, 1982). 11

Figure 2.6. Layout of load-extension test apparatus developed at Strathclyde University. (a) In-isolation confined. (b) In-soil confined (McGown and Andrawes, 1982). 12

Figure 2.7. In-soil confined load-extension test data for three geotextiles (McGown and Andrawes, 1982). 13

Figure 2.8. In-soil confined load-extension test data for Propex 6067 (McGown *et al.*, 1982). 14

Figure 2.9. Sample box (El-Fermaoui and Nowatzki, 1982). 15

Figure 2.10. Geotextile specimen widths versus horizontal deformation in unconfined loading (El-Fermaoui and Nowatzki, 1982). 17

Figure 2.11. Stress-strain curves of geotextiles under 383.2 kPa normal stress for various cover and support materials (El-Fermaoui and Nowatzki, 1982). 18

Figure 2.12. Stress-strain curves of geotextiles tested under various normal stresses in #30 Ottawa sand (El-Fermaoui and Nowatzki, 1982). 19

Figure 2.13. Log E_i and log E_{sec20} versus log σ_n for Polyfilter X (woven fabric); cover and support material is dry #30 Ottawa sand. (El-Fermaoui and Nowatzki, 1982). 19

Figure 2.14. Effect of the test strain rate on the load-extension relationships for different geotextiles (a) slit film woven polypropylene, (b) continuous filament melt-bonded polypropylene/polyethylene; (c) continuous filament needle-punched polyester (Andrawes *at al.*, 1984). . 21

Figure 2.15. In-soil load-elongation test apparatus developed by Leshchinsky and Field (1987). 22

Figure 2.16. Load-elongation curves for a nonwoven geotextile (Leshchinsky and Field, 1987). 22

Figure 2.17. Modified shear box proposed by Kokkalis and Papacharisis (1989). 23

Figure 2.18. In isolation and in-soil load-extension curves of selected geotextiles (Kokkalis and Papacharisis, 1989). 26

Figure 2.19. Test configuration of Resl (1990). 27

Figure 2.20. Torn geotextile sample (Resl, 1990). 27

Figure 2.21. Tensile test apparatus with 200mm (left) and 3mm (right) gauge length (Resl, 1990). 28

Figure 2.22. Load-deformation relationships of a spun-bonded nonwoven geotextile under aspect ratio of 8 and 2% strain per minute (Ling *et al.*, 1990). 29

Figure 2.23. Modified triaxial apparatus to be used in tensile-extension tests (Wu, 1991). 30

Figure 2.24. Load-extension relationships of a needle-punched nonwoven geotextile (Wu, 1991). 30

Figure 2.25. Load-extension relationships of Geotextile A and B (needle-punched) (Ballegeer and Wu, 1993). 32

Figure 2.26. Load-extension relationships of Geotextile C and D (heat-bonded) (Ballegeer and Wu, 1993). 32

Figure 2.27. Load-extension relationships of Geotextile E (woven) (Ballegeer and Wu, 1993). 33

Figure 2.28. (a) In-soil test apparatus, (b) configuration of soil specimen (Ling *et al.*, 1992). 34

Figure 2.29. Particle gradation curve of Toyoura sand (Ling *et al.*, 1992). . . . 35

Figure 2.30. In-air test results for spun bonded geotextile with various aspect ratios (Ling *et al.*, 1992). 36

Figure 2.31. Load-deformation relationships of geotextiles under in-membrane conditions (Ling *et al.*, 1992). 38

Figure 2.32. Modified (after McGown, 1982) test apparatus of Wilson-Fahmy *et al.* (1993). 39

Figure 2.33. Load-extension behaviour of woven and nonwoven heat-bonded geotextiles (Wilson-Fahmy *et al.*, 1993). 39

Figure 2.34. Load-extension behaviour of nonwoven needle-punched geotextiles (Wilson-Fahmy *et al.*, 1993). 40

Figure 2.35. Influence of strain rate on woven geotextiles under in-isolation conditions at 100mm gauge length (Boyle *et al.*, 1996). 43

Figure 2.36. Influence of gauge length on nonwoven geotextiles under in-isolation conditions at 10% strain/min (Boyle *et al.*, 1996). 43

Figure 2.37. 5% secant stiffness versus gauge length from in-isolation tests for NW1 and NW2 compared with secant stiffness values obtained from 100 mm gauge length confined tests on the same type of geotextile specimens (Boyle *et al.*, 1996). 44

Figure 2.38. Schematic view of the unit cell device proposed by Boyle *et al.* (1996). 45

Figure 2.39. Confined test results of needle punched nonwoven geotextile; (a) Load-strain relationships, (b) Strength and initial stiffness-confining pressure relationships (Ling *et al.*, 2007). 46

Figure 2.40. Layout for comparative wall designs (Ling *et al.*, 2007). 47

Figure 2.41. Schematic view of the confined extension test apparatus (Elias *et al.*, 1998) 47

Figure 2.42. Influence of soil thickness on load-strain behaviour of nonwoven geotextile (Elias *et al.*, 1998). 49

Figure 2.43. Influence of soil confining pressure and soil type on load-strain behaviour of needle-punched nonwoven geotextile (Elias *et al.*, 1998). 49

Figure 2.44. Influence of soil confining pressure and soil type on load-strain behaviour of multi-filament woven geotextile (Elias *et al.*, 1998). . . 50

Figure 2.45. Influence of soil confining pressure and soil type on load-strain behaviour of mono-filament woven geotextile (Elias *et al.*, 1998). . . 50

Figure 2.46. Influence of soil confining pressure and soil type on load-strain behaviour of extruded geogrid geotextile (Elias *et al.*, 1998). 51

Figure 2.47. Influence of soil thickness on load-strain behaviour of woven geogrid (Elias *et al.*, 1998). 51

Figure 2.48. Increase of secant stiffness values (Elias *et al.*, 1998). 52

Figure 2.49. The apparatus and specimen used in tests (a) specimen detail, unit: mm (b) schematic view of apparatus (Wang, 2001). 52

Figure 2.50. Tensile test results of Sample A, nonwoven needle-punched geotextile (Wang, 2001). 53

Figure 2.51. Tensile test results of Sample B, nonwoven needle-punched geotextile (Wang, 2001). 53

Figure 2.52. Schematic view of the apparatus developed by Mendes *et al.* (2007). 54

Figure 2.53. Load-strain curves for tests on geotextiles GB and GD under 100 kPa confining stress (Mendes *et al.*, 2007). 55

Figure 2.54. Influence of confining stress on secant tensile stiffness of geotextile GD for different strain levels: (a) wooden blocks; (b) soil SA; (c) soil SC (Mendes *et al.*, 2007). 56

Figure 2.55. Influence of geotextile impregnation on secant tensile stiffness under 100 kPa confining stress: (a) geotextile GB and (b) geotextile GD impregnated with glass beads (GLB) (Mendes *et al.*, 2007). 56

Figure 2.56. Influence of particle shape of impregnating material; confining stress of 100 kPa and λ=4: (a) geotextile GB; (b) geotextile GD (Mendes *et al.*, 2007). 57

Figure 2.57. Schematic diagram of apparatus used by Woo and Kim (2007). . . 58

Figure 2.58. Schematic diagram of apparatus used by Balakrishnan and Viswanadham (2017). 59

Figure 2.59. Effect of strain rate on tensile load-strain behaviour of geogrid (Balakrishnan and Viswanadham, 2017). 59

Figure 2.60. Effect of confining pressure on tensile load-strain behaviour of geogrid (Balakrishnan and Viswanadham, 2017). 60

Figure 2.61. Effect of soil type on tensile load-strain behaviour of geogrid (Balakrishnan and Viswanadham, 2017). 61

Figure 2.62. Effect of sand-sandwiched layer on tensile load-strain behaviour of geogrid (Balakrishnan and Viswanadham, 2017). 62

Figure 2.63. Schematic sectional side view of modified pull-out test device (Morsy *et al.*, 2019). 63

Figure 2.64. Average displacement ratio of upper passive reinforcement layers at various average displacements of active reinforcement layers: (a) u_{av} = 2 mm; (b) u_{av} = 5 mm; and (c) u_{av} = 10 mm (Morsy *et al.*, 2019). 63

Figure 2.65. Frontal tensile load-displacement curves: (a) at normal stress, σ_v = 50 kPa; and (b) at normal stress, σ_v = 21 kPa. (Morsy *et al.*, 2019). 64

Figure 3.1. In-soil wide width test apparatus. 69

Figure 3.2. Numerical model of in-soil wide width test apparatus. 70

Figure 3.3. Cross sections used to determine the box length (in gauge direction). 71

Figure 3.4. Normal stress acting on box wall in the end of test. 72

Figure 3.5. Total displacements (under 100 kPa surcharge). 72

Figure 3.6. Normal stress acting on box wall (to determine box height). 73

Figure 3.7. Schematic view of the segmental test box (measures are in mm). . 74

Figure 3.8. Slippage of specimen due to poor clamp design. 75

Figure 3.9. Final design of the clamp with sufficient slippage performance. . . 75

Figure 3.10. Clamping of the geosynthetics used in the study. 76

Figure 3.11. Geometry of the clamp (in cm). 76

Figure 3.12. Control panel. 77

Figure 3.13. Menu of the control panel. 77

Figure 3.14. User interface of the software. 79

Figure 3.15. Measuring devices. 80

Figure 3.16. Calibration of load cell. 80

Figure 3.17. Washing out the particles finer than 0.075 mm. 82

Figure 3.18. Gradation curves of sand (SW) and gravel (GW with sand). . . . 84

Figure 3.19. Sieving equipment. 84

Figure 3.20. Soil after sieving (sand). 85

Figure 3.21. Comparison of particle shape and size. 86

Figure 3.22. Particle shape of sand. 86

Figure 3.23. Particle shape of gravel. 87

Figure 3.24. Specific gravity test on sand. 88

Figure 3.25. Maximum unit weight (min void ratio) test on sand. 89

Figure 3.26. Minimum unit weight (max void ratio) test on sand. 89

Figure 3.27. Air pluviation setup used for sand placement. 90

Figure 3.28. Preparation of nonwoven geotextile samples. 93

Figure 3.29. Preparation of woven geotextile samples. 94

Figure 3.30. Preparation of geogrid samples. 95

Figure 3.31. Procedure of Single Layer Test. 96

Figure 3.32. Calculation of average (gross) load-strain curve. 97

Figure 3.33. Procedure to determine clamp friction in single layer test. 98

Figure 3.34. Gross curve, frictional curve and net curve. 99

Figure 3.35. Procedure of Multi-layer Test. 99

Figure 3.36. Procedure to determine clamp friction in multi-layer test. 101

Figure 3.37. In-air wide width test setup for various reinforcements. 103

Figure 4.1. In-air test set up for all investigated geosynthetics. 107

Figure 4.2. An example of in-soil test set up; (a) Single-layer (b) Multi-layer. . 107

Figure 4.3. In-air test setup and result of nonwoven geotextile test. 110

Figure 4.4. Load-strain result of in-air test on nonwoven geotextile. 111

Figure 4.5. Change of secant stiffness with strain for nonwoven geotextile (in-air test). 111

Figure 4.6. In-air test of woven geotextile specimen; (a) beginning of test, (b) end of test. 112

Figure 4.7. Load-strain result of in-air test on woven geotextile. 112

Figure 4.8. Change of secant stiffness with strain for woven geotextile (in-air test). 113

Figure 4.9. In-air test of geogrid specimen; (a) beginning of test, (b) end of test.114

Figure 4.10. Load-strain result of in-air test on geogrid. 114

Figure 4.11. Change of secant stiffness with strain for geogrid (in-air test). . . . 114

Figure 4.12. Apparatus developed by Balakrishnan and Viswanadham (2017). . 116

Figure 4.13. Clamp pull-out test in sand for single-layer tests (upper half is also filled with sand after taking the photograph). 117

Figure 4.14. Displacement of loading plate (at 30% strain). 118

Figure 4.15. Results of clamp pull-out test in sand. 119

Figure 4.16. Results of clamp pull-out test in sand (after area correction). . . . 119

Figure 4.17. Peak tensile strength and interface friction angle. 120

Figure 4.18. Tensile secant modulus at 5% strain for clamp pull-out in sand. . . 121

Figure 4.19. Nonwoven geotextile confined in sand (upper half of box is also filled with sand); (a) beginning of test, (b) end of test.. 122

Figure 4.20. Displacement of loading plate (up to 30% strain). 123

Figure 4.21. Results of tests on nonwoven geotextile in sand. 123

Figure 4.22. Tensile secant modulus of nonwoven geotextile in sand. 126

Figure 4.23. Displacement of rear and front end of loading plate with respect to strain. 127

Figure 4.24. Change in tensile secant modulus with respect to unconfined (in-air) test. 127

Figure 4.25. Tensile secant modulus at 5% strain for nonwoven geotextile in sand.128

Figure 4.26. Woven geotextile confined in sand (upper half of box is also filled with sand); (a) beginning of test, (b) end of test. 129

Figure 4.27. Displacement of loading plate (at T_{ult} load). 129

Figure 4.28. Results of tests on woven geotextile in sand. 130

Figure 4.29. Tensile secant modulus of woven geotextile in sand. 132

Figure 4.30. Change in tensile secant modulus with respect to unconfined (in-air) test. 133

Figure 4.31. Tensile secant modulus at 5% strain for woven geotextile in sand. . 133

Figure 4.32. Geogrid confined in sand (upper half of box is also filled with sand); (a) beginning of test, (b) end of test. 134

Figure 4.33. Displacement of loading plate (at T_{ult} load). 135

Figure 4.34. Results of tests on geogrid in sand. 136

Figure 4.35. Tensile secant modulus of geogrid in sand. 137

Figure 4.36. Displacement of rear and front end of loading plate with respect to strain. 138

Figure 4.37. Change in tensile secant modulus with respect to unconfined (in-air) test. 138

Figure 4.38. Tensile secant modulus at 5% strain for geogrid in sand. 139

Figure 4.39. Clamp pull-out test in gravel for single-layer tests (upper half is also filled with gravel after taking the photograph). 140

Figure 4.40. Displacement of loading plate (at 30% strain). 141

Figure 4.41. Results of clamp pull-out test in gravel. 141

Figure 4.42. Peak tensile strength and interface friction angle. 143

Figure 4.43. Tensile secant modulus at 5% strain for clamp pull-out in gravel. . 143

Figure 4.44. Nonwoven geotextile confined in gravel; (a)beginning of test, (b)end of test. 145

Figure 4.45. Displacement of loading plate (up to 30% strain). 145

Figure 4.46. Results of tests on nonwoven geotextile in gravel. 146

Figure 4.47. Tensile secant modulus of nonwoven geotextile in gravel. 148

Figure 4.48. Change in tensile secant modulus with respect to unconfined (in-air) test. 149

Figure 4.49. Tensile secant modulus at 5% and 10% strains for nonwoven geotextile in gravel. 149

Figure 4.50. Woven geotextile confined in gravel (upper half of box is also filled with gravel); (a) beginning of test, (b) end of test. 151

Figure 4.51. Displacement of loading plate (at T_{ult} load). 152

Figure 4.52. Results of tests on woven geotextile in gravel. 152

Figure 4.53. Tensile secant modulus of woven geotextile in gravel. 153

Figure 4.54. Displacement of rear and front end of loading plate with respect to strain. 154

Figure 4.55. Change in tensile secant modulus with respect to unconfined (in-air) test. 154

Figure 4.56. Tensile secant modulus at 5% and 10% strain for woven geotextile in gravel. 155

Figure 4.57. Geogrid confined in gravel (upper half of box is also filled with gravel); (a) beginning of test, (b) end of test. 157

Figure 4.58. Displacement of loading plate (at T_{ult} load). 157

Figure 4.59. Results of tests on geogrid in gravel. 158

Figure 4.60. Tensile secant modulus of geogrid in gravel. 159

Figure 4.61. Change in tensile secant modulus with respect to unconfined (in-air) test. 160

Figure 4.62. Tensile secant modulus at 5% and 10% strain for geogrid in gravel. 161

Figure 4.63. Results of clamp pull-out test in sand and gravel. 163

Figure 4.64. Results of tensile tests on nonwoven geotextile in sand and gravel. 163

Figure 4.65. Results of tensile tests on woven geotextile in sand and gravel. . . 163

Figure 4.66. Results of tensile tests on geogrid in sand and gravel. 164

Figure 4.67. Clamp pull-out test in sand for multi-layer test of (a) nonwoven geotextile, (b) woven geotextile, (c) geogrid. 166

Figure 4.68. Displacement of loading plate for nonwoven geotextile (at 30% strain).167

Figure 4.69. Displacement of loading plate for woven geotextile (at 30% strain). 167

Figure 4.70. Displacement of loading plate for geogrid (at 30% strain). 168

Figure 4.71. Results of clamp pull-out test in sand for nonwoven geotextile (a) actual, (b) scaled. 168

Figure 4.72. Results of clamp pull-out test in sand for woven geotextile (a) actual, (b) scaled. 168

Figure 4.73. Results of clamp pull-out test in sand for geogrid (a) actual, (b) scaled. 169

Figure 4.74. Multi-layer test of nonwoven geotextile confined in sand (for 50% strain); (a) s_v=25 mm (also representative for 50 mm), (b) s_v=100 mm. 170

Figure 4.75. Displacement of loading plate (up to 30% strain). 171

Figure 4.76. Results of multi-layer test of nonwoven geotextile in sand. 171

Figure 4.77. Tensile secant modulus of nonwoven geotextile in sand. 172

Figure 4.78. Change in tensile secant modulus with respect to unconfined (in-air) test. 173

Figure 4.79. Tensile secant modulus at 5% strain for nonwoven geotextile in sand.173

Figure 4.80. Multi-layer test of woven geotextile confined in sand (for ε_{ult} ≈26% strain); (a) s_v=25 mm, (b) s_v=50 mm, (c) s_v=100 mm. 175

Figure 4.81. Displacement of loading plate (at T_{ult} load). 175

Figure 4.82. Results of multi-layer test of woven geotextile in sand. 176

Figure 4.83. Tensile secant modulus of woven geotextile in sand. 176

Figure 4.84. Change in tensile secant modulus with respect to unconfined (in-air) test. 177

Figure 4.85. Tensile secant modulus at 5% strain for woven geotextile in sand. . 178

Figure 4.86. Multi-layer test of geogrid confined in sand (for ε_{ult} ≈12% strain), s_v=25 mm. 179

Figure 4.87. Displacement of loading plate (at T_{ult} load). 179

Figure 4.88. Results of multi-layer test of geogrid in sand. 180

Figure 4.89. Tensile secant modulus of geogrid in sand. 180

Figure 4.90. Change in tensile secant modulus with respect to unconfined (in-air) test. 181

Figure 4.91. Tensile secant modulus at 5% strain for geogrid in sand. 182

Figure 4.92. Clamp pull-out test in gravel for multi-layer test of nonwoven geotextile (s_v=50 mm and for 35% strain). 184

Figure 4.93. Clamp pull-out test in gravel for multi-layer test of woven geotextile (s_v=25 mm and for 35% strain). 184

Figure 4.94. Clamp pull-out test in gravel for multi-layer test of geogrid (s_v=25 mm and for 35% strain). 185

Figure 4.95. Displacement of loading plate for nonwoven geotextile (at 30% strain).186

Figure 4.96. Displacement of loading plate for woven geotextile (at 30% strain). 186

Figure 4.97. Displacement of loading plate for geogrid (at 30% strain). 186

Figure 4.98. . Results of clamp pull-out test in gravel for nonwoven geotextile (a) actual, (b) scaled. 187

Figure 4.99. Results of clamp pull-out test in gravel for woven geotextile (a) actual, (b) scaled. 187

Figure 4.100. Results of clamp pull-out test in gravel for geogrid (a) actual, (b) scaled. 187

Figure 4.101. Multi-layer test (s_v=25 mm) of nonwoven geotextile confined in gravel (for 35% strain); (a) test specimen, (b) passive (upper) reinforcement (s_v=25mm). 189

Figure 4.102. Displacement of loading plate (up to 30% strain). 190

Figure 4.103. Results of multi-layer test of nonwoven geotextile in gravel. 190

Figure 4.104. Tensile secant modulus of nonwoven geotextile in gravel. 191

Figure 4.105. Change in tensile secant modulus with respect to unconfined (in-air) test. 192

Figure 4.106. Tensile secant modulus at 5% and 10% strain for nonwoven geotextile in gravel. 193

Figure 4.107. Multi-layer test of woven geotextile confined in gravel. 194

Figure 4.108. Displacement of loading plate (at T_{ult} load). 195

Figure 4.109. Results of multi-layer test of woven geotextile in gravel. 195

Figure 4.110. Tensile secant modulus of woven geotextile in gravel. 196

Figure 4.111. Change in tensile secant modulus with respect to unconfined (in-air) test. 196

Figure 4.112. Tensile secant modulus at 5% strain for woven geotextile in gravel. 197

Figure 4.113. Multi-layer test of geogrid confined in gravel (for ε_{ult} ≈11% strain), s_v=25 mm. 198

Figure 4.114. Displacement of loading plate (at T_{ult} load). 199

Figure 4.115. Results of multi-layer test of geogrid in gravel. 199

Figure 4.116. Tensile secant modulus of geogrid in gravel. 200

Figure 4.117. Change in tensile secant modulus with respect to unconfined (in-air) test. 201

Figure 4.118. Tensile secant modulus at 5% strain for geogrid in gravel. 202

Figure A.1. Noise of the apparatus. 214

Figure A.2. Clamp pull-out tests in sand (single-layer, 25 kPa). 214

Figure A.3. Clamp pull-out tests in sand (single-layer, 50 kPa). 215

Figure A.4. Clamp pull-out tests in sand (single-layer, 75 kPa). 215

Figure A.5. Clamp pull-out tests in sand (single-layer, 125 kPa). 215

Figure A.6. Clamp pull-out tests in gravel (single-layer, 25 kPa). 216

Figure A.7. Clamp pull-out tests in gravel (single-layer, 50 kPa). 216

Figure A.8. Clamp pull-out tests in gravel (single-layer, 75 kPa). 216

Figure A.9. In-air tests of NWGT. 217

Figure A.10. In-air tests of WGTX. 217

Figure A.11. In-air tests of WOGD. 217

Figure A.12. Single-layer NWGT in sand (25 kPa). 218

Figure A.13. Single-layer NWGT in sand (50 kPa). 218

Figure A.14. Single-layer NWGT in sand (75 kPa). 218

Figure A.15. Single-layer WGTX in sand (25 kPa). 219

Figure A.16. Single-layer WGTX in sand (50 kPa). 219

Figure A.17. Single-layer WGTX in sand (75 kPa). 219

Figure A.18. Single-layer WOGD in sand (25 kPa). 220

Figure A.19. Single-layer WOGD in sand (50 kPa). 220

Figure A.20. Single-layer WOGD in sand (75 kPa). 220

Figure A.21. Single-layer WOGD in sand (125 kPa). 221

Figure A.22. Single-layer NWGT in gravel (25 kPa). 221

Figure A.23. Single-layer NWGT in gravel (50 kPa). 221

Figure A.24. Single-layer NWGT in gravel (75 kPa). 222

Figure A.25. Single-layer WGTX in gravel (25 kPa). 222

Figure A.26. Single-layer WGTX in gravel (50 kPa). 222

Figure A.27. Single-layer WGTX in gravel (75 kPa). 223

Figure A.28. Single-layer WOGD in gravel (25 kPa). 223

Figure A.29. Single-layer WOGD in gravel (50 kPa). 223

Figure A.30. Single-layer WOGD in gravel (75 kPa). 224

Figure A.31. Clamp pull-out tests in sand (multi-layer, NWGT, 25 mm). 224

Figure A.32. Clamp pull-out tests in sand (multi-layer, NWGT, 50 mm). 224

Figure A.33. Clamp pull-out tests in sand (multi-layer, NWGT, 100 mm). . . . 225

Figure A.34. Clamp pull-out tests in sand (multi-layer, WGTX, 25 mm). 225

Figure A.35. Clamp pull-out tests in sand (multi-layer, WGTX, 50 mm). 225

Figure A.36. Clamp pull-out tests in sand (multi-layer, WGTX, 100 mm). . . . 226

Figure A.37. Clamp pull-out tests in sand (multi-layer, WOGD, 25 mm). 226

Figure A.38. Clamp pull-out tests in sand (multi-layer, WOGD, 50 mm). 227

Figure A.39. Clamp pull-out tests in sand (multi-layer, WOGD, 100 mm). . . . 227

Figure A.40. Clamp pull-out tests in gravel (multi-layer, NWGT, 25 mm). . . . 227

Figure A.41. Clamp pull-out tests in gravel (multi-layer, NWGT, 50 mm). . . . 228

Figure A.42. Clamp pull-out tests in gravel (multi-layer, NWGT, 100 mm). . . 228

Figure A.43. Clamp pull-out tests in gravel (multi-layer, WGTX, 25 mm). . . . 228

Figure A.44. Clamp pull-out tests in gravel (multi-layer, WGTX, 50 mm). . . . 229

Figure A.45. Clamp pull-out tests in gravel (multi-layer, WGTX, 100 mm). . . 229

Figure A.46. Clamp pull-out tests in gravel (multi-layer, WOGD, 25 mm). . . . 229

Figure A.47. Clamp pull-out tests in gravel (multi-layer, WOGD, 50 mm). . . . 230

Figure A.48. Clamp pull-out tests in gravel (multi-layer, WOGD, 100 mm). . . 230

Figure A.49. Multi-layer NWGT in sand (25 mm). 230

Figure A.50. Multi-layer NWGT in sand (50 mm). 231

Figure A.51. Multi-layer NWGT in sand (100 mm). 231

Figure A.52. Multi-layer WGTX in sand (25 mm). 231

Figure A.53. Multi-layer WGTX in sand (50 mm). 232

Figure A.54. Multi-layer WGTX in sand (100 mm). 232

Figure A.55. Multi-layer WOGD in sand (25 mm). 233

Figure A.56. Multi-layer WOGD in sand (50 mm). 233

Figure A.57. Multi-layer WOGD in sand (100 mm). 233

Figure A.58. Multi-layer NWGT in gravel (25 mm). 234

Figure A.59. Multi-layer NWGT in gravel (50 mm). 234

Figure A.60. Multi-layer NWGT in gravel (100 mm). 234

Figure A.61. Multi-layer WGTX in gravel (25 mm). 235

Figure A.62. Multi-layer WGTX in gravel (50 mm). 235

Figure A.63. Multi-layer WGTX in gravel (100 mm). 235

Figure A.64. Multi-layer WOGD in gravel (25 mm). 236

Figure A.65. Multi-layer WOGD in gravel (50 mm). 236

Figure A.66. Multi-layer WOGD in gravel (100 mm). 236

Figure B.1. Model geometry in FEM. 238

Figure B.2. Change of Jsec5 of NWGT with pressure for laboratory and FEM tests. 239

Figure B.3. Change of Jsec5 of WGTX with pressure for laboratory and FEM tests. 239

Figure B.4. Modified FEM models to reach laboratory results. 240

Figure B.5. Inherent $J_{sec5,r}$. 241

LIST OF TABLES

Table 2.1. Geotextiles investigated by Shrestha and Bell (1982). 7

Table 2.2. Strip tensile test series studied by Shrestha and Bell (1982). 7

Table 2.3. Changes from unconfined in-isolation load-strain curves due to confinement in-soil at 100 kPa confining stress (McGown *et al.*, 1989). 14

Table 2.4. Summary of test program (all soils were air dry except where noted) 16

Table 2.5. Characteristics of geotextiles tested in the experiments (Kokkalis and Papacharisis, 1989) 24

Table 2.6. Comparison of tensile strengths (DIN 53857) (Resl, 1990) 28

Table 2.7. Properties of the geotextiles used in study of Ballegeer and Wu (1993) 31

Table 2.8. Index properties of geotextiles (Ling *et al.*, 1992) 34

Table 2.9. Test program (Ling *et al.*, 1992). 36

Table 2.10. Change of secant modulus with confinement pressure for nonwoven needle-punched geotextiles (Wilson-Fahmy *et al.*, 1993) 40

Table 2.11. Geotextiles tested by Boyle *et al.* (1996) 41

Table 2.12. Soil properties used by Boyle *et al.* (1996). 45

Table 2.13. Properties of geosynthetics used in the study of Elias *et al.* (1998) 48

Table 2.14. Soil properties used by Mendes *et al.* (2007) 54

Table 2.15. Nonwoven needle-punched geotextile properties used by Mendes *et al.* (2007) 55

Table 2.16. Summary of previous studies on confined extension test 67

Table 3.1. Materials used in FEM model 71

Table 3.2. MSE wall reinforced fill particle size distribution requirement (Berg *et al.* 2009) 82

Table 3.3. Particle size distribution of sand and gravel used in the study . . . 83

Table 3.4. Index and engineering properties of sand 88

Table 3.5. Air pluviation test results 91

Table 3.6. Gravel tamping in proctor mold 91

Table 3.7. Technical specifications of GeoTeknik 5000 PP 92

Table 3.8. Technical specifications of TenCate Geolon PP 40 93

Table 3.9. Technical specifications of ForTex GG 35/20 P 94

Table 3.10. Test program of single layer in-soil tests (also includes in-air tests) 104

Table 3.11. Test program of multi-layer in-soil tests 105

Table B.1. Materials used in FEM model 238

LIST OF SYMBOLS

C_c	Coefficient of curvature (D_{30}^2 / D_{10} x D_{60})
C_u	Coefficient of uniformity (D_{60} / D_{10})
D_{10}	The particle size such that 10% of the particles are smaller
D_{30}	The particle size such that 30% of the particles are smaller
D_{50}	Mean diameter
D_{60}	The particle size such that 60% of the particles are smaller
D_r	Relative density (%)
E_i	Initial tangent modulus
e_{max}	Maximum void ratio
e_{min}	Minimum void ratio
E_{sec20}	Secant modulus for 20% strain
G_s	Specific gravity
$J_{air,10}$	Unconfined tensile secant modulus (stiffness) at 10% strain
$J_{air,5}$	Unconfined tensile secant modulus (stiffness) at 5% strain
J_{sec}	Tensile secant modulus (stiffness)
$J_{sec,5}$	Confined tensile secant modulus (stiffness) at 5% strain
$J_{sec,r}$	Tensile secant modulus (stiffness) ratio
l	Length
$\emptyset_{ps}$	Plane strain angle of internal friction
$\emptyset'_{peak}$	Peak angle of internal friction (Direct Shear Test)
$\emptyset'_{res}$	Residual angle of internal friction (Direct Shear Test)
R^2	Coefficient of determination
s_v	Vertical spacing
T	Tensile load
T_{ult}	Ultimate tensile load
w	Width

γ_d	Dry unit weight
γ_{dmax}	Maximum dry unit weight
γ_{dmin}	Minimum dry unit weight
δ	Deformation
ε	Strain
ε_{ult}	Strain at ultimate tensile load
ρ_d	Dry density
ρ_{dmax}	Maximum dry density
ρ_{dmin}	Minimum dry density
σ_n	Normal stress
σ_T	Equivalent tensile stres

LIST OF ACRONYMS/ABBREVIATIONS

ASTM	The American Society for Testing Materials
GRS	Geosynthetic Reinforced Soil
HB	Heat-bonded
LVDT	Linear Variable Differential Transformer
MD	Machine Direction
NA	Data Not Available
NP	Needle-punched
NW	Nonwoven Geotextile
NW or NWGT	Nonwoven Geotextile
PES	Polyester
PET	Polyethylene
PP	Polypropylene
PVC	Polyvinyl Chloride
UCD	Unit Cell Device
USCS	Unified Soil Classification System
W	Woven Geotextile
WGTX	Woven Geotextile
W or WGTX	Woven Geogrid
XD	Cross-machine Direction

1. INTRODUCTION

The approach of adding inclusions to soil to improve its engineering properties has been followed for centuries. Reinforced soil concept is still used throughout the world and a preferred option in many situations. The first examples of inclusions and reinforcements in the history are natural materials (wood, cotton, etc.) which have high degradability. Thanks to the advanced technology (mid 20^{th} century), engineers used polymers to create more durable materials to reinforce the soil. Thenceforward, geosynthetics -a product of polymers- are largely used to reinforce the soil.

In order to use geosynthetics in design, their properties (especially load-strain behaviour) should be known. Consequently, determining the most realistic tensile behaviour by tensile tests became one of the most important goals of geotechnical engineers working on this field. Nowadays, wide-width tensile test is the most common method to determine the load-strain behaviour of geosynthetics. However, it overrules the influence of environmental factors (soil type, confinement, etc.) on load-strain behaviour by proposing an unconfined in-air tensile test. In other words, the common unconfined in-air test methods (ASTM D4595, ASTM D6637, EN ISO 10319, etc.) can't simulate the most realistic tensile load-strain behaviour of the reinforcement under operational conditions. This led many researchers to study in-soil test methods.

Determination of the in-soil load-strain behaviour of geosynthetics dates to the study of McGown and Andrawes (1982). In their pioneering study, they investigated the in-soil load-strain behaviour of nonwoven geotextiles like most of the consequent researchers. Results of various studies showed that there is an undeniable improvement in load-strain behaviour of the nonwoven geotextile (especially needle-punched) when they are tested in soil under confinement pressures. Several test methods were proposed since 1980s to determine the in-soil load-strain behaviour of the geosynthetics. The woven geotextiles and geogrids are seldomly investigated in studies.

In this study the in-soil tensile strength and behaviour of geosynthetic reinforcements were investigated. 160 tests were conducted in scope of this study to investigate the influence of variables such as soil type, vertical pressure and passive reinforcement on tensile behaviour of different geosynthetic types. For this reason, a new apparatus which can perform both in-air and in-soil tests was developed (Figure 1.1). The new apparatus enables user to use coarse soils contrary to the apparatuses used in previous studies. As a result, site conditions can be simulated more realistically for various soil types.

The tests in the scope of this study can be divided into 3 main groups. First group is the control group in which the geosynthetics were tested under unconfined in-air conditions. A regular wide width tensile test method was applied to this group as described in ASTM D4595, ASTM D6637 and EN ISO 10319 with constant strain rate of 2% strain/min.

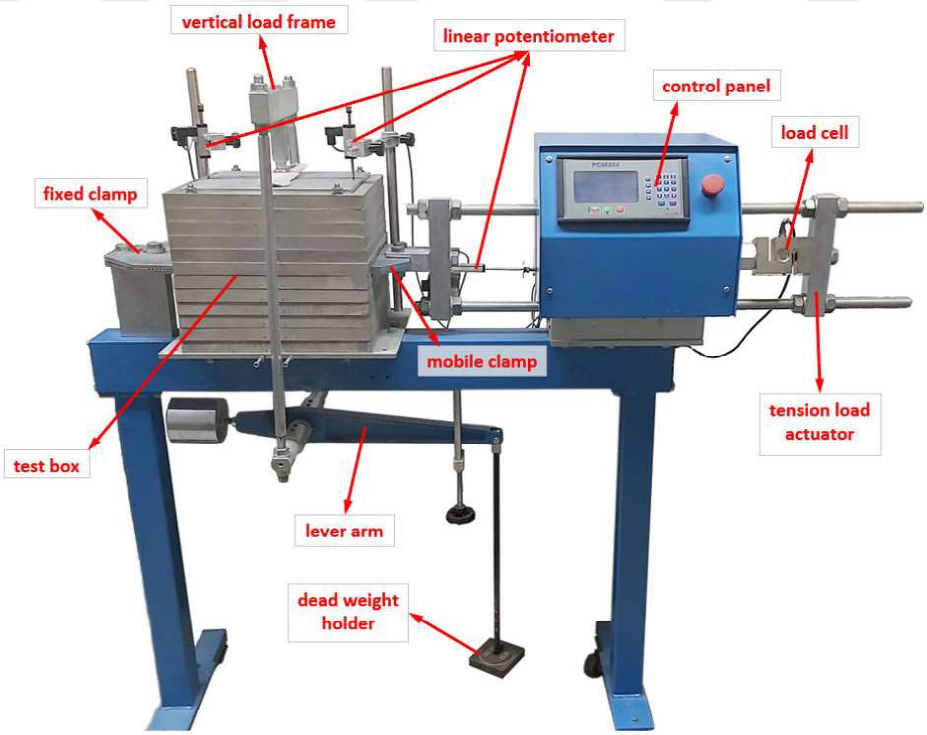


Figure 1.1. In-soil wide width test apparatus.

In second test group, geosynthetics were tested under confined in-soil conditions. In this test group, the influences of vertical pressure and soil type on geosynthetic tensile behaviour were investigated separately. Vertical pressure of 25, 50 and 75 kPa were applied during the in-soil wide width tensile test. This group is called "single-layer test group" (Figure 1.2).

In third test group, again, geosynthetics were tested under confined in-soil conditions. In this test group, the influence of the passive reinforcement on the test specimen was investigated for various vertical spacing values. 1 layer of passive reinforcement above and below the test specimen were placed in the box and fixed to the box at the rear end. Vertical pressure of 50 kPa was applied during the in-soil wide width tensile test. Vertical spacing (s_v) values of 25, 50 and 100 mm were applied separately, and the load-strain behaviour of test specimen was observed for each case. This group is called "multi-layer test group". The box of the apparatus was designed accordingly. Each segment of the box also works as a clamp for passive reinforcement (Figure 1.2).

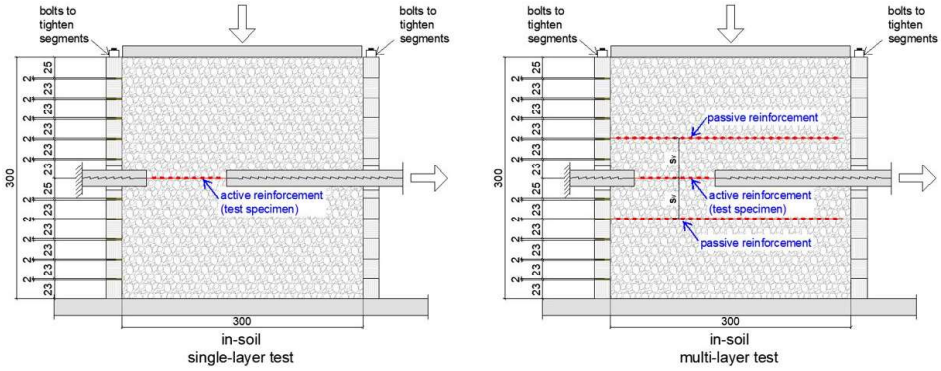


Figure 1.2. Schematic view of the segmental test box and in-soil test types (measures are in mm).

The vast majority of the previous studies were on nonwoven geotextiles (Andrawes *et al.* (1984), Leschinsky and Field (1987), Kokkalis and Papacharisis (1989), Wu (1991), Ling *et al.* (1992), Ling *et al.* (1997), Wang (2001), Mendes *et al.* (2007), Won and Kim (2007)). There is insufficient research on common geosynthetic rein-

forcements such as woven geotextile and geogrid. This study was carried out on 3 types of geosynthetics. Geosynthetics used in the study are needle-punched nonwoven geotextile (GeoTeknik 5000 PP), woven geotextile (TenCate Geolon PP 40) and woven geogrid (ForTex GG35/20P).

Fine sand (up to 2 mm) and rubber/membrane were used in most of the previous studies in the literature (McGown and Andrawes (1982), McGown *et al.* (1982), Andrawes *et al.* (1984), Wu (1991), Ballegeer and Wu (1993), Ling *et al.* (1992), Wilson-Fahmy *et al.* (1993), Boyle *et al.* (1996), Ling *et al.* (1997), Elias *et al.* (1998), Wang (2001), Mendes *et al.* (2007), Balakrishnan and Viswanadham (2017)). For a better simulation of site conditions, soils commonly used in reinforced soil applications on site were included in this study. In-soil tests were performed in 2 types of soils. According to USCS, the soil types used in tests are classified as Well Graded Sand and Well Graded Gravel with Sand (45% sand content).

In this study, in-air and in-soil tests were carried out to plot load-strain curves of geosynthetics. Behaviour and properties of the geosynthetics (T_{ult}, ε_{ult}, stiffness, etc.) under various conditions (confinement, soil type, vertical pressure, vertical spacing) were determined, evaluated, and compared. The changes in behaviour were interpreted and possible reasons were discussed. Especially, the change in stiffness was interpreted for small strains which are commonly used in design (5% strain) and change with respect to the pressure was described numerically. Thanks to the proposed equations, in future applications, the in-soil stiffness of the geosynthetics can be directly estimated without performing in-soil test.

2. LITERATURE REVIEW

2.1. Introduction

Reinforcing the soil by adding inclusions were commenced centuries ago, but the inclusions in early examples were natural materials which were destined to decay in a relatively short time. In 1960s, French architect-engineer Henri Vidal developed the reinforced earth in which steel strips were used to improve the soil's tensile strength. Then, steel reinforcements were substituted with geosynthetic reinforcements (Das, 2011).

Tensile load-extension behaviour of the reinforcement governs the design of reinforced soils. Consequently, determining the most realistic tensile behaviour by tensile tests became one of the most important goals of geotechnical engineers working on this field. Textile scientists propounded to modify existing small-scale tensile tests of textile industry while geotechnical engineers were tended to alter existing soil test methods to measure geotextile properties (Ball, 1982).

ASTM and ISO (and EN standards based on ISO) test methods to determine tensile load-extension behaviour of geosynthetics are accepted worldwide. Load-extension tests are performed by following wide width strip test standards, ISO 10319 (for all geosynthetics), ASTM D 4595 (for geotextiles) and ASTM D 6637 (for geogrids). Both ASTM tests are conducted at a constant strain rate of 10±3%/min whereas it is 20±5%/min in ISO tests. Specimen dimensions should be 200 mm wide and 100 mm long (gauge length) according to ASTM D 4595 (2011) and ISO 10319 (2015). Likewise, geogrid specimen is prepared to be minimum 200 mm wide (or at least 5 ribs in the cross-test direction) by 300 mm long (or at least 2 apertures in the test direction) (ASTM D 6637, 2015).

Tests included in the mentioned ASTM and ISO standards are carried out under in-air (in-isolation) conditions which is not the best method to represent the geosynthetic behaviour in field. In order to simulate the most realistic tensile load-extension behaviour of the reinforcement under operational conditions, many researchers studied in-soil test methods and proposed various test procedures.

2.2. Previous Studies

As aforementioned, tensile load-extension characteristics of geosynthetics must be measured to be used in geotechnical designs. Earliest studies were carried out by considering the textile industry's applications but need of geotechnical-specific tests came to light. Within the scope of this need, load-extension test method proposals came out. The studies can be divided into two groups mainly, such as in-isolation and in-soil methods. Previous studies in the literature related to the mentioned methods are discussed in this section chronologically.

Shrestha and Bell (1982) carried out an unconfined in-isolation strip tensile test program to determine the effects of some variables on tension-extension results. The investigated variables were specimen size and aspect ratio, strain rate, test method and sample variability. 6 geotextiles were used in research (Table 2.1). All samples were taken in machine direction (MD). Laboratory temperature and humidity were 68^{o}F to 82^{o}F and 20% to 58%. Test program is given in Table 2.2.

Table 2.1. Geotextiles investigated by Shrestha and Bell (1982).

Number	Fiber-Polymer	Construction
NW-1	Continuous Polyester	Nonwoven, Resin bonded
NW-3	Continuous Polypropylene	Nonwoven, Heat bonded
NW-5	Continuous Polypropylene	Nonwoven, Needlepunched
NW-6	Staple Polypropylene	Nonwoven, Needlepunched
W-4	Monofilament Polypropylene	Woven
C-1	Slit Film Polypropylene	Woven, Needled nap

Table 2.2. Strip tensile test series studied by Shrestha and Bell (1982).

Series Number	Test Method	Width x Gauge Length (mm)	Strain Rate (% per minute)	Fabrics Tested	Specimens Each Test
1	Strip	200 x 25 MD	5	6	5
		200 x 50 MD	5	6	5
		200 x 100 MD	5	6	5
		200 x 200 MD	5	6	5
2	Strip	25 x 100 MD	5	6	5
		50 x 100 MD	5	6	5
		100 x 100 MD	5	6	5
		150 x 100 MD	5	6	5
3	Strip	200 x 100 MD	1-1/4	6	3
		200 x 100 MD	12-1/2	6	5
4	Plane-Strain	200 x 100 MD	5	6	5

After performing tests in 200 mm specimen width, they found out that gauge length has little or no effect on ultimate tensile strength of geotextiles. However, the failure strains were influenced significantly by gauge length. The influence becomes less visible if the gauge length was equal or greater than 100 mm. Tensile loads at 10% strain also supported the finding that influence of the gauge length decreases after 100 mm. The mentioned findings are summarized in Figure 2.1.

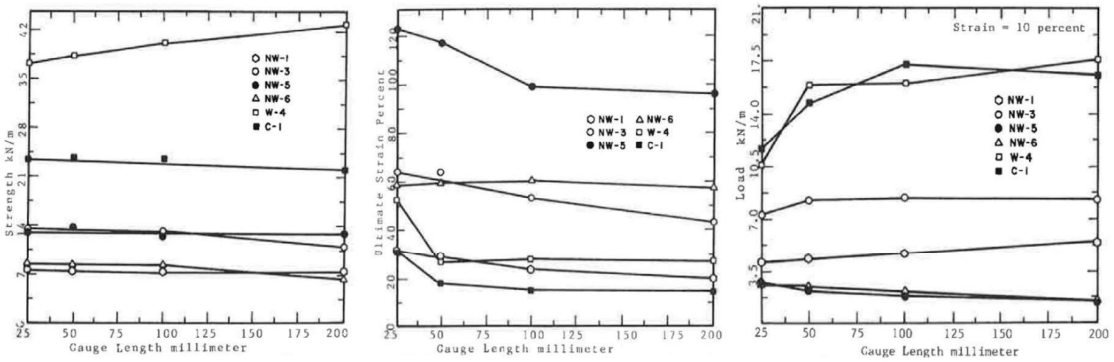


Figure 2.1. Change of ultimate tensile strength, strain at failure and tensile load at 10% strain with gauge length (Specimen width: 200 mm) (Shrestha and Bell, 1982).

After finding that the minimum gauge length should be 100 mm, they also studied the effect of specimen width, thus aspect ratio, on ultimate tensile strength and strain at failure. Results of series 1 and 2 (study on specimen dimensions and aspect ratio) in test program were summarized for 10% strain in Figure 2.2. Load-aspect ratio trends for non-woven geotextiles are almost same, while woven geotextiles showed a different trend. The loads and strains were most influenced by aspect ratios greater than 4.0 for woven geotextiles, whereas the nonwoven fabrics were most influenced by aspect ratios less than 2.0. As a result, specimen dimension of 200 mm width x 100 mm gauge length was recommended by Shrestha and Bell for routine laboratory testing. Moreover, findings of series 4 also proved that at this specimen size, plane-strain loading conditions on geotextiles can be approximated without use of a restraining device to limit necking of specimens during strip tensile tests (Shrestha and Bell, 1982).

Shrestha and Bell's study showed that there is no consistent trend with variation in strain rates. This finding of the study is controversial because recent studies showed that the strain rate has influence on load-strain behaviour of geotextiles. In general, increase of strain rate causes a more brittle trend in load-strain curves by increasing the ultimate tensile load and decreasing the ultimate strain. The behaviour can be observed in following studies included in this chapter.

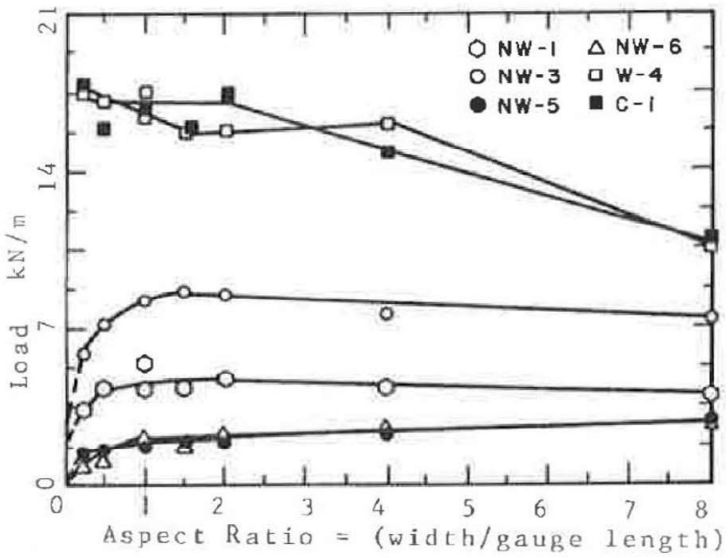


Figure 2.2. Load at 10% strain vs. Aspect ratio (Shrestha and Bell, 1982).

One of the primal studies on in-soil tensile behaviour of geosynthetic reinforcements was conducted by McGown and Andrawes (1982). McGown and Andrawes started their research by describing the in-isolation and in-soil test conditions. Main difference between in-isolation and in-soil test is the use of soil as a confining material. Latter refers to the test in which reinforcement is embedded in soil. In-isolation test can be performed under confined or unconfined conditions, but in-soil test is only performed under confined conditions (Figure 2.3). Murray and McGown (1982) also used the same description and emphasized that one method of test shouldn't be used for all purposes. In detail, in-isolation tests are useful for quality control, but in-soil tests are better for design purposes.

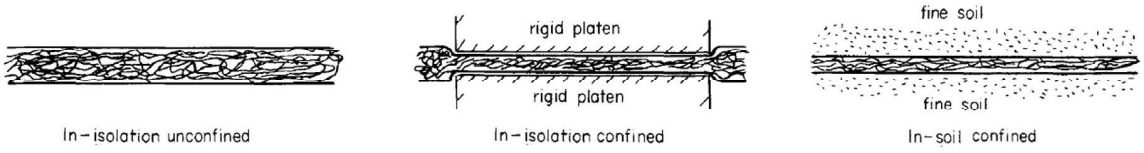


Figure 2.3. In-isolation and in-soil test methods (McGown and Andrawes, 1982).

Besides the influence of the confinement, they also stated that the stress distribution over the reinforcement is influential. In-isolation tests are performed by using plate-like elements such as rigid platen, pressure bellows, etc. Therefore, the stress distribution over the reinforcement is considered uniform. However, the stress distribution over the reinforcement strongly depends on the soil type (size and angularity of particles, particle size distribution, etc.). McGown and Andrawes stated that the confined in-isolation and confined in-soil tests may not give the same result. Result of these two tests is expected to be closer when fine grained soil is used in confined in-soil tests.

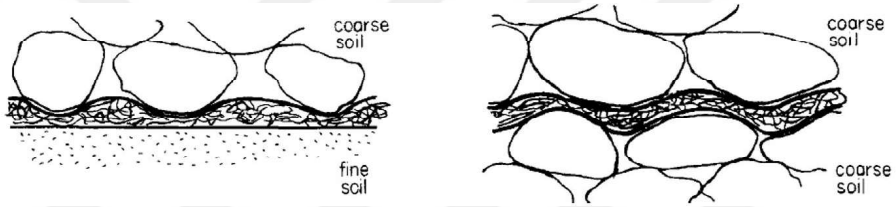


Figure 2.4. Uniformity of compression in different soils (McGown and Andrawes, 1982).

Prior to reinforcement testing, dimensions of the test sample were determined by McGown and Andrawes. They tested different geotextile types and concluded that the minimum dimension in any direction should be 100 mm to avoid local variations in uniformity of structure. As a second step in dimension research, width to length ratio was investigated with a thick needle punched nonwoven geotextile (one of the most sensitive geotextiles to edge effects). Widths ranging from 50 mm to 500 mm were used in their research. It can be seen in Figure 2.5 that minimum width of test specimen should be 200 mm when the length of specimen is 100 mm. As a result, minimum width to length ratio is determined as 2:1 by McGown and Andrawes (1982). However, larger width to length ratios up to 5:1 may be necessary when testing more loosely connected reinforcements, such as staple fibre needle punched products.

MMcGown and Andrawes (1982) developed a new apparatus by considering 2:1 width to length ratio. The apparatus was capable of testing load-extension behaviour of geotextiles under both in-isolation and in-soil confined conditions. It can also perform load-extension test in different rates of strain, creep test, repeated and cyclic loading tests. Schematic view of proposed apparatus is given in Figure 2.6.

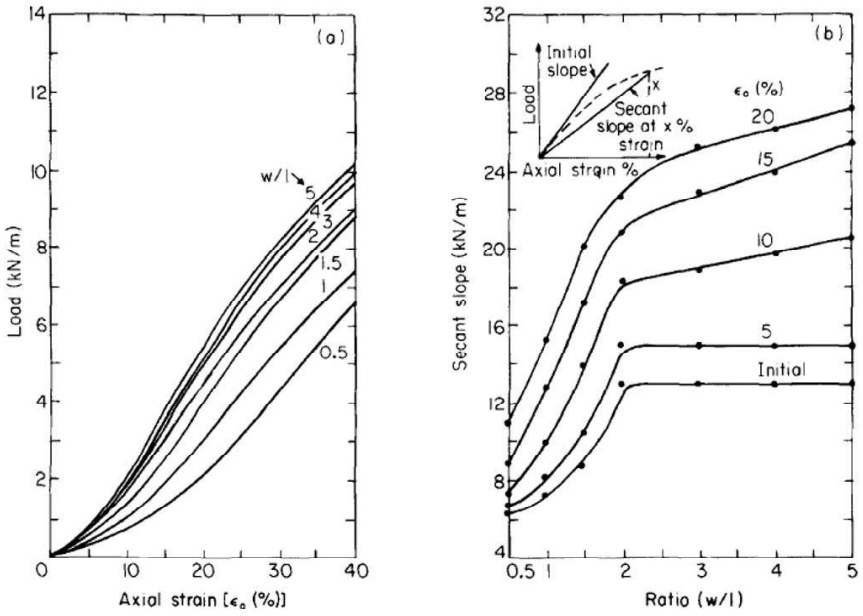


Figure 2.5. Influence of width to length ratio of test specimens on the load-extension behaviour of a geotextile (McGown and Andrawes, 1982).

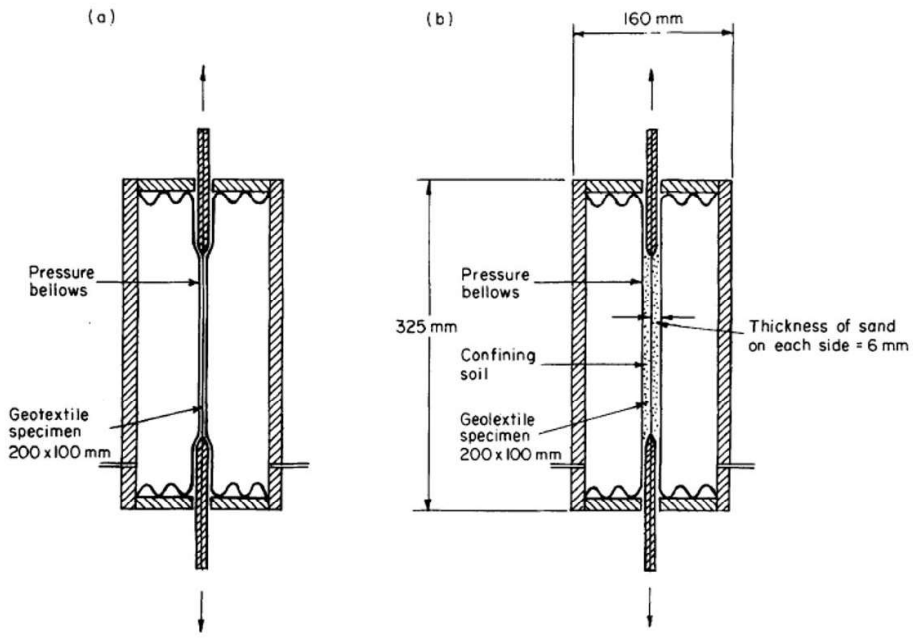


Figure 2.6. Layout of load-extension test apparatus developed at Strathclyde University. (a) In-isolation confined. (b) In-soil confined (McGown and Andrawes, 1982).

By using the proposed apparatus, McGown and Andrawes tested 3 different geotextiles under confined, in-isolation and in-soil conditions. Leighton Buzzard sand (0.3-2.0 mm) was used in in-soil test group. Geotextiles used in the tests were:

- Needle punched non-woven geotextile (Bidam U24),
- Melt bonded non-woven geotextile (Terram 1000),
- Flat split tape woven geotextile (Lotrak 16/15).

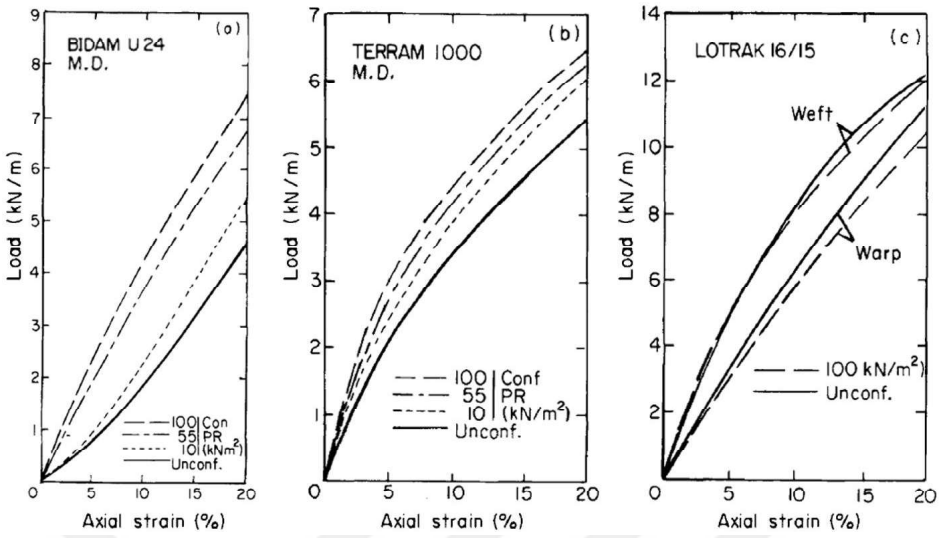


Figure 2.7. In-soil confined load-extension test data for three geotextiles (McGown and Andrawes, 1982).

As clearly seen in Figure 2.7, confinement has an irrefutable influence on load-extension behaviour of nonwoven geotextiles (Figure 2.7a and Figure 2.7b). However, there is almost no influence on the woven geotextile. McGown and Andrawes (1982) explains this change by the compressibility of the nonwoven geotextiles. Confinement changes the internal structure of the nonwoven geotextile by altering the inter-fibre friction and surface texture. Change in the structure of reinforcement directly effects the load-extension behaviour.

As woven geotextile (Figure 2.7c) is almost incompressible, influence of confinement on geotextile structure is limited. According to McGown and Andrawes, lower results in confined case (woven geotextile) is probably due to the soil particles which cause further splitting of the tapes. Moreover, tapes are always aligned in weft direction during the test, so influence of confinement on filament structure is little. In warp direction, however, filaments pass over and under the cross filaments. Therefore, movement of filaments in warp direction are restricted as a result of confinement in-soil. Hence, geotextile structure is affected while tested in warp direction (Andrawes *et al.*, 1984).

In their another study, McGown *et al.* (1982) quantified the changes in the load-strain curves with regards to slopes (initial and secant stiffnesses). The changes in slopes were calculated in terms of percentage. Comparison was made between unconfined in-isolation and confined in-soil for 100kPa (Table 2.3).

Table 2.3. Changes from unconfined in-isolation load-strain curves due to confinement in-soil at 100 kPa confining stress (McGown *et al.*, 1989).

MEASURED VALUE	BIDAM U24	TERRAM 1000	LOTRAK 16/15 (weft)	PROPEX 6067*
Initial Slope	+270%	+78%	+8%	+254%
5% Secant Slope	+206%	+46%	+1%	+39%
20% Secant Slope	+64%	+16%	-1%	+16% (18% strain)

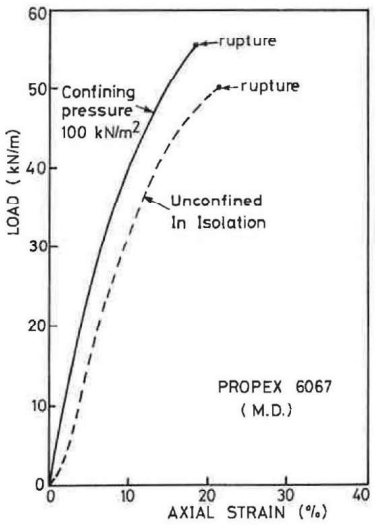


Figure 2.8. In-soil confined load-extension test data for Propex 6067 (McGown *et al.*, 1982).

As shown in Table 2.3, they tested an extra reinforcement in this study, Propex 6067. Propex 6067 is a composite geotextile (combination of woven and needle punched nonwoven geotextile). It is 100% polypropylene, specific gravity is 0.91, 650 g/m2 and nominal thickness is 3.5mm. Load-strain curve is given Figure 2.8.

McGown and Andrawes (1982) concludes that the use of confined in-soil testing is essential. The complex relationship between geotextile, confinement and soil forces the designer to conduct case specific in-soil confined tests. On the other hand, in-isolation unconfined tests are more practical. Therefore, in-isolation unconfined tests can be performed for quality control and specifications, but not for design.

El-Fermaoui and Nowatzki (1982) developed a different test method to investigate the in-soil behaviour of geotextiles. They designed a square box with interior dimensions of 63.5x63.5x38.1mm (Figure 2.9). Various soil materials can be used in upper and lower sections of the box. A direct shear device was used to apply tensile force to the geotextile. Influence of confinement, cover and support material, soil moisture content were studied with the proposed test apparatus. Prior to these ones they monitored the necking effect on different geotextiles and summarized them in a graph.

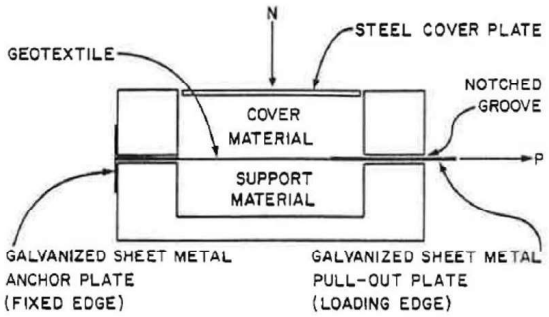


Figure 2.9. Sample box (El-Fermaoui and Nowatzki, 1982).

Geotextile samples were cut in a 5.08 cm square. It is known from previous studies that the width to length ratio should be at least 2, but 1 was used in this study. Normal stresses applied on tests were 47.9, 95.8, 191.6 and 383.2 kPa. Two types of soils were used in the study as #30 Ottawa sand and fine river run uniform gravel. Dry unit weights of soils were 14.13 and 16.96 kN/m^3 respectively. Strain rate was 1.27 mm/min (2.5% strain/min) and test stops at geotextile failure or at 25% strain.

Dry and wet tests were conducted to assess the influence of soil moisture content. In wet tests, the box was prepared and soaked in water for 24 hours before the beginning of test. Tests were performed on woven and non-woven geotextiles which were Polyfilter X, Mirafi 100x and Mirafi 500x (woven) and Mirafi 140S, Typar 3601, Bidim C-34 (non-woven). Summary of test program is given in Table 2.4.

Table 2.4. Summary of test program (all soils were air dry except where noted).

GEOTEXTILE TYPE	SAND-SAND INTERFACE	GRAVEL-SAND INTERFACE	GRAVEL-GRAVEL INTERFACE
Polyfilter X	X*	X	X
Mirafi 100X	X	-	-
Mirafi 500X	X	-	-
Mirafi 140S	X*	X	X
Typar 3601	X	-	-
Bidim C-34	X	-	-
* Tests were also performed for wet interfaces.			

Instead of using tensile force per unit width (kN/m) in the test outputs, El-Fermaoui and Nowatzki (1982) preferred to use equivalent tensile stress (σ_T). σ_T is the ratio of tensile force to the reinforcement cross sectional area (width x thickness of geotextile). Since reinforcement width (thus cross-sectional area) has tendency to change with horizontal displacement during test, they measured the change in geotextile width during unconfined tests and plotted a graph (Figure 2.10). They assumed that width changes in confined test are same with the ones in unconfined tests. It is obvious in the graph that the necking due to horizontal displacement is negligible in woven geotextile while significant in nonwoven geotextiles.

Following necking tests, they investigated the effect of cover and support material under same confining pressure (383.2 kPa). Tensile stresses of samples in #30 Ottawa sand were found higher than the ones in gravel (Figure 2.11). Researchers reported that higher shear stresses along soil-geotextile interfaces were mobilized when #30 Ottawa

sand was used, because of the larger contact area of sand when compared to the gravel.

Another variable of this test group was the influence of moisture content on in-soil behaviour of geotextiles. Only #30 Ottawa sand was used in this test group. Compared to the dry tests, no change was observed when woven and non-woven geotextiles were tested in wet sand under zero normal stress.

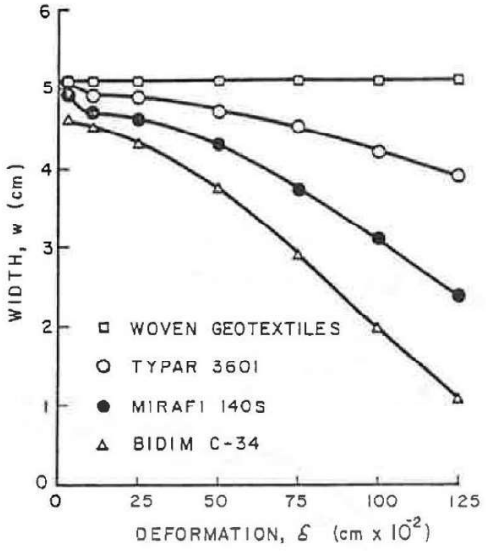


Figure 2.10. Geotextile specimen widths versus horizontal deformation in unconfined loading (El-Fermaoui and Nowatzki, 1982).

When normal stress was applied, wet sand caused a reduction in tensile strength of woven geotextile. This is caused by the lubricant effect of water on interface which makes slip of woven geotextile easier. Contrary to woven geotextile, strength of non-woven geotextile slightly increased under wet conditions. This is explained by the drainage capability of non-woven geotextiles. As a result of drainage, effective stress of soils on the interface increases and soils densify. This leads approximately 5% increase in tensile strength.

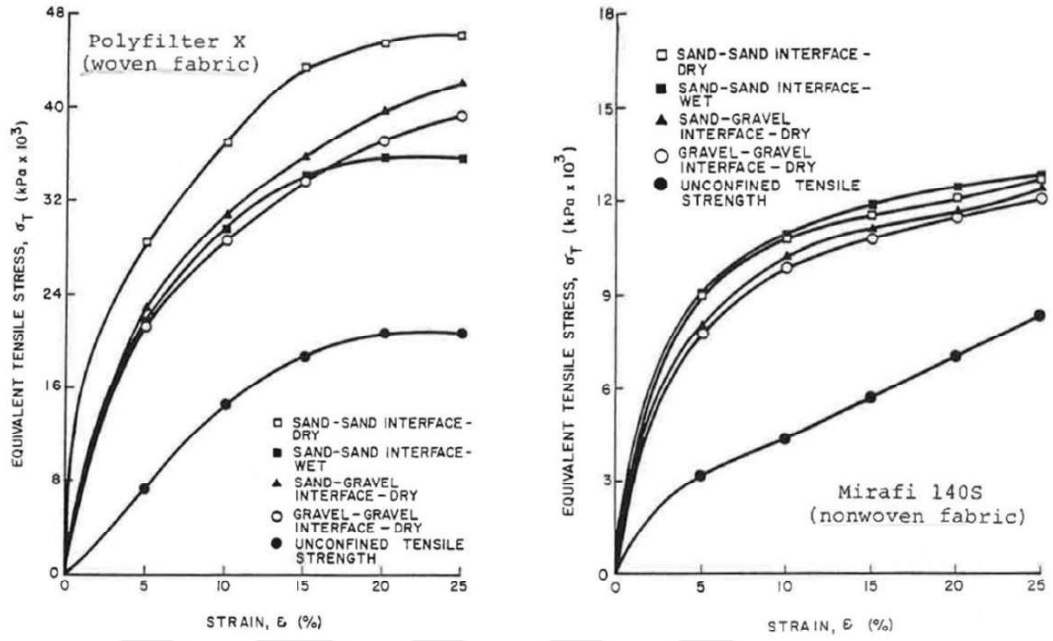


Figure 2.11. Stress-strain curves of geotextiles under 383.2 kPa normal stress for various cover and support materials (El-Fermaoui and Nowatzki, 1982).

The final test group was established to measure the influence of normal stress on tensile strength. Only dry #30 Ottawa sand was used in this test group. It appears that tensile strength increases with the normal stress both for woven and nonwoven geotextile (Figure 2.12).

Initial tangent modulus (E_i) and secant modulus for 20% strain (E_{sec20}) values for various normal stress conditions were plotted in logarithmic scale. Graph exhibits the linear relationship of log σ_n and stiffness values (Figure 2.13). By using these results, secant values and stress-strain curves for other normal stresses can be calculated and used in design. It should be noted that results are specific to the applied conditions (soil type, moisture content, etc.).

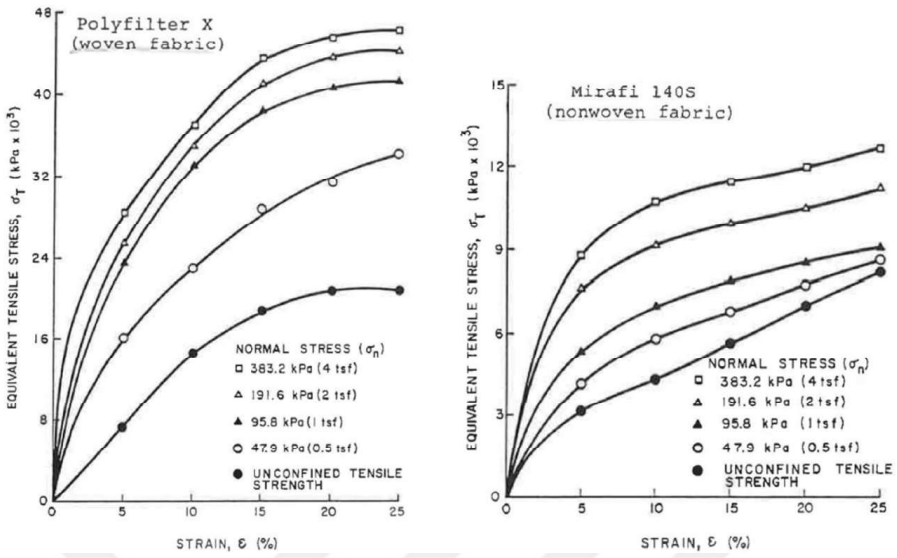


Figure 2.12. Stress-strain curves of geotextiles tested under various normal stresses in #30 Ottawa sand (El-Fermaoui and Nowatzki, 1982).

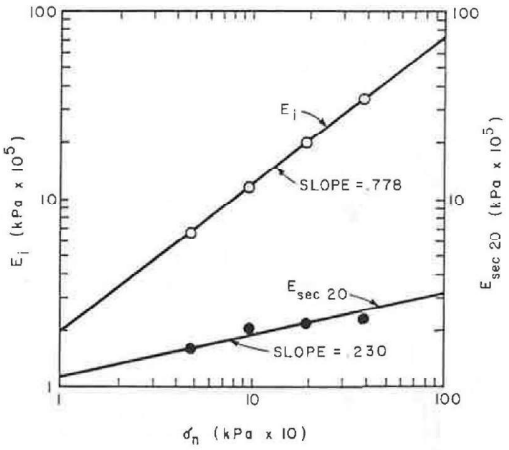


Figure 2.13. Log E_i and log E_{sec20} versus log σ_n for Polyfilter X (woven fabric); cover and support material is dry #30 Ottawa sand. (El-Fermaoui and Nowatzki, 1982).

In 1984, Andrawes *et al.* published a paper that can be considered an extension of McGown and Andrawes (1982). Influence of temperature, humidity, strain rate and confinement on load-extension behaviour was investigated. The test group which includes the effect of confinement is also given in the study of McGown and Andrawes

(1982). Remarkable part of their study is the influence of strain rate. Same 3 geotextiles given previously were used in tests, namely;

- Needle punched non-woven geotextile (Bidam U24),
- Melt bonded non-woven geotextile (Terram 1000),
- Flat split tape woven geotextile (Lotrak 16/15).

Dimensions of specimens were 200 mm wide and 100 mm long. Tests were performed under 20^{o}C. Constant strain rates of 0.2, 2 and 20% strain per minute were used to evaluate the influence of strain rate on different reinforcements. Tests were carried out under in-isolation (unconfined) conditions. Results of the tests are given in Figure 2.14. It can be clearly seen that the geotextile with the loosest structure (needle-punched, non-woven) is not influenced by the changes in strain rate. In contrary, woven geotextile which has aligned filaments and tight structure is affected by strain rate most.

It is stated by McGown and Andrawes (1982) that the total elongation is a combination of the deformations of individual filaments and rearrangement of the internal structure. Deformation of polymer filaments are sensitive to strain rate while internal structure is sensitive to confinement. Therefore, woven geotextile which has aligned filaments is the most sensitive one in this test group (Andrawes *et al.*, 1984).

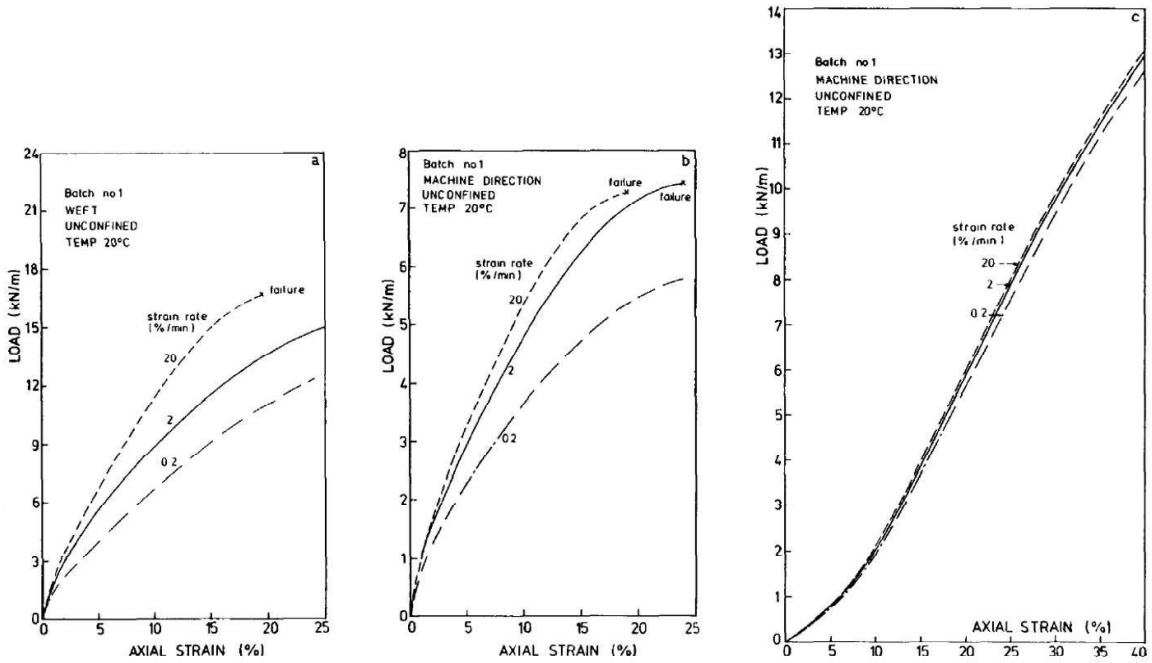


Figure 2.14. Effect of the test strain rate on the load-extension relationships for different geotextiles (a) slit film woven polypropylene, (b) continuous filament melt-bonded polypropylene/polyethylene; (c) continuous filament needle-punched polyester (Andrawes *at al.*, 1984).

Leshchinsky and Field (1987) modified direct shear apparatus in which bending of the geotextile was inhibited. The geotextile specimen was rested on a lubricated rigid bottom plates instead of soil to prevent settlement based out-of-plane bending of the specimen (Figure 2.15). Nonwoven geotextiles were used in tests. An increase in stiffness parallel to the confining pressure was observed. Authors also concluded that interface friction between geotextile and soil was not significantly affected by change in confining pressure and failure strain was found almost same for all confining pressures.

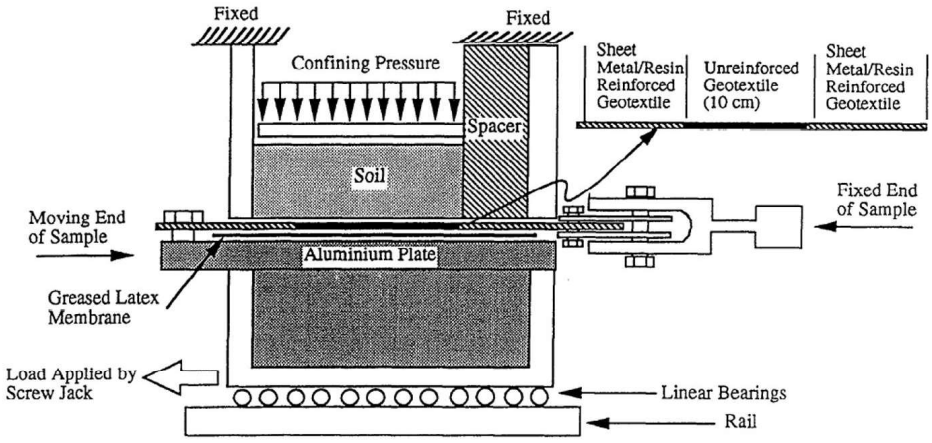


Figure 2.15. In-soil load-elongation test apparatus developed by Leshchinsky and Field (1987).

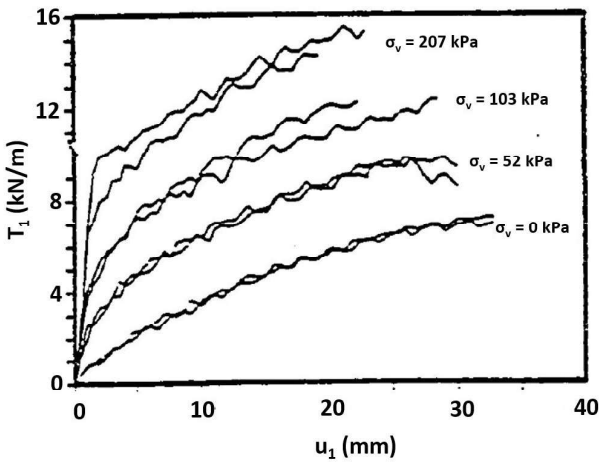


Figure 2.16. Load-elongation curves for a nonwoven geotextile (Leshchinsky and Field, 1987).

Kokkalis and Papacharisis (1989) also investigated the in-soil behaviour of geotextiles. They asserted that normal stresses imposed on geotextiles (due to the overlying material) mobilize shear stresses along the soil-geotextile interface. Mobilized shear stresses limit any dimensional change, especially in tension direction. Elongation and reorientation of the individual geotextile yarns constitute the extension of whole geotextile. The component of the extension due to reorientation of the geotextile yarns can

be constrained by the compressive confinement. As a result, confinement increases the elastic modulus and ultimate strength of geotextile. However, effect of confinement is limited when the geotextile has a regular tight structure (e.g., woven geotextile). The effect is considerable on geotextiles with loose structure (e.g., non-woven geotextile, especially needle-punched) (Kokkalis and Papacharisis, 1989).

Complex structure and limited availability of the apparatus proposed by McGown (Figure 2.6) led Kokkalis and Papacharisis (1989) to design a simpler apparatus. They also emphasized other drawbacks of the former apparatus. According to the mentioned researchers, shallow thickness of the soil, vulnerability of the air bellows to sharp objects limit the capability of the former apparatus. Due to these reasons, simulating gravelly environment or using angular aggregates with the former apparatus might be problematic.

Kokkalis and Papacharisis (1989) emphasized the importance of simulating field conditions in laboratory by following a simple test method. Then, they modified the large (30 x 30 cm) shear box apparatus to perform in-soil tests in the Road Laboratory of the University of Thessaloniki. They proposed the apparatus because of its simplicity and availability in almost every laboratory (Figure 2.17).

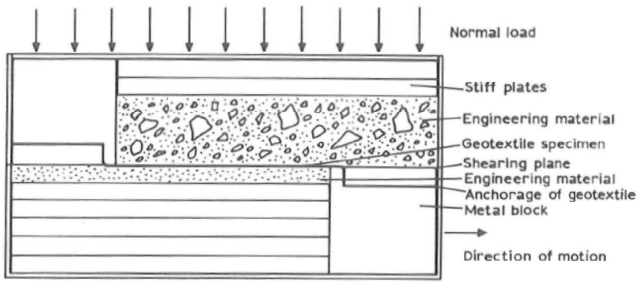


Figure 2.17. Modified shear box proposed by Kokkalis and Papacharisis (1989).

Sample dimensions were selected by considering width to length ratio, which should be at least 2. Sample dimensions (stressed part) were 15 cm long by 30 cm wide. Upper half and lower half of the apparatus can be filled with different materials

to reconstruct the situation in the field. During the sample preparation, materials were compacted by both mechanical effort and static compression (static compression was applied as normal stress during the test). Load cell and dial gauge (0.01 mm min. reading) were used to determine load-extension graphs.

However, this apparatus had some drawbacks. The first one is to maintain the required thickness of the soil in the lower half. Thickness of the soil has to be in a certain level to that the geotextile coincides with shear plane. Therefore, special care must be given while preparing the sample box. Second drawback is the friction between metal clamps and soil, which misleads the test results. Researchers solved this problem by performing initial tests to determine the friction between soil and clamps, then they subtracted the friction results from actual tests. Therefore, they obtained net load-extension results of geotextile specimen. Thirdly, imperfections in clamping may cause false results for the first 1-2 mm of displacement. This problem is relatively easy to identify and correct.

In their research, Kokkalis and Papacharisis (1989) used 3 different geotextiles given in Table 2.5.

Table 2.5. Characteristics of geotextiles tested in the experiments (Kokkalis and Papacharisis, 1989).

Composition	Type of Construction	Weight per unit area (g/m^2)	Thickness (mm)	Identification number
67% polypropylene + 33% polyethylene	non-woven melt-bonded	140	0.7	1
67% polypropylene + 33% polyethylene	non-woven melt-bonded	230	1.0	2
100% polyester	non-woven needle-punched	270	2.3	3

Kokkalis and Papacharisis (1989) carried out the research under 3 main groups. All tests were conducted at 2% strain/min. Results of tests are given in Figure 2.18.

- First group consists of tests performed under in-isolation conditions. Load-extension characteristics of 3 geotextile types were obtained in this group.
- Second group tests were performed to compare the results of their modified shear box apparatus with the previously proposed more specialized apparatus (McGown and Andrawes, 1982). In this group, only geotextile 1 was used with Leighton Buzzard sand. Thickness of the sand layer was applied 2 cm above and beneath the geotextile. Confining pressure was applied as 10, 55 and 100 kPa.
- Third test group includes the tests in which reinforced road pavement was simulated. In order to simulate reinforced road pavement, researchers applied 2cm thick clay soil beneath the reinforcement and 6 cm thick sand-gravel soil above reinforcement. Confining pressure was applied as 152, 304 and 457 kPa. All 3 geotextile types were used in tests.

Conclusion of Kokkalis and Papacharisis (1989) coincides with the other studies. They concluded that the confinement influences the behaviour of geotextiles. Modulus of elasticity is directly proportional to the value of confinement pressure. However, influence of confinement also depends on the structure of geotextile. Loose structures like needle-punched non-woven geotextiles have the highest potential to be influenced under confinement, whereas melt-bonded non-woven geotextiles (relatively tighter structure) are influenced less.

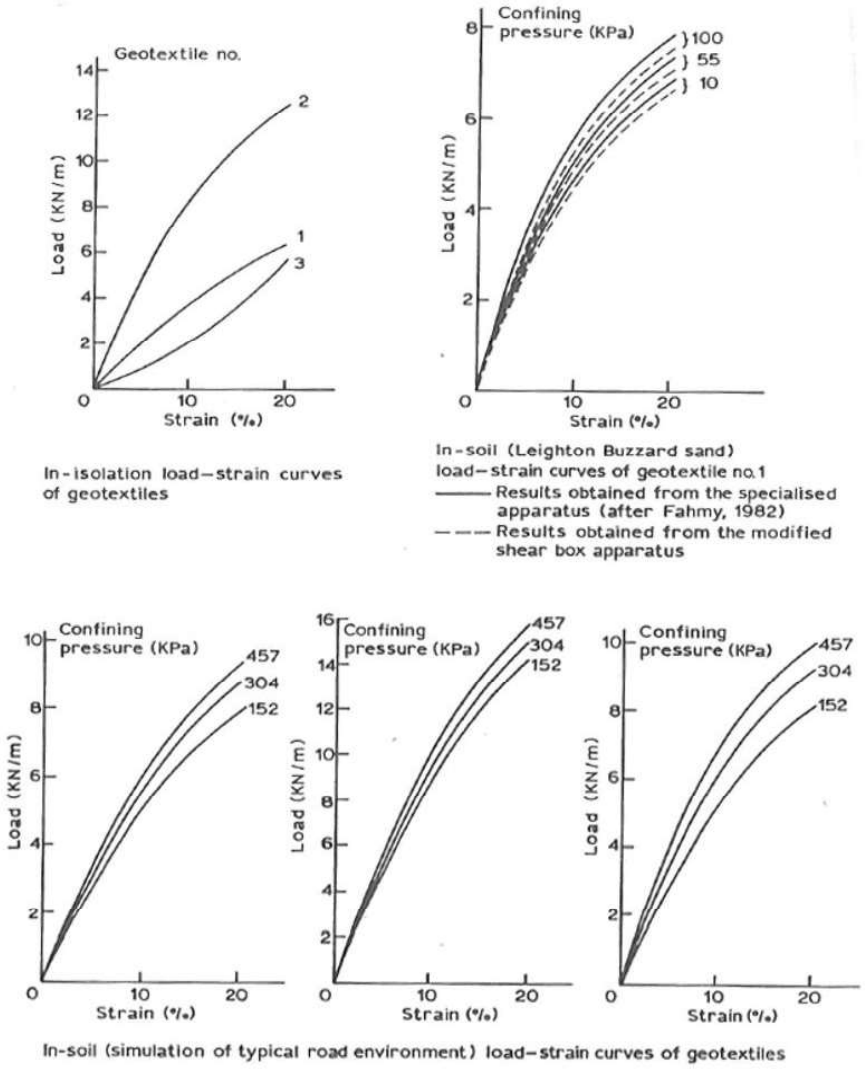


Figure 2.18. In isolation and in-soil load-extension curves of selected geotextiles (Kokkalis and Papacharisis, 1989).

Resl (1990) conducted model tests on geosynthetic reinforced (nonwoven geotextile) steep slopes (Figure 2.19). Based on the results of model tests, Resl (1990) stated that the conventional design methods lead to overdesign. Furthermore, he stated that the standard geotextile test methods (e.g., DIN 53857, ASTM D 4595, etc.) are unsuitable to simulate the in-soil load-extension behaviour of the reinforcement. First reason is the same with other researchers, effect of confinement on geotextile structure (higher stiffness). Second reason has emerged after observing the torn geotextile in the end of loading tests. As shown in Figure 2.20, the geotextile around the torn part is

neither stretched nor affected. This means that the geotextile in soil is clamped very close to the failure line. In other words, gauge length is close to the zero gap tests contrary to standard tensile tests (100 mm gauge length).

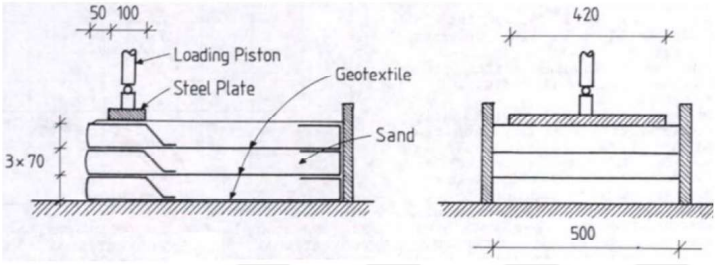


Figure 2.19. Test configuration of Resl (1990).

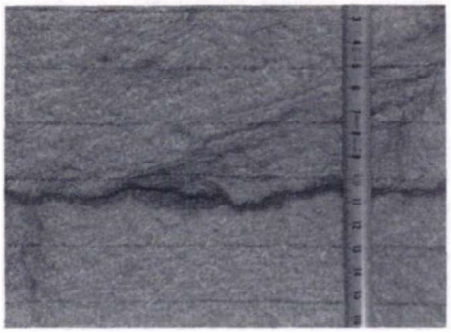


Figure 2.20. Torn geotextile sample (Resl, 1990).

Resl (1990) also investigated the influence of gauge length in geotextile load-extension behaviour. His aim was to describe a test method which gives more realistic (closer to in-soil behaviour) results. He performed in-isolation tests with gauge lengths of 200 and 3 mm (at 50 mm width) and compared the results (Figure 2.21). Results showed the increase in tensile strength by reduced gauge length (Table 2.6). However, indicating the gauge length as the only reason of tensile strength increase can be misleading. Since Resl (1990) didn't mention the strain rate in his research, it can be speculated that strain rate was not the same with longer samples but increased with decreased gauge length. If the displacement rate was kept constant (not the strain

rate), strain rate in 3 mm test is approximately 67 times greater than the strain rate in 200 mm test. This means that most likely the contribution of the strain rate was not considered in Resl's research.

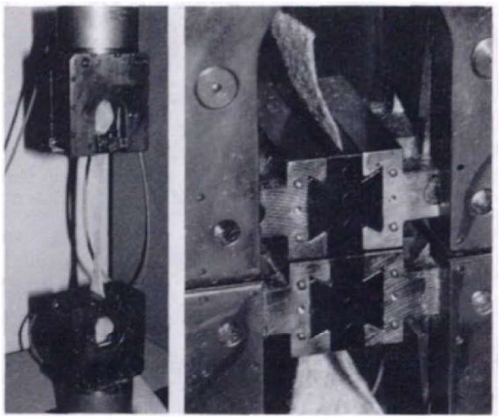


Figure 2.21. Tensile test apparatus with 200mm (left) and 3mm (right) gauge length (Resl, 1990).

Table 2.6. Comparison of tensile strengths (DIN 53857) (Resl, 1990).

Geotextile Type	Mass (g/m^2)	L=200 mm (kN/m)	L=3 mm (kN/m)	Increase (%)
PP Continuous filament needle-punched nonwoven	60	2.74	6.14	124
	90	5.08	11.46	126
	400	20.6	33.92	65
PP slit film woven	130	19.46	26	34
	380	63.16	81.32	29
	540	68.74	89.8	31

Wu (1991) proposed a modified triaxial test apparatus to determine inherent load-extension behaviour of geotextiles under confinement. Contrary to the previous studies, which are considered model tests, the purpose of the Wu's research was to maintain an "element test" by preventing relative movement between soil and geotextile. Element test gives the inherent load-extension properties of geotextiles. By

excluding the contribution of shear on soil-geotextile interface, load-extension results are obtained in a more conservative way according to researcher. On the other hand, avoiding interface shear would enable the use of different materials (like rubber) instead of soil in confined tests. Comparison of test results under various confinement conditions which were presented in Ling *et al.* (1990) also encouraged the use of rubber instead of soil (Figure 2.22).

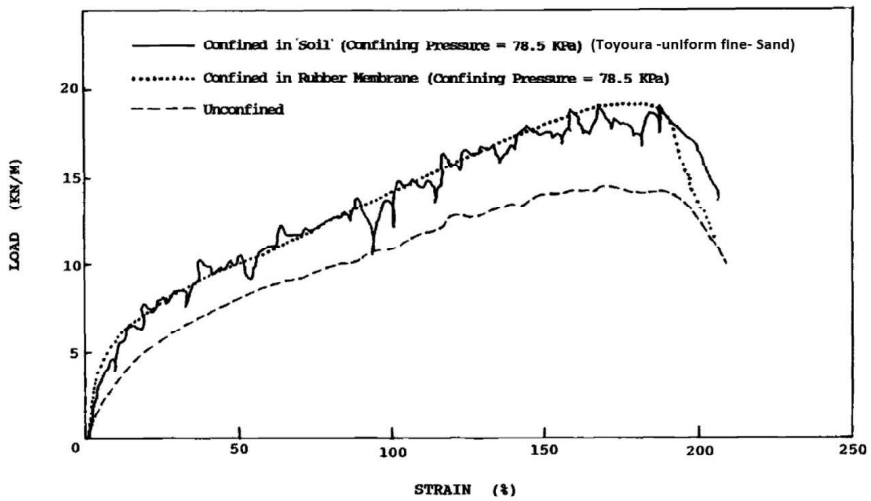


Figure 2.22. Load-deformation relationships of a spun-bonded nonwoven geotextile under aspect ratio of 8 and 2% strain per minute (Ling *et al.*, 1990).

The designed apparatus was only tested with nonwoven needle-punched geotextile in fine uniform Ottawa sand. Specimen dimensions were 50.8x152.4 mm and geotextile was tested under 69 kPa and at a constant strain rate of 2% per minute.

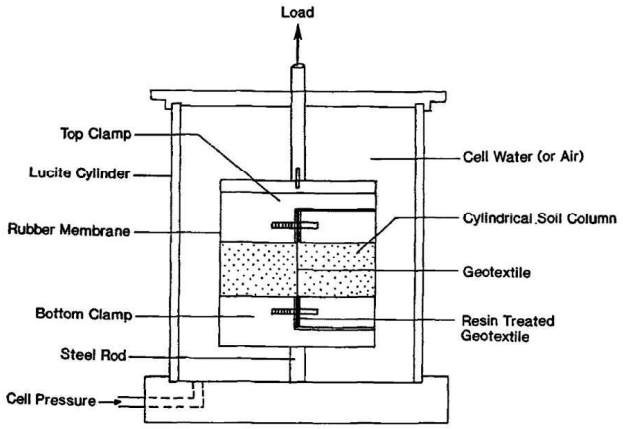


Figure 2.23. Modified triaxial apparatus to be used in tensile-extension tests (Wu, 1991).

The results needed to be corrected to eliminate the influence of soil's load-extension behaviour. Therefore, correction test was carried out to determine the soil's load-extension curve and subtract it from the actual tests. The results showed a significant increase in secant stiffness of the needle-punched nonwoven geotextile. The 5% secant stiffness was increased from 300 to 620 kN/m^2 (Figure 2.24).

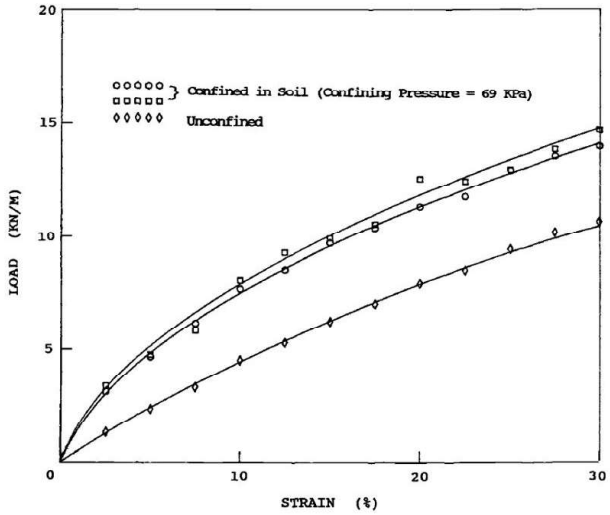


Figure 2.24. Load-extension relationships of a needle-punched nonwoven geotextile (Wu, 1991).

Apparatus (Figure 2.23) developed by Wu (1991) was used to advance the investigations by Ballegeer and Wu (1993). In scope of this study, 4 nonwoven geotextiles and 1 woven geotextile were tested (Table 2.7) at a constant rate of 2% strain per minute. Aspect ratio of samples was 6, dimensions of test samples were 25 mm (gauge length) to 150 mm (width). Instead of soil, rubber was used in confined tests. A constant confining pressure of 80 kPa was applied to the specimens by vacuuming the rubber.

Table 2.7. Properties of the geotextiles used in study of Ballegeer and Wu (1993).

Geotextile Properties	Geotextile A	Geotextile B	Geotextile C	Geotextile D	Geotextile E
Structure	NW, NP	NW, NP	NW, HB	NW, HB	W
Polymer Type	PES	PES	PP	PP	PP
Thickness (mm) (ASTM D 1777-64)	2.4	3.2	0.3	0.38	0.51
Mass Per Unit Area (g/m^2) (ASTM D 3776-84)	241	339	98	136	136
Grab Tensile / Elongation (kN, %) (ASTM D 4632-86)	0.934 / 60	1.357 / 60	0.534 / 60	0.578 / 50	0.890 / 15
Wide Width Strength / Elongation, Machine Direction (kN/m, %) (ASTM D 4595-86)	17.1 / 65	26.8 / 74	NA	NA	24.5 / 12

Results of confined and unconfined tests are presented in the following figures. Needle-punched nonwoven geotextiles are the most sensitive to the confinement due to their loose structure. Influence of the confinement reduces when the strains exceed 10%.

Results of confined and unconfined tests are presented in the following figures. Needle-punched nonwoven geotextiles are the most sensitive to the confinement due

to their loose structure. Influence of the confinement reduces when the strains exceed 10%.

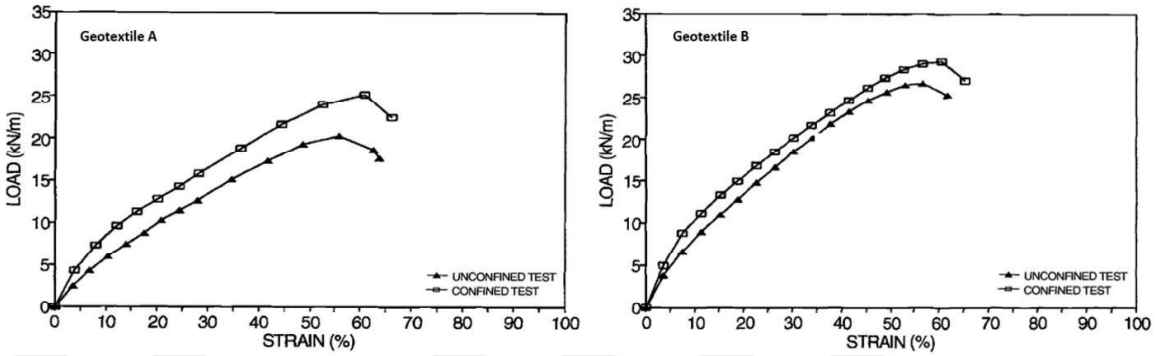


Figure 2.25. Load-extension relationships of Geotextile A and B (needle-punched) (Ballegeer and Wu, 1993).

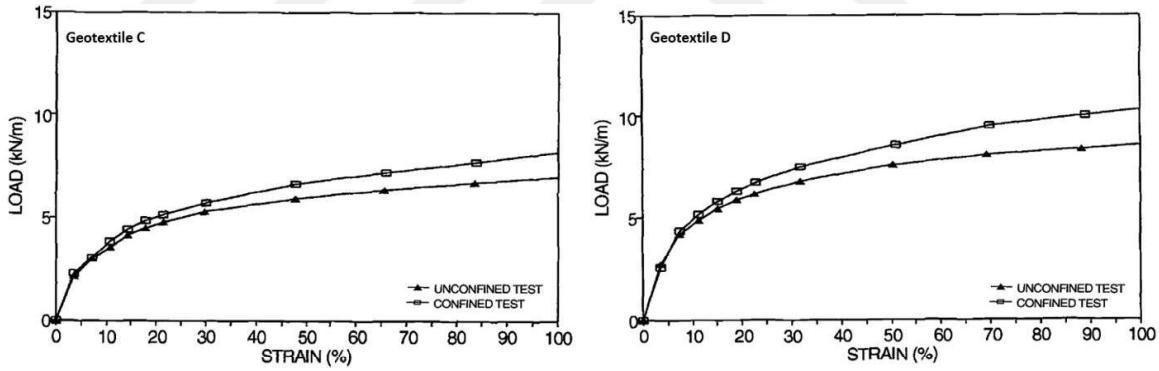


Figure 2.26. Load-extension relationships of Geotextile C and D (heat-bonded) (Ballegeer and Wu, 1993).

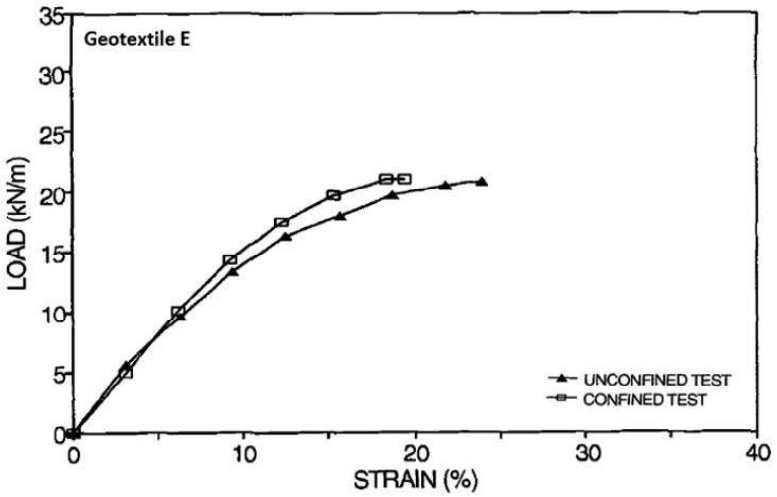


Figure 2.27. Load-extension relationships of Geotextile E (woven) (Ballegeer and Wu, 1993).

Likewise Wu (1991), Ling *et al.* (1992) claimed that the relative movement (slippage) between soil and geotextile does not occur under operational conditions. It occurs when a failure state is approached. According to Ling *et al.*, the previous test methods which involve the combination of frictional forces and confinement effect overestimates the strength and stiffness of geotextiles. They developed an apparatus (Figure 2.28) which allows soil and geotextile move together during the test (theoretically, slippage of geotextile is avoided). By following this method, the measured load-extension results did not comprise the effects of the frictional force. According to the Ling *et al.* (1992), results of the proposed tests were only influenced by the confinement.

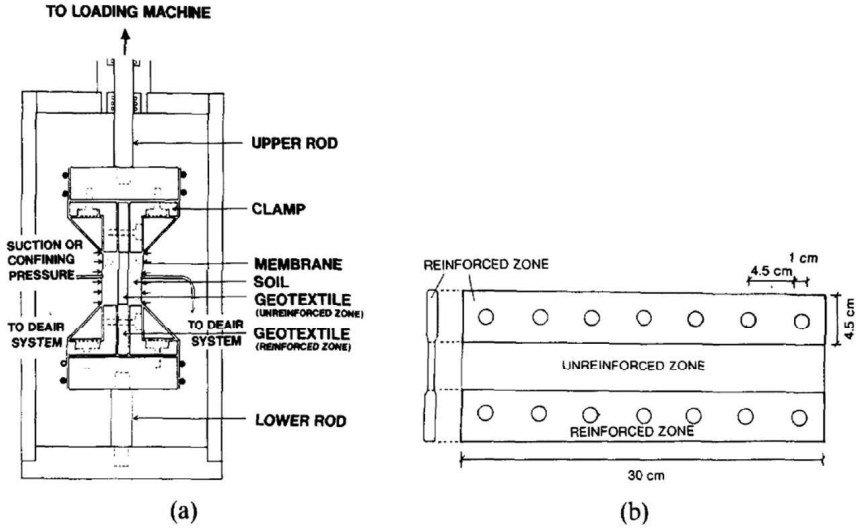


Figure 2.28. (a) In-soil test apparatus, (b) configuration of soil specimen (Ling *et al.*, 1992).

Table 2.8. Index properties of geotextiles (Ling *et al.*, 1992).

Geotextile	Bonding Process	Polymer type	Weight per unit area (g/m^2)	Thickness (mm)
Bidim b5	Needle-punched	Polyester	235	3
Tafnel U-60	Spun-bonded	Polypropylene	300	3
Typar 3301	Heat-bonded	Polypropylene	105	0.5

Clamped zones of the geotextiles were reinforced by epoxy. Three nonwoven geotextiles were tested under unconfined (in-air) and confined conditions (in-soil and in-membrane). For the in-soil tests; fine grained, uniform Toyoura sand was used. Properties of the geotextiles and gradation curve of the sand is given in Table 2.8 and Figure 2.29 respectively.

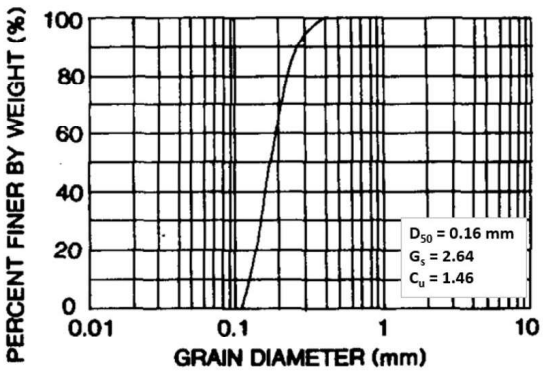


Figure 2.29. Particle gradation curve of Toyoura sand (Ling *et al.*, 1992).

All tests were performed in machine direction of geotextiles, under constant strain rate of 2% per minute and the temperature was kept at 20^{o}C. The test program was set to investigate the following effects:

- the aspect ratio of specimen,
- confinement stress,
- confinement type (in-soil, in-membrane) and
- geotextile type.

The variables implemented in the tests are also given in Table 2.9. The influence of soil and rubber to the load-strain output is diminished by testing soil and rubber separately in the apparatus. Obtained results were subtracted from the confined test results to determine corrected load-strain behaviour of geotextiles.

Spun bonded geotextile was tested in air with various aspect ratios such as 5, 6, 8 and 12 (at a width of 300mm). These tests were performed to determine a sufficiently large aspect ratio to use in confined tests. Test results (Figure 2.30) showed that the influence of aspect ratio is negligible when it is 8 or greater. In accordance with results, aspect ratio of 8 was used in tests. Needle punched geotextile was also tested under aspect ratio of 2 (at a width of 200 mm) which is commonly used in the literature.

Table 2.9. Test program (Ling *et al.*, 1992).

Group	Geotextile Type	Aspect Ratio	Confining pressure (kgf/cm^2)
In-air test	Spun-bonded	5, 6, 8, 12	0
	Needle-punched	2, 8 (2 tests)	0
	Heat-bonded	8	0
In-soil test	Spun-bonded	8	0.80 (78.48 kPa)
	Needle-punched	2 (2 tests)	0.56 (54.94 kPa)
		8	0.75 (73.58 kPa)
	Heat-bonded	8	0.75 (73.58 kPa)
In-membrane test	Spun-bonded	8	0.50 (49.05 kPa)
		8 (2 tests)	0.80 (78.48 kPa)
	Needle-punched	2	0.56, 0.75 (54.94, 73.58 kPa)
		8	0.75 (73.58 kPa)
	Heat-bonded	8	0.75 (73.58 kPa)

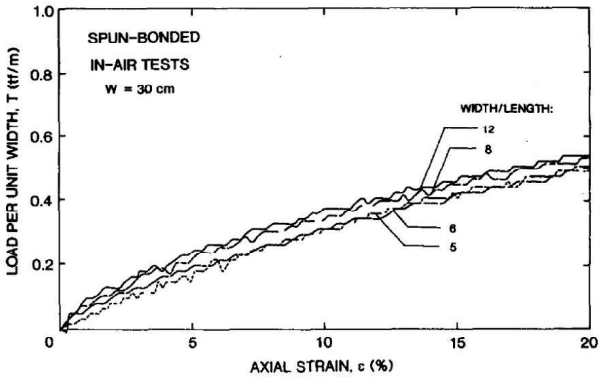


Figure 2.30. In-air test results for spun bonded geotextile with various aspect ratios (Ling *et al.*, 1992).

Another aim of the Ling *et al.* (1992) study was to determine the differences between in-soil and in-isolation (i.e., in-membrane) tests. Load-strain results of in-

membrane and in-soil tests gave similar results and the difference between two methods were found negligible. For needle-punched geotextile, in-membrane method gave slightly higher stiffness than in-soil method when strains exceed 5%. In-membrane tests of spun bonded geotextile under 0.80 kgf/cm^2 also proved the method's repeatability. In-membrane test was found more repeatable, easier to perform and less time-consuming than in-soil test. Ling *et al.* (1992) recommended the use of in-membrane test to determine the properties of geotextiles under confined situations.

In-membrane load-extension test results of 3 different geotextiles are shown in Figure 2.31. Under confined conditions, geotextiles with looser structures (spun-bonded and needle-punched) acted as stiffer materials and ultimate tensile was increased. According to researchers, heat-bonded geotextile, which has a denser fabric structure, subjected to less influence of the confinement. However, they consider a large range of strain in this conclusion (up to 70%). In operational conditions (<10% strain), influence of confinement is considerable even for heat-bonded geotextile. As mentioned in previous studies, geotextiles with looser structures become more compact with confinement. This makes the effect of confinement more visible on load-deformation curves.

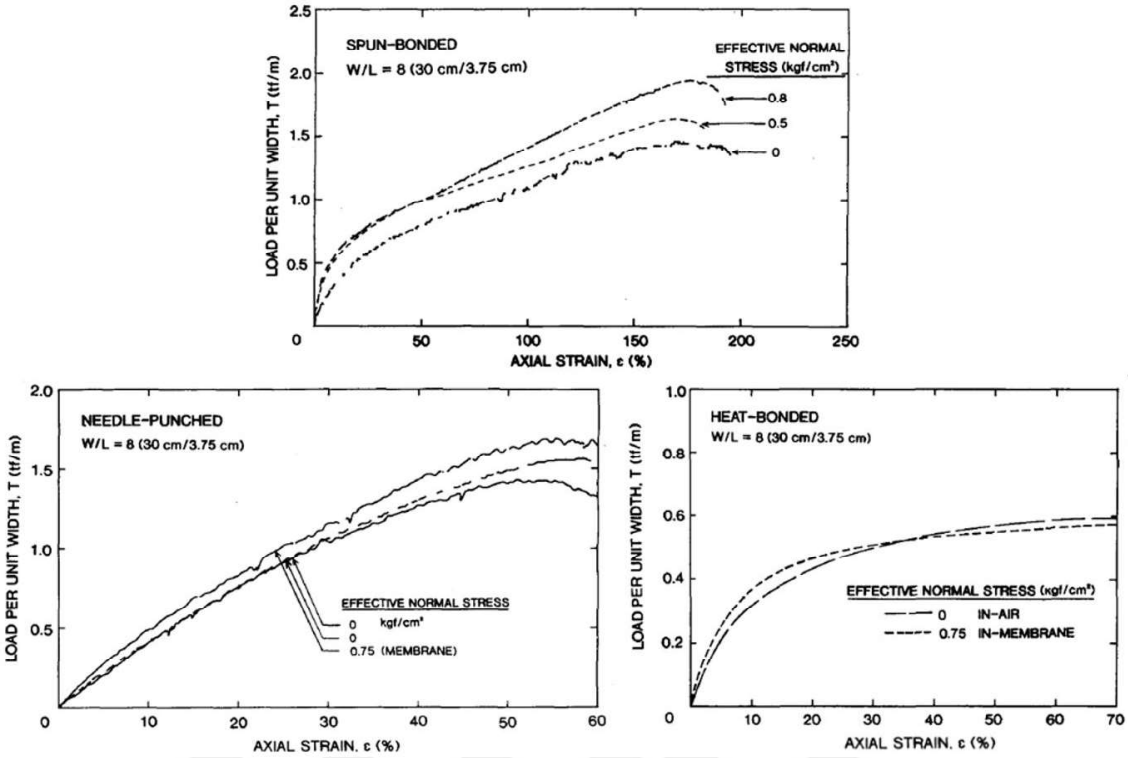


Figure 2.31. Load-deformation relationships of geotextiles under in-membrane conditions (Ling *et al.*, 1992).

Wilson-Fahmy *et al.* (1993), tested a wide range of geosynthetics (Woven and Non-woven Geotextiles, Geomembranes, Geosynthetic Clay Liners, Geonets) under confinement pressures up to 138 kPa and compared them with the unconfined test results. Geosynthetics mentioned above are tested by a modified version (changed its position to horizontal) of test device developed by McGown and Andrawes (1982). Tested area of the specimens is 202 mm at width and 102 mm at gauge length. An important difference from the other research studies was the strain rate which was applied at a constant strain rate at 10.2 mm/min (10% strain/min). Details of sand is not given but it's expected to be fine uniform sand as McGown (1982) used in his studies.

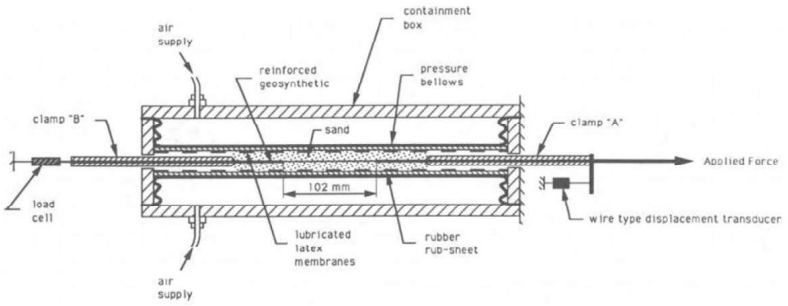


Figure 2.32. Modified (after McGown, 1982) test apparatus of Wilson-Fahmy *et al.* (1993).

Load-extension behaviour of woven geotextile was not influenced by the confining pressure. Nonwoven heat-bonded geotextile also wasn't influenced by confining pressures up to 10% strain. However, confinement pressure became important at higher strain values (>15%). According to the researchers, higher tensile loads cause deterioration of fiber crossover bonds. At mentioned load levels, soil confinement is expected to prevent the sudden rupture of fibers and deterioration of bonds by the frictional resistance. See Figure 2.33 for load-extension behaviour of woven geotextile and nonwoven heat-bonded geotextile.

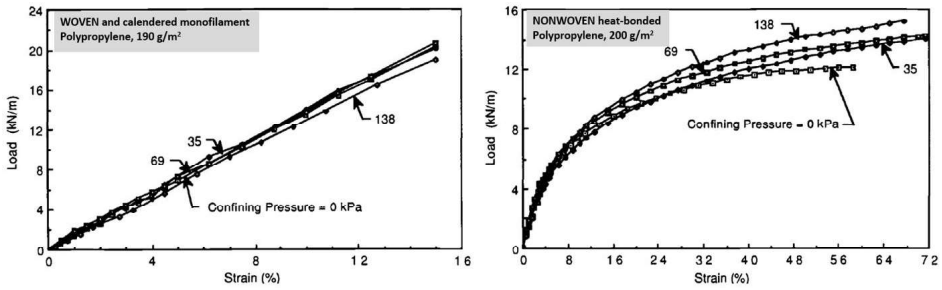


Figure 2.33. Load-extension behaviour of woven and nonwoven heat-bonded geotextiles (Wilson-Fahmy *et al.*, 1993).

Effect of confinement pressure on load-extension behaviour was clearly observed in nonwoven needle-punched geotextiles. Influence on ultimate tensile strength was relatively small but increase in modulus at 5% strain increased up to 4.8 times (Fig-

ure 2.34 and Table 2.10).

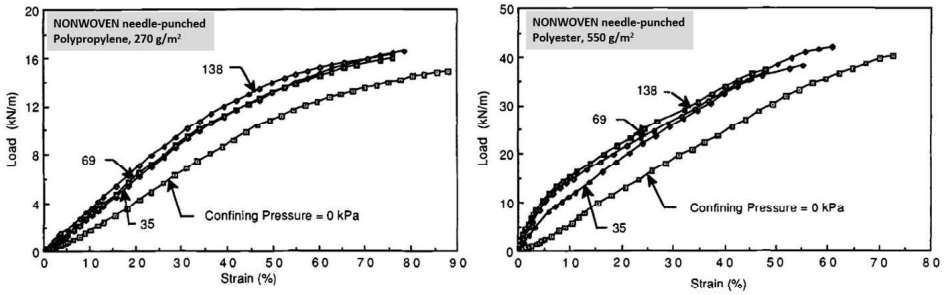


Figure 2.34. Load-extension behaviour of nonwoven needle-punched geotextiles (Wilson-Fahmy *et al.*, 1993).

Table 2.10. Change of secant modulus with confinement pressure for nonwoven needle-punched geotextiles (Wilson-Fahmy *et al.*, 1993).

Geotextile Type	Confining Pressure (kPa)	Secant modulus at 5% strain, kN/m
Nonwoven needle-punched 270 g/m^2	0	14
	35	25
	69	27
	138	33
Nonwoven needle-punched 550 g/m^2	0	44
	35	140
	69	193
	138	210

Wilson-Fahmy *et al.* (1993) finalized their research by stating that the load-extension behaviour of geomembranes (2 types, HDPE and PVC), geosynthetic clay liners (2 types) and geonet (polyethylene) was not influenced by the confining pressure under operational conditions (up to 10% strain).

Boyle *et al.* (1996) divided their research into two groups as in-isolation and in-soil test. In isolation group contained the investigation of strain rate (0.01% to 10% strain/minute) and gauge length (25 to 115 mm) influence on woven and nonwoven geotextiles, respectively whereas in-soil test questioned the effect of confining pressure on load-extension behaviour of woven and nonwoven geotextiles. Strain rate and gauge length investigations under in-isolation conditions provide very valuable data because in-soil test may -indirectly- change the gauge length, thus strain rate of the specimen during the test. Findings of in-isolation tests may let us to simulate (by changing strain rate and gauge length) in-soil behaviour of the geosynthetics under in-isolation conditions in a more practical way. All test specimens were 200 mm wide with a 100 mm gauge length as required by ASTM D4595. Geosynthetics given in Table 2.11 were used in test program.

Table 2.11. Geotextiles tested by Boyle *et al.* (1996).

Geotextile	Description	Mass (g/m^2)	Thickness (mm)	Wide Width Strength (kN/m) (ASTM D 4595)	Elongation (%) (ASTM D 4595)
PP1	Woven, slit-film	-	0.4	26	15
PP2	Woven, slit-film, 2 layer stitch-bonded	-	0.7	49	15
PP3	Woven, slit-film, 3 layer stitch-bonded	-	1.4	77	15
PET1	Woven, multi-filament	-	-	215	10
PET2	Woven, multi-filament	-	1.8	175	10
NW1	Nonwoven,needle-punched (PP)	268	2.6	16	95
NW2	Nonwoven,needle-punched (PP)	532	4.3	26	95

PP1 and PET1 is directly exhumed from the demolition of Rainier Avenue wall in Seattle, Washington, USA (Allen *et al.*, 1992). PP2 and PP3 has the same material with PP1 whilst PET2 has the same material with PET1.

In-isolation tests conducted on woven geotextiles showed that strength and stiffness of PP1, PP2, PP3 are sensitive to the strain rate whilst PET2 specimens have very little sensitivity (Figure 2.35). The 5% secant stiffness values of PP1, PP2 and PP3 decreased by 50% when strain rate was decreased from 10 to 0.01%/minute. It was decreased by only 15 to 20% in case of PET2.

In-isolation tests were performed at 10% strain/minute on nonwoven geotextiles (NW1 and NW2). The goal of these tests was to determine if a correlation could be established between in-isolation and in-soil load-extension behaviour. Based on the findings of Wang *et al.* (1990) and Resl (1990), an increase at strength was expected with decreasing gauge length. Contrary to the previous results reported by Wang *et al.* (1990) and Resl (1990), strength values of NW1 and NW2 weren't influenced by gauge length according to results of Boyle *et al.* (1996) (Figure 2.36). The possible explanation of the difference in results can be the strain rate. Wang and Resl didn't keep the strain rate constant during the test. As a result, decreasing gauge length caused an increase in strain rate which changed the load-extension behaviour of specimen.

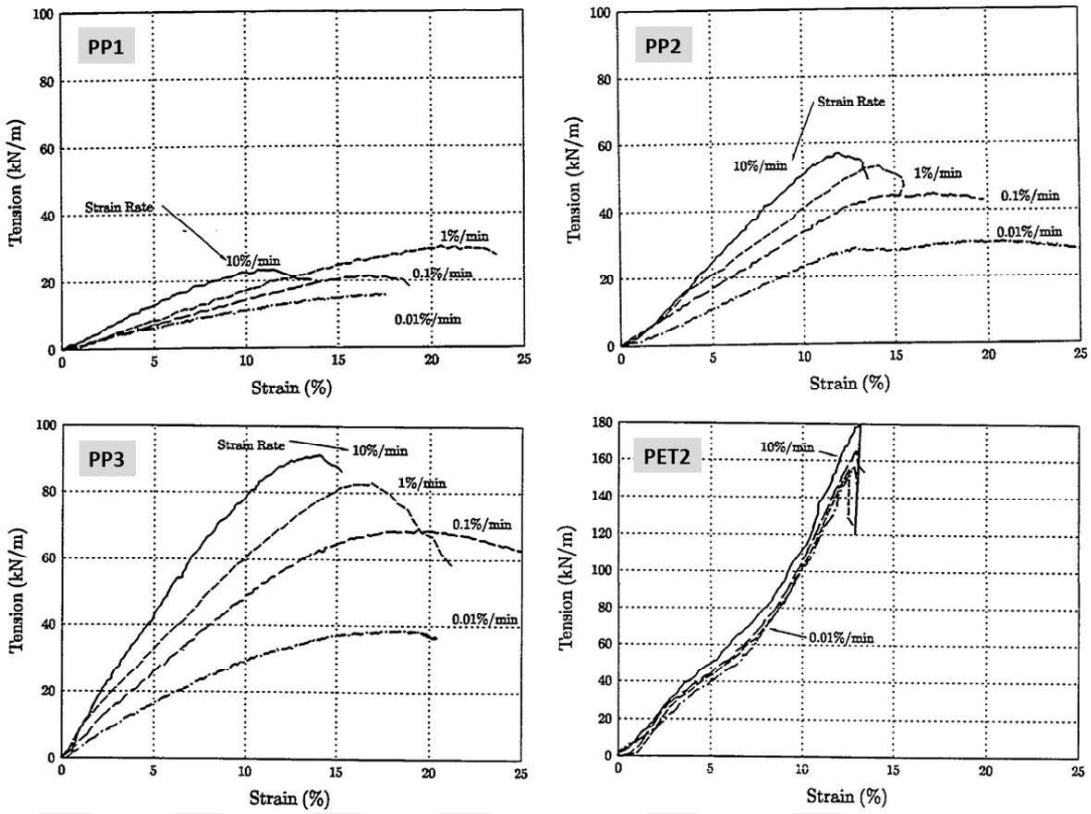


Figure 2.35. Influence of strain rate on woven geotextiles under in-isolation conditions at 100mm gauge length (Boyle *et al.*, 1996).

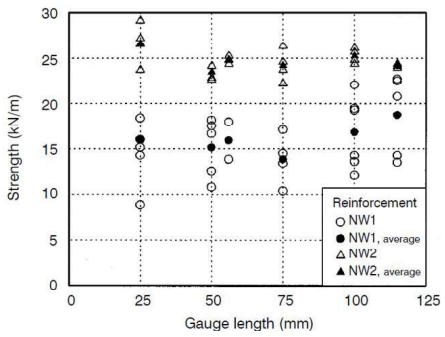


Figure 2.36. Influence of gauge length on nonwoven geotextiles under in-isolation conditions at 10% strain/min (Boyle *et al.*, 1996).

Although increase was not observed in strength of NW1 and NW2, 5% secant stiffness values were increased by decreasing gauge length. Increase in 5% stiffness

reached 130% for NW1 and 65% for NW2 when the gauge length was decreased from 115 mm to 25 mm. The linear regression of in-isolation results (Figure 2.37) showed that the stiffness value at zero-gauge length (zero gap) is still below the in-soil test results of McGown *et al.* (1982). No correlation between the "zero" gauge length in-isolation stiffness and the confined stiffness could be made (Boyle *et al.*, 1996).

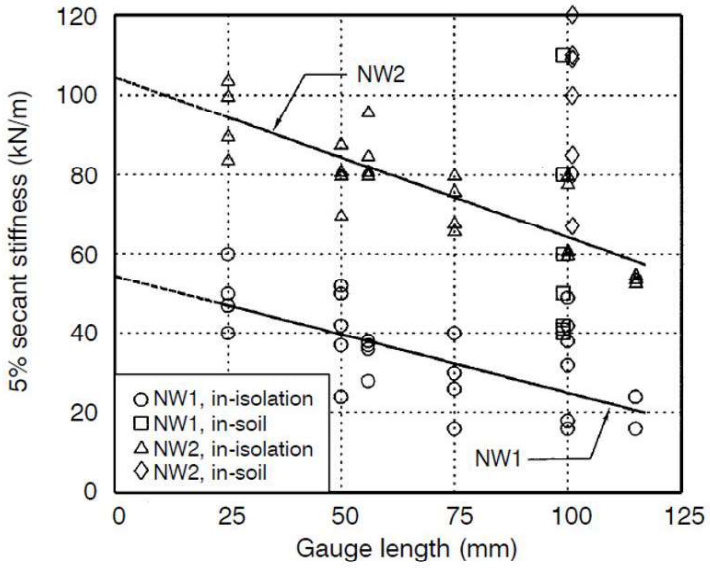


Figure 2.37. 5% secant stiffness versus gauge length from in-isolation tests for NW1 and NW2 compared with secant stiffness values obtained from 100 mm gauge length confined tests on the same type of geotextile specimens (Boyle *et al.*, 1996).

Second part of the research of Boyle and co-workers included in-soil confined testing. A unit cell device (UCD) shown in Figure 2.38 was developed to simulate the behaviour in a GRS wall. UCD is a load-controlled test apparatus. Vertical pressure is applied from bladders located at top and bottom of soil cell. Left box is free to move horizontally with the increasing vertical stress. Ottawa sand (Soil O) and a local glacial outwash sand (Soil R) was used in test program. Properties of the sands are given in Table 2.12.

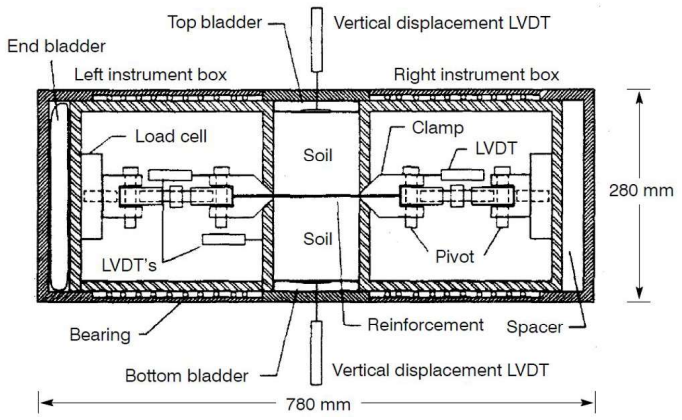


Figure 2.38. Schematic view of the unit cell device proposed by Boyle *et al.* (1996).

Table 2.12. Soil properties used by Boyle *et al.* (1996).

Soil	D_{60} (mm)	C_u	C_c	Specific Gravitiy	Minimum Void Ratio	Maximum Void Ratio	$\emptyset_{ps}$
Soil O	0.28	1.6	1	2.65	0.51	0.75	42
Soil R	0.61	4.1	1	2.73	0.46	0.76	55

Nonwoven (NW1, NW2) and woven (PP1, PP2, PP3, PET1 and PET2) geotextiles are tested in UCD. When compared with the standard ASTM D 4595 test, increase in stiffness of nonwoven geotextiles were observed as expected. However, stiffness values of woven geotextiles were found smaller in in-soil test results. This was explained by the reduction of strain rate, which was between 0.05 and 0.035% strain/min in UCD tests. This means that the woven geotextiles in UCD were tested up to 300 times slower than the standard ASTM method (10% strain/min). Since woven geotextiles are sensitive to strain rate, results can be explained by change in strain rate.

A correlation between in-isolation and in-soil tests can't be developed after research of Boyle and coworkers. Moreover, the results can't be correlated with the previous studies, too. First reason is the variable confining pressure during the test. In order to interpret test results and compare with the previous studies and with in-isolation results, load extension behaviour under a constant confining pressure needs

to be established. Second reason is the load control of the test method (instead of strain control). Variable strain rate during the test renders a correlation impossible with previous studies.

Ling *et al.* (1997) performed a comparative design of a granular soil retaining wall based on a limit equilibrium approach. Nonwoven needle-punched geotextile was considered in design which has a mass of 360 g/m^2. The wall was designed by using both in-air and in-soil test results of nonwoven geotextile. The plane-strain apparatus previously presented (see Figure 2.28) was used to obtain tensile load-strain behaviour of the geotextile. Confining pressure during tests were applied by using vacuumed rubber in lieu of soil.

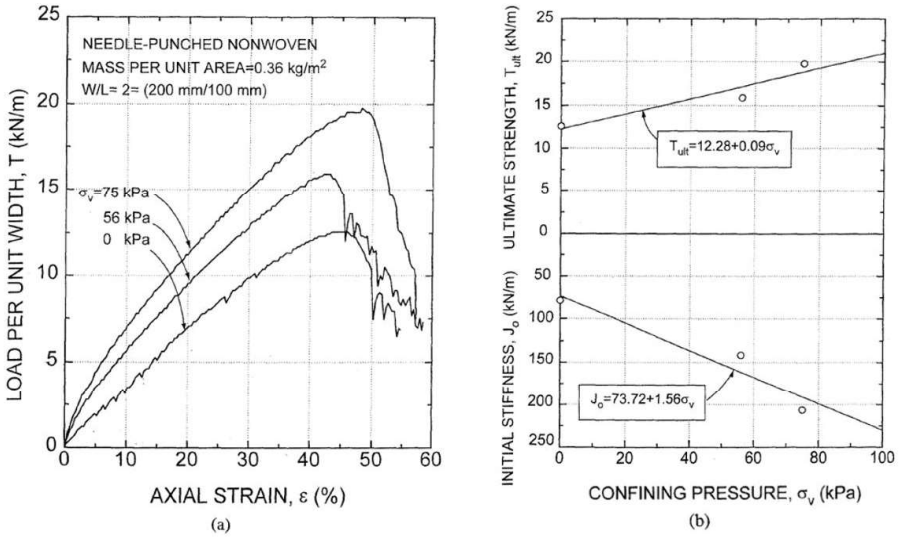


Figure 2.39. Confined test results of needle punched nonwoven geotextile; (a) Load-strain relationships, (b) Strength and initial stiffness-confining pressure relationships (Ling *et al.*, 2007).

A vertical reinforced soil wall of 3 m height was designed by taking both unconfined and confined test results of geotextile (Wall 1 and Wall 3 respectively). Walls are depicted in Figure 2.40. The reinforcement vertical spacing was increased to 0.38 m from 0.30 m when confined behaviour of the geotextile was considered. This led to a more economical design by reducing the amount of reinforcement 20%.

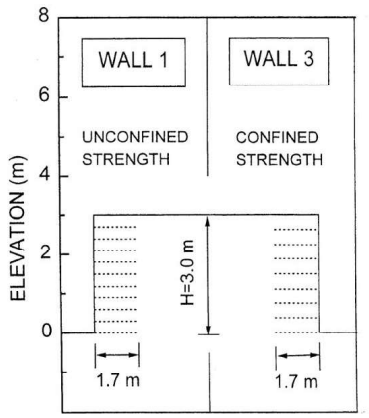


Figure 2.40. Layout for comparative wall designs (Ling *et al.*, 2007).

Elias *at al.* (1998) proposed a testing protocol for Federal Highway Administration (FHWA). An apparatus was designed and fabricated (Figure 2.41) similar to the one developed by McGown (1982). Effect of confining pressure was investigated by comparing the unconfined results with the results of 10 psi (69 kPa) and 20 psi (138 kPa).

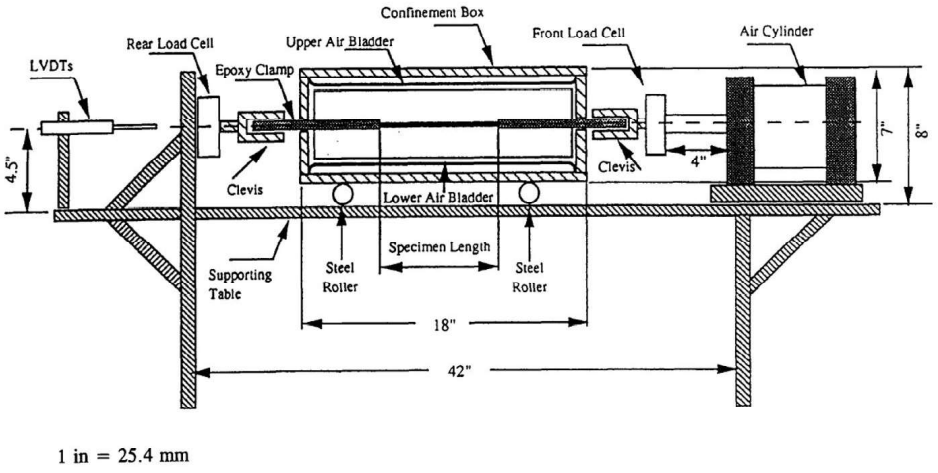


Figure 2.41. Schematic view of the confined extension test apparatus (Elias *et al.*, 1998)

Two types of soil, poorly graded sand (Beach sand; 98% sand and 2% fines) and Silty Sand (1% gravel, 77% sand and 22% fines), were used in the study. 5 types of

geotextiles were used as shown in Table 2.13. All tests were performed under a constant rate of 10% strain/min to be compared with ASTM D 4595. Aspect ratio of 1/2 was used with dimensions 100x200 mm for nonwoven and woven geotextiles. Geogrid gauge length was selected as 2 apertures.

Table 2.13. Properties of geosynthetics used in the study of Elias *et al.* (1998).

ID	Filament	Structure	Polymer	Mass (g/m^2)	Ultimate Tensile strength (kN/m)
10	Staple filament	Nonwoven	Polypropylene	272	19.7
11	Slit-film multi-filament	Woven	Polypropylene	-	70
12	Mono filament	Woven	Polypropylene	-	40.3
13	-	Extruded Geogrid	Polyethylene	-	86
14	Multi-filament	Woven Geogrid with PVC coating	Polyester	-	85.4

Test on confining soil thickness (10, 25, 51, 76 mm) showed that soil thickness should be at least 25 mm. Furthermore, increase in soil thickness after 25 mm didn't yield a significant change in behaviour (Figure 2.42). Elias and co-workers used 76 mm soil thickness in their further investigations.

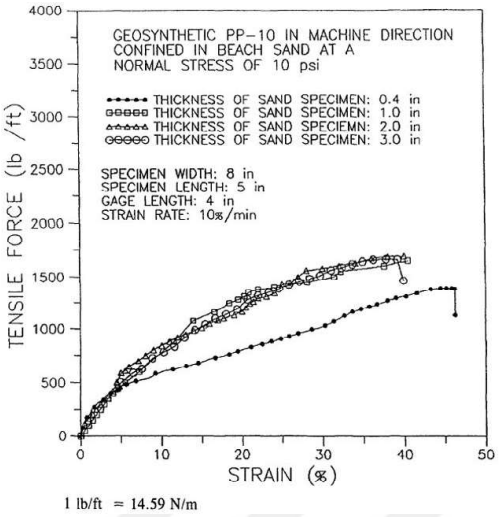


Figure 2.42. Influence of soil thickness on load-strain behaviour of nonwoven geotextile (Elias *et al.*, 1998).

For needle-punched nonwoven geotextile, soil confinement enhances both modulus and ultimate tensile strength while reducing the strain at peak and break. The mentioned effects were more pronounced in beach sand cases. The influence was observed less in rest of the reinforcements tested in scope of the study.

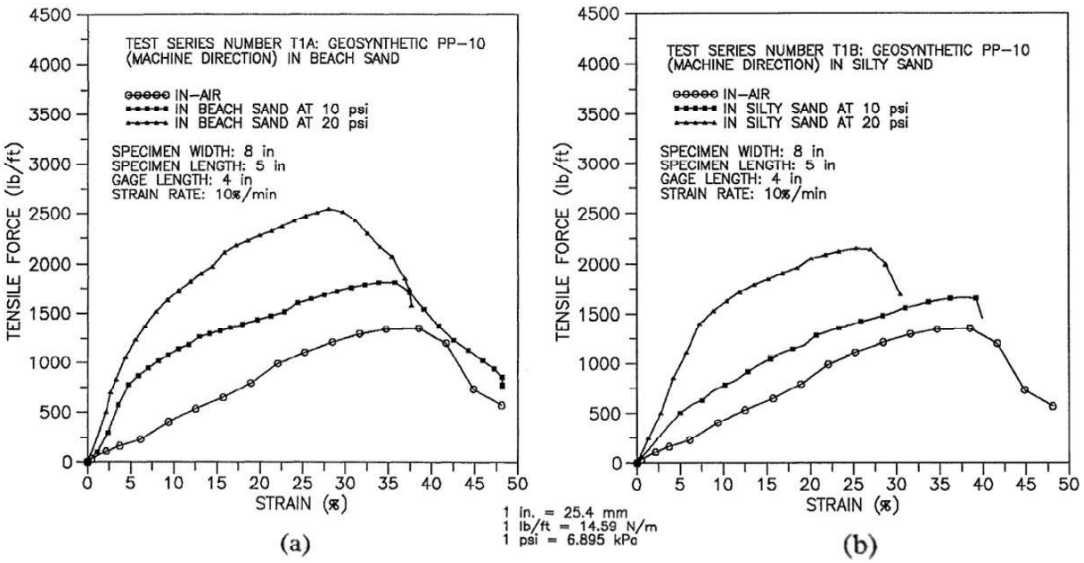


Figure 2.43. Influence of soil confining pressure and soil type on load-strain behaviour of needle-punched nonwoven geotextile (Elias *et al.*, 1998).

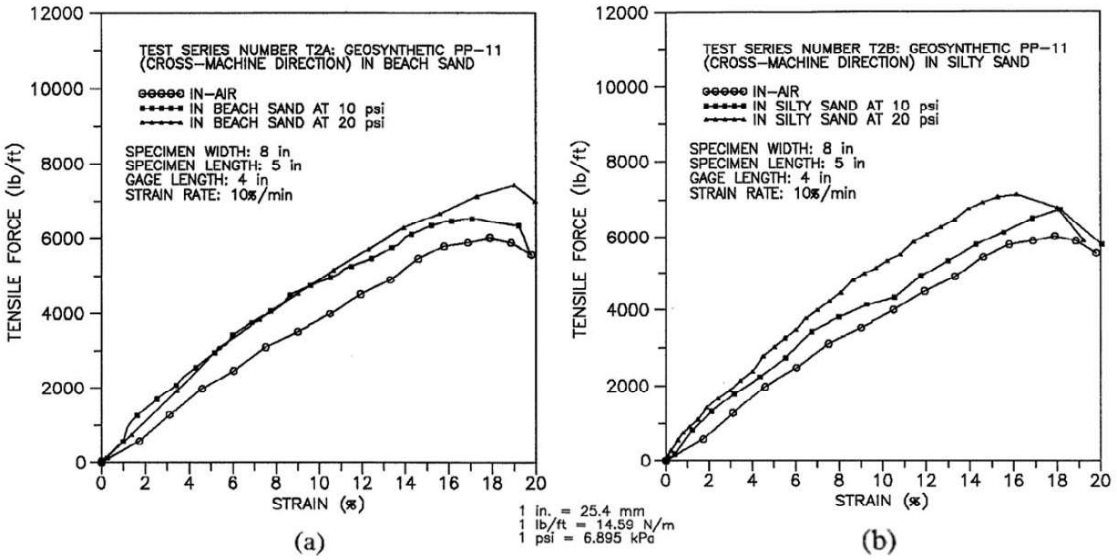


Figure 2.44. Influence of soil confining pressure and soil type on load-strain behaviour of multi-filament woven geotextile (Elias *et al.*, 1998).

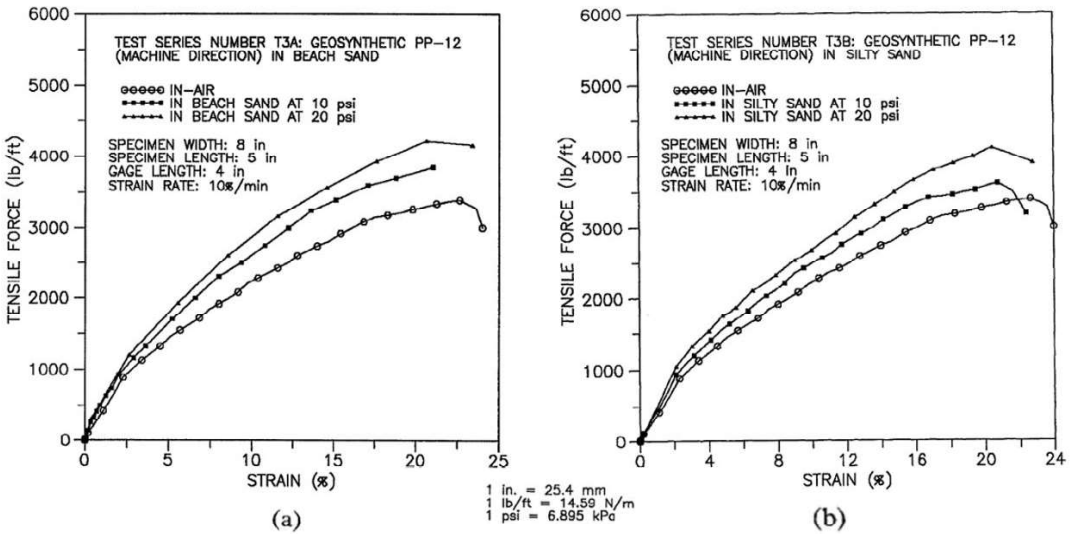


Figure 2.45. Influence of soil confining pressure and soil type on load-strain behaviour of mono-filament woven geotextile (Elias *et al.*, 1998).

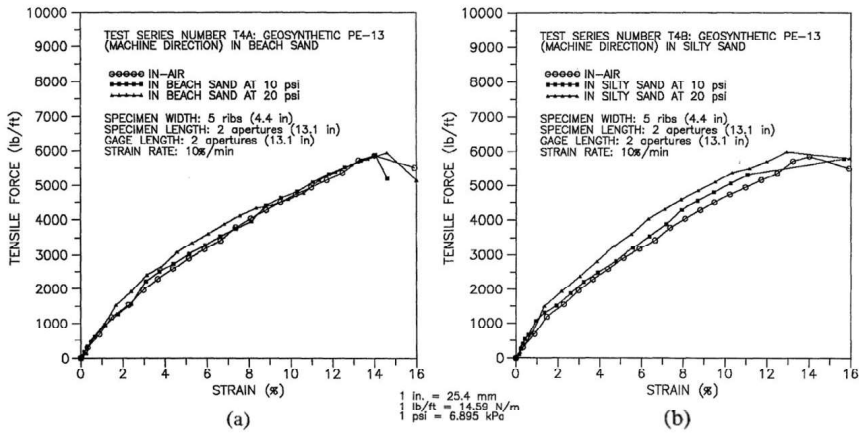


Figure 2.46. Influence of soil confining pressure and soil type on load-strain behaviour of extruded geogrid geotextile (Elias *et al.*, 1998).

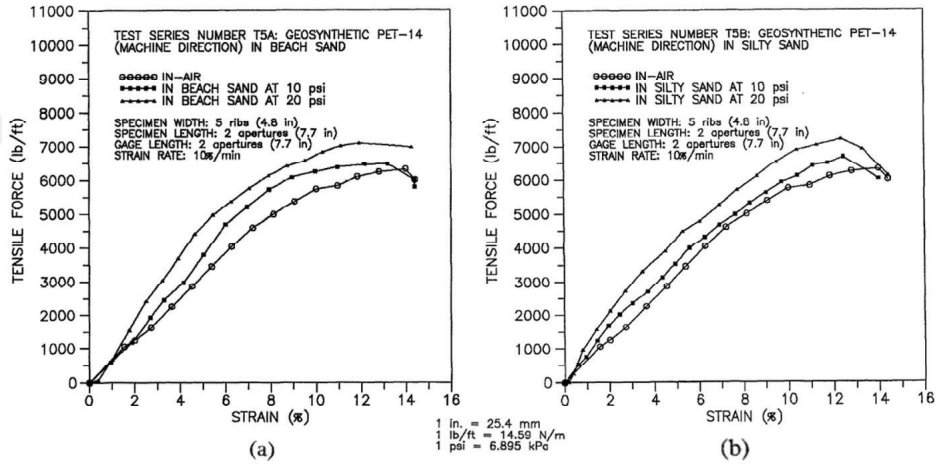


Figure 2.47. Influence of soil thickness on load-strain behaviour of woven geogrid (Elias *et al.*, 1998).

Based on the load-strain results, increase in secant stiffness at various strains are given in Figure 2.48. The most useful outcome of the study is to see the behaviour of geogrid under confined conditions. In-soil behaviour of geogrid, which is widely used as reinforcement nowadays, was not investigated in previous studies of other researchers. Elias and co-workers reported the influence of confining pressure even in the use of geogrid.

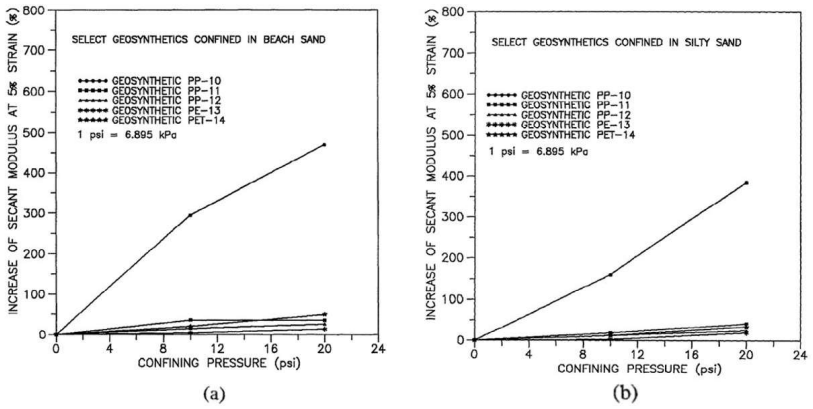


Figure 2.48. Increase of secant stiffness values (Elias *et al.*, 1998).

Wang (2001) claimed that the in-soil test apparatus proposed by McGown *et al.* (1982) can't be used for various geosynthetic reinforcement tests due to its thin clamp assembly and he developed a new apparatus which was a modified version of McGown's apparatus. In this apparatus confining pressure was applied by air bladders (Figure 2.49).

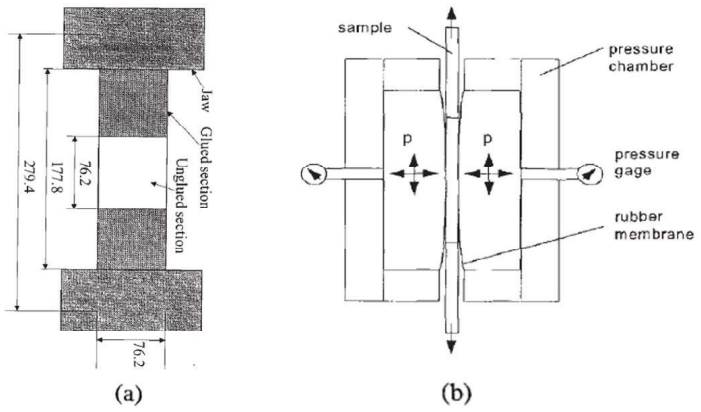


Figure 2.49. The apparatus and specimen used in tests (a) specimen detail, unit: mm (b) schematic view of apparatus (Wang, 2001).

2 nonwoven needle-punched geotextiles of polypropylene, namely Polyfelt TS 650 (Sample A) and Polyfelt TS 750 (Sample B), were tested under unconfined and confined conditions. Specimens were prepared in both machine direction (MD) and cross machine direction (XD). The unit mass of geotextiles was 360 g/m^2. Tests were conducted

at a constant displacement rate of 20 mm/min (26% strain/min), which is very high when compared to the other studies and ASTM standards. 9.0 kPa and 9.7 kPa confining pressures were applied during confined tests of Sample A and B, respectively. Even these low confining pressures (with respect to other studies), an increase in stiffness was observed (Figure 2.50 and Figure 2.51).

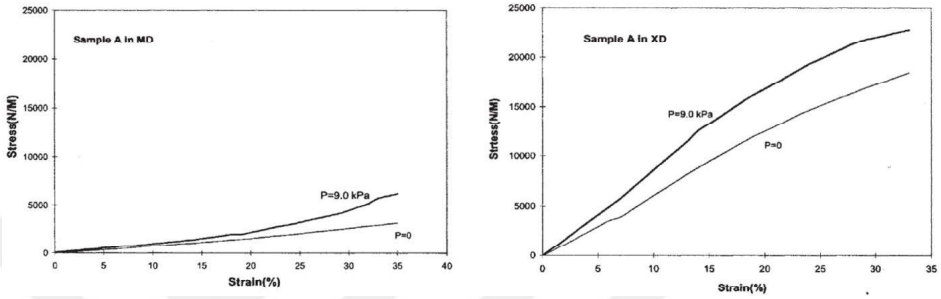


Figure 2.50. Tensile test results of Sample A, nonwoven needle-punched geotextile (Wang, 2001).

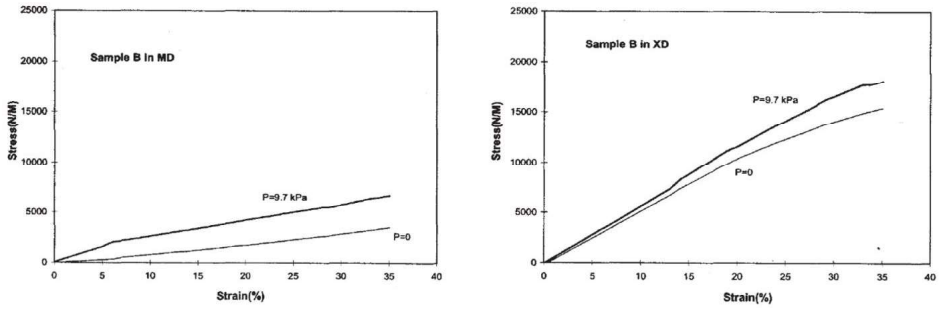


Figure 2.51. Tensile test results of Sample B, nonwoven needle-punched geotextile (Wang, 2001).

Mendes *et al.* (2007) investigated the load-extension behaviour of virgin and damaged nonwoven geotextiles. Influence of intruded soil and soil's shape on load-extension behavior of geotextiles were also determined. Authors developed a new apparatus by following the theory of Wu (1991) in which friction between soil and geotextile is negligible (Figure 2.52). Investigating influence of soil intrusion on tensile behaviour and influence of confinement on damaged geotextiles are valuable outcomes

of this study since there are no information in the literature on these topics. Results are helpful to understand how confinement affects the tensile behaviour of geotextiles.

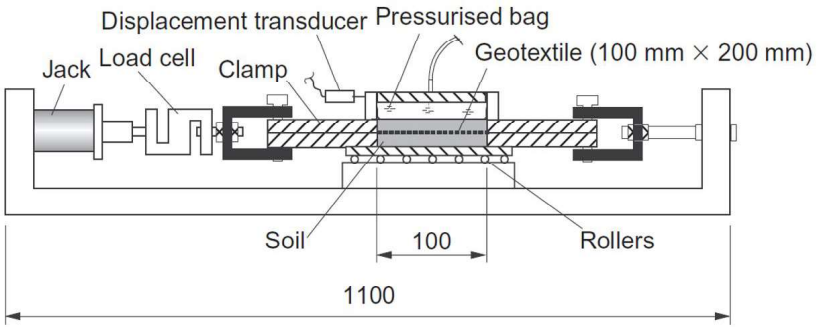


Figure 2.52. Schematic view of the apparatus developed by Mendes *et al.* (2007).

5 types of nonwoven needle punched geotextiles (designated GA to GE) were used in the tests. 5 different soil types (designated SA to SD) and glass beads (GLB) were used as confinement material. Wooden plates were also used at top and bottom of geotextile as an alternative confining material. Since there is no friction between geotextile and confining material during the test, it is investigated if a different material than soil could be used in tests. Materials used are listed in Table 2.14 and Table 2.15. All tests were performed under 2% strain/min and dimensions of the specimens are 200 mm wide and 100 mm long.

Table 2.14. Soil properties used by Mendes *et al.* (2007).

Property	SA	SB	SC	SD	GLB
Particle density (g/cm^3)	2.66	2.58	2.68	2.68	2.44
D10 (mm)	0.60	0.64	0.61	0.034	0.042
D50 (mm)	0.80	1.14	0.2	0.07	0.058
D85 (mm)	1.05	1.68	0.38	0.10	0.071
D95 (mm)	1.12	1.86	0.41	0.13	0.085
Cu	1.30	1.40	4.10	2.30	1.40

Table 2.15. Nonwoven needle-punched geotextile properties used by Mendes *et al.* (2007).

Property	GA	GB	GC	GD	GE
Mass per unit area (g/m^2)	150	200	300	400	600
Thickness (mm)	1.5	2	2.6	3.3	4.5
Tensile stiffness (kN/m)	10	21	31	42	59
Tensile strength (kN/m)	6.2	9.9	15	19.2	25.1
Maximum tensile strain (%)	67	58	63	63	65

Tests performed under 100 kPa confining stress with geotextiles GB and GD showed that load-strain curves determined under confinement of wooden plates, SA and SC were similar. Authors concluded that the confining material type doesn't have a significant influence on load-strain behaviour, except the influence of soil intrusion into geotextile (Figure 2.53).

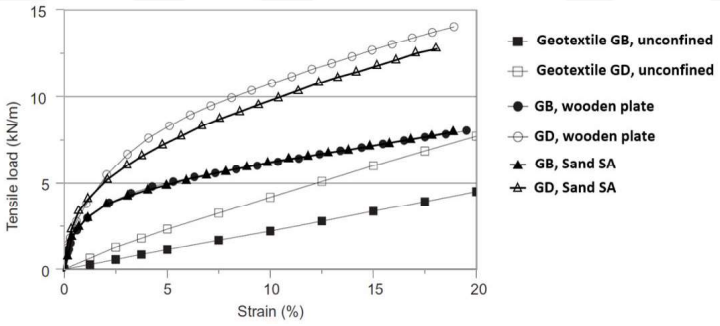


Figure 2.53. Load-strain curves for tests on geotextiles GB and GD under 100 kPa confining stress (Mendes *et al.*, 2007).

Another valuable outcome of the study is the change of secant stiffness with respect to various confinement methods. Results for GD is given in Figure 2.54. The change of secant stiffness with respect to the confining pressure follows a linear trend for geotextile GD.

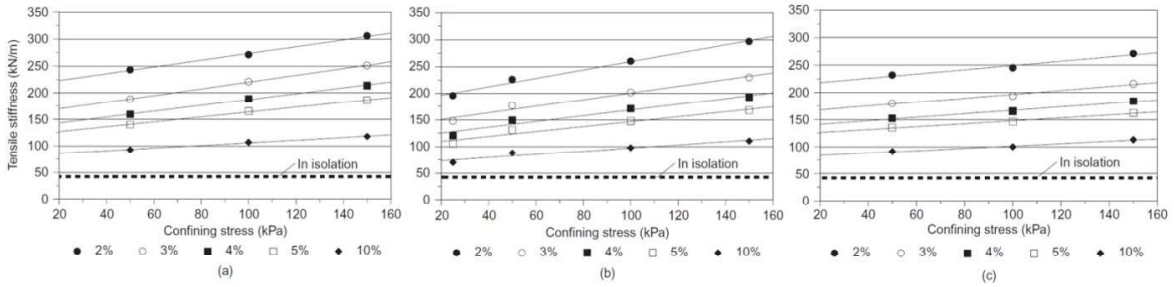


Figure 2.54. Influence of confining stress on secant tensile stiffness of geotextile GD for different strain levels: (a) wooden blocks; (b) soil SA; (c) soil SC (Mendes *et al.*, 2007).

Mendes and co-workers also investigated the influence of soil intrusion on secant stiffness of geotextile. Soil was spread over geotextile and vibrated to impregnate the geotextile. Level of impregnation, λ, was quantified in terms of mass of intruded soil particles per unit area divided by the mass of fibres per unit area. By soil impregnation into the geotextile matrix, pores of the geotextile decrease. As a result of filled pores, fibres can't have enough space to stretch during geotextile extension and stiffness of the geotextile increases. Results presented in Figure 2.55 determines that the lighter geotextile (GB) was not influenced by impregnation when compared to a denser geotextile (GD). According to authors, even after impregnation there is still enough space for fibers to stretch.

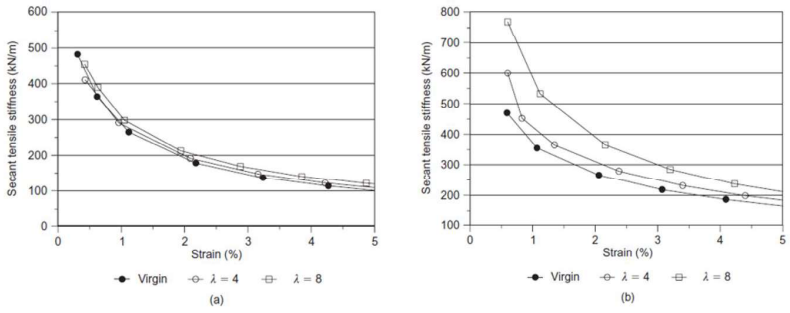


Figure 2.55. Influence of geotextile impregnation on secant tensile stiffness under 100 kPa confining stress: (a) geotextile GB and (b) geotextile GD impregnated with glass beads (GLB) (Mendes *et al.*, 2007).

Additionally, particle shape was also investigated in impregnation test program. Fine sand SD (angular) and rounded glass beads (GLB), which have similar particle gradation, were compared in tests. It can be concluded that in-soil stiffness of the geotextile increases with angularity of the soil.

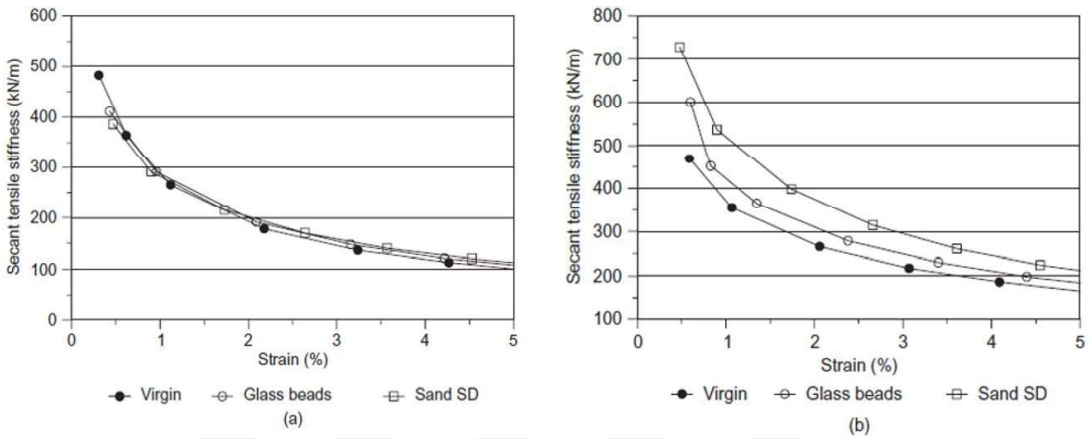


Figure 2.56. Influence of particle shape of impregnating material; confining stress of 100 kPa and λ=4: (a) geotextile GB; (b) geotextile GD (Mendes *et al.*, 2007).

Won and Kim (2007) investigated the deformation behaviour of reinforcements within GRS walls. In Won and Kim's (2007) study, laboratory (in-soil, confined) and field tests (on 5m walls) were conducted, and measured strains were compared. In the lab part of the study, 100x200 mm nonwoven needle-punched (PET) geotextile was tested under 70 kPa of confining pressure. Strain rate and load-strain results were not reported.

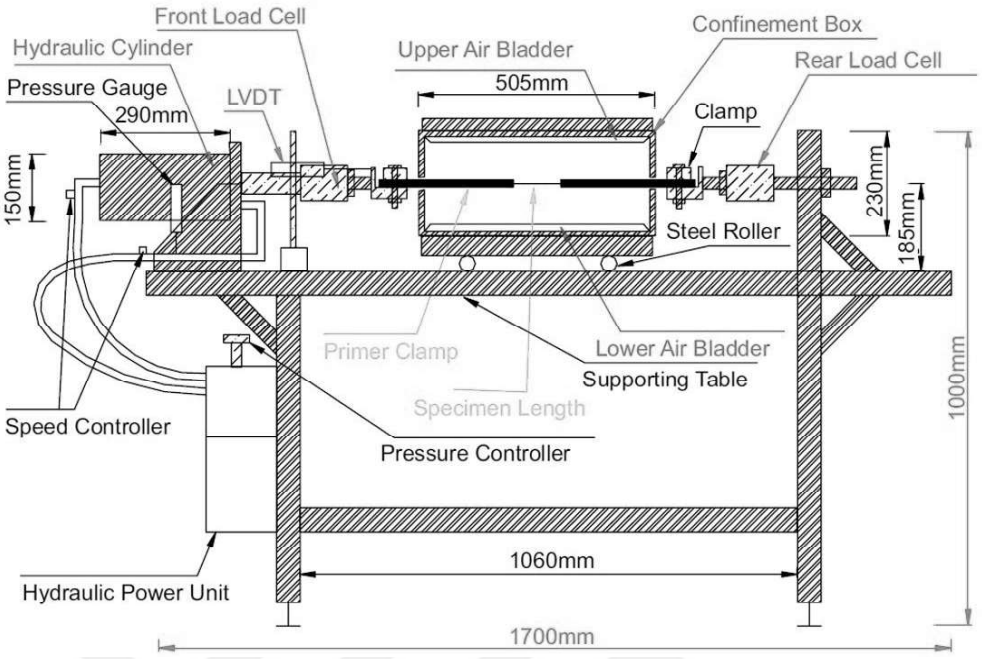


Figure 2.57. Schematic diagram of apparatus used by Woo and Kim (2007).

The local strain was measured by strain gauge while total strain was measured by LVDT. Results of local and total strain measurements were compared. It was reported that, up to 15% total strain, the confined local strain was half of the local strain measured under in-isolation conditions. The apparatus used is shown in Figure 2.57.

Balakrishnan and Viswanadham (2017) developed a displacement controlled in-soil test apparatus to investigate the influence of strain rate, confining pressure and soil type on load-strain behaviour of geogrid (Figure 2.58). A scaled down geogrid was used in tests. Both longitudinal and transverse ribs were 0.01mm wide and aperture dimensions are 3.5x3.5 mm which leads to a percentage open area of 97.43%. Specimen dimension was 100 mm in gauge length and 200 mm wide. In-isolation tests were conducted to investigate the effect of strain rate on load-strain behaviour of geogrid. Results of tests which were performed at constant displacement rates of 1.25 mm/min and 0.5 mm/min were compared. Secant stiffness of the geogrid was increased with increasing strain rate (Figure 2.59).

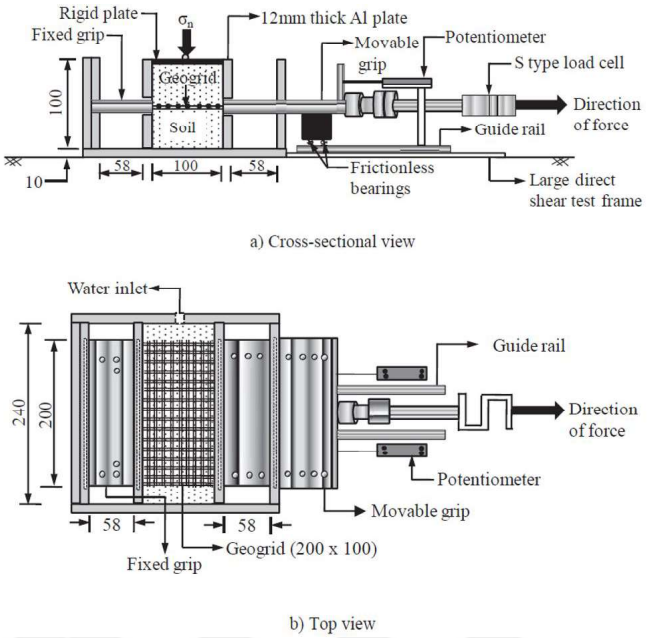


Figure 2.58. Schematic diagram of apparatus used by Balakrishnan and Viswanadham (2017).

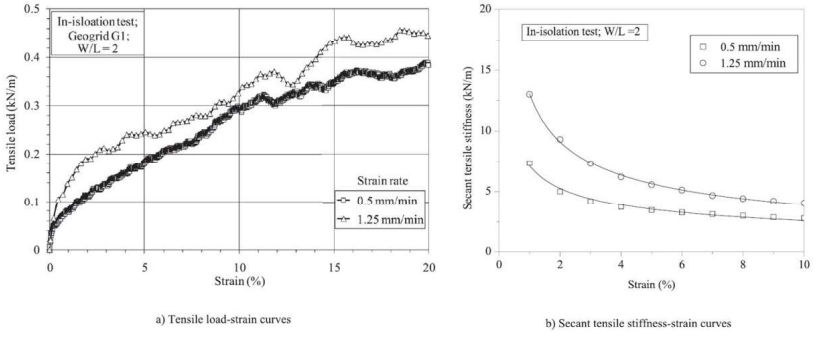


Figure 2.59. Effect of strain rate on tensile load-strain behaviour of geogrid (Balakrishnan and Viswanadham, 2017).

Two soil types were used in in-soil tests. Soil A (fine sand) is a poorly graded sand according to USCS. Particles of Soil A were smaller than 0.425 mm and larger than 0.075 mm (no fines) and D_{50}=0.23 mm. Soil B (marginal soil) which contained 42% of fines (smaller than 0.075 mm) was classified as silty sand according to USCS. Since the ratio of opening size of geogrid (97.43%) to D_{50} of soil was greater than 5,

both Soil A and Soil B were considered to have a good contact with geogrid (Springman *et al.*, 1992). All in-soil tests were carried out at a constant displacement rate of 1.25 mm/min. Confining pressures of 25, 50, 100 and 150 kPa were applied to geogrid in Soil A during the test to determine the effect of confining pressure on tension load-strain behaviour. Increase in secant stiffness was observed with increasing confining pressure (Figure 2.60). At 5% strain, secant stiffness increase ranged from 1.34 to 2.42 times with respect to in-isolation test.

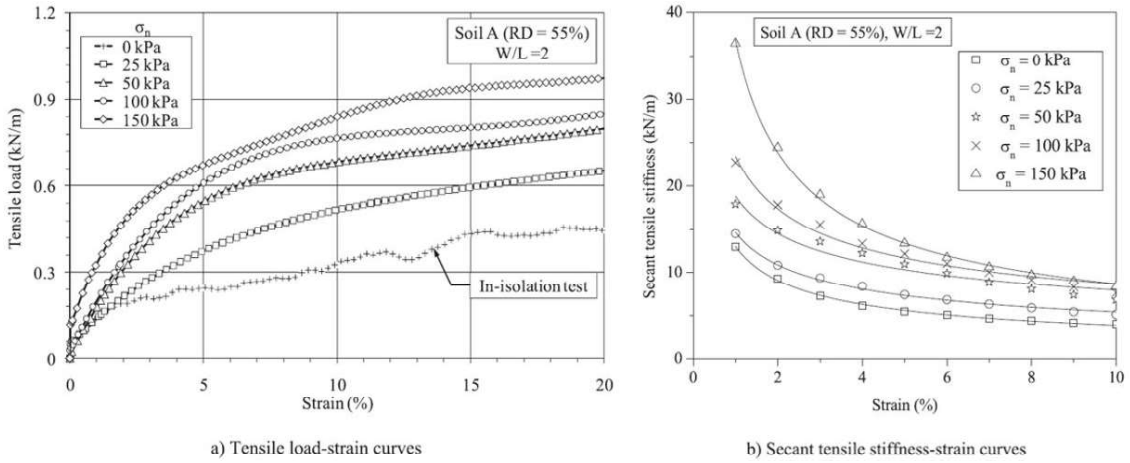


Figure 2.60. Effect of confining pressure on tensile load-strain behaviour of geogrid (Balakrishnan and Viswanadham, 2017).

Comparison of in-soil tests with various soil types also showed the influence of soil type on load-strain behaviour of geogrid. Geogrid tested in Soil A (fine sand) lead to higher stiffness values when compared to Soil B (marginal soil with 42% fines). Results of tests under 100 kPa were depicted in Figure 2.61.

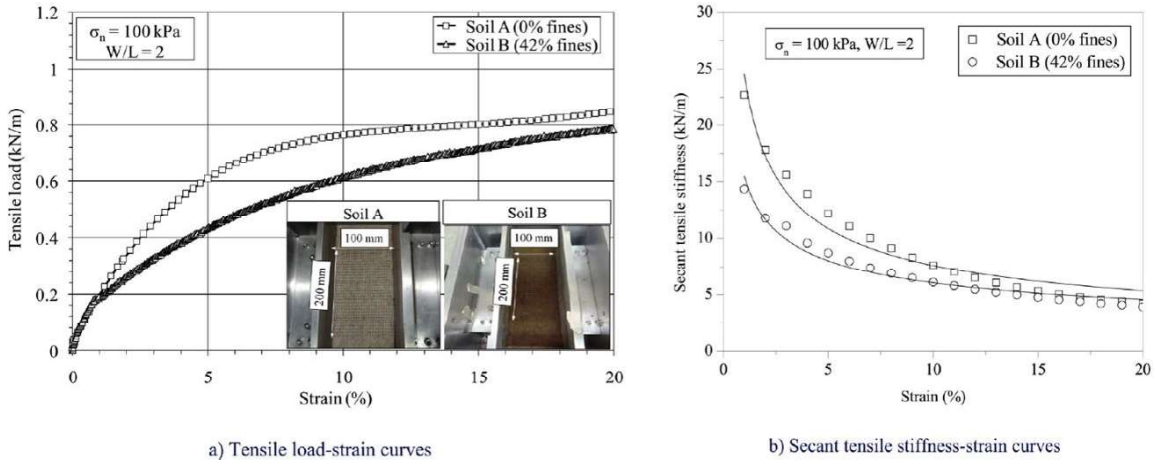


Figure 2.61. Effect of soil type on tensile load-strain behaviour of geogrid (Balakrishnan and Viswanadham, 2017).

In the study of Balakrishnan and Viswanadham (2017), Soil B (marginal soil, 42% fines) was improved by applying a thin silica sand layer (grade-2 silica sand) above and below the reinforcement. In other words, geogrid tested in Soil B was sandwiched in silica sand. The thickness of sand layer was selected 5 mm above and below the geogrid (10 mm in total). The positive influence of proposed sand sandwiched layer on marginal soil was determined by performing a series of pull-out tests (Balakrishnan, 2016). When 10 mm sand sandwiched layer was applied to Soil B and confining pressure was 100 kPa, secant stiffness of the geogrid was improved 1.22, 1.77 and 1.84 times at 2%, 5% and 10% strain, respectively (Figure 2.62).

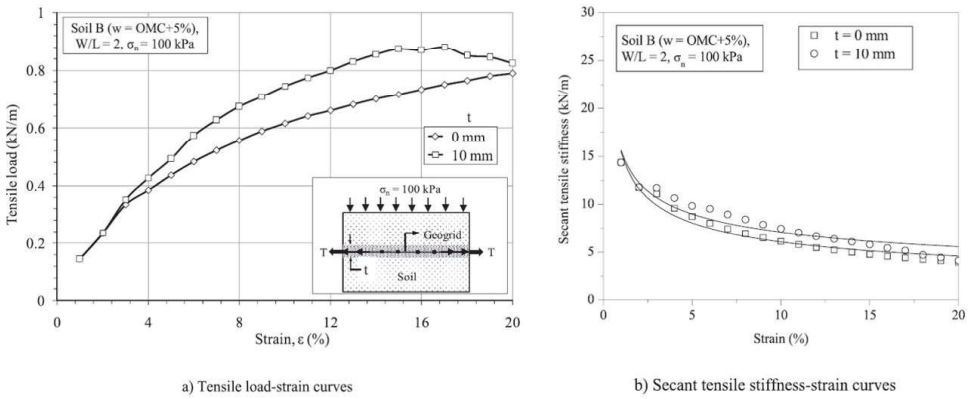


Figure 2.62. Effect of sand-sandwiched layer on tensile load-strain behaviour of geogrid (Balakrishnan and Viswanadham, 2017).

Although Morsy *et al.* (2019) study is not directly related to the effect of confinement on the tensile load-strain behaviour of geosynthetics, it sheds light to the soil-reinforcement interaction, especially if there is not only one layer of reinforcement, but there are other geosynthetic reinforcement elements in the near vicinity. Morsy *et al.* (2019) discussed the soil-reinforcement interaction based on the experimental results. The experiments are performed in a modified pull-out test box. Regular pull-out test method was modified by the addition of passive reinforcements above and below the active reinforcement (Figure 2.63). The active reinforcement was subjected to tensile load to be pulled-out whereas passive reinforcements were only fixed to the rear end of the box.

The influence of the vertical spacing between passive and active reinforcements on the behaviour of a reinforced soil mass was investigated. The vertical spacing range from 0.05 to 0.40 m was used in experiments under 21 and 50 kPa surcharge pressures. Reinforced soil mass in the study consists of AASHTO No. 8 gravel and polyester woven geotextile. Morsy *et al.* (2019) concluded that the critical vertical spacing value is 0.15 m in terms of the behaviour. In detail, based on the soil and reinforcement conditions provided in tests, no interaction between reinforcements were observed when vertical spacing exceeds 0.15m. This conclusion is based on the ratio of passive reinforcement displacement to active reinforcement displacement (Figure 2.64). However, it has been

observed that the influence of the reinforcement interaction is negligible in terms of frontal tensile load monitored in the active reinforcement (Figure 2.65).

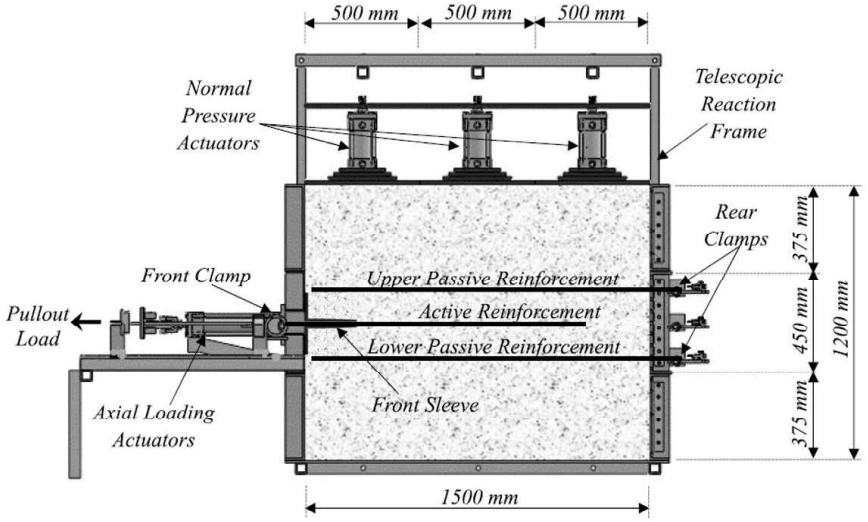


Figure 2.63. Schematic sectional side view of modified pull-out test device (Morsy *et al.*, 2019).

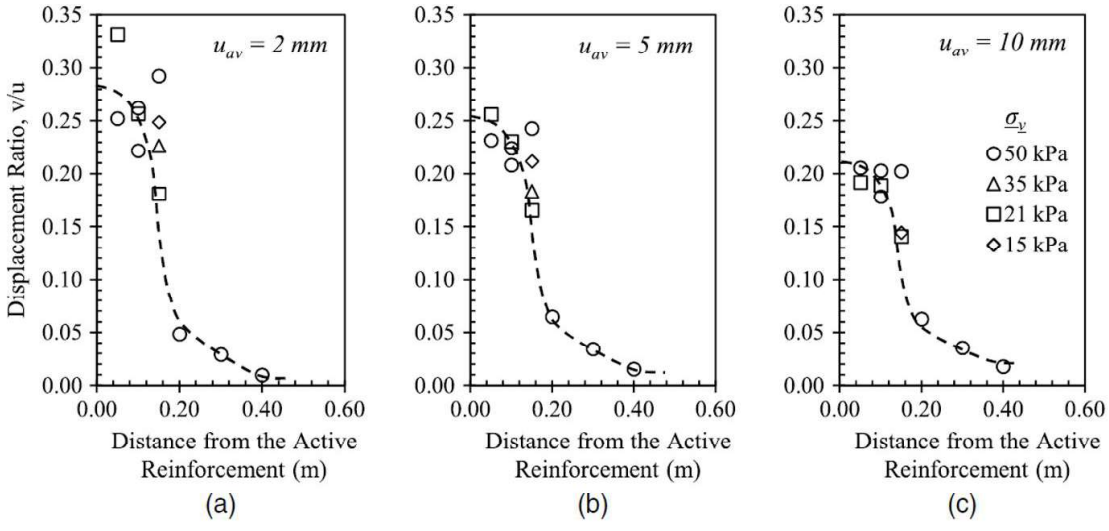


Figure 2.64. Average displacement ratio of upper passive reinforcement layers at various average displacements of active reinforcement layers: (a) u_{av} = 2 mm; (b) u_{av} = 5 mm; and (c) u_{av} = 10 mm (Morsy *et al.*, 2019).

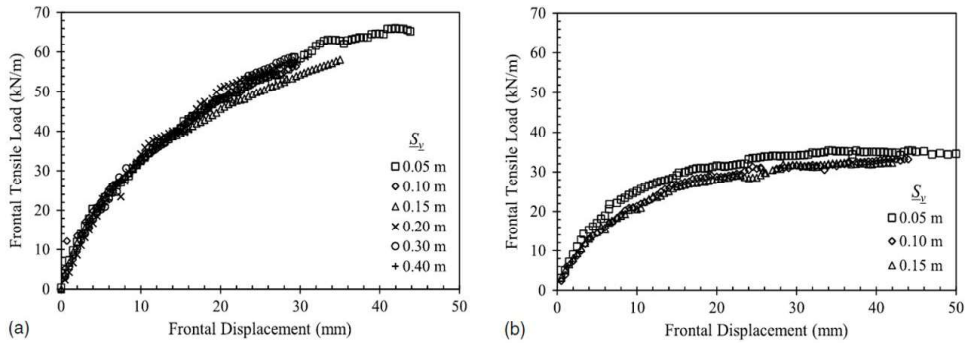


Figure 2.65. Frontal tensile load-displacement curves: (a) at normal stress, $\sigma_v = 50$ kPa; and (b) at normal stress, $\sigma_v = 21$ kPa. (Morsy *et al.*, 2019).

2.3. Evaluation of Previous Studies

Research studies on in-soil load-extension behaviour of geosynthetics starting from early 1980s were summarized in this section. To understand in-soil tests, a general understanding on wide width test method is also required. Therefore, a few in-air research studies in which influence of aspect ratio, gauge length, sample dimension, strain rate were investigated are also included in this section. A summary of the previous studies on confined tests are presented in Table 2.16. Investigations in which confined tests weren't performed but included in this section are not given in this table.

Test methods used in previous studies to investigate tensile load-extension behaviour of geosynthetics can be divided into 2 main groups, namely Type A and Type B. Type A and Type B deviates from each other in terms of the soil-geosynthetic interaction during the test. In Type A method, strain incompatibility (relative movement between soil and geosynthetic) occurs between soil and geosynthetic which leads a frictional force. Earlier studies constitute Type A (McGownand Andrawes, 1982; El-Fermaoui and Nowatzki, 1982; Leshchinsky and Field, 1987; Kokkalis and Papacharisis, 1989; Wilson-Fahmy *et al.*, 1993).

In Type B, strain compatibility is considered by modifying the apparatus used in Type A tests (Wu, 1991; Ling *et al.*, 1992; Boyle *et al.*, 1996; Mendes *et al.*, 2007;

Balakrishnan and Viswanadham, 2017). In the apparatus used in Type B tests, the box wall is a clamp as well. Therefore, by displacing the clamp (thus reinforcement), soil displaces as well. As a result, strain compatibility is maintained by keeping the relative movement between soil and geosynthetic at minimum. Therefore, the friction between soil and geosynthetic was not included to tensile load-strain results of the tests and more conservative results were obtained. Type B method measures the properties of reinforcements independent from the confining material, thus researchers used various materials to confine the reinforcements (soil, wooden plate, membrane, vacuumed rubber).

However, Type B approach was described more applicable for extensible reinforcement like nonwoven needle-punched geotextiles (Wu, 1991). On the other hand, strain compatibility during operational life of the reinforcement is a complex issue and still needs to be explained.

In general, confined test results showed that stiffness of the geosynthetics increase in most cases. The increase of stiffness depends on the structure of the material. Geosynthetics with looser structure, such as nonwoven needle-punched geotextile, have a great tendency to improve under confined conditions. Stiffness of nonwoven geotextile depends on the friction between the fibers and the elongation capability of individual fibers. Confinement leads higher friction between fibers, and it restricts the movement (aligning with tension) of fibers. Increase of stiffness in nonwoven geotextiles are explained in this way.

Intrusion of soil into the pores of nonwoven geotextile is another parameter which increases the stiffness of nonwoven geotextile during the test. Intrusion of soil is more pronounced when applied to a denser nonwoven geotextile (when compared to a looser nonwoven geotextile). Since looser geotextile has more pores, pores can't be filled effectively to change the behaviour. In looser nonwoven geotextiles, fibers still find place to elongate after intrusion (Mendes *et al.*, 2007).

Intrusion tests on nonwoven geotextiles (Mendes *et al.*, 2007) and regular confined tests on nonwoven geotextiles (Elias *et al.*, 1998) showed that angularity of soil leads to more stiffness increase in nonwoven geotextiles. On the other hand, the influence of particle angularity of soil is less in woven geotextile and geogrid according to the investigation of Elias and co-workers (1998).

There is not sufficient research on woven geotextile and geogrid. Especially, confinement effect on geogrids -which are widely used as reinforcement in modern day- has to be studied. Available studies demonstrated relatively slighter increase for these types of reinforcements. In stiff reinforcements like extruded geogrid, confinement can't influence the structure of the material but increase in stiffness can be mentioned (Elias *et al.*, 1998). This can be explained by another effect of confined test. Under confined conditions, gauge length decreases and causes an increase in strain rate accordingly. Therefore, the increase in strain rate can be considered one of the reasons of increase in stiffness for all geosynthetics.

Table 2.16. Summary of previous studies on confined extension test.

Investigator	Geosynthetic Type	Confining Material	Geosynthetic Dimensions L x W (mm)	Strain Rate (%)	Confinement (kPa)
McGown and Andrawes (1982)	-Nonwoven -Woven Gt.	-Leighton Buzzard Sand	100x200	2	10-55-100
McGown et al. (1982)	-Nonwoven -Woven Gt. -Composite	-L. B. Sand	100x200	2	10-55-100
El-Fermaoui and Nowatzki (1982)	-Nonwoven -Woven Gt.	-Ottawa Sand -Uniform Gravel	50.8x50.8	2.5	48-96-192-383
Andrawes et al. (1984)	-Nonwoven	-L. B. Sand	100x200	2	10-55-100
Leshchinsky and Field (1987)	-Nonwoven	-Sand	100 x n/a	n/a	52-103-207
Kokkalis and Papacharisis (1989)	-Nonwoven	-L. B Sand -Clayey at bottom and sand-gravel at top	150x300	2	10-55-100 152-304-457
Wu (1991)	-Nonwoven	-Ottawa Sand	50.8x152.4	2	69
Ling et al. (1992)	-Nonwoven	-Toyoura Sand -Membrane	100x200 37.5x300	2	49-74-79
Ballegeer and Wu (1993)	-Nonwoven -Woven Gt.	-Rubber (with suction)	25x150	2	80
Wilson-Fahmy et al. (1993)	-Nonwoven -Woven Gt. -Geomembrane -GCL -Geonet	-Sand	102x202	10.2	35-69-138
Boyle et al. (1996)	-Nonwoven -Woven Gt.	-Ottawa Sand -Glacial Sand	100x200	Load contr.	Not constant
Ling et al. (1997)	-Nonwoven	-Rubber (with suction)	100x200	n/a	56-75
Elias et al. (1998)	-Nonwoven -Woven Gt. -Geogrid	-Beach Sand -Silty Sand	100x200	10	69-138
Wang (2001)	-Nonwoven	-Air Bladder	76.2x76.2	26	9-9.7
Mendes et al. (2007)	-Nonwoven (virgin/damaged)	-Sand -Glass Beads -Wooden plate	100x200	2	25-50-100-150
Won and Kim (2007)	-Nonwoven	n/a	100x200	n/a	70
Balakrishnan and Viswanadham (2017)	-Geogrid (Scaled down)	-Fine Sand -Silty Sand	100x200	1.25	25-50-100-150

Especially in Type A tests, behaviour is dependent to the soil type. Pressure distribution changes with the soil particle size (McGown and Andrawes, 1982) and particle shape (Mendes *et al.*, 2007; Elias *et al.*, 1998). Therefore, a direct comparison between studies is not applicable since they use different confining materials and apparatuses.

Previous investigations encourage for further investigation on this topic. In this study, the following points were considered while planning the research work.

- Majority of the researchers interpret Type B as unrealistic since relative movement may occur under operational conditions because of the stiffness difference between soil and geosynthetic. Proposed study should follow Type A method. Furthermore, considering the friction between soil and reinforcement will lead a better simulation of field conditions.
- As soil, fine confining material (fine sand, silty sand) was used almost in all previous studies. Further investigations with various soil types, especially with the ones used in the field (coarse sand, gravel) should be investigated.
- For Type A method, in general, thickness of confining material is very small (around 10 mm) in previous studies. This doesn't allow the use of coarser soil in tests. A new apparatus with thicker confinement material space had to be designed to investigate the behaviour in coarser soils.
- Aspect ratio and dimensions differ in previous studies. For a better comparison with the ASTM standards and with majority of the studies, 100 mm long and 200 mm wide specimen should be used.
- Nonwoven geotextiles were widely used as reinforcement in 1980s. Therefore, most of the studies in the literature were performed on nonwoven geotextiles. However, woven geotextiles and especially geogrids are widely used nowadays. For this reason, further investigations on woven geotextile and on geogrid should be carried out.
- In addition to confinement effect, interlocking effect on geogrids should be investigated for various soil gradations.
- The further investigations mentioned above should be performed at a constant strain rate (in this case 2% strain/min) to make it comparable.
- Various confinement scenarios should be investigated (e.g. additional reinforcements located at top and below the test specimen).

3. METHODOLOGY

In scope of this study, an in-soil test apparatus is developed and used to investigate the in-soil behaviour of various geosynthetic reinforcements. First, in-air wide width tests are performed as a control group to be compared with the results of in-soil wide width tensile tests. In soil tests on 3 different geosynthetics are performed in two different soil types and under 3 different confinement pressures. Moreover, effect of adjacent reinforcements to the test specimen is also investigated. The mentioned tests are explained in detail in the following sections.

This chapter covers the properties of the newly developed test apparatus, procedure of the tests, test program, material properties and their preparation.

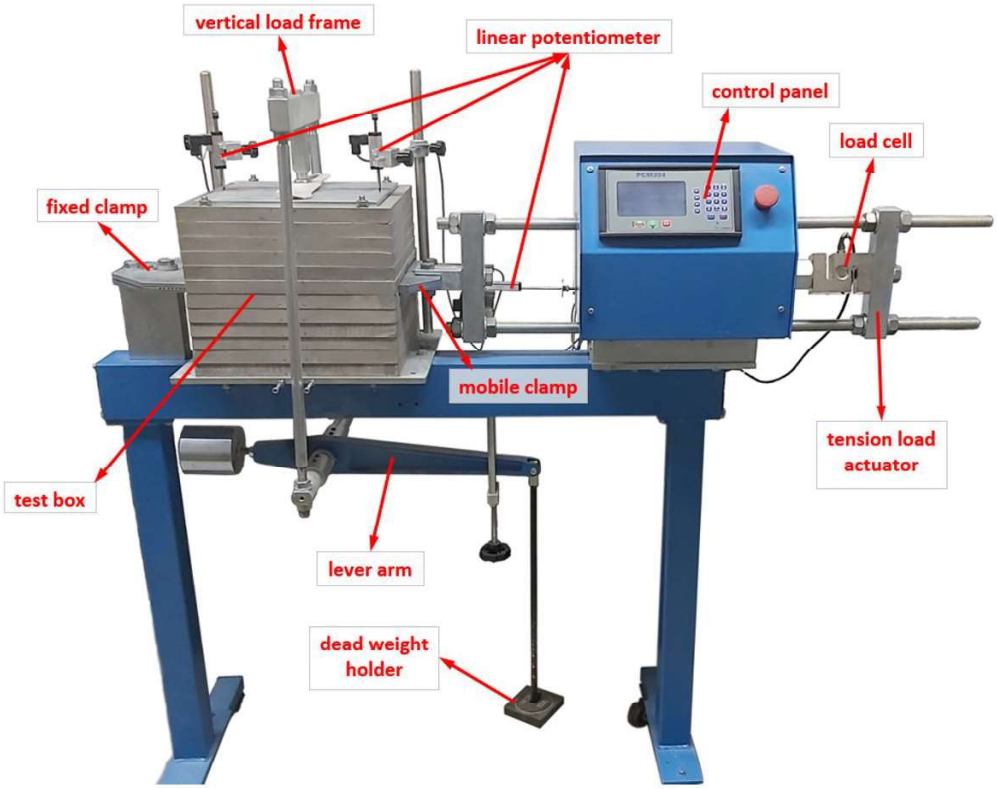


Figure 3.1. In-soil wide width test apparatus.

3.1. In-Soil Wide Width Test Apparatus

The apparatus (Figure 3.1) is capable of testing geosynthetics either in-air or in-soil. The purpose of the apparatus is to study the influence of soil conditions and vertical pressures on the tensile behaviour of the geosynthetics. It is also capable of investigating the effect of vertical spacing (multi-layer test) on the test specimen. The box is designed in segmental form to allow multi-layer testing. The detailed properties of the apparatus are given in this section.

3.1.1. Test Box

Finite element analyses have been performed to determine the dimensions of test box. The problem can be considered plane-strain, so plane-strain model of Plaxis 2D has been used in analyses. Since the FEM model was built prior to planning of the laboratory tests, material properties used in FEM model do not comply with the ones used in lab tests. However, results are reliable because stress distribution and deformation behaviour with respect to the box geometry has been investigated. The model is sufficient to reflect the behaviour in lab tests.

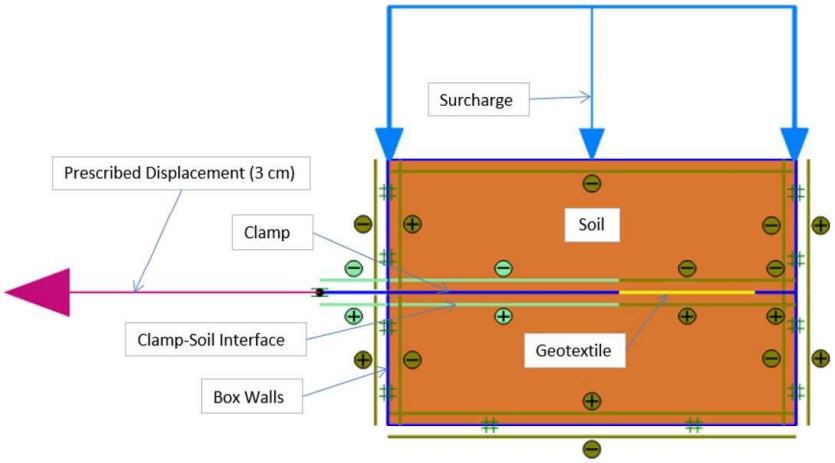


Figure 3.2. Numerical model of in-soil wide width test apparatus.

Table 3.1. Materials used in FEM model.

Material	Material Model	Parameters
Dense Sand	Mohr Coulomb (Drained)	γ=20 kN/m^3, E=50 MPa, Φ'=37^o, c=1 kPa, ν=0.3
Geotextile	Linear Elastic	T=20 kN/m at 10% $\rightarrow$ EA=200 kN/m
Steel plate (t=2cm)	Linear Elastic	EA=4000 MN/m, EI=133.33 kNm^2/m, w=1.172 kN/m/m for γ=78.6 kN/m3, ν=0.2
Interface Element	-	R=0.7 (between geotextile and sand) R=0.1 (between steel clamp and sand)

Based on the results mentioned in the literature survey, it was determined that the tested sample shall be 10 cm long. Considering this, analyses have been conducted for various box lengths (20, 30, 40, 50, 100cm) to determine the optimum box length (in gauge direction). In order to see whether the confining pressure has an effect on this optimum dimension, tests under three confinement pressures (0, 50, 100 kPa) were conducted. Cross sections of the analyzed models and other related calculation results are given in following figures Figure 3.3, Figure 3.4 and Figure 3.5.

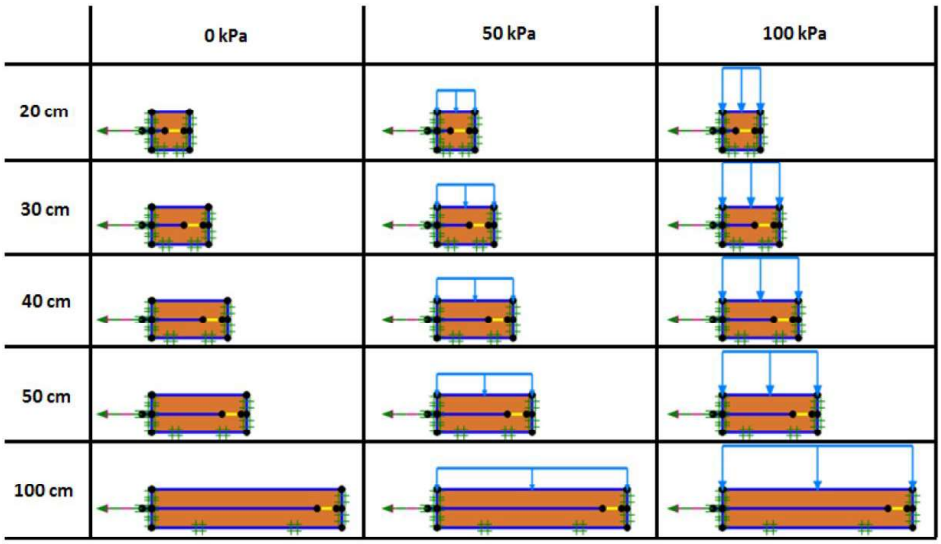


Figure 3.3. Cross sections used to determine the box length (in gauge direction).



Figure 3.4. Normal stress acting on box wall in the end of test.

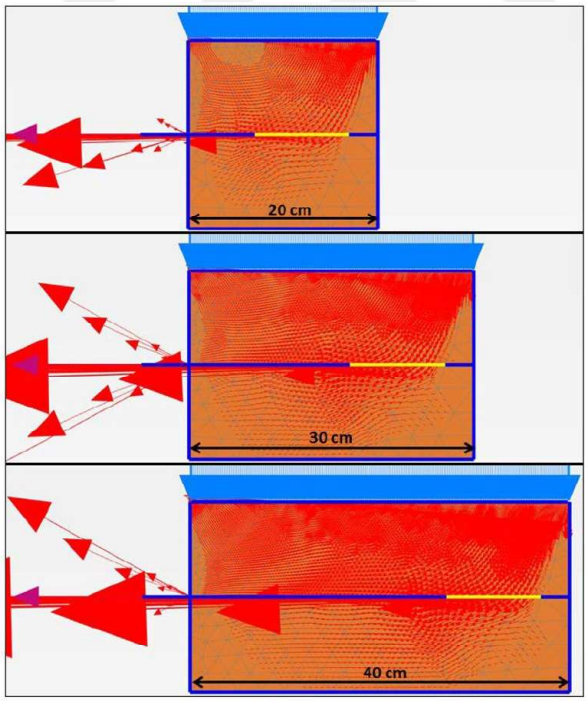


Figure 3.5. Total displacements (under 100 kPa surcharge).

When Figure 3.4 is considered, the change in stress distribution on the wall is clearly visible in case of 100 kPa surcharge. It is observed that the behaviour changes when the length of the box exceeds 20 cm. According to the normal stress distribu-

tion, minimum box length should be 30 cm. The deformation behaviour observed in Figure 3.5 also supports this finding. When box length is shorter than 30 cm, soil displacements form a swirl pattern and pushing the loading plate upwards on the front end whereas displacement pattern becomes horizontal and does not change when the box length is equal or greater than 30 cm. On the other hand, to keep friction between soil and clamp at a minimum (longer clamp means more friction which misleads results) and for the ease of setup (performing test in small box becomes easier), box with length of 30 cm is considered optimum.

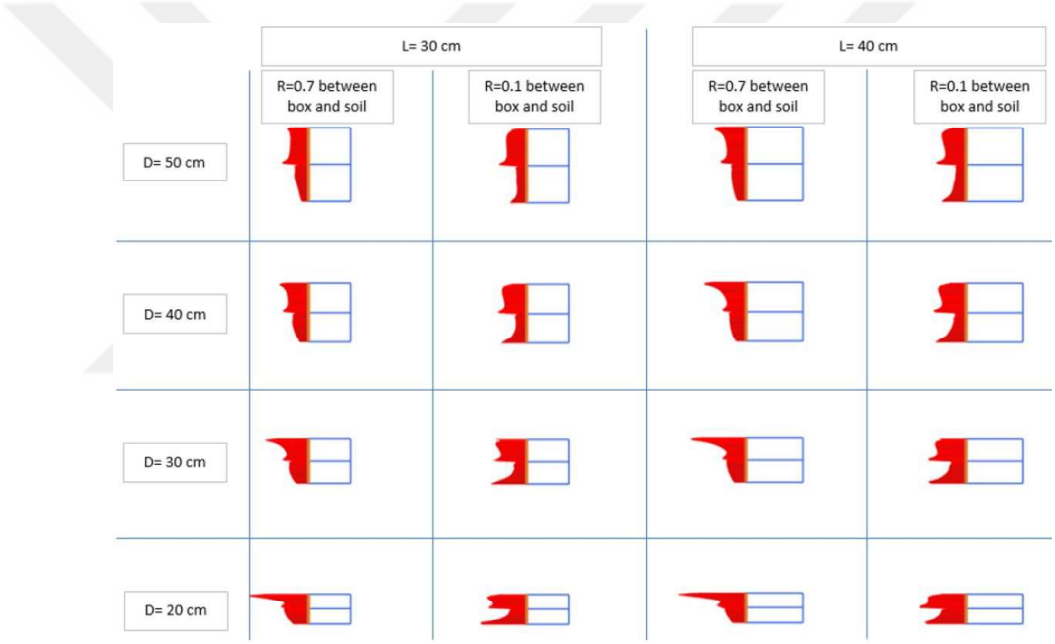


Figure 3.6. Normal stress acting on box wall (to determine box height).

Effect of height of the box is also analysed by running FEM analyses. The models have been built for 30 cm and 40 cm long boxes. Two different box-soil interface situations (R=0.7 and R=0.1) have been investigated. When normal stresses on box wall are considered (Figure 3.6) for the selected length of the box (30 cm), stress distribution of the box with height of 20 cm deviates from other boxes. In other words, stress distribution becomes similar for heights larger than 30 cm. Therefore, it is decided to use 30 cm for the box height based on FEM results. The selected box height complies with the finding of Elias *et al.* (1998) in which the height of the box

was selected as 152 mm based on experimental results. Unlike the study of Elias *et al.* (1998), coarse soil is also planned to be used in this study. Therefore, box height should be greater than 152 mm. As a result, the net box dimensions are selected as 30x30x30 cm.

Test box must be designed in at least 2 halves (upper and lower half). However, test box used in the study has been designed in segmental form in which each segment is 25 mm in depth (12 segments in total). Each segment can also be used as a clamp, so the apparatus becomes capable of conducting multi-layer in-soil tests. Segments are tightened by screwing the bolt at the uppermost segment (Figure 3.7).

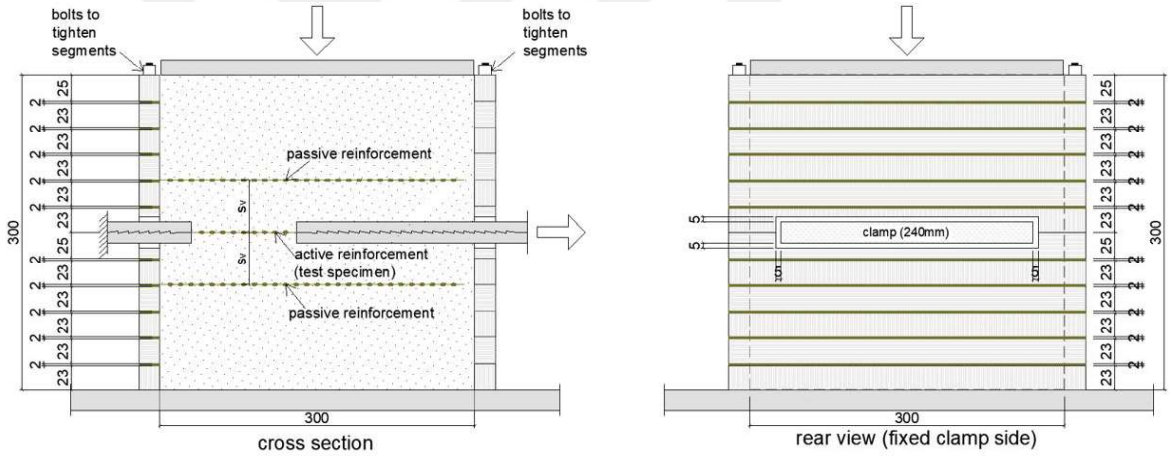


Figure 3.7. Schematic view of the segmental test box (measures are in mm).

3.1.2. Clamps

One of the most important part of the apparatus is the clamp. The clamp should be tight enough to prevent slip of the specimen, but it should also not damage the specimen while holding it. Several clamp types have been tried in scope of this study. In Figure 3.8, the gap between red line and the edge of clamp shows the amount of the slippage in the end of a test.

Final clamp design sufficiently prevented the slippage of the nonwoven reinforcement. However, it damaged the woven geotextile and geogrid. To prevent specimen damage, a cushion layer made of nonwoven geotextile has been used inside the clamps. Therefore, nonwoven geotextile has been attached to the clamp without cushion layer while woven geotextile and geogrid have been attached with cushion layer.

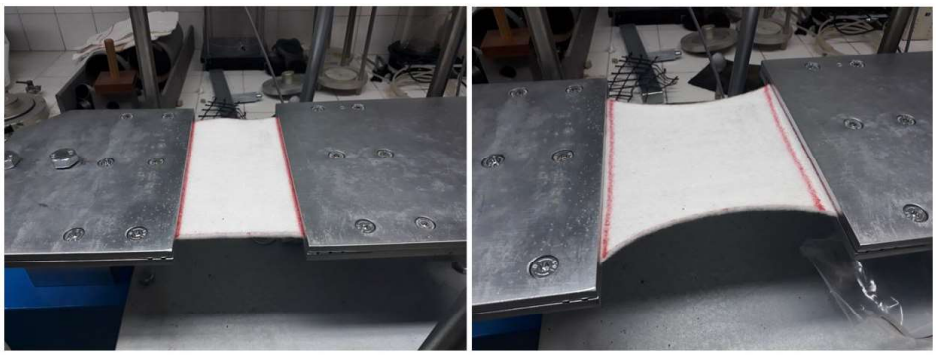


Figure 3.8. Slippage of specimen due to poor clamp design.

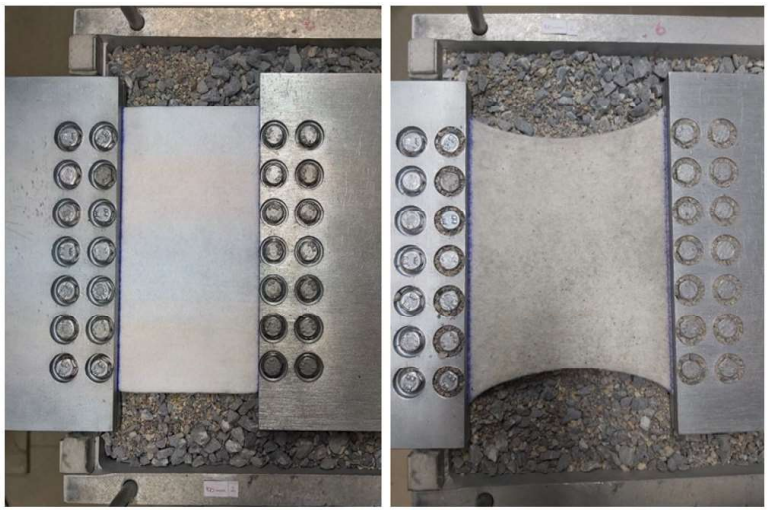


Figure 3.9. Final design of the clamp with sufficient slippage performance.

Continuous planar reinforcements like nonwoven and woven geotextiles are perforated to let clamp be bolted. Soldering iron is used to perforate the geotextiles which creates a stable hole without damaging the structure of the geotextile. Since bolt plan

has been designed according to the geogrid's openings, no special adjustment has been needed to attach geogrid to clamps. The geometry of the clamps is given in Figure 3.11. 1.5 cm of the fixed clamp stays inside the box, while 18 cm of mobile clamp stays inside the box (initial position). The thickness of both clamps is 1.8 cm.

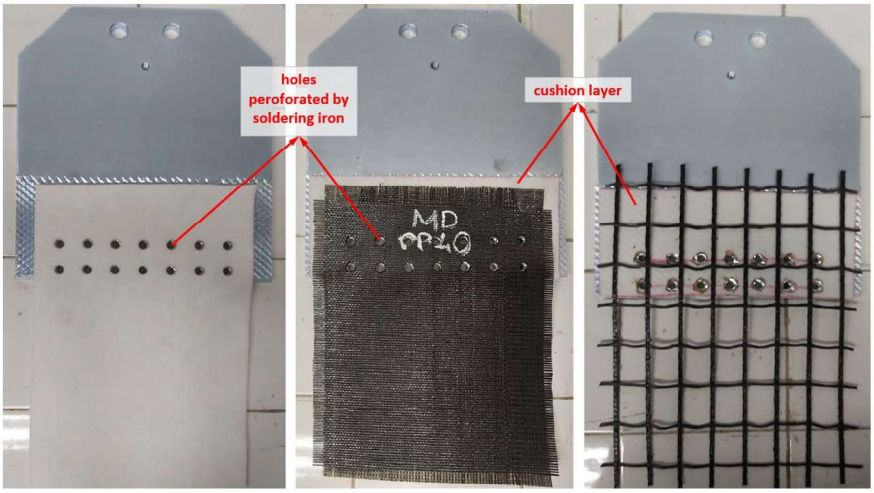


Figure 3.10. Clamping of the geosynthetics used in the study.

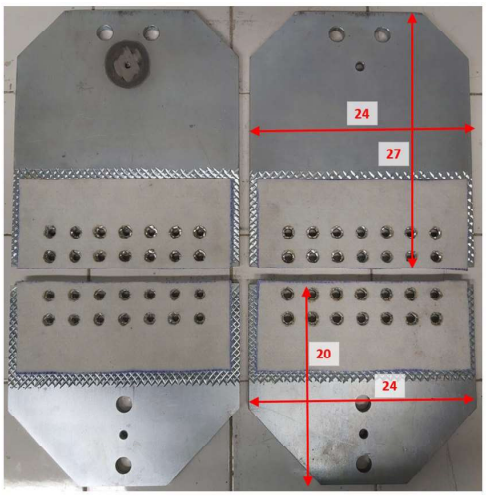


Figure 3.11. Geometry of the clamp (in cm).

3.1.3. Control Panel

The control panel has a built-in data logger with 4 channels. In this study, 3 linear potentiometers and a load cell has been used. Control panel also lets the user to adjust the displacement rate (from 0.001 to 15 mm/min), calibrating the potentiometers and load cell. Threshold force at which device starts to log the results can be adjusted. Moreover, end force (fracture sensing) at which test ends can be entered in percentage of the ultimate load.

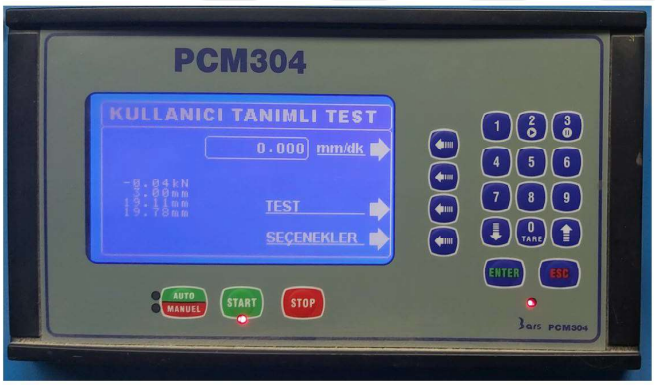


Figure 3.12. Control panel.

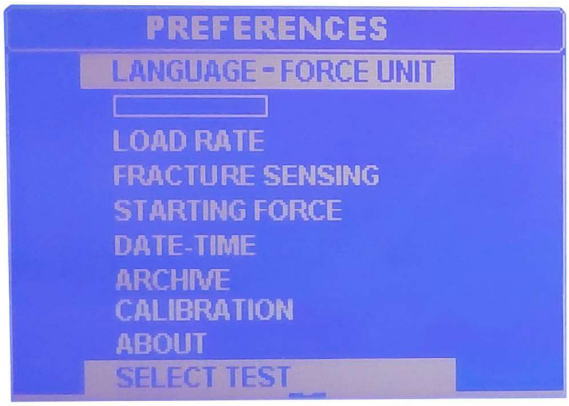


Figure 3.13. Menu of the control panel.

Main menu of the control panel is illustrated in Figure 3.13. The contents of the sub menus are as follows:

- "Language-Force Unit" lets the user to select the desired language (English or Turkish) and force unit (kN or kgf).
- The second menu which has no name has been implemented to determine some parameters to adjust the step motor. The password needs to be entered is 2277 for this menu. Parameters in this menu are in Turkish and must be determined as below. User must hit ENTER button in the panel to save and exit the menu.
  (i) Hareket Yonu: Sag
  (ii) Reduktor Orani: 32000
  (iii) Mikrostep Katsayisi: 6400
  (iv) Hızlanma Orani: 4
- Displacement rate of the apparatus can be adjusted from "Load Rate". As aforementioned it can be selected from 0.001 to 15 mm/minute.
- In "Fracture Sensing", the force which stops the machine (ends test) can be adjusted in percentage of ultimate force observed during the test.
- "Starting Force" menu lets the user to select the force at which data logging starts. Minimum force can be selected as 5 N.
- As the name suggests, date-time can be adjusted under "Date-Time" menu.
- A specific test can be called from the archive based on its date and test number. "Archive" menu should be used for this purpose.
- Calibration of potentiometers and load cell can be performed under "Calibration" menu. Password (which is 2277) needs to be entered to enter this menu. User is allowed to define the capacity of the device and calibrate it either in 2 points or 5 points. For example, while using 2 points calibration:
  (i) Enter the first value and press START button on the panel,
  (ii) Then enter the second value and press ENTER button on the panel,
  (iii) Save and exit.
- "About" menu gives info about the machine and the manufacturer. The contact info of the manufacturer is included in this menu.
- "Select Test" can be used to call a specific test based on date and test number of the test.

In order to log the test data, a laptop/pc should be plugged in via a digitus-usb connection. A software is used to simultaneously transfer and log the data to laptop/pc. Data is collected ten rows per second and software can convert the collected data file to text file. Furthermore, displacement rate can be selected by using the software (as an alternative to the control panel of apparatus). Software also has a graph plotter.

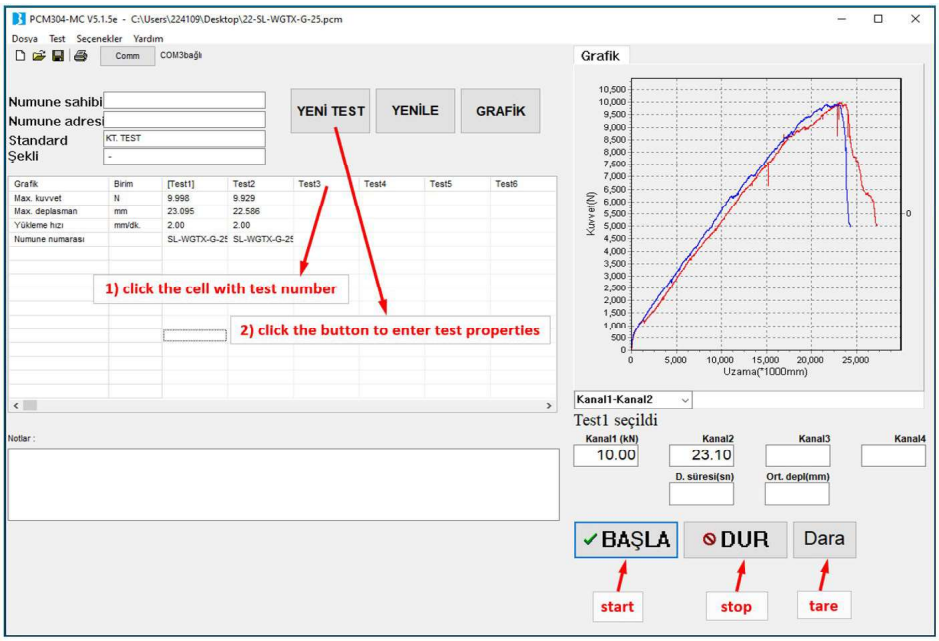


Figure 3.14. User interface of the software.

3.1.4. Measuring Devices

As aforementioned, 4 measuring devices have been used in the study. 1^{st} channel belongs to the load cell which has 35 kN compression and tension capacity. 1 potentiometric linear transducer (2^{nd} channel) with capacity of 50 mm has been used to measure the displacement of the clamp, thus strain of the test specimen. 2 potentiometric linear transducers (3^{rd} and 4^{th} channel) with capacity of 25 mm have been used to measure the vertical displacements of the loading plate, thus vertical displacements of soil. Prior to the tests, all measuring devices have been calibrated in the laboratory.

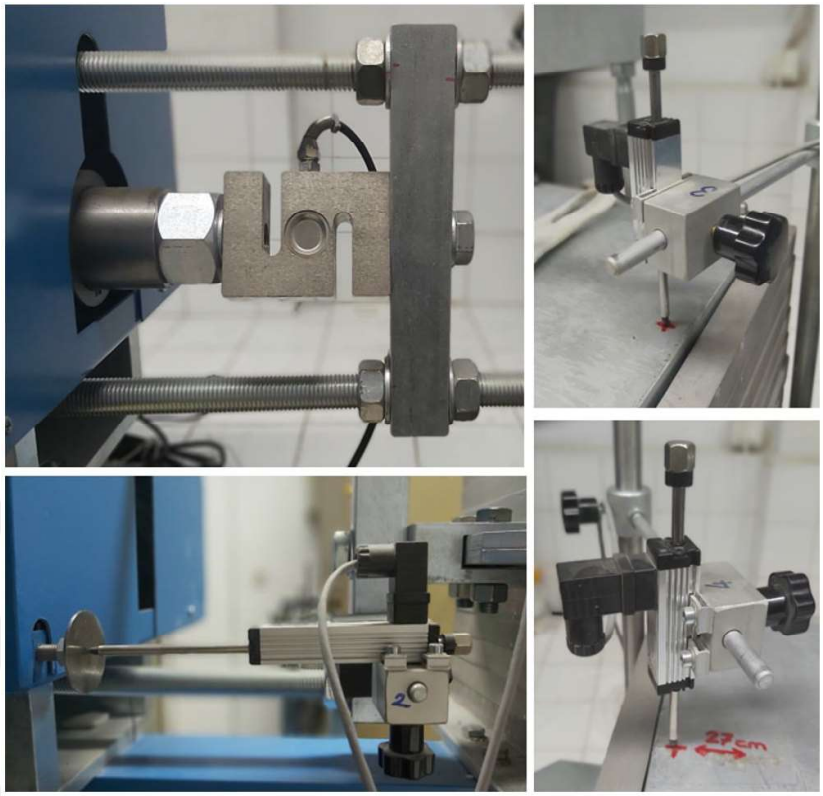


Figure 3.15. Measuring devices.

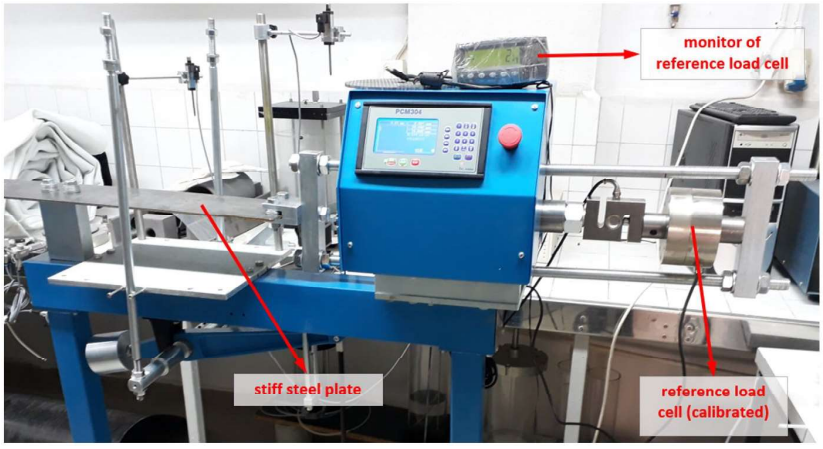


Figure 3.16. Calibration of load cell.

3.1.5. Vertical Load Frame

Confinement pressure is applied by the dead weight. A regular load frame is used in the apparatus which is similar to the ones used in oedometer and direct shear apparatuses. A lever arm of 1/10 ratio is used in the apparatus to magnify the applied dead weight.

3.2. Materials

Materials used in the study consist of 2 different soil types and 3 different geosynthetic types. Technical properties of materials and their preparation are presented in this chapter.

3.2.1. Soil

To investigate the influence of soil type in load-strain behaviour, two different soil types are used in the study. The soils used in the study are granular and non-cohesive. Mainly, these soil types can be mentioned as sand and gravel. Details are given in following sections.

Prior to sieve analyses and other index tests on soils, they have been cleaned. Particles finer than 0.075 mm were also washed out by wet sieving method (Figure 3.17). Wet and cleaned soil was dried in the oven at 110±5^{o}C.



Figure 3.17. Washing out the particles finer than 0.075 mm.

3.2.1.1. Gradation Curve and Soil Classification. Particle size distribution of soils used in the study are given in Table 3.3 and they both satisfy the reinforced fill gradation criteria of FHWA-NHI-10-024 (Berg *et al.*, 2009) shown in Table 3.2.

Table 3.2. MSE wall reinforced fill particle size distribution requirement (Berg *et al.* 2009).

U.S. Sieve Size	Percent Passing
4 in. (102 mm)	100
No. 40 (0.425 mm)	0-60
No. 200 (0.075 mm)	0-15

Requirements given in Table 3.2 provided a base, a starting point to determine the soil properties. Other considered points on gradation of soils are as follows.

- Parallel gradation curves were used to have a better comparison of soil influence on the behaviour,
- Studies in literature are dominantly on sand. Therefore, one of the soil types used in the study was selected as gravel which is more realistic when use in industry is considered.

- Well graded soils were selected to have a better compaction and lessen voids.
- In-soil tests are performed in a relatively small box (30x30 cm) and the minimum vertical spacing in multi-layer test is 25 mm. Because of these two reasons, maximum grain size must be limited as small as possible. Therefore, maximum grain size in gravel is kept below 9.5 mm. Particle size distributions of the gravel and sand were generated accordingly. This also satisfies the upper limit requirement, 19 mm, stated in FHWA-NHI-00-044 (Elias, 2000). According to FHWA, particle size shouldn't exceed 19 mm to prevent damage of reinforcement. Otherwise, site damage factor must be increased.

Based on all the mentioned points above, the particle size distribution of sand and gravel are presented in Table 3.3. Gradation curves and the characteristic particle diameters are illustrated in Figure 3.18.

Table 3.3. Particle size distribution of sand and gravel used in the study.

Sieve No.	Sieve Opening (mm)	Percent Passing, Cumulative (Sand)	Percent Passing, Cumulative (Gravel)
3/8"	9.5	100	100
5/16"	8	100	80
#4	4.75	100	45
#10	2	64.3	20
#20	0.85	34	0
#40	0.425	17.6	0
#70	0.212	4.4	0
#100	0.149	1.9	0
#200	0.075	0	0

According to the Unified Soil Classification System (ASTM D2487-11), the proposed soil types are SW (well graded sand) and GW with sand (Well graded gravel with sand), respectively.

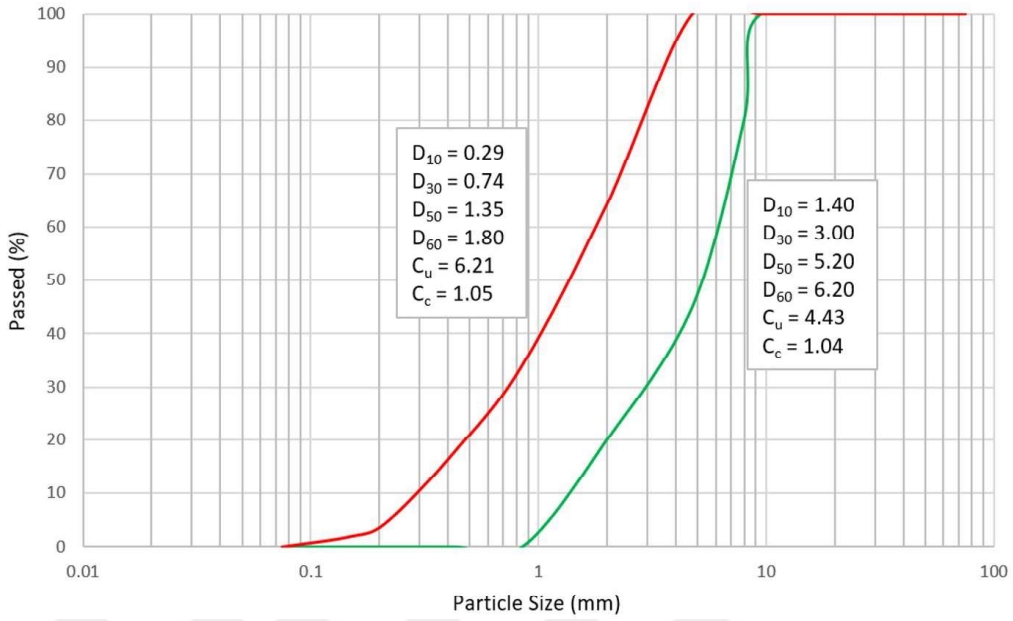


Figure 3.18. Gradation curves of sand (SW) and gravel (GW with sand).

To obtain the proposed gradation curves of SW and GW with Sand, sieve analyses have been performed on dry soils. Sieve analyses have been performed by using a stack of sieves on a sieve shaker, EFL 2000/2 (Figure 3.19). Therefore, certain particle size ranges have been determined (Figure 3.20) and then mixed to obtain the gradation curves given in Figure 3.18.



Figure 3.19. Sieving equipment.



Figure 3.20. Soil after sieving (sand).

3.2.1.2. Particle Shape. One of the important factors in the in-soil testing of reinforcements is particle shape. In the previous studies, fine sand has been mostly used as soil which has rounded shape. On the other hand, there is no sufficient study in the literature to interpret the influence of particle shape. In this study, two soil types (sand and gravel) are also distinguished from each other by particle shape. Sand consists of rounded particles whilst angular particles constitute gravel. The roundness coefficients of the materials have been determined by the method proposed by Zheng and Hryciw (Zheng and Hryciw, 2015). The roundness values for sand and gravel are calculated as 0.68 and 0.45, respectively. As a result, generated gravel mixture has more angular shaped particles when compared to the sand mixture.



Figure 3.21. Comparison of particle shape and size.

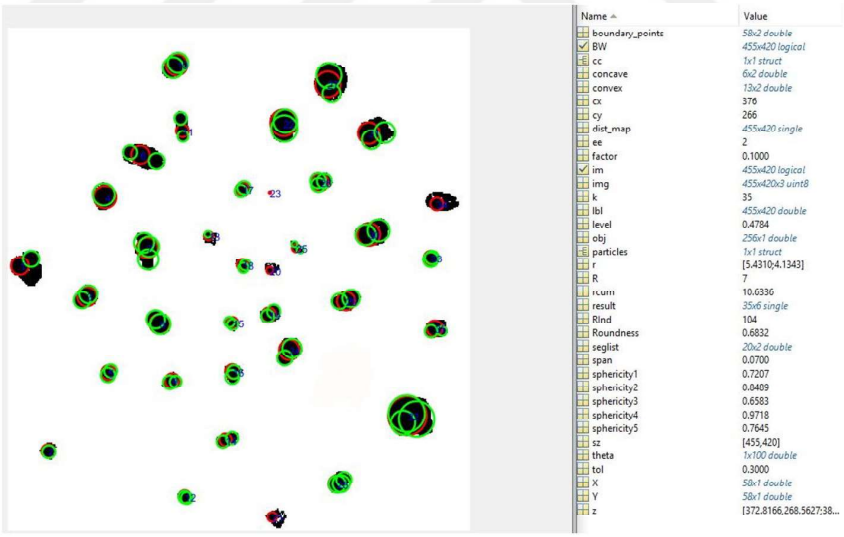


Figure 3.22. Particle shape of sand.

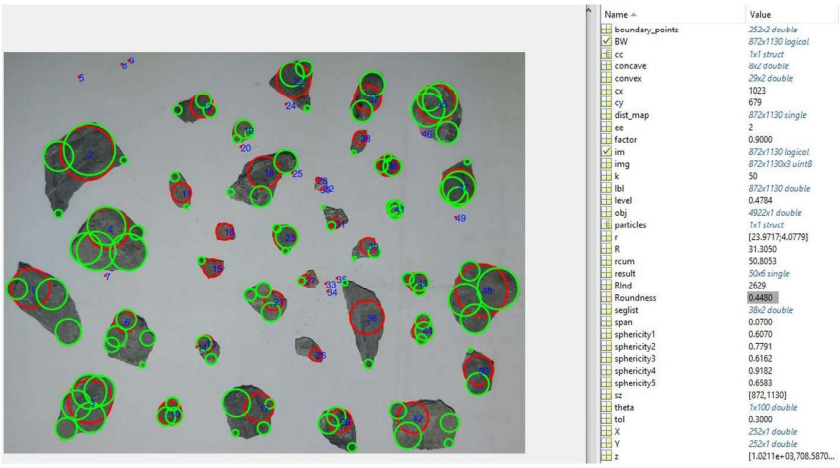


Figure 3.23. Particle shape of gravel.

3.2.1.3. Index Properties of Sand. In-soil tensile tests should be performed under same soil conditions. To keep the relative density of sand constant on each test, a specific relative density (D_r) should be determined. In order to calculate relative density of sand, index properties should be determined by laboratory tests. ASTM standards have been followed while carrying out the mentioned tests (ASTM-D854-14, ASTM-D4253-14 and ASTM-D4254-14). Tests have been repeated to satisfy the deviation requirements of the codes. As a result, mentioned parameters for the sand have been calculated as follows. The shear angle of sand has been determined by performing direct shear tests.

Table 3.4. Index and engineering properties of sand.

Property	Unit	Value
G_s	-	2.6962
e_{min}	-	0.51
e_{max}	-	0.62
ρ_{dmin}	gr / cm^3	1.6279
ρ_{dmax}	gr / cm^3	1.7522
γ_{dmin}	kN / m^3	15.9648
γ_{dmax}	kN / m^3	17.1838
$\emptyset'_{peak}$	^{o}	42.5
$\emptyset'_{res}$	^{o}	34.9



Figure 3.24. Specific gravity test on sand.

The vibratory table has been run for 8 minutes in 60 Hz for the maximum unit weight test.



Figure 3.25. Maximum unit weight (min void ratio) test on sand.



Figure 3.26. Minimum unit weight (max void ratio) test on sand.

3.2.1.4. Placing the Sand and Gravel to the Test Box. As mentioned in previous section, in-soil test should be performed under constant soil conditions to provide a sustainable test medium. To satisfy the mentioned requirement, air pluviation has been used to fill the test box with sand. Thanks to air pluviation, a uniform sand medium at a certain relative density can be constituted for the in-soil test. For this purpose, an air pluviation vessel has been developed out of a 19 litre plastic carboy. A spherical

1-inch gas valve with a flow diameter of 23 mm has been attached to the carboy to control the flow of sand. The air pluviation assembly has been carried by a mobile crane.



Figure 3.27. Air pluviation setup used for sand placement.

In air pluviation method, relative density of sand mainly depends on drop height and the valve opening. The relative density of sand is computed as

$$D_r = \frac{\rho_{dmax}\left(\rho_d - \rho_{dmin}\right)}{\rho_d\left(\rho_{dmax} - \rho_{dmin}\right)} 100. \tag{3.1}$$

Drop height is limited by the capability of mobile crane which can reach up to 19cm with respect to top of the test box. To achieve the highest relative density, sand has been dropped from 19 cm height. Test box is filled 3 times to determine the dry density (thus relative density). The average dry density of ρ_d=1.6933 gr/cm^3 (unit

weight, γ_d=16.61 kN/m^3) has been reached by 0.6% deviation. The system can be considered consistent. Results of tests are presented in Table 3.5. According to ASTM D4254-14 (Eq. 3.1), relative density (D_r) is calculated as 54% (ρ_{dmin}=1.6279 gr/cm^3 and ρ_{dmax}=1.7522 gr/cm^3). D_r=54% corresponds to medium dense sand.

Table 3.5. Air pluviation test results.

Test No	Soil Mass (gr)	Net Volume of Box (cm^3)	ρ_d (gr/cm^3)
1	44400	26145	1.6982
2	44272	26145	1.6933
3	44143	26145	1.6884

Test box has dimensions of 30x30x30 cm, which leads to a gross volume of 27000 cm$_3$. Net volume of the box in Table 3.5 is calculated by subtracting the volume of clamps (855 cm^3) from the gross volume of the test box, because pluviation tests have been performed while clamps were inside the box.

When gravel is used in in-soil tests, the box has been filled with the gravel by tamping. The unit weight of the gravel has been determined after tests performed in proctor mold. Proctor mold has been filled with gravel by tamping and reached density has been used in in-soil tests. The average dry density of ρ_d=1.5518 gr/cm^3 (γ_d=15.22 kN/m^3) has been reached by 1.3% deviation. Results of tests are presented in Table 3.6. This corresponds to 40571 gr of gravel in test box. Gravel has been placed to the test box in 25 mm layers and desired density has been achieved by tamping for each layer.

Table 3.6. Gravel tamping in proctor mold.

Test No	Soil Mass (gr)	Volume of Mold (cm^3)	ρ_d (gr/cm^3)
1	1445	926.25	1.5601
2	1440	926.25	1.5547
3	1427	926.25	1.5406

3.2.2. Geosynthetics

In-soil behaviour has been investigated for 3 types of geosynthetic reinforcements. Vast majority of the literature includes the in-soil tests on nonwoven geotextiles. In addition to nonwoven geotextile, woven geotextile and woven geogrid have been used in this study.

3.2.2.1. Nonwoven Geotextile. GeoTeknik 5000 PP is the nonwoven geotextile used in the study. It is a needle punched and thermally calendered (on both sides) nonwoven geotextile. It's made of polypropylene. The technical specifications are given in Table 3.7.

Table 3.7. Technical specifications of GeoTeknik 5000 PP.

Properties	Standard	Unit	Values
Weight	EN ISO 9864	gr/m^2	500
Thickness (at 2 kPa)	EN ISO 9863-1	mm	3.5
Tensile strength (CD/MD)	EN ISO 10319	kN/m	28/35
Elongation at Break (CD/MD)	EN ISO 10319	%	min. 50
Static Puncture Test	EN ISO 12236	N	4500
Cone Drop Test	EN ISO 13433	mm	7
Water Permeability, V_{H50}	EN ISO 11058	mm/s	40
Opening Size, O_{90}	EN ISO 12956	mm	0.071

Test samples of nonwoven geotextile have been cut out from the roll in 200x250 mm. Since in soil tests are performed under wide width requirements, width of the reinforcement is 200 mm. The total length in gauge direction is 250 mm but 75 mm was kept inside the clamp which makes the net gauge length 100 mm. Sharp scissors is used to keep the disturbance of the material at minimum while cutting out.

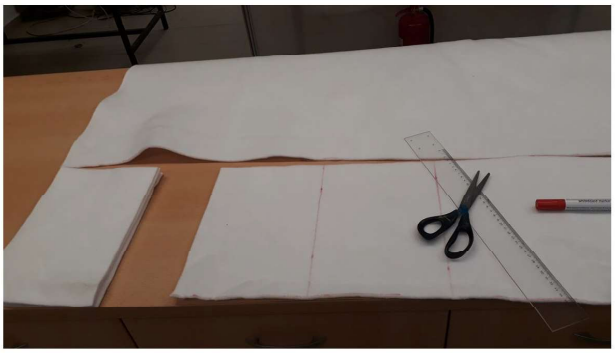


Figure 3.28. Preparation of nonwoven geotextile samples.

3.2.2.2. Woven Geotextile. TenCate Geolon PP 40, which is composed of polypropylene fibres, has been used in the study as woven geotextile. The technical specifications are given in Table 3.8.

Table 3.8. Technical specifications of TenCate Geolon PP 40.

Properties	Standard	Unit	Values
Tensile Strength, (MD)	EN ISO 10319	kN/m	38-40
Tensile Strength, (CD)	EN ISO 10319	kN/m	37-40
Elongation at min. strength (MD)	EN ISO 10319	%	17
Elongation at min. strength (CD)	EN ISO 10319	%	12
Static Puncture Test	EN ISO 12236	N	5000
Cone Drop Test	EN ISO 13433	mm	11
Water Permeability, VH50	EN ISO 11058	mm/s	13
Opening Size, O90	EN ISO 12956	mm	0.25

Like nonwoven geotextile, woven geotextiles were cut out from the roll at dimensions of 200x250 mm. In fact, the width of the sample was cut greater than 200 mm, then fibers on each side were unraveled to reach 200 mm width. Following this rigorous preparation, samples with an exact width of 200 mm was maintained by avoiding damage on fibres.



Figure 3.29. Preparation of woven geotextile samples.

3.2.2.3. Geogrid. Since negligible in-soil effect is expected in extruded geogrids, a woven geogrid was used in the study. As the woven geogrid, ForTex GG35/20P was used in this study. This geogrid consists of polymer coated polyester fibers. Due to the interaction of individual fibres and their behaviour under pressure, in-soil behaviour of the mentioned geogrid type is expected to be different than the one observed in in-air tests. The technical specifications are given in Table 3.9.

Table 3.9. Technical specifications of ForTex GG 35/20 P.

Properties	Standard	Unit	Values
Tensile Strength, (MD)	TS EN ISO 10319	kN/m	35
Tensile Strength, (CD)	TS EN ISO 10319	kN/m	20
Elongation at break (MD)	EN ISO 10319	%	10(±2)
Elongation at break (CD)	EN ISO 10319	%	10(±2)
Opening (MD)	-	mm	30(±2)
Opening (CD)	-	mm	26(±2)

Like geotextiles, woven geogrid was cut out from the roll at dimensions of 200x250 mm. Since in soil tests are performed under wide width requirements, width of the reinforcement is 200 mm. The total length in gauge direction is 250 mm but 75 mm was kept inside the clamp which makes the net gauge length 100 mm.

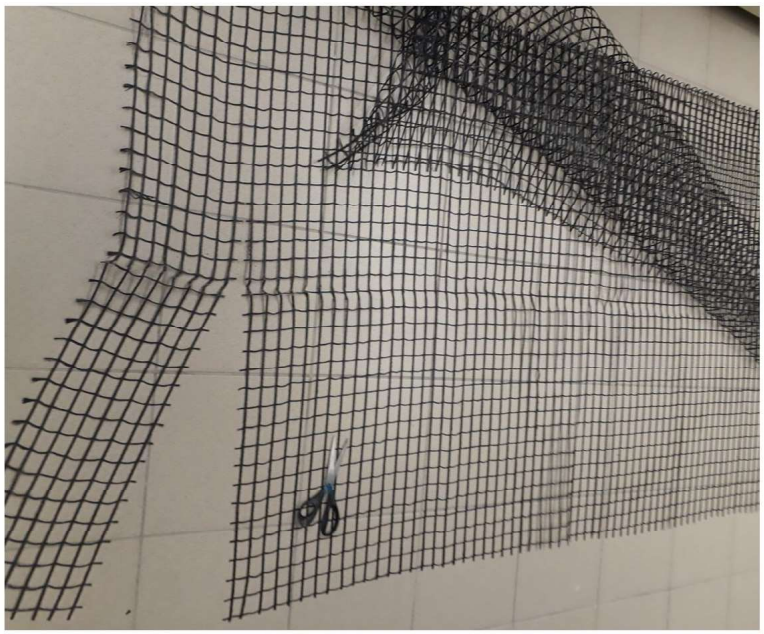


Figure 3.30. Preparation of geogrid samples.

3.3. Test Procedure

The goal of this study is to investigate the in-soil tensile behaviour of geosynthetics through tensile load-strain curves. In scope of this study two types of in-soil tests were conducted. These tests are called “Single Layer Test” and “Multi-layer Test”.

In single layer tests, a regular in-soil test procedure is performed. In detail, test sample is sandwiched in soil and subjected to tension load during the test. In other words, a wide width tensile test inside the soil is carried out. Single layer test results lead the researcher to investigate the influence of soil type and confinement pressure on tensile behaviour of different geosynthetic reinforcements. The procedure of the single layer test is illustrated in Figure 3.31.

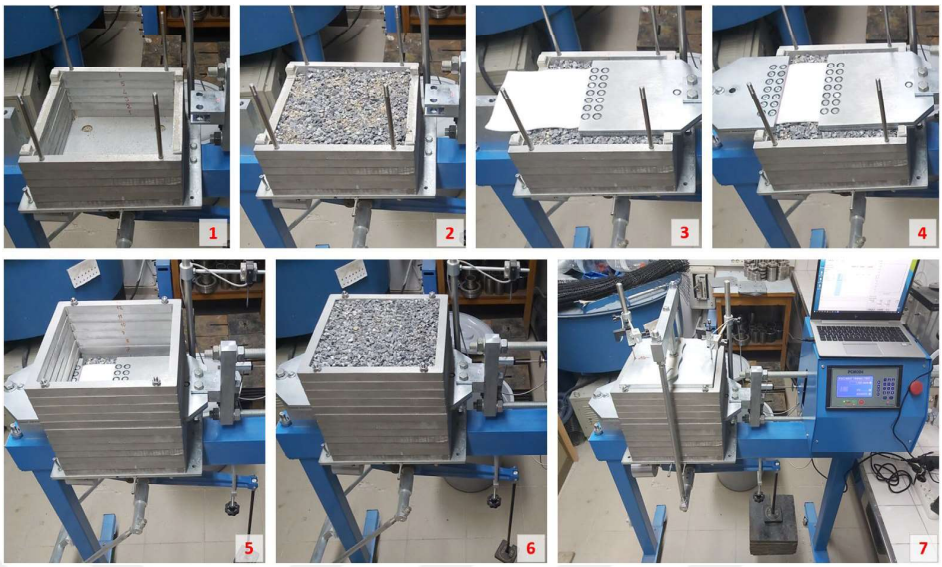


Figure 3.31. Procedure of Single Layer Test.

- Step 1: Assembly the lower half of the box.
- Step 2: Fill in the lower half of the box with soil (sand or gravel in this study). For tests performed in sand, air pluviation method is used while tamping is used in case of gravel.
- Step 3: Attach test sample to the active clamp (the clamp which moves during the test). Then, attach the clamp to the apparatus.
- Step 4: Attach test sample to the fixed clamp (the clamp which is stationary).
- Step 5: Assembly the upper half of the box.
- Step 6: Fill in the upper half of the box by using the method in Step 2.
- Step 7: Place steel loading plate and measurement devices (2 vertical potentiometers on loading plate to determine the movement of it and 1 horizontal potentiometer to measure the clamp displacement). Attach the required dead mass to lever arm to apply 25, 50, 75 and 125 kPa confinement pressure on test sample (20, 43, 66 and 112 kg of dead mass respectively). Note that mass of soil and loading plate are also taken into account while adding the dead mass to lever arm.

The procedure explained above has to be repeated at least two times until reaching a negligible deviation between load-strain curves. An average load-strain curve is calculated by taking all test results into account. The average (gross) load-strain curve calculation method is illustrated in Figure 3.32.

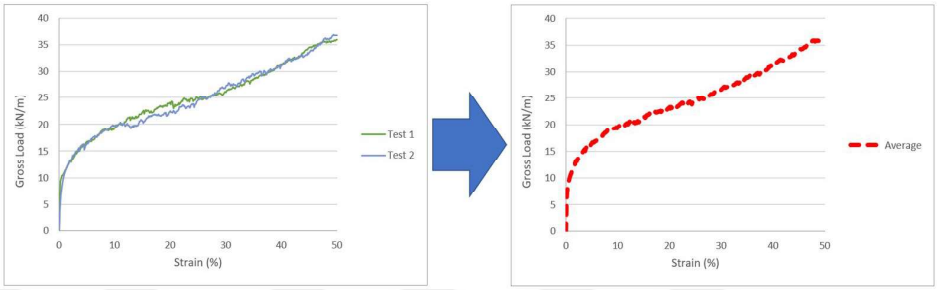


Figure 3.32. Calculation of average (gross) load-strain curve.

However, the result of this test would be erroneous due the friction between clamp and soil. Therefore, the procedure explained above gives the "gross" tensile load-strain curve. "Net" tensile load-strain curve, in which influence of the clamp friction is subtracted, should be determined for this study. In order to prevent the influence of clamp friction, the frictional loads need to be subtracted from the gross results. Clamp friction is determined by following the procedure given in Figure 3.33.

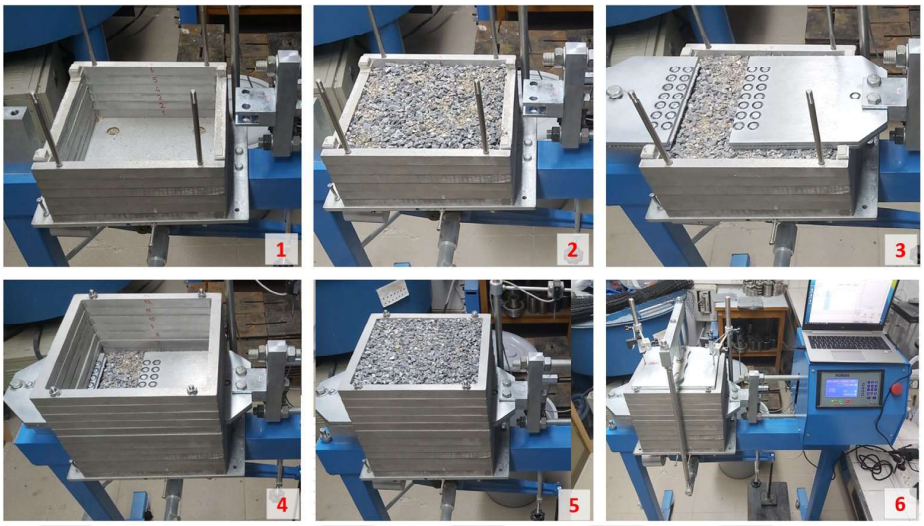


Figure 3.33. Procedure to determine clamp friction in single layer test.

The procedure to determine clamp friction for single layer test is as follows:

- Step 1: Assembly the lower half of the box.
- Step 2: Fill in the lower half of the box with soil (sand or gravel in this study). For tests performed in sand, air pluviation method is used while tamping is used in case of gravel.
- Step 3: Place both clamps in the box (no reinforcement attached).
- Step 4: Assembly the upper half of the box.
- Step 5: Fill in the upper half of the box by using the method in Step 2.
- Step 6: Place steel loading plate and measurement devices (2 vertical potentiometers on loading plate to determine the movement of it and 1 horizontal potentiometer to measure the clamp displacement). Attach the required dead mass to lever arm to apply 25, 50, 75 and 125 kPa confinement pressure on test sample (20, 43, 66 and 112 kg of dead mass respectively). Note that mass of soil and loading plate are also taken into account while adding the dead mass to lever arm.

The net tensile load-strain curves are calculated by subtracting the result of friction test from the actual test. Net tensile load-strain curves are used in evaluations.

This approach is illustrated in Figure 3.34.

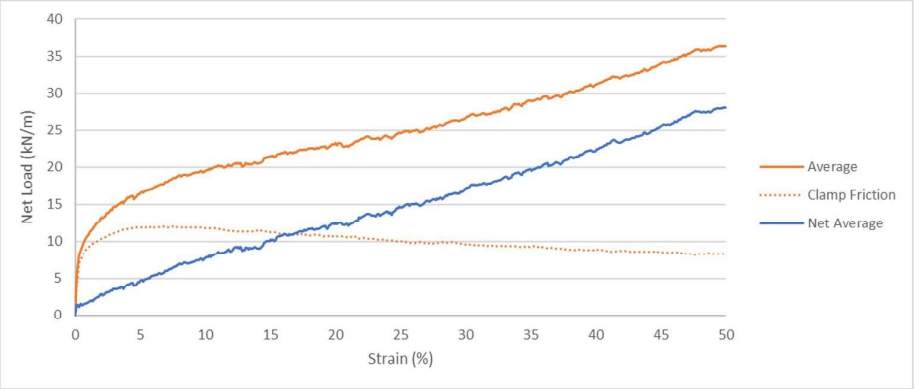


Figure 3.34. Gross curve, frictional curve and net curve.

The multi-layer test is similar to single layer test. In multi-layer test, two additional reinforcements are also placed in the box. These reinforcements are called passive reinforcements. Passive reinforcements are placed in upper half and lower half of the box. The distance of a passive reinforcement to the test sample (active reinforcement) is called vertical spacing "s_v". Multi-layer tests have been performed to investigate the influence of vertical spacing on in-soil tensile behaviour of geosynthetics. Vertical spacing values used in tests are 25, 50 and 100 mm. On every single test, s_v was equal at above and below the test sample. Confinement pressure has been kept constant in all tests as 50 kPa. The procedure of the multi-layer test is illustrated in Figure 3.35.

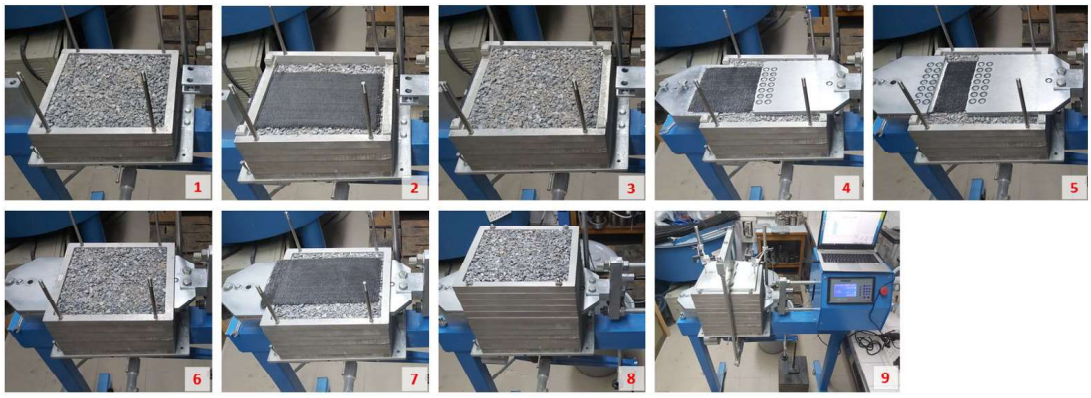


Figure 3.35. Procedure of Multi-layer Test.

- Step 1: Assembly the lower half of the box up to the level of lower passive reinforcement. Fill in the box with soil (sand or gravel in this study). For tests performed in sand, air pluviation method is used while tamping is used in case of gravel.
- Step 2: Place the lower passive reinforcement and assembly the box up to the test sample (active reinforcement).
- Step 3: Fill in the box with soil up to the level of test sample by using the method in Step 1.
- Step 4: Attach test sample to the active clamp (the clamp which moves during the test). Then, attach the clamp to the apparatus.
- Step 5: Attach test sample to the fixed clamp (the clamp which is stationary).
- Step 6: Assembly the upper half of the box up to the level of upper passive reinforcement. Fill in the box with soil by using the method in Step 1.
- Step 7: Place the upper passive reinforcement and assembly the box up to the uppermost level.
- Step 8: Fill in the upper half of the box by using the method in Step 1.
- Step 9: Place steel loading plate and measurement devices (2 vertical potentiometers on loading plate to determine the movement of it and 1 horizontal potentiometer to measure the clamp displacement). Attach the required dead mass to lever arm to apply 50 kPa confinement pressure on test sample (43 kg of dead mass). Note that mass of soil and loading plate are also taken into account while adding the dead mass to lever arm.

The procedure explained above is repeated at least two times until reaching a negligible deviation between load-strain curves. An average load-strain curve is calculated by taking all test results into account. The average (gross) load-strain curve calculation method is illustrated in Figure 3.32.

However, the result of this test would be erroneous due the friction between clamp and soil. Therefore, the procedure explained above gives the “gross” tensile load-strain curve. “Net” tensile load-strain curve, in which influence of the clamp

friction is subtracted, should be determined separately for each test group. In order to prevent the influence of clamp friction, the frictional loads need to be subtracted from the gross results. Clamp friction is determined by following the procedure given in Figure 3.36.

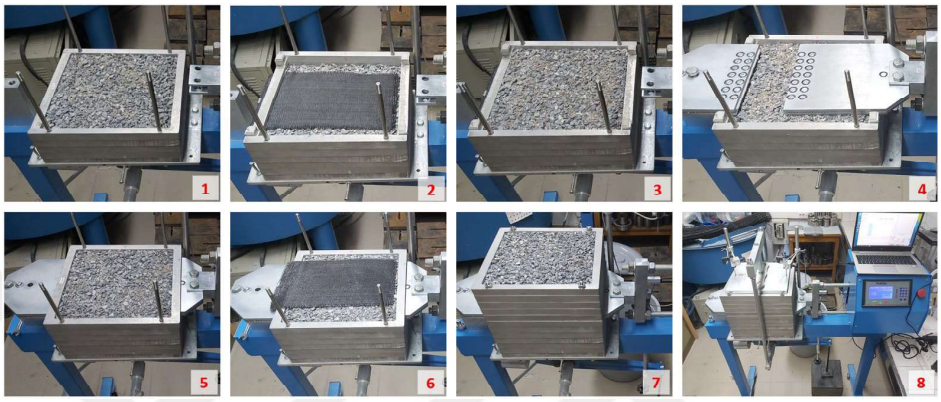


Figure 3.36. Procedure to determine clamp friction in multi-layer test.

The procedure to determine clamp friction for multi-layer test is as follows:

- Step 1: Assembly the lower half of the box up to the level of lower passive reinforcement. Fill in the box with soil (sand or gravel in this study). For tests performed in sand, air pluviation method is used while tamping is used in case of gravel.
- Step 2: Place the lower passive reinforcement and assembly the box up to the level of clamps.
- Step 3: Fill in the box with soil up to the level of clamps by using the method in Step 1.
- Step 4: Place both clamps in the box (no reinforcement attached).
- Step 5: Assembly the upper half of the box up to the level of upper passive reinforcement. Fill in the box with soil by using the method in Step 1.
- Step 6: Place the upper passive reinforcement and assembly the box up to the uppermost level.
- Step 7: Fill in the upper half of the box by using the method in Step 1.

- Step 8: Place steel loading plate and measurement devices (2 vertical potentiometers on loading plate to determine the movement of it and 1 horizontal potentiometer to measure the clamp displacement). Attach the required dead mass to lever arm to apply 50 kPa confinement pressure on test sample (43 kg of dead mass). Note that mass of soil and loading plate are also taken into account while adding the dead mass to lever arm.

The net tensile load-strain curves are calculated by subtracting the result of friction test from the actual test. Net tensile load-strain curves are used in evaluations. This approach is illustrated in Figure 3.34.

Prior to the in-soil tests explained above, in-air (unconfined) wide width tests have been performed (Figure 3.37). The mentioned in-air tests constitute the control group to be compared with the in-soil tests. For in-soil and in-air tests, the criteria given below are satisfied.

- In geotextiles, specimen width was selected 200 mm while gauge length of the specimen was 100 mm as specified in ASTM D 4595.
- In geogrid, specimen width was selected 200 mm while gauge length was maintained by having 2 apertures (3 junctions) in gauge direction as specified in ASTM D 6637. For the chosen geogrid this also corresponds to 100 mm.
- Tests were performed at a constant strain rate of 2% per minute. This corresponds to the 2 mm/min when the gauge length is 100mm as mentioned above.
- Confinement pressures were 25, 50 and 75 kPa in in-soil tests. 125 kPa is also applied for single test in-sand performed on geogrid. This is explained in Chapter 4 (Test Results and Evaluation).

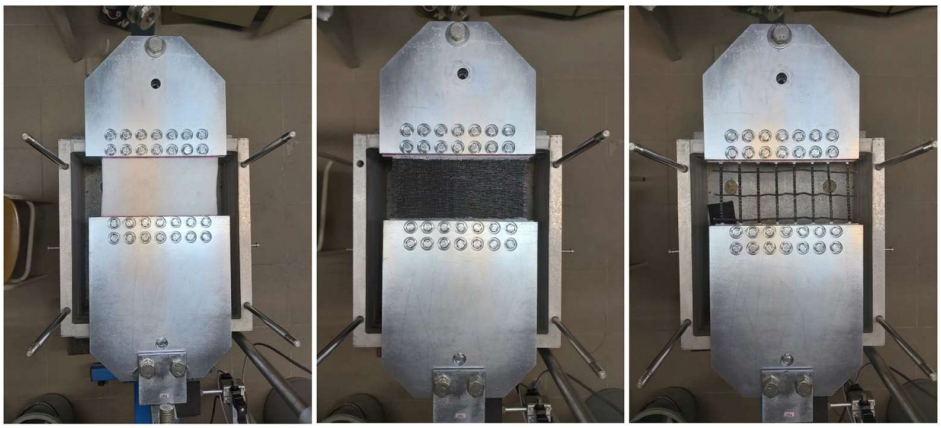


Figure 3.37. In-air wide width test setup for various reinforcements.

3.4. Test Program

Test apparatus developed for this study has been used to carry out wide width tensile tests (in-air and in-soil) on geosynthetics. 160 tests were conducted to investigate the in-soil load-extension behaviour of geosynthetics. The tests can be divided mainly into 5 groups as follows:

- In-air (unconfined) wide width tests,
- Single layer (confined) tests,
- Single layer (confined) tests for clamp friction,
- Multi-layer (confined) tests,
- Multi-layer (confined) tests for clamp friction,

Single layer tests have been performed to investigate the influence of confinement pressure in various soil types on load-strain behaviour of geosynthetics. Multi-layer tests have been performed to investigate the influence of vertical spacing in various soil types on load-strain behaviour of geosynthetics. The test program is given in Table 3.10 and Table 3.11.

In Table 3.10 and Table 3.11, NWGT is nonwoven geotextile, WGTX is woven geotextile and WOGD is woven geogrid. For soil type; SW is well graded medium dense sand and GW is well graded gravel with sand. As aforementioned strain rate is 2% strain/min in all tests.

Table 3.10. Test program of single layer in-soil tests (also includes in-air tests).

Test ID	Geosynthetic Type	Backfill	s_v (mm)	Confinement Pressure (kPa)	Explanation
2	No Reinforcement	GW	-	25	performed to determine the friction between clamp and soil
3			-	50	
4			-	75	
5		SW	-	25	
6			-	50	
7			-	75	
7a			-	125	
14	NWGT	in-air	-	-	control group of NWGT to determine the in-soil behaviour of NWGT under various confinement pressure values
15		GW	-	25	
16			-	50	
17			-	75	
18		SW	-	25	
19			-	50	
20			-	75	
21	WGTX	in-air	-	-	control group of WGTX to determine the in-soil behaviour of WGTX under various confinement pressure values
22		GW	-	25	
23			-	50	
24			-	75	
25		SW	-	25	
26			-	50	
27			-	75	
28	WOGD	in-air	-	-	control group of WOGD to determine the in-soil behaviour of WOGD under various confinement pressure values
29		GW	-	25	
30			-	50	
31			-	75	
32		SW	-	25	
33			-	50	
34				75	
34a			-	125	

Table 3.11. Test program of multi-layer in-soil tests.

Test ID	Geosynthetic Type	Backfill	s_v (mm)	Confinement Pressure (kPa)	Explanation
35	WGTX (only passive)	GW	25	50	only upper and lower reinforcements exist. performed to determine the friction between clamp and soil
36			50	50	
37			100	50	
38		SW	25	50	
39			50	50	
40			100	50	
41	WOGD (only passive)	GW	25	50	only upper and lower reinforcements exist. performed to determine the friction between clamp and soil
42			50	50	
43			100	50	
44		SW	25	50	
45			50	50	
46			100	50	
100	NWGT (only passive)	GW	25	50	only upper and lower reinforcements exist. performed to determine the friction between clamp and soil
101			50	50	
102			100	50	
103		SW	25	50	
104			50	50	
105			100	50	
47	WGTX	GW	25	50	to determine the in-soil behaviour of WGTX under various vertical spacing values
48			50	50	
49			100	50	
50		SW	25	50	
51			50	50	
52			100	50	
53	WOGD	GW	25	50	to determine the in-soil behaviour of WOGD under various vertical spacing values
54			50	50	
55			100	50	
56		SW	25	50	
57			50	50	
58			100	50	
110	NWGT	GW	25	50	to determine the in-soil behaviour of NWGT under various vertical spacing values
111			50	50	
112			100	50	
113		SW	25	50	
114			50	50	
115			100	50	

4. TEST RESULTS AND EVALUATION

4.1. Introduction

Test apparatus developed for this study has been used to carry out wide width tensile tests (in-air and in-soil) on geosynthetics. 160 tests were conducted to investigate the in-soil load-extension behaviour of geosynthetics. As discussed in Chapter 3, each test is performed at least twice to reduce the deviation and average of the repetitive test outputs is given in this section. Raw load-extension test results are given in Appendix A.

Some important aspects of the tests are as follows:

- Tests were performed at a constant strain rate of 2% per minute.
- Confinement pressures were 25, 50 and 75 kPa in in-soil tests.
- In geotextiles, specimen width was selected 200 mm while gauge length of the specimen was 100 mm as specified in ASTM D 4595.
- In geogrid, specimen width was selected 200 mm while gauge length was maintained by having 2 apertures (3 junctions) in gauge direction as specified in ASTM D 6637. For the chosen geogrid this also corresponds to 100 mm.

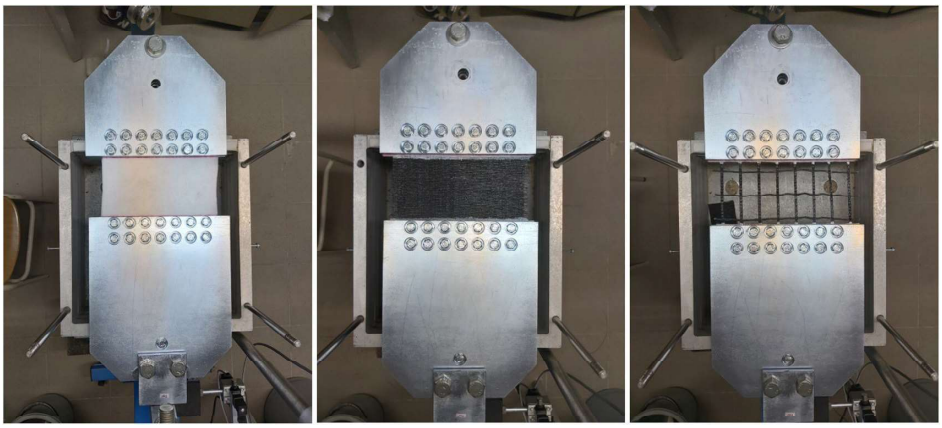


Figure 4.1. In-air test set up for all investigated geosynthetics.

Prior to in-soil tests, in-air tensile tests were performed (control group) to be compared with in-soil test results (Figure 4.1). As aforementioned in Chapter 3 in-soil tests are mainly divided into 2 groups in terms of used geosynthetic pattern. From this point on, mentioned in-soil test groups are referred as "single-layer test" and "multi-layer test". Single-layer test is a regular in-soil tensile test of geosynthetics under confinement pressure. In multi-layer test, in addition to the test specimen in single-layer, a layer of geosynthetic is placed at upper half and at lower half of the test box (Figure 4.2). The reinforcements at upper and lower half of the box are called passive reinforcements. Details are given in Chapter 3.



Figure 4.2. An example of in-soil test set up; (a) Single-layer (b) Multi-layer.

Test results are evaluated by investigating the following test outputs.

Load-Strain Curve (T-ε): This is a regular, tensile load-strain curve. Since woven geotextile and geogrid break at strains lower than 30%, results presented in this chapter are limited to 30% strain at most. In general, large strains (>10% approx.) are meaningless in terms of design considerations, so the behaviour at a reasonable strain for design such as 5% is investigated. Load-strain behaviour of the geosynthetics under various conditions are compared. Both load-extension and load-strain terms refer to the same curve in this chapter.

- **Secant Stiffness-Strain Curve (J_{sec}-ε)**: As name suggests, secant stiffness values are plotted with corresponding strain values. Derived from load-extension curve. Secant stiffness is computed as

$$J_{sec} = \frac{Tension\ Load\ \ (T)\ \ at\ Strain\ \varepsilon}{Strain\ \varepsilon}. \tag{4.1}$$

- **Secant Stiffness-Strain Curve ($J_{sec,r}$-ε)**: This is a valuable parameter to directly see the stiffness change due to confinement or vertical spacing. Secant stiffness ratio is computed as

$$J_{sec,r} = \frac{J_{sec}\ from\ in-soil\ test}{J_{sec}\ from\ in-air\ test}. \tag{4.2}$$

Secant Stiffness at 5% Strain-Normal Pressure Curve ($J_{sec,5} - \sigma_n$): This is an outcome of single-layer test results. The mentioned stiffness value is calculated for all confining scenarios. In the end, $J_{sec,5}$ values are plotted against confining pressures. The plotted points for in-soil test are represented by a linear trendline to describe the change of $J_{sec,5}$ depending on the confining pressure. The aim of describing the relationship by a σ_n dependent equation is to calculate $J_{sec,5}$ for a certain vertical spacing value without performing in-soil test.

Secant Stiffness at 10% Strain-Normal Pressure Curve ($J_{sec,10} - \sigma_n$): The procedure is same as the one in $J_{sec,5} - \sigma_n$ graph. However, this is only applied in the single-layer tests performed in gravel. The non-deterministic results in tests required

more parameters to interpret the behaviour.

Secant Stiffness at 5% Strain-Vertical Spacing Curve ($J_{sec,5} - s_v$): This is an outcome of multi-layer test results. The mentioned stiffness value is calculated for all vertical spacing scenarios. In the end, $J_{sec,5}$ values are plotted against vertical spacing values. The plotted points for in-soil test are represented by a linear trendline to describe the change of $J_{sec,5}$ depending on the vertical spacing. The aim of describing the relationship by a s_v dependent equation is to calculate $J_{sec,5}$ for a certain vertical spacing value without performing in-soil test.

4.2. In-Air (Unconfined) Load-Extension Tests

As base of comparison, specimens have been tested under unconfined situation (in-air test). This test group (in-air group) is considered control group in this study. In-soil test results are evaluated with respect to in-air test results.

4.2.1. Nonwoven Geotextile

Nonwoven geotextile has an ultimate strain greater than 50%. Since the displacement limit of the apparatus is 50mm (50% strain), ultimate tensile load (rupture of geotextile) can't be reached within the displacement limits of the apparatus. Therefore, ultimate tensile load and ultimate strain (T_{ult} and ε_{ult}) couldn't be determined.

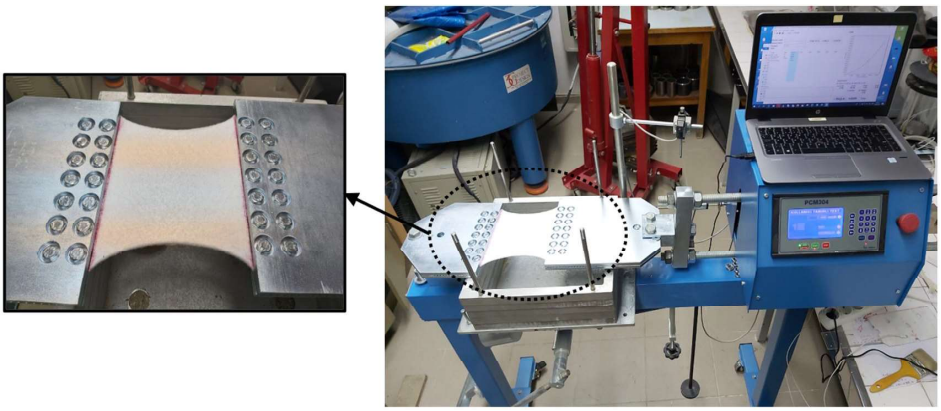


Figure 4.3. In-air test setup and result of nonwoven geotextile test.

The apparatus successfully performed in-air test of nonwoven geotextile. Edges of the specimen were marked to examine the slippage of the geotextile out of the clamp (Figure 4.3). In the end of test, it was seen that clamp sufficiently works for the nonwoven geotextile. Neither slippage nor rupture of geotextile occurs during the test.

Needle-punched nonwoven geotextile, which has one of the loosest structures among all geosynthetics, was used in tests. Load-strain output of the test is illustrated in Figure 4.4. In the beginning of the test, geotextile has a very low stiffness due to its loose structure. However, entangled fibers of the nonwoven geotextile become aligned with the extension of the geotextile and aligned fibers lead the nonwoven geotextile to act like a stiffer material at greater strains. The increase in stiffness is almost linear with increasing strain (Figure 4.5).

Nonwoven geotextile wasn't subjected to pre-tension and no threshold load was defined in the tests. This is another, but negligible cause of the low stiffness value at very low strains.

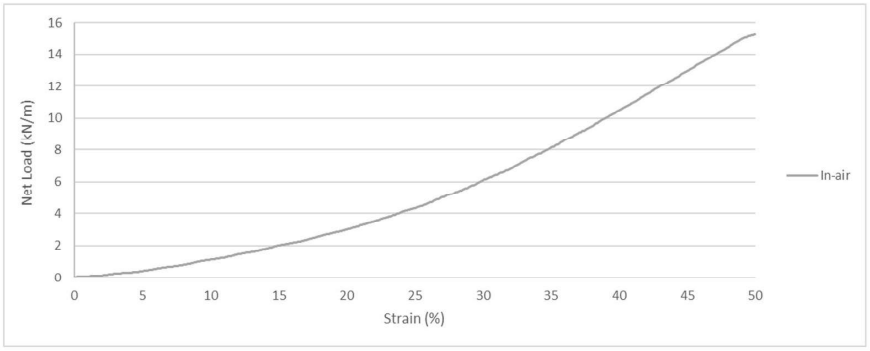


Figure 4.4. Load-strain result of in-air test on nonwoven geotextile.

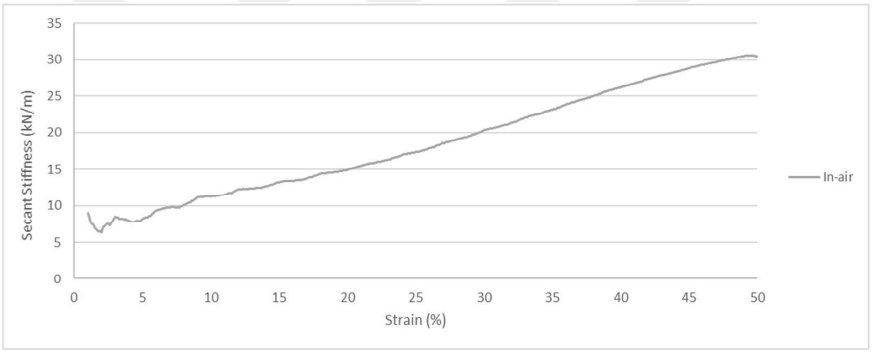


Figure 4.5. Change of secant stiffness with strain for nonwoven geotextile (in-air test).

4.2.2. Woven Geotextile

Inner (sharp) faces of the clamps were supported by nonwoven geotextile to successfully hold the woven geotextile during the test. Nonwoven support of clamp prevented both slippage and damage of specimen on the edges. This is also explained in "Chapter 3 – Methodology". Edges were marked to assess the capability of the clamp against slippage and satisfactory results were obtained. The end of test situation is shown in Figure 4.6. This white marks on both ends of the geotextile proves that there is no slippage thanks to the nonwoven cushion layer inside the clamp.

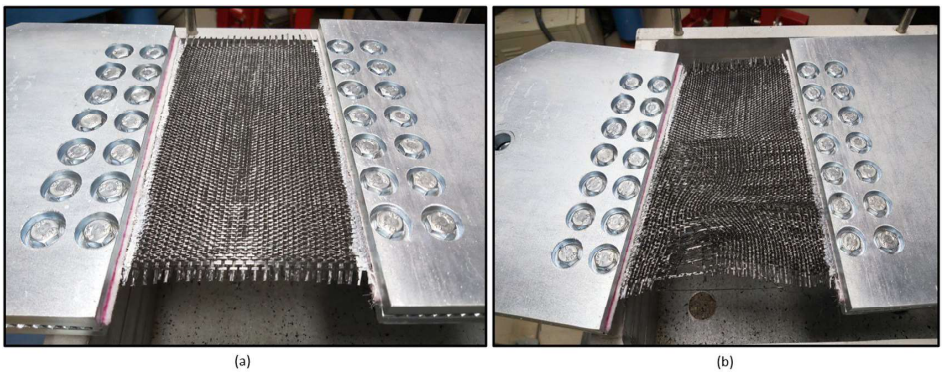


Figure 4.6. In-air test of woven geotextile specimen; (a) beginning of test, (b) end of test.

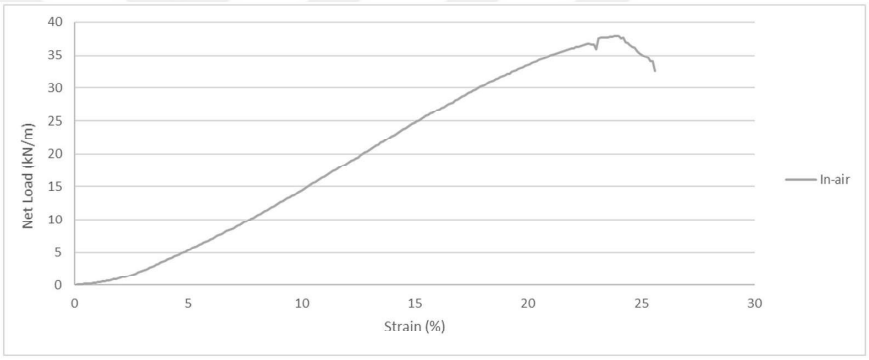


Figure 4.7. Load-strain result of in-air test on woven geotextile.

As aforementioned, no pre-tension was applied to the specimen during the test and no threshold load was defined in the test. This yields lower stiffness values in small strains (<1%) but an effective approach to see the raw results (Figure 4.7). The change in secant stiffness is illustrated in Figure 4.8.

Ultimate tensile load (T_{ult}) for the woven geotextile tested in unconfined condition is 37.9 kN/m corresponding to an ultimate strain (ε_{ult}) of 23.9%. In the specification of the material (Tencate Geolon PP 40), the mentioned values are given as 38 40 kN/m and 17% for T_{ult} and ε_{ult} respectively. Results in the specification are obtained by following BS EN ISO 10319 standard in which strain rate is 20±5% while it is 2% in scope of this study. It is known that the decreasing strain rate causes a more

ductile behaviour in woven geotextile by increasing the ultimate strain and keeping tensile strength almost constant (Andrawes *et al.*, 1984). Because of this ε_{ult} difference (23.9% and 17%) is observed between test results and specification as expected. It can be concluded that results obtained by using the new apparatus complies with the material properties determined by the manufacturer.

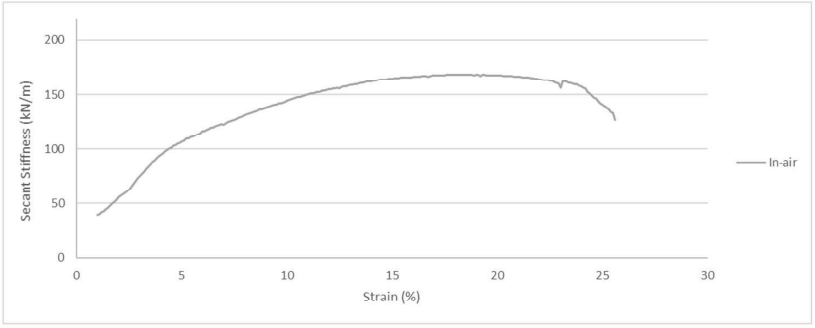


Figure 4.8. Change of secant stiffness with strain for woven geotextile (in-air test).

4.2.3. Geogrid

Clamping of the geogrid was also problematic as encountered in woven geotextile case. The nonwoven cushion solution used in woven geotextile tests leads satisfactory results when used in geogrid testing. Nonwoven geotextile cushion holds the geogrid specimen strong enough to prevent slippage without damaging its structure. Edges of specimen were marked to assess the capability of the clamp against slippage and no slippage was encountered (Figure 4.9).



Figure 4.9. In-air test of geogrid specimen; (a) beginning of test, (b) end of test.

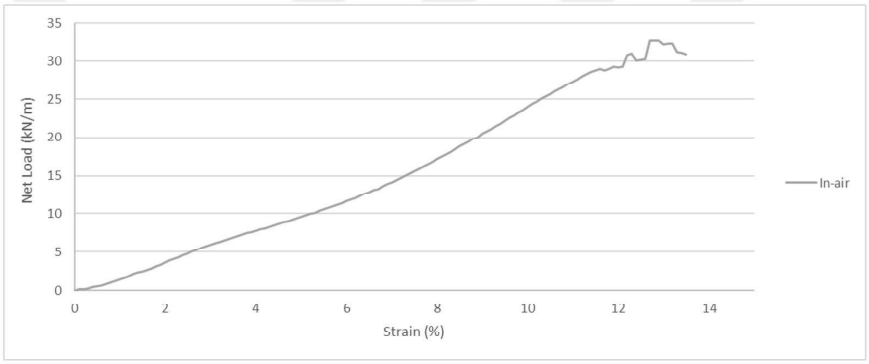


Figure 4.10. Load-strain result of in-air test on geogrid.

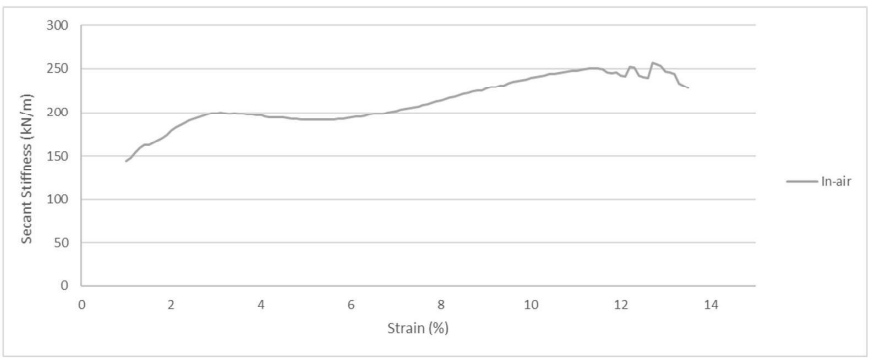


Figure 4.11. Change of secant stiffness with strain for geogrid (in-air test).

As aforementioned, no pre-tension was applied to the specimen during the test and no threshold load was defined in the test. This yields lower stiffness values in

small strains (<1%) but an effective approach to see the raw results (Figure 4.10). The change in secant stiffness is illustrated in Figure 4.11.

Ultimate tensile load (T_{ult}) for the geogrid tested in unconfined condition is 32.2 kN/m corresponding to an ultimate strain (ε_{ult}) of 13.1%. In the specification of the material (ForTex GG 35/20 P), the mentioned values are given as 35 kN/m and 10±2% for T_{ult} and ε_{ult} respectively. Results in the specification are obtained by following BS EN ISO 10319 standard in which strain rate is 20±5% while it is 2% in scope of this study. Andrawes *et al.*, 1984 studied on woven and nonwoven geotextiles and concluded that strain rate influences the behaviour of stiffer materials. Therefore, decreasing strain rate causes a more ductile behaviour in geogrid by increasing the ultimate strain and keeping tensile strength almost constant. Because of this, ε_{ult} difference (13.1% and 10±2%) is observed between test results and specification as expected. It can be concluded that results obtained by using the new apparatus complies with the material properties determined by the manufacturer.

In-air (unconfined) tests will be used as control group in investigation of in-soil behaviour of the geosynthetic reinforcements. Following sections will present the results of in-soil test results (single-layer and multi-layer tests), their evaluation and the comparison of them with in-air behaviour.

4.3. Single-Layer Tests in Sand

4.3.1. Friction Between Sand and Clamp (Clamp Pull-Out Tests)

To investigate the in-soil behaviour of the geosynthetic specimen, the specimen must stay in the soil during the test from beginning to the end. In one of the latest studies (Balakrishnan and Viswanadham, 2017), clamps are located at the edges of box which causes specimen to get out of soil after the very first strain while they are kept inside the box in most of the previous studies. As shown in Figure 4.12, having test specimen out of soil media during the test is a considerable issue for in-soil tests.

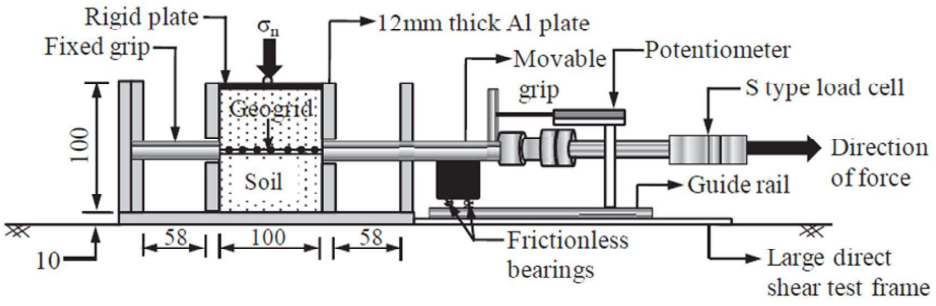


Figure 4.12. Apparatus developed by Balakrishnan and Viswanadham (2017).

The author of this study upholds the approach of keeping the clamp, thus geosynthetic specimen, inside the box during the test. The clamps are kept inside the box in the developed apparatus to prevent this side effect of the apparatus of Balakrishnan and Viswanadham (2017).

However, keeping the clamp inside the box arises another important drawback of the test. This drawback is the friction between soil and clamp during the test. There will be unignorable contribution of the clamp friction to the test results of the geosynthetics. To eliminate the influence of mentioned frictional loads to the test results, clamp pull-out tests were performed to determine the clamp friction for each scenario (Figure 4.13). Tensile load-strain curves were plotted for each pull-out test. The mentioned results are subtracted from actual test results to obtain "net tensile load-strain" curves of geosynthetics.



Figure 4.13. Clamp pull-out test in sand for single-layer tests (upper half is also filled with sand after taking the photograph).

Since in-soil single-layer tests are planned to be performed under 25, 50 and 75 kPa (also 125 for geogrid) confinement pressures, clamp pull-out tests are also performed under same pressures. Load-strain results of the tests for various confinement pressures are given in Figure 4.15. Prior to the load-strain results, the displacement of the loading plate is also checked to determine any abnormal volume change of soil (Figure 4.14). In plate displacement figures, position of the plate is shown in initial position (beginning of test) and final position (at 30% strain). Measured maximum settlements are always at the fixed clamp side (rear side) and ranges from 1.1 to 1.5 mm. These findings show that vertical pressure has a minor effect on the settlement and there is no significant change in the soil volume during the test.

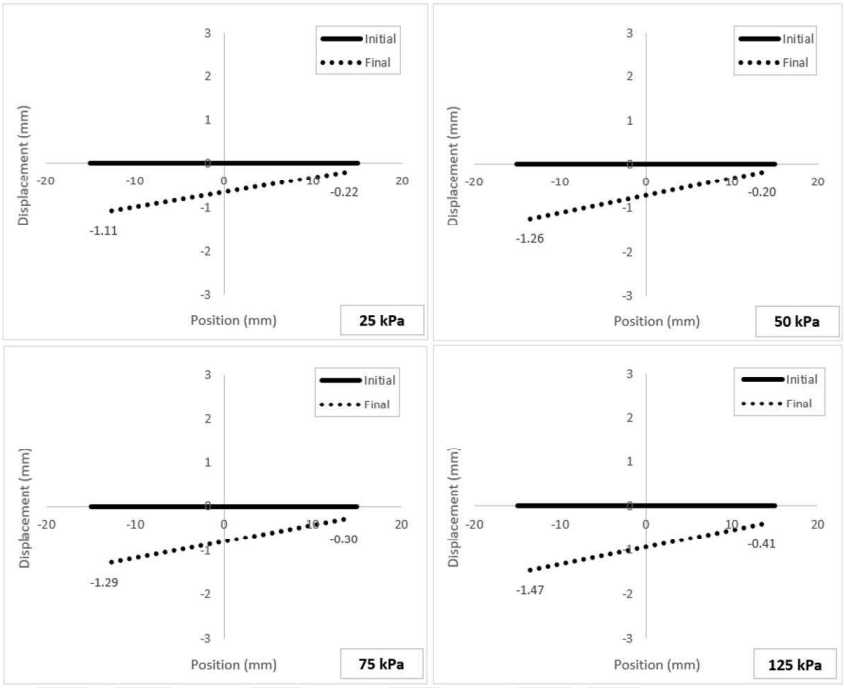


Figure 4.14. Displacement of loading plate (at 30% strain).

Since there's no specimen in pull-out tests, using the term "strain" can be confusing. However, to be able to calculate the friction at each displacement of the clamp, an equivalent strain has been defined. Here the equivalent strain is calculated with respect to the imaginary geosynthetic sample. For example, 10 mm displacement of the clamp (pull-out) is shown as 10% strain in graphs because the theoretical sample has a length of 100 mm.

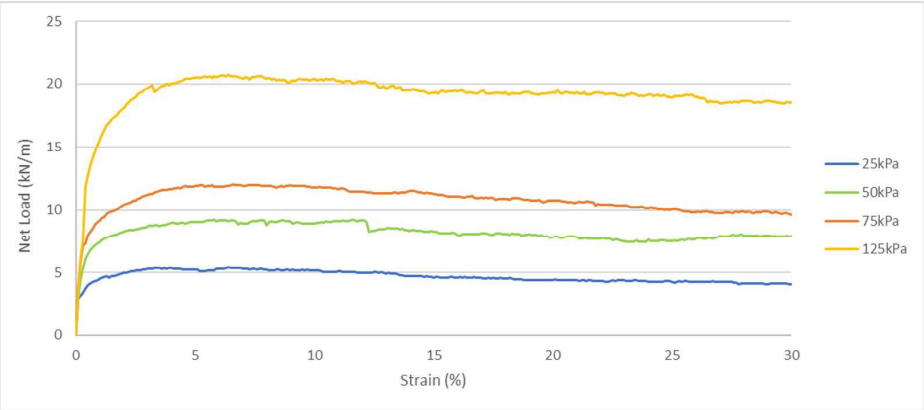


Figure 4.15. Results of clamp pull-out test in sand.

Load-strain graph of clamp friction (Figure 4.15) proves that there is a certain strain (clamp displacement) level at which frictional force fully mobilizes. This activation strain increases with increased normal stress. Under the conditions of this study, mentioned strains are lower than 5%.

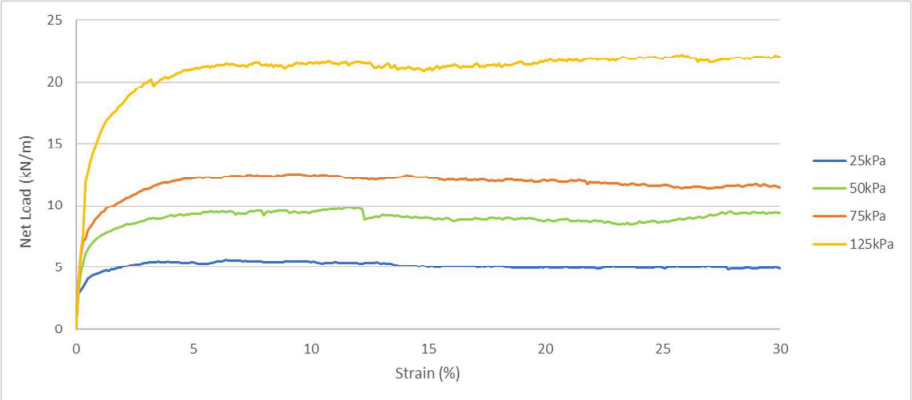


Figure 4.16. Results of clamp pull-out test in sand (after area correction).

It can be seen in Figure 4.15 that frictional forces decrease with strain. Since clamp friction test results will be directly subtracted from actual test results, clamp area correction can't be applied. In Figure 4.15, The reduction in frictional forces at higher strains caused by this approach. When area correction is applied (Figure 4.16), frictional forces become almost constant after peak value. The curves after area correc-

tion are given in Figure 4.16 just for additional information to interpret the frictional behaviour (reduction with strain in Figure 4.15) of steel clamp in sand. They are not directly used in calculations, results given in Figure 4.15 are used instead.

The friction angle between sand and clamp can be calculated by using the results of Figure 4.15. The peak frictional load between clamp and sand is determined for each normal stress situation separately and the plot showed a clear linear relationship which proves a pure frictional behaviour (intersects the origin). As a result, friction angle between sand and clamp is calculated as 19.7^o.

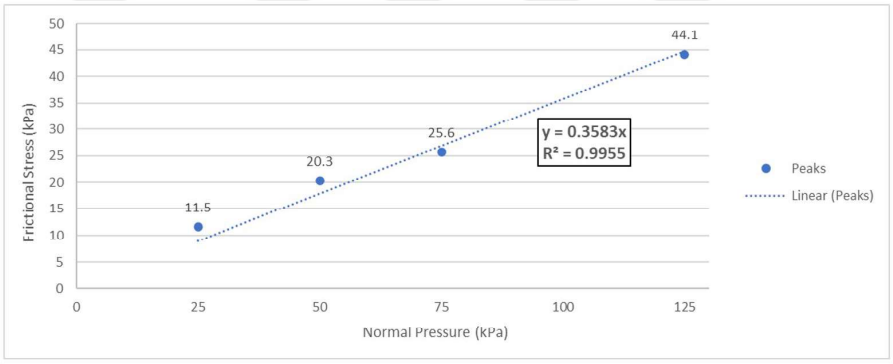


Figure 4.17. Peak tensile strength and interface friction angle.

As mentioned in Section 4.1, tensile secant modulus at 5% strain will be investigated for in-soil (confined in sand) behaviour of the geosynthetics. For this reason, secant modulus at 5% strain becomes important. The change of the stiffness is plotted in Figure 4.18.

In fact, the tensile secant modulus of the clamp friction has no physical meaning, but it is necessary to calculate the stiffness values of geosynthetic reinforcements. Therefore, equivalent $J_{sec,5}$ value for clamp friction was calculated for various normal pressures. When secant modulus at 5% strain for clamp friction is investigated in detail, it can be observed that friction is almost directly proportional to the confinement pressure (Figure 4.18). A linear equation represents change of secant modulus at 5% with respect to the confinement (σ_n) could be derived with R^2=0.997. Thanks to the

almost perfectly linear behaviour, secant modulus at 5% can be computed as

$$J_{sec,5} = 3.31\ \sigma_n. \tag{4.3}$$

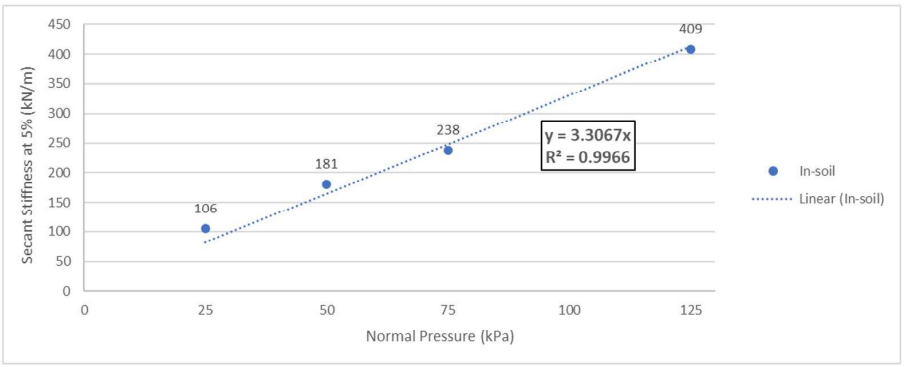


Figure 4.18. Tensile secant modulus at 5% strain for clamp pull-out in sand.

4.3.2. Behaviour of (Single-Layer) Nonwoven Geotextile Confined in Sand

Nonwoven geotextiles were subjected to wide width in-soil tensile tests in sand under confinement pressures of 25, 50 and 75 kPa. All tests were performed at a constant strain rate of 2% per minute. The initial and final situations of the specimen depicted in Figure 4.19. The photographs are taken to investigate the failure (rupture) and slippage of the reinforcement. Rupture couldn't be observed since the strains are lower than 50%. Thanks to clamp design, slippage of the reinforcement wasn't observed as well.

In this section, tensile load-strain curves and related curves are plotted to investigate the in-soil behaviour (Figure 4.21). Change of secant stiffness is also determined to establish a numerical description that represents the in-soil behaviour of nonwoven geotextile in sand (Figure 4.22). The results given in this section include net loads acting on nonwoven geotextile (clamp friction is subtracted from gross results). Nonwoven geotextile has been tested up to 50% strain values and breaking load couldn't be reached. Operational strains in design are mostly kept below 10%, so results in this

section are limited up to 30% to obtain more detailed plots in small strains. Each test is performed at least twice, and the average of the performed tests are presented in this section. Raw test results in which load-strain curves of each test is plotted separately are given in Appendix A.



Figure 4.19. Nonwoven geotextile confined in sand (upper half of box is also filled with sand); (a) beginning of test, (b) end of test.

Prior to the load-strain results, the displacement of the loading plate is also checked to determine any abnormal volume change of soil (Figure 4.20). In plate displacement figures, position of the plate is shown in initial position (beginning of test) and final position (at 30% strain). Measured maximum settlements are always at the fixed clamp side (rear side) and ranges between 1.3 and 1.6 mm. These findings show that vertical pressure has a minor effect on the settlement and there is no significant change in the soil volume during the test.

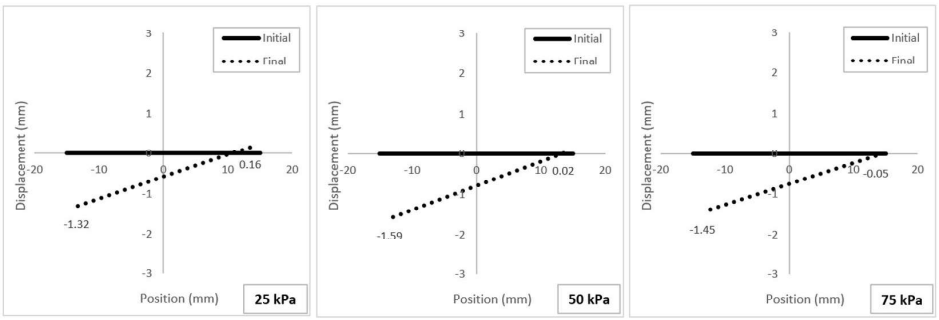


Figure 4.20. Displacement of loading plate (up to 30% strain).

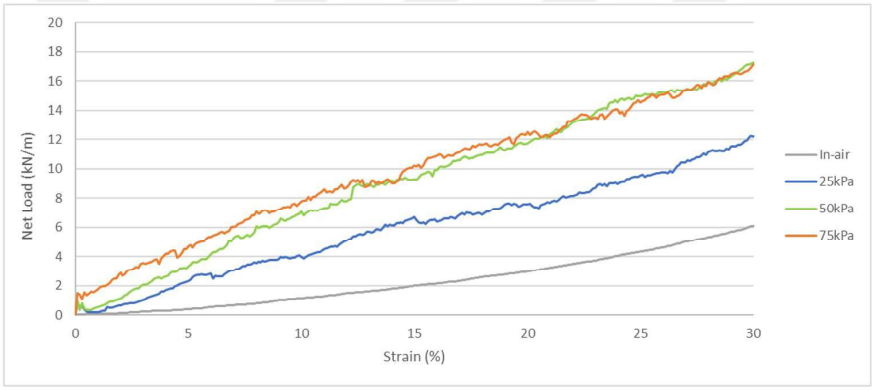


Figure 4.21. Results of tests on nonwoven geotextile in sand.

Load-strain curves in Figure 4.21 clearly shows the influence of confinement pressure on tensile behaviour of nonwoven geotextiles. The observed increase in stiffness has two reasons. They are internal and external effects of confinement. The internal effect includes the changes in the internal structure of geotextile and can be considered "inherent" while external effect is based directly on the friction between the geotextile and soil.

Nonwoven geotextile used in the study is a needle-punched geotextile which has one of the loosest structures among all geotextiles. Nonwoven needle-punched geotextile is made of entangled fibers. Inherent tensile behaviour of the specimen is proportional to the bonding and friction between individual fibers, their orientation and mobility. Therefore, the effect of confinement can be explained by interpreting the change in the

geotextile structure under confinement. In detail, the change in behaviour with respect to the confinement pressure can be explained as follows.

One of the effects of the confinement is increase in inter-fiber friction. Applying confinement compresses the specimen, increases the friction between fibers and increases the overall stiffness of the specimen. This is considered the main factor of change in inherent load-strain behaviour.

Second effect is the intrusion of small soil particles in geotextile. Large openings of nonwoven needle-punched geotextile let small soil particles to intrude into geotextile. Intrusion of soil particles into fiber matrix limits fiber stretching and yields to increase in stiffness (Mendes et al., 2007). In unconfined case, the response of nonwoven geotextile to tension is the alignment of fibers during loading. Alignment of fibers and carrying the tension load in unconfined case occurs in large displacements. However, intrusion of soil into the fiber matrix prevents them from being aligned, thus they had to start carrying load without being aligned. This means that fibers start to carry tension even in small displacements which yields an increased stiffness in overall behaviour.

Friction caused by the confinement also acts like a clamp. Therefore, a ruptured individual fiber could be hold via confinement effect. This would lead to a more progressive failure mechanism and an increase in strength (Wilson Fahmy, 1993).

On the other hand, having small fictional clamps (due to confinement) along the gauge length of the specimen would have more side effects by shortening the gauge length. In general, smaller specimen size (shorter gauge length) leads to a stronger behaviour in all materials because of reduced imperfections on specimen. However, this effect can be classified as a minor effect.

Tests are performed at a constant displacement rate of 2 mm/min (2% strain per minute). Increased strain rate (due to the assumption of shorter gauge length caused

by vertical pressure) may also increase the stiffness of the test specimen. However, this is also considered a minor effect and falsifiable because Andrawes et al. (1984) proved that influence of strain rate on nonwoven geotextile is negligible.

The friction between geotextile and sand also causes an increase in stiffness. When compared to in-air test, geotextile is subjected to friction from the beginning of the test which increases the load monitored during the test.

The test is modeled by using Finite Element Method (FEM) to determine the external and internal contributions of confinement separately. Details of the FEM analyses and the evaluation of results are given in Appendix B. The results of FEM analyses showed that the stiffness of geotextile in FEM is smaller than the one measured in laboratory. This is reasonable while FEM is not capable to simulate the change in internal structure of the geotextile.

To sum up, there are two main reasons of stiffness increase in in-soil tests namely, external and internal. The first one is the influence of interface friction between the reinforcement and soil which contributes to stiffness increase significantly (Appendix B). The latter isthe influence of confinement on internal structure of reinforcement. In short, increase in fiber friction and intrusion of soil particles into fiber matrix increase the stiffness of nonwoven geotextile. It should also be noted that effect of confinement is not eternal, it can be observed up to a certain confinement pressure. The similar load strain curves at 50 and 75 kPa proves this theory. The change in tensile behaviour reduces when the vertical pressure exceeds 50 kPa.

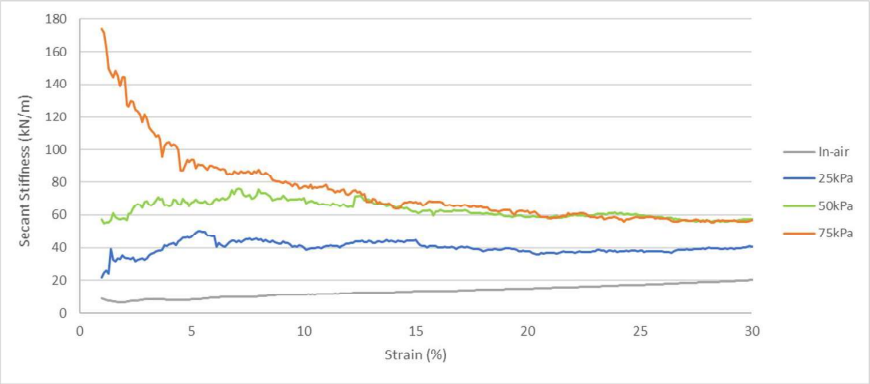


Figure 4.22. Tensile secant modulus of nonwoven geotextile in sand.

In order to evaluate the influence of confinement, change of secant stiffness with respect to confinement is also investigated (Figure 4.22). The figure shows that the nonwoven geotextile acts in a stiffer way even in small strains when the vertical pressure is 75 kPa. The reduction in stiffness at 75 kPa test can be explained by the well-established grab mechanism (confinement) at high pressure levels. The mentioned effect reduces due to the relocation of soil particles and change of the soil structure (thus load transfer on sample) because of clamp displacement and strain of geotextile (strain of geotextile causes the movement of soil). In other words, increasing vertical stress increases the stiffness in static situation (i.e., in the beginning of the test). However, with the displacement of the clamp and strain of reinforcement, this effect can't be kept. The changing volume of the sand (due to clamp displacement and strain in geotextile) also changes the pressure acting on geotextile. The relocation of particles and change of soil structure (volume) can't be observed on the plate displacement clearly. This is happening because of relatively thin shear band of sand. The displacement of plate follows almost the same trend under all vertical pressures (Figure 4.23).

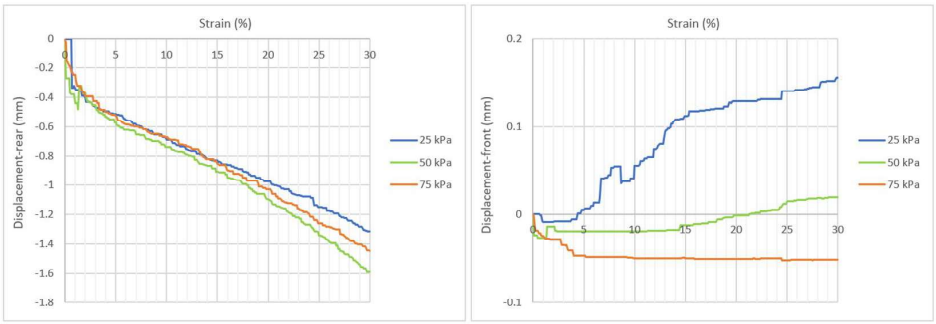


Figure 4.23. Displacement of rear and front end of loading plate with respect to strain.

Another reason of descending stiffness curve at 75 kPa can be the dilation of soil during the test. Since the sand is medium dense sand there is no proof of dilation at loading plate (Figure 4.20 and Figure 4.23) it can be troublesome to explain the stiffness reduction in terms of dilation.

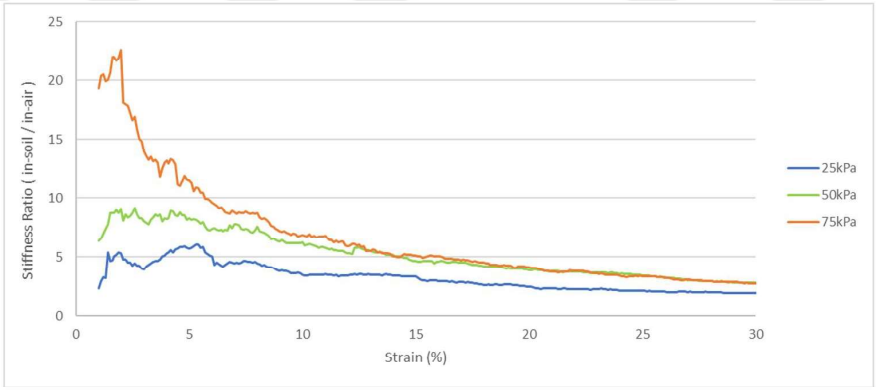


Figure 4.24. Change in tensile secant modulus with respect to unconfined (in-air) test.

In Figure 4.24, the stiffness ratio ($J_{sec,r}$) shows the change in stiffness in confined test with respect to the unconfined (in-air) situation. Tensile secant modulus at 5% strain ($J_{sec,5}$) increases 5.7, 8.3 and 11.5 times under 25, 50 and 75 kPa confinement pressures, respectively. The increase in the tensile secant modulus points that nonwoven geotextile can be used in geosynthetic reinforced structures. This finding is also beneficial to avoid the overdesign of geosynthetic reinforced structures.

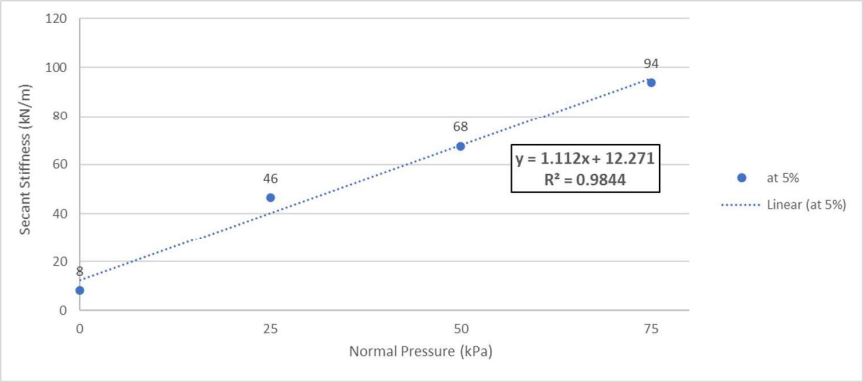


Figure 4.25. Tensile secant modulus at 5% strain for nonwoven geotextile in sand.

The change in tensile secant modulus at 5% strain is plotted in Figure 4.25. A linear equation represents change of secant modulus at 5% with respect to the confinement pressure (σ_n) could be derived with R^2=0.984. Thanks to the almost perfectly linear behaviour, secant modulus at 5% can be computed as

$$J_{sec,5} = 1.112\sigma_n + 12.3. \tag{4.4}$$

4.3.3. Behaviour of (Single-Layer) Woven Geotextile Confined in Sand

Like the nonwoven geotextile presented in previous section, woven geotextile was tested under confined conditions as shown in Figure 4.26. The figure proves that clamp with nonwoven cushions has proven a successful performance against slippage.

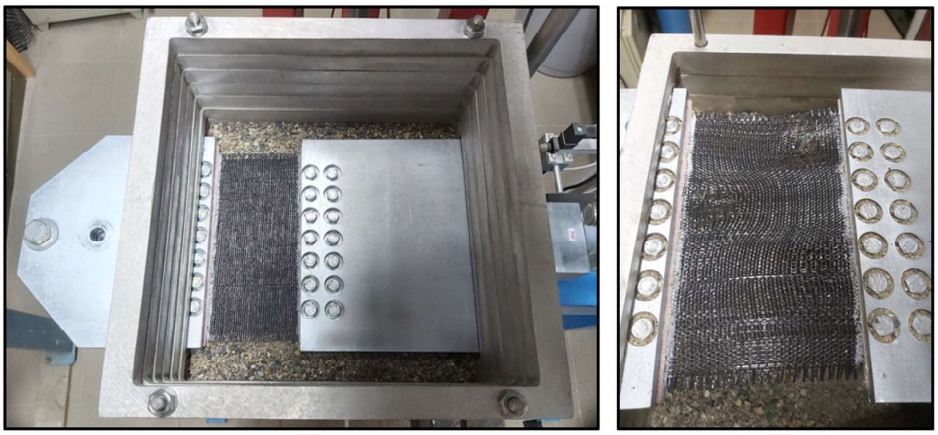


Figure 4.26. Woven geotextile confined in sand (upper half of box is also filled with sand); (a) beginning of test, (b) end of test.

Prior to the load-strain results, the displacement of the loading plate is also checked to determine any abnormal volume change of soil (Figure 4.27). In plate displacement figures, position of the plate is shown in initial position (beginning of test) and final position (at T_{ult} load). Measured maximum settlements are always at the fixed clamp side (rear side) and ranges from 1.0 to 1.3 mm. These findings show that vertical pressure has a minor effect on the settlement and there is no significant change in the soil volume during the test.

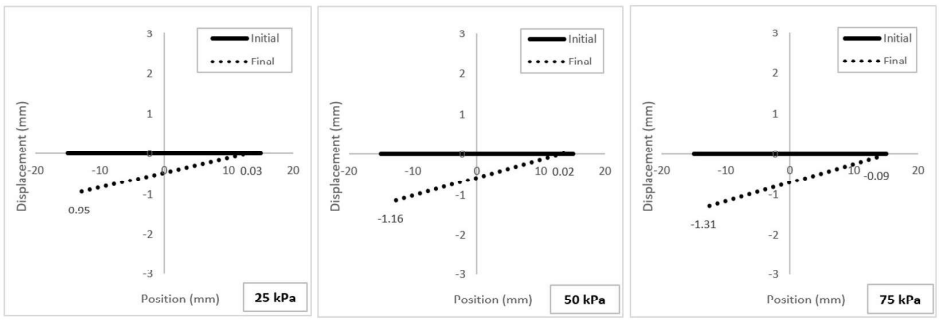


Figure 4.27. Displacement of loading plate (at T_{ult} load).

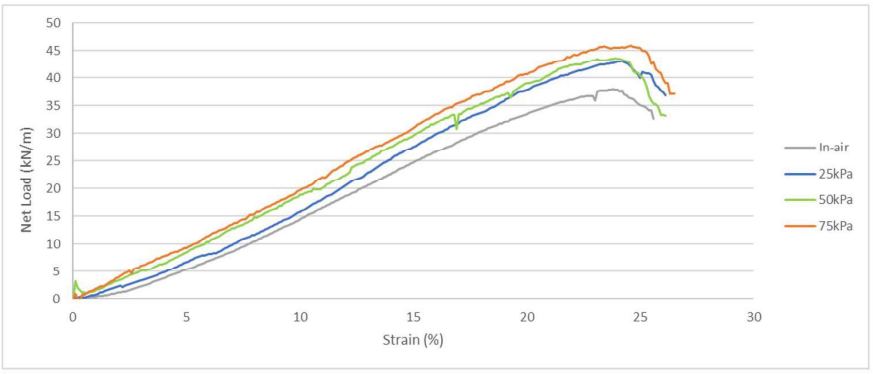


Figure 4.28. Results of tests on woven geotextile in sand.

According to the in-soil test results in Figure 4.28, confinement increases the stiffness and strength of woven geotextile. When compared to the nonwoven geotextile, the influence on woven geotextile is smaller due to its lower compressibility. Confinement has a limited influence on the internal structure of the woven geotextile due to the lower compressibility of the woven geotextile (tighter structure).

As aforementioned in previous section (nonwoven geotextile in sand), the influence of the confinement can be classified as external and internal. The interface friction between geotextile and sand and it's contribution to stiffness increase are similar to the one observed in nonwoven geotextile. As performed in nonwoven case, FEM model was built for woven geotextile tests, too. Stiffness increase in FEM results are lower than the ones observed in laboratory tests (Appendix B). This is reasonable while FEM is not capable to simulate the change in internal structure of the geotextile.

Instead of entangled fibers (like in nonwoven geotextile), woven geotextile consists of filaments aligned in weft (cross-machine direction) and warp (machine direction) directions. Filaments in warp direction pass over and under the filaments in weft direction, so filaments in load direction are not totally flat. Therefore, under in-air conditions, filaments become aligned when they are tensed. Confinement limits the filament movement and doesn't let them to be aligned under tension. Hence, geotextile behaves as a stiffer material by carrying the same load with less strain. As stated

before, filaments of woven geotextile are oriented in two perpendicular directions while nonwoven geotextile consists of randomly entangled fibers (via needle punching). This makes the woven geotextile less sensitive against vertical pressure (confinement).

It is mentioned before that confinement may reduce the gauge length by acting like fictive clamps. In addition to the structural change, confinement may also increase the strain rate of the test by decreasing the gauge length. Contrary to the nonwoven geotextiles, woven geotextiles are sensitive to strain rate during the test. Increase in strain rate increases the stiffness of the woven geotextile. Finally, stiffness increase observed in results may also be explained by increased strain rate.

Friction caused by the confinement also acts like a clamp. Therefore, a ruptured individual filament could be hold via confinement effect. This would lead to a more progressive failure mechanism and an increase in strength (Wilson Fahmy, 1993).

Ultimate tensile load (T_{ult}) for the woven geotextile tested changes from 37.9 kN/m (under 0 kPa) to 45.9 kN/m (under 75 kPa). However, corresponding ultimate strain (ε_{ult}) is almost same for all tests, 23.8% to 24.6%.

The change in behavior is more pronounced up to 50 kPa confinement pressure. Increasing the confinement pressure from 50 kPa to 75 kPa didn't influence the results as much as observed between 25 kPa to 50 kPa (although the same amount of increase in confinement pressure).

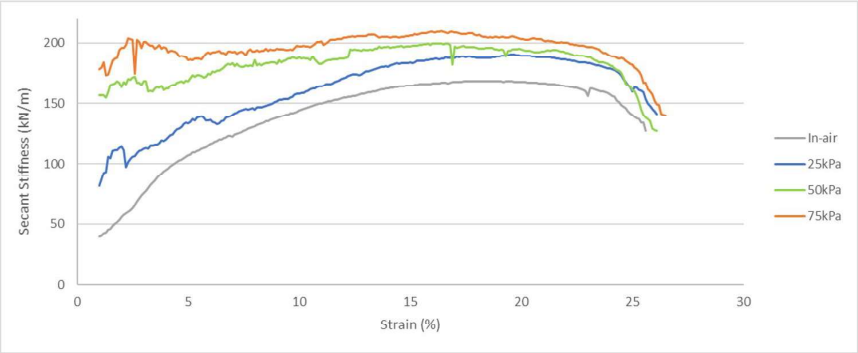


Figure 4.29. Tensile secant modulus of woven geotextile in sand.

As depicted in Figure 4.29, stiffness of the material increases at greater strain levels and this behaviour is more pronounced in lower vertical pressures. A reduced scale of "alignment effect" mentioned in nonwoven case is also visible in woven geotextile. According to the mentioned effect, filaments become aligned with increasing strain and aligned filaments act in a stiffer way by carrying load together. It means that at greater strain levels, filaments carry the load together and more uniformly.

Another reason of low stiffness at the low strains is the test conditions, namely preloading. Prior to test a preloading is not applied to the test specimen and specimen started test in a relatively loose state. Therefore, specimen demands displacement (strain in graph) to start carrying tensile load. This causes relatively low stiffness values at the very beginning of the test (at low strains in graph). In other words, increasing vertical stress increases the stiffness in static situation (or in the beginning of the test). However, with the displacement of the clamp and strain of reinforcement, this affect can't be kept. The changing geometry inside the sand (due to clamp displacement and strain in geotextile) also changes the pressure acting on geotextile.

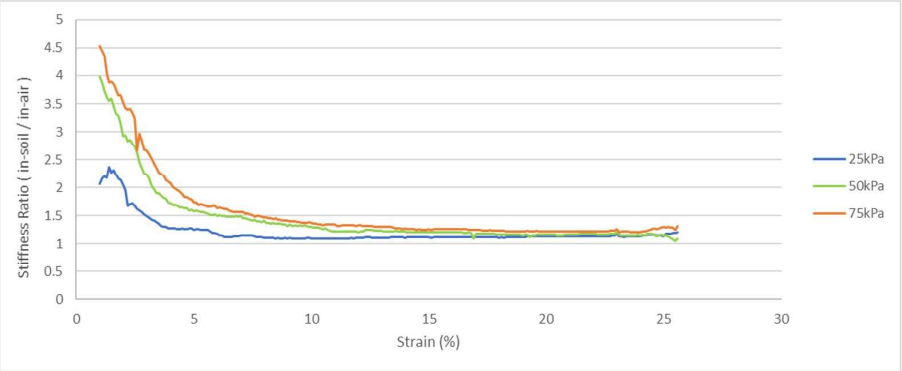


Figure 4.30. Change in tensile secant modulus with respect to unconfined (in-air) test.

The change of stiffness ratio with strain value is plotted in Figure 4.30. When stiffness ratio ($J_{sec,r}$) against in-air test is evaluated, tensile secant modulus at 5% strain ($J_{sec,5}$) increases 1.2, 1.6 and 1.7 times under 25, 50 and 75 kPa confinement pressures, respectively.

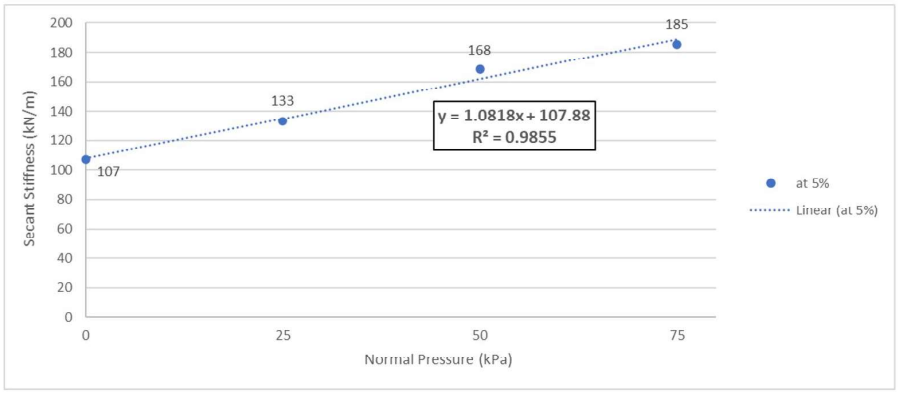


Figure 4.31. Tensile secant modulus at 5% strain for woven geotextile in sand.

The change in tensile secant modulus at 5% strain is plotted in Figure 4.31. A linear equation represents change of secant modulus at 5% with respect to the confinement (σ_n) could be derived with R^2=0.986. Thanks to the almost perfectly linear behaviour, secant modulus at 5% can be computed as

$$J_{sec,5} = 1.082\sigma_n + 107.9. \tag{4.5}$$

As given in ($J_{sec,5}$ equation of nonwoven geotextile in sand), the slope of the linear trendline is 1.112 for nonwoven geotextile. As can be seen, the slope has reduced to 1.082 in case of woven geotextile. This means that nonwoven geotextile is more sensitive to the vertical pressure. This is an expected result when the structures of two geotextiles are compared. The looser structure of nonwoven geotextile causes the more increase in inter-fiber friction under vertical pressure.

4.3.4. Behaviour of (Single-Layer) Geogrid Confined in Sand

Geogrid was tested under confined conditions as shown in Figure 4.32. The figure proves that clamp with nonwoven cushions has proven a successful performance in terms of slippage.



Figure 4.32. Geogrid confined in sand (upper half of box is also filled with sand); (a) beginning of test, (b) end of test.

Prior to the load-strain results, the displacement of the loading plate is also checked to determine any abnormal volume change of soil (Figure 4.33). In plate displacement figures, position of the plate is shown in initial position (beginning of test) and final position (at T_{ult} load). Measured maximum settlements are always at the fixed clamp side (rear side) and ranges from 0.4 to 0.8 mm. These findings show that vertical pressure has a minor effect on the settlement and there is no significant change in the soil volume during the test.

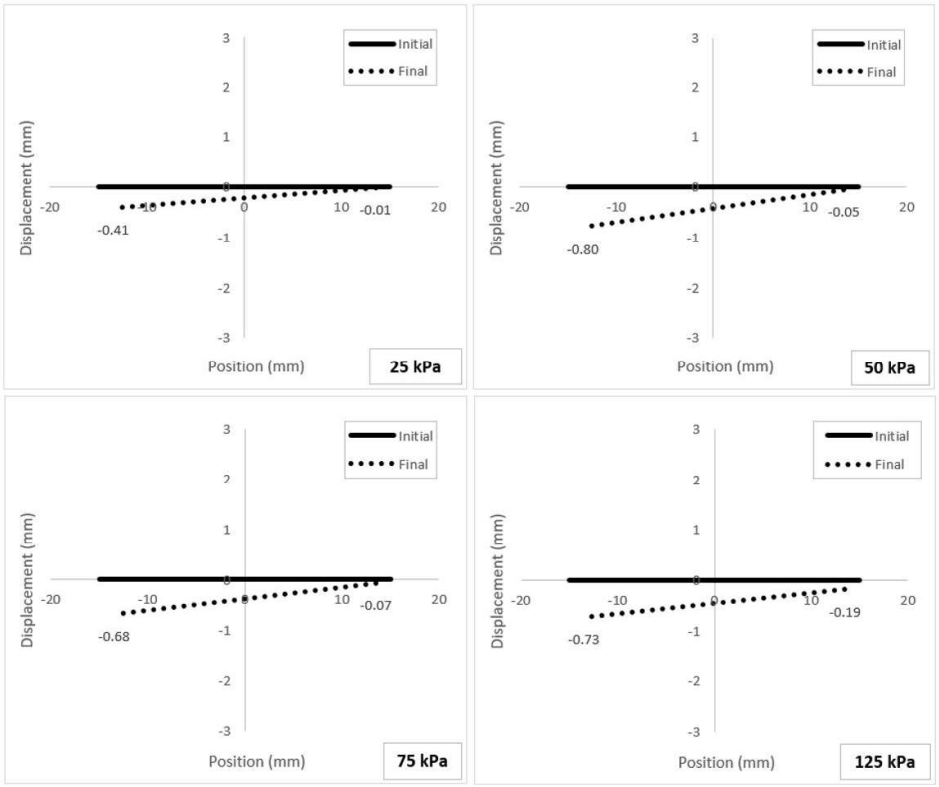


Figure 4.33. Displacement of loading plate (at T_{ult} load).

A uniaxial woven geogrid, ForTex GG 35/20 P was used in the investigations. The geogrid is made of woven polyester fibers and PVC coated. Internal structure (inter friction of polyester fibers) affects the tensile stiffness and strength of the geogrid. Therefore, confinement influences the tensile behaviour by changing the internal structure. Since internal structure of the geogrid is tight and stable it is less sensitive to confinement pressure when compared to nonwoven geotextile.

The load-strain results (Figure 4.34) showed that vertical pressure must be greater than 50 kPa to influence the behaviour. Having such a pressure threshold (50 kPa) is reasonable according to the tight structure of geogrid. However, effect of vertical pressure on change of the internal structure is limited due to the geogrid's tight structure. In other words, confinement can compress the geogrid (and increase inter-fiber friction) up to a certain level. To determine the upper boundary of confinement effect, further tests were performed under 125 kPa (this confinement is only used in assessment of

single-layer geogrid in sand). It is clear that influence of confinement reaches its upper boundary when the vertical pressure raches 75 kPa.

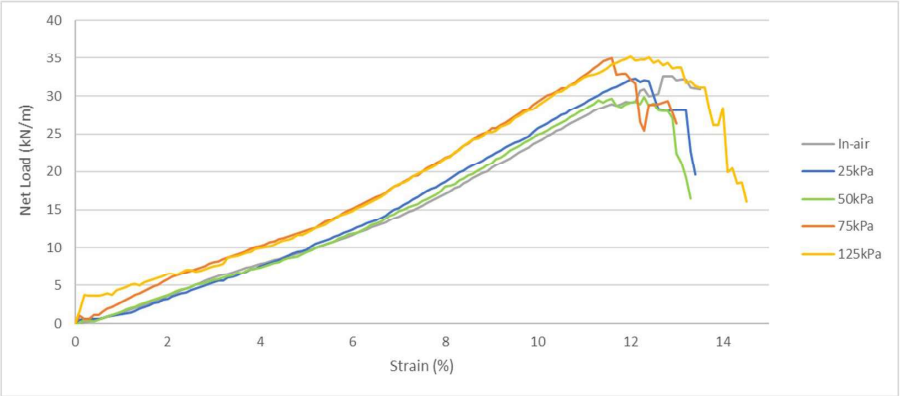


Figure 4.34. Results of tests on geogrid in sand.

In addition to the change on internal structure, another possible reason of the change in behaviour under confinement may be the fictive clamps mentioned in previous sections and/or interlocking mechanism (McGown *et al.*, 1995). Gauge length decreases with confinement during the test and strain rate increases in case of constant displacement rate. Since stiffer materials are more sensitive to strain rate (greater strain rate leads to more brittle behaviour), geogrid stiffness increases with confinement.

Ultimate tensile load (T_{ult}) for the woven geogrid is not proportional to the applied confinement pressure. Change in Tult can only be pronounced for confinement pressures greater than 50 kPa. However, corresponding ultimate strain (ε_{ult}) is almost same for all tests, 11.6% to 12.3%.

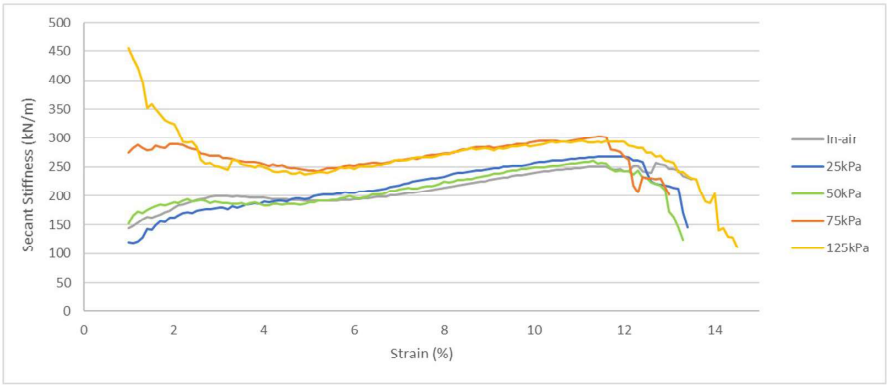


Figure 4.35. Tensile secant modulus of geogrid in sand.

In order to evaluate the influence of confinement, change of secant stiffness with respect to confinement pressure is also investigated (Figure 4.35). The figure shows that the geogrid has a descending stiffness trend in small strains at high pressures (especially in 125 kPa). The reduction in stiffness at small strains can be explained by the well-established grab mechanism (confinement) at high pressure levels. The mentioned effect reduces due to the degradation of soil structure (thus load transfer on sample) because of clamp displacement. In other words, increasing vertical stress increases the stiffness in static situation (or in the beginning of the test). However, with the displacement of the clamp and strain of reinforcement, this effect can't be kept. The relocation of the sand (due to clamp displacement and strain in geogrid) also changes the pressure acting on geogrid. The relocation of particles and change of soil structure (volume) can't be observed on the plate displacement clearly. This is happening because of relatively thin shear band of sand. The displacement of loading plate follows almost the same trend for all vertical pressures (Figure 4.36).

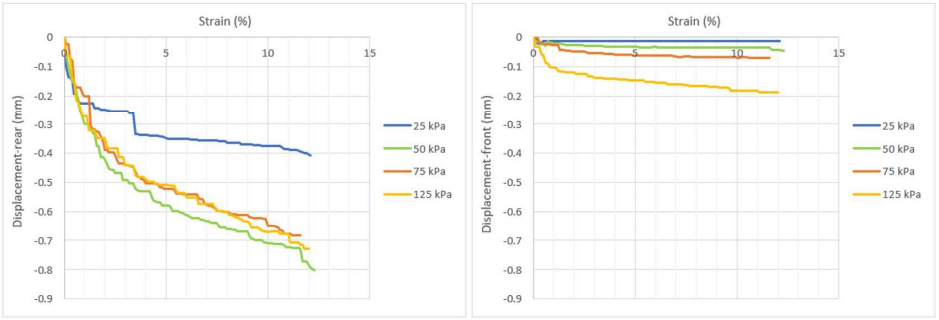


Figure 4.36. Displacement of rear and front end of loading plate with respect to strain.

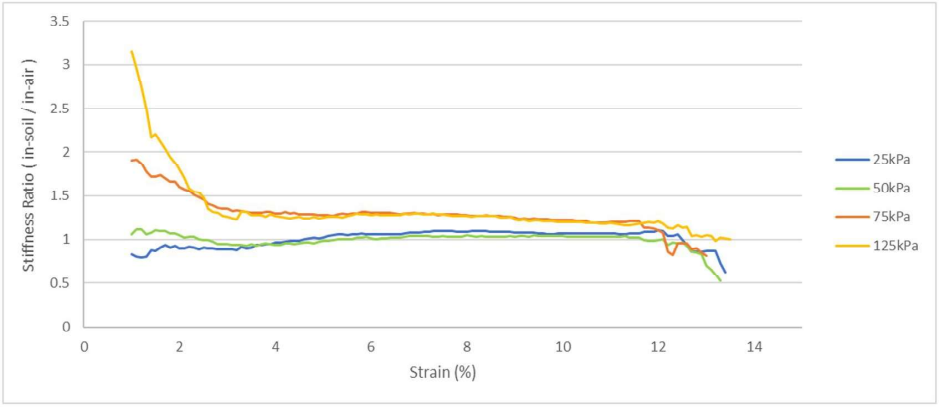


Figure 4.37. Change in tensile secant modulus with respect to unconfined (in-air) test.

The change of stiffness ratio with strain value is plotted in Figure 4.37. Stiffness ratio ($J_{sec,r}$) shows the change in stiffness in confined test with respect to the unconfined (in-air) situation. Tensile secant modulus at 5% strain ($J_{sec,5}$) increases 1.0, 1.0, 1.3 and 1.3 times under 25, 50, 75 and 125 kPa confinement pressures, respectively.

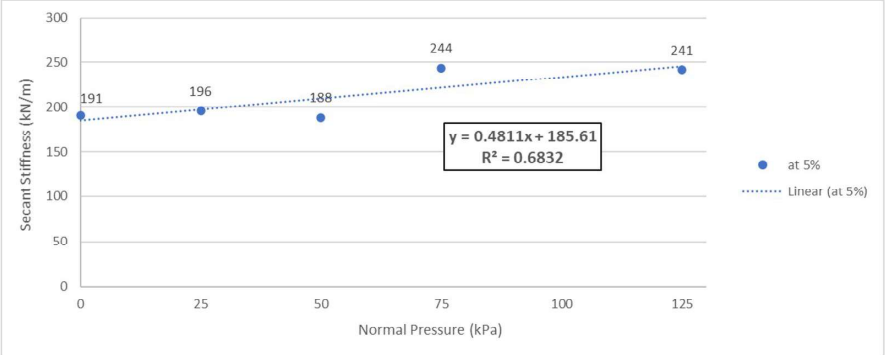


Figure 4.38. Tensile secant modulus at 5% strain for geogrid in sand.

The change in tensile secant modulus at 5% strain is plotted in Figure 4.38. A linear equation represents change of secant modulus at 5% with respect to the confinement (σ_n) could be derived with R^2=0.683. Contrary to the results obtained for nonwoven and woven geotextiles, trend is less linear for geogrids. To define the trend in a more accurate way, more test results should be used. The linear equation of $J_{sec,5}$ should be used by staying on the conservative side. Therefore, $J_{sec,5}$ can be computed as

$$J_{sec,5} = 0.481\sigma_n + 185.6. \tag{4.6}$$

The slope of the trendline of $J_{sec,5}$ is 1.112 and 1.082 for nonwoven and woven geotextiles, respectively. As can be seen, the slope has reduced to 0.481 in case of woven geogrid. This means that nonwoven and woven geotextiles are more sensitive to the vertical pressure. This is an expected result when the structures of the geosynthetics are compared. The looser structures of nonwoven and woven geotextiles cause the more increase in inter-fiber friction under vertical pressure. In addition, the contact area of geogrid with the soil is less than the geotextiles. This can also reduce the effect of confinement on behaviour of geogrid.

4.4. Single-Layer Tests in Gravel

4.4.1. Friction Between Gravel and Clamp (Clamp Pull-Out Tests)

As mentioned in Section 4.3.1., friction between clamp and soil (gravel) should be determined. To eliminate the influence of mentioned frictional loads to the test results, clamp pull-out tests were performed to determine the clamp friction for each scenario (Figure 4.39). Tensile load-strain curves were plotted for each pull-out test. The mentioned results are subtracted from actual test results to obtain "net tensile load-strain" curves of geosynthetics. Briefly, same methodology introduced in Section 4.3.1. is applied by changing the soil type as gravel.



Figure 4.39. Clamp pull-out test in gravel for single-layer tests (upper half is also filled with gravel after taking the photograph).

Since in-soil single-layer tests are planned to be performed under 25, 50 and 75 vertical pressures, clamp pull-out tests are also performed under same pressures. Load-strain results of the tests for various confinement pressures are given in Figure 4.41. Prior to the load-strain results, the displacement of the loading plate is also checked to determine any abnormal volume change of soil (Figure 4.40). In plate displacement

figures, position of the plate is shown in initial position (beginning of test) and final position (at 30% strain). Measured maximum settlements are always at the fixed clamp side (rear side) and around 0.8 mm. These findings show that vertical pressure has a minor effect on the settlement and there is no significant change in the soil volume during the test.

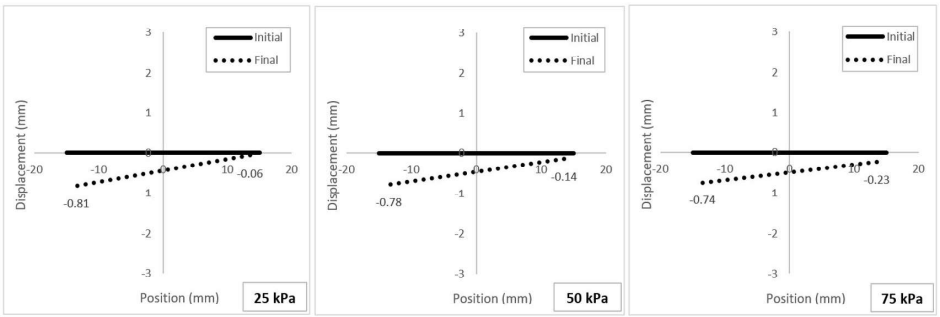


Figure 4.40. Displacement of loading plate (at 30% strain).

Since there's no specimen in pull-out tests, using the term "strain" can be confusing. However, to be able to calculate the friction at each displacement of the clamp, an equivalent strain has been defined. Here the equivalent strain is calculated with respect to the imaginary geosynthetic sample. For example, 10 mm displacement of the clamp (pull-out) is shown as 10% strain in graphs because the theoretical sample has a length of 100 mm.

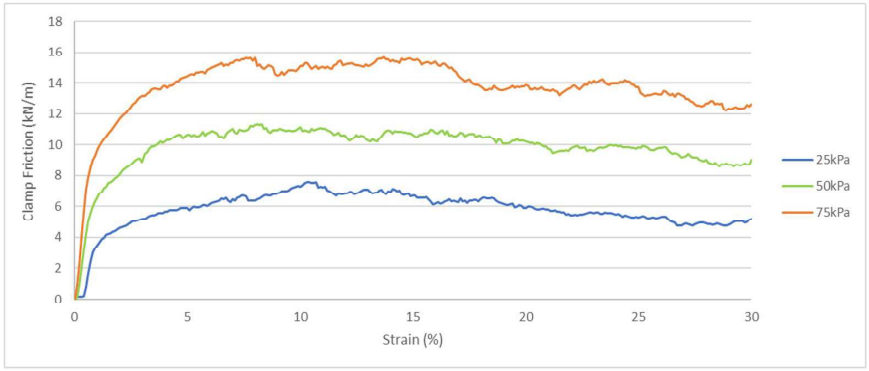


Figure 4.41. Results of clamp pull-out test in gravel.

Load-strain graph of clamp friction (Figure 4.41) proves that there is a certain strain (clamp displacement) level at which frictional force fully mobilizes. The displacement demand to reach the peak friction load is higher than the ones observed in sand (approx. <5% in sand and >5% in gravel). Additionally, in gravel, interface friction between clamp and soil is higher when compared to tests performed in sand. However, results of gravel group deviate more in each vertical pressure test set. This is caused by the more angular and irregular shape of the gravel. As also observed in sand (but in a more irregular way) there is a slightly descending trend of load at higher displacement values. This is caused by the reducing clamp area during the test as also observed in sand group. The comparison of the behaviour with respect to the soil type is investigated in Section 4.5, in detail.

The friction angle between gravel and clamp can be calculated by using the results of Figure 4.42. The peak frictional load between clamp and gravel is determined for each normal stress situation separately and the plot showed a clear linear relationship which proves a pure frictional behaviour (intersects the origin). As a result, friction angle between gravel and clamp is calculated as 25.9^o.

As given in Section 4.3.1 (friction of clamp-sand interface), the friction angle is 19.7^o for clamp-sand interface. As can be seen, the angle has increased to 25.9^o at gravel-clamp interface. Interface friction between soil and clamp has been found higher for gravel. This is a reasonable result when the angularity of the gravel is considered.

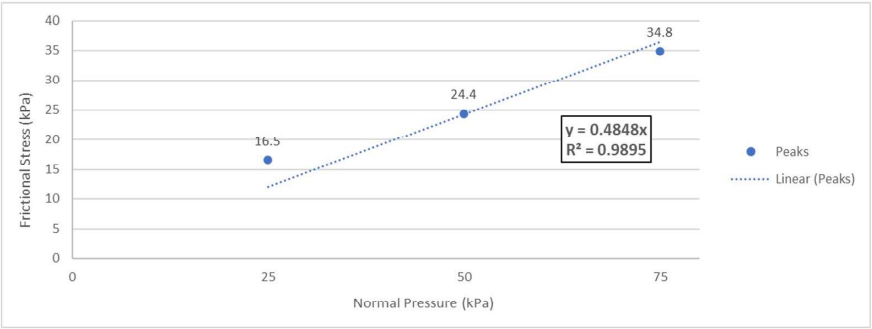


Figure 4.42. Peak tensile strength and interface friction angle.

As mentioned in Section 4.1, tensile secant modulus at 5% strain will be investigated for in-soil (confined in gravel) behaviour of the geosynthetics (Figure 4.43). For this reason, secant modulus at 5% strain becomes important.

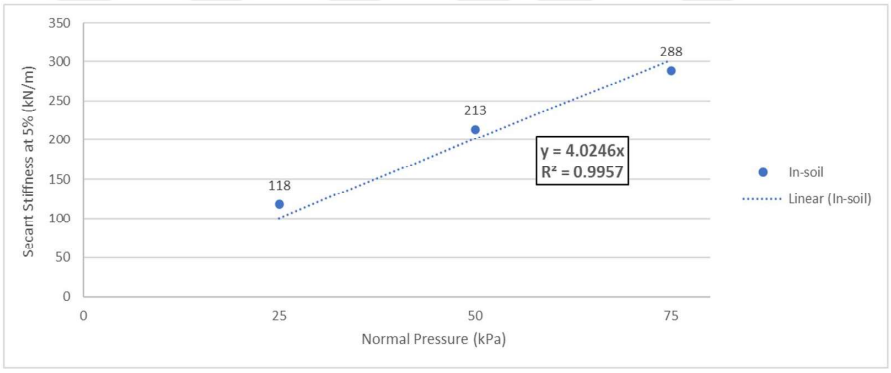


Figure 4.43. Tensile secant modulus at 5% strain for clamp pull-out in gravel.

In fact, the tensile secant modulus of the clamp friction has no physical meaning, but it is necessary to calculate the stiffness values of geosynthetic reinforcements. Therefore, equivalent $J_{sec,5}$ value for clamp friction was calculated for various vertical pressures. When secant modulus at 5% strain for clamp friction is investigated in detail, it can be observed that friction is almost directly proportional to the vertical pressure (Figure 4.43). A linear equation represents change of secant modulus at 5% with respect to the confinement (σ_n) could be derived with R^2=0.996. Thanks to the

almost perfectly linear behaviour, secant modulus at 5% can be computed as

$$J_{sec,5} = 4.025\sigma_n \tag{4.7}$$

4.4.2. Behaviour of (Single-Layer) Nonwoven Geotextile Confined in Gravel

Nonwoven geotextiles were subjected to wide width in-soil tensile tests in gravel under vertical pressures of 25, 50 and 75 kPa. All tests were performed at a constant strain rate of 2% per minute. The stage before plate placement and final situation of the specimen depicted in Figure 4.44. The photographs are taken to investigate the failure (rupture) and slippage of the reinforcement. Rupture couldn't be observed since the strains are lower than 50%. Thanks to clamp design, slippage of reinforcement wasn't observed as well.

Tensile load-strain curves and related curves are plotted to investigate the in-soil behaviour. Change of secant stiffness is also determined to establish a numerical description that represents the in-soil behaviour of nonwoven geotextile in gravel. The results given in this section include net loads acting on nonwoven geotextile (clamp friction is subtracted from gross results). Nonwoven geotextile has been tested up to 50% strain values and breaking load couldn't be reached. Operational strains in design are mostly kept below 10%, so results in this section are limited up to 30% to obtain more detailed plots in small strains. Each test is performed at least twice, and the average of the performed tests are presented in this section. Raw test results in which load-strain curves of each test is plotted separately are given in Appendix A.



Figure 4.44. Nonwoven geotextile confined in gravel; (a)beginning of test, (b)end of test.

Prior to the load-strain results, the displacement of the loading plate is also checked to determine any abnormal volume change of soi (Figure 4.45). In plate displacement figures, position of the plate is shown in initial position (beginning of test) and final position (at 30% strain). Measured maximum settlements are always at the fixed clamp side (rear side) and ranges from 0.3 to 0.7 mm. These findings show that vertical pressure has a minor effect on the settlement and there is no significant change in the soil volume during the test.

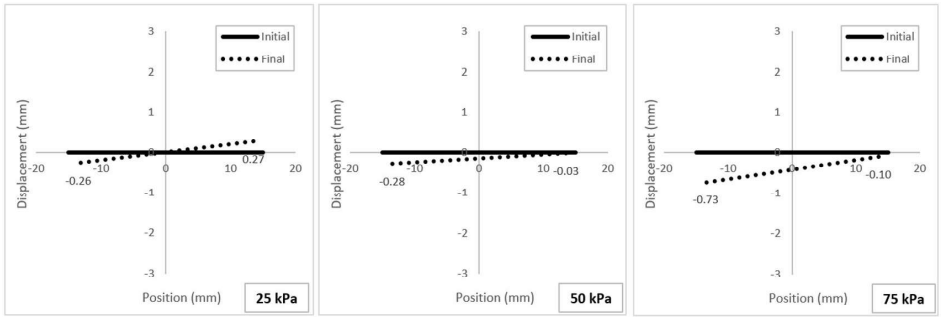


Figure 4.45. Displacement of loading plate (up to 30% strain).

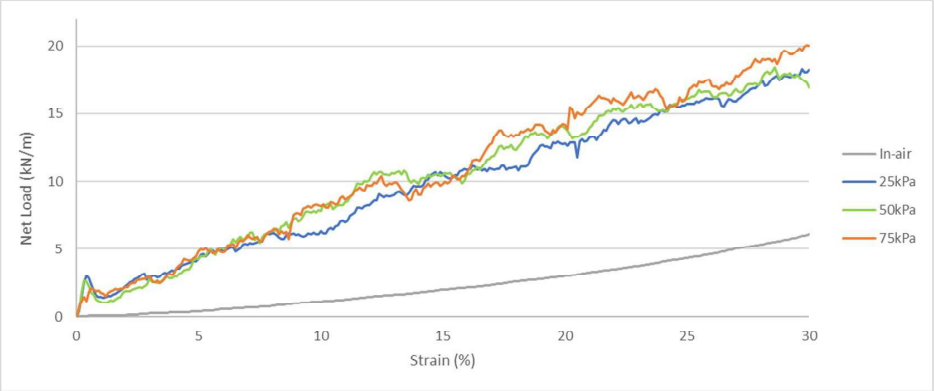


Figure 4.46. Results of tests on nonwoven geotextile in gravel.

Load-strain curves in Figure 4.46 clearly show the influence of confinement pressure on tensile behaviour of nonwoven geotextiles. Nonwoven geotextile used in the study is a needle-punched geotextile which has one of the loosest structures among all geotextiles.

Nonwoven needle-punched geotextile is made of entangled fibers. Tensile behaviour of the specimen is proportional to the friction between individual fibers, their orientation and mobility. Therefore, the effect of confinement can be explained by interpreting the change in the geotextile structure. The effects of confinement on nonwoven geotextile in gravel are mostly same with the one in sand. For this reason, evaluations of confinement effect in gravel given below are mostly same with the ones in sand. They mostly cause the same change in the material structure, but in different magnitudes. Gravel specific reasons of the change in load-strain behaviour are also explained below.

One of the effects of the confinement is increase in inter-fiber friction. Applying confinement compresses the specimen, increases the friction between fibers and increases the overall stiffness of the specimen. This is considered the main factor of change in load-strain behaviour.

Second effect is the intrusion of small soil particles in geotextile. Large openings of nonwoven needle-punched geotextile let small soil particles to intrude into geotextile. Intrusion of soil particles into fiber matrix limits fiber stretching and yields to increase in stiffness (Mendes *et al.*, 2007). In unconfined case, the response of nonwoven geotextile to tension is the alignment of fibers during loading. Alignment of fibers and carrying the tension load in unconfined case occurs in large displacements. However, intrusion of soil into the fiber matrix prevents them from being aligned, thus they had to start carry load without being aligned. This means that fibers start to carry tension even in small displacements which yields an increased stiffness in overall behaviour.

Friction caused by the confinement also acts like a clamp. Therefore, a ruptured individual fiber could be held via confinement effect. This would lead to a more progressive failure mechanism and an increase in strength (Wilson Fahmy, 1993).

On the other hand, having small fictional clamps (due to confinement) along the gauge length of the specimen would have more side effects by shortening the gauge length. In general, smaller specimen size (shorter gauge length) leads to a stronger behaviour in all materials because of reduced imperfections on specimen. However, this effect can be classified as a minor effect.

Tests are performed at a constant displacement rate of 2 mm/min (2% strain per minute). Increased strain rate (due to the assumption of shorter gauge length caused by vertical pressure) may also increase the stiffness of the test specimen. However, this is also considered a minor effect and falsifiable because Andrawes *et al.* (1984) proved that influence of strain rate on nonwoven geotextile is negligible.

To sum up, the effect of stiffness increase is mostly caused by the change in the loose structure of nonwoven geotextile. In short, increase in fiber friction and intrusion of soil particles into fiber matrix increase the stiffness of nonwoven geotextile. It should also be noted that effect of confinement is not eternal, it can be observed up to a certain confinement pressure. The similar load strain curves at 25, 50 and 75 kPa proves this

theory. The change in tensile behaviour reduces when the vertical pressure exceeds 25 kPa. Contrary to the behaviour of nonwoven geotextile in sand, geotextile reaches its highest load-strain capacity even under 25 kPa vertical pressure and it does not change by increasing pressure (up to 75 kPa).

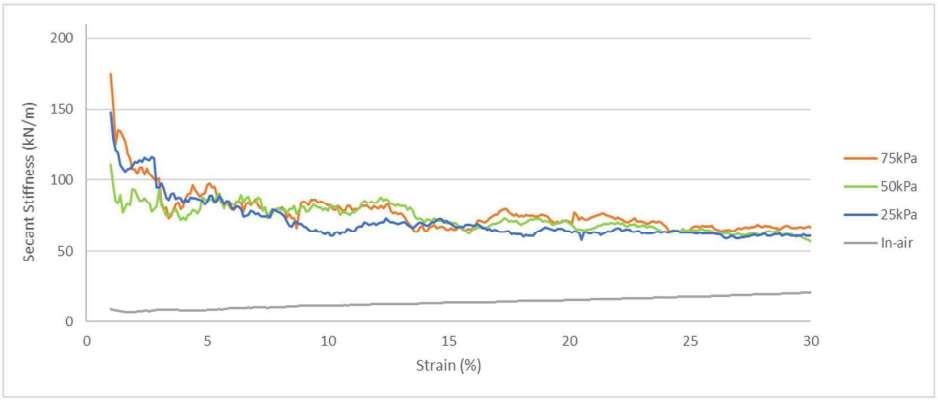


Figure 4.47. Tensile secant modulus of nonwoven geotextile in gravel.

In order to evaluate the influence of confinement, change of secant stiffness with respect to confinement is also investigated (Figure 4.47). The figure shows that the nonwoven geotextile acts in a similar way independent from the vertical pressure. The stiffness increases with the vertical pressure when compared to the in-air results but doesn't change by the pressure increments. The behaviour shows that the geotextile reaches its upper limit even in 25 kPa vertical pressure when confined in gravel.

Additionally, stiffness values are at their highest levels at the beginning of the test. This is caused by the high friction between geotextile and gravel at the beginning of the test (static situation). By increasing the displacement, soil relocates (mobilizes) and geotextile strains. As a result, friction between soil and geotextile decreases.

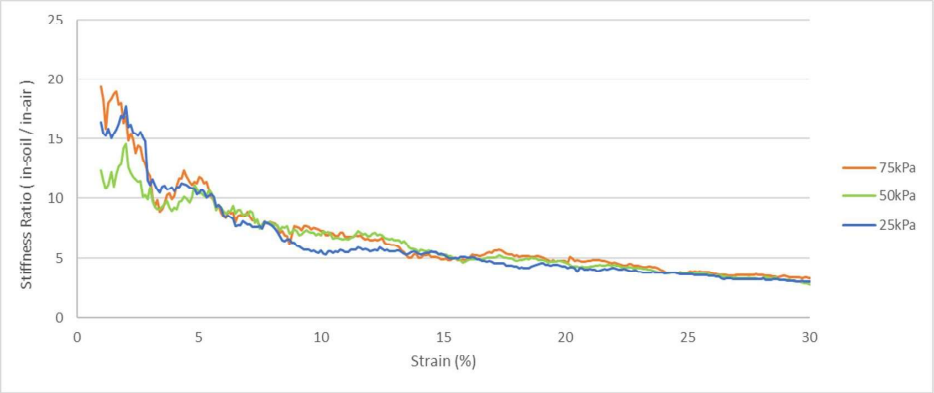


Figure 4.48. Change in tensile secant modulus with respect to unconfined (in-air) test.

In Figure 4.48, the stiffness ratio ($J_{sec,r}$) shows the change in stiffness in confined test with respect to the unconfined (in-air) situation. Tensile secant modulus at 5% strain ($J_{sec,5}$) increases 10.4 times under 25 and 50 kPa while it's 11.8 times under 75 kPa confinement pressure. The difference among in-soil secant stiffness values reduces at 10% strain. The increase in the tensile secant modulus supports the idea of using the nonwoven geotextile as a reinforcement in design of small structures. This finding is also beneficial to avoid the overdesign of geosynthetic reinforced structures.

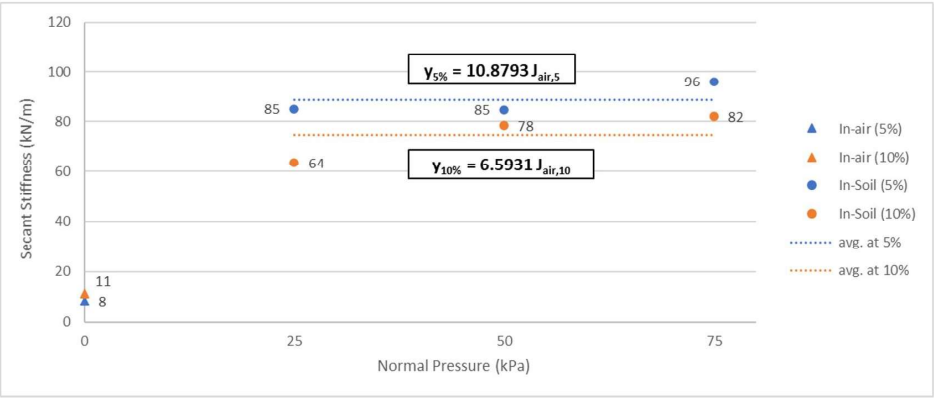


Figure 4.49. Tensile secant modulus at 5% and 10% strains for nonwoven geotextile in gravel.

The change in tensile secant modulus at 5% and 10% strain are plotted in Figure 4.49. However, a linear regression line wouldn't be realistic due to the almost

constant value of stiffness at each strain level (5% and 10% strains).

Instead of a linear regression line, the influence of confinement on secant stiffness is represented by a horizontal line and the line is defined in terms of secant stiffness values of unconfined tests ($J_{air,5}$ and $J_{air,10}$). The in-soil secant stiffness at a certain strain point is assumed to be constant at all confinement levels, because load-strain curves show that the increase in stiffness of the geotextile for gravel is achieved by the grab mechanism rather than the magnitude of the pressure (for pressures higher than 25 kPa). Therefore, it is independent from the vertical pressure (for pressures from 25 kPa to 75 kPa).

Magnitude of the horizontal line is average of in-soil secant stiffnesses for each strain level separately. As mentioned, secant stiffness at 10% strain is also investigated to interpret the results in a wider range (only for gravel cases). The mentioned relationship between in-air and in-soil stiffness values are formulated. However, performing a case specific test is suggested to be used in designs. Therefore, $J_{sec,5}$ and $J_{sec,10}$ can be computed as

$$J_{sec,5} = 10.879 J_{air,5} \tag{4.8}$$

$$J_{sec,10} = 6.593 J_{air,10} \tag{4.9}$$

respectively.

When these values are compared with the results of the test with sand (Eq. 4.4), $J_{sec,5}$ is proportionally increasing with the vertical pressure (for sand, $J_{sec,5} = 1.112\ \sigma_n + 12.3$). It can be concluded that the nonwoven geotextile reaches the upper boundary of its load-strain curve even under 25 kPa when confined in gravel. This is considered due to the mobilized grab mechanism in gravel even in low pressures, such as 25 kPa. The higher angularity of the gravel is considered the reason of the high grab potential.

4.4.3. Behaviour of (Single-Layer) Woven Geotextile Confined in Gravel

Like the nonwoven geotextile presented in previous section, woven geotextile was tested under confined conditions as shown in Figure 4.50. The figure proves that clamp with nonwoven cushions has proven a successful performance against slippage. The procedure explained in previous sections (sand case) is followed by using gravel.

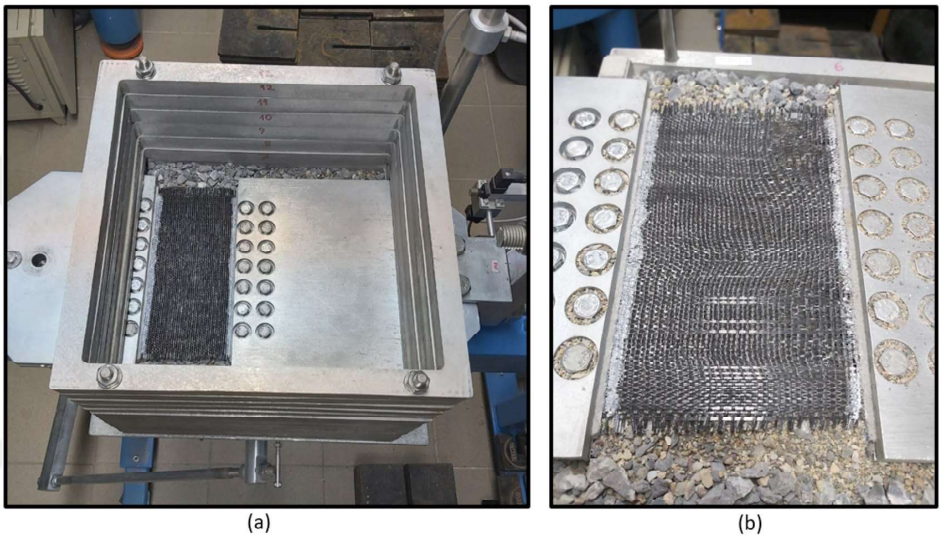


Figure 4.50. Woven geotextile confined in gravel (upper half of box is also filled with gravel); (a) beginning of test, (b) end of test.

Prior to the load-strain results, the displacement of the loading plate is also checked to determine any abnormal volume change of soil (Figure 4.51). In plate displacement figures, position of the plate is shown in initial position (beginning of test) and final position (at T_{ult}). Measured maximum settlements are always at the fixed clamp side (rear side) and around 0.4 mm. These findings show that vertical pressure has a minor effect on the settlement and there is no significant change in the soil volume during the test.

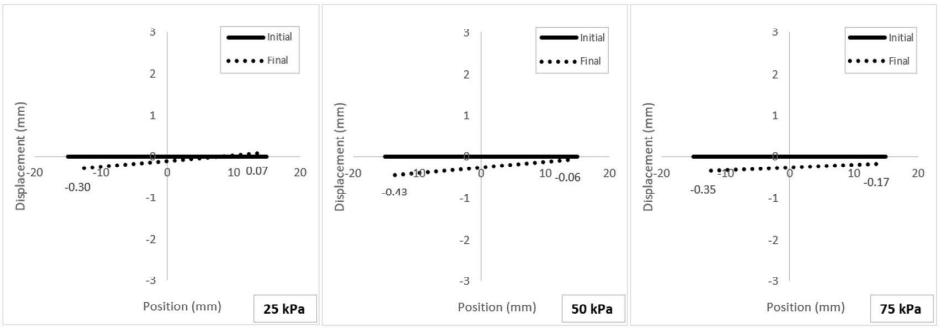


Figure 4.51. Displacement of loading plate (at T_{ult} load).

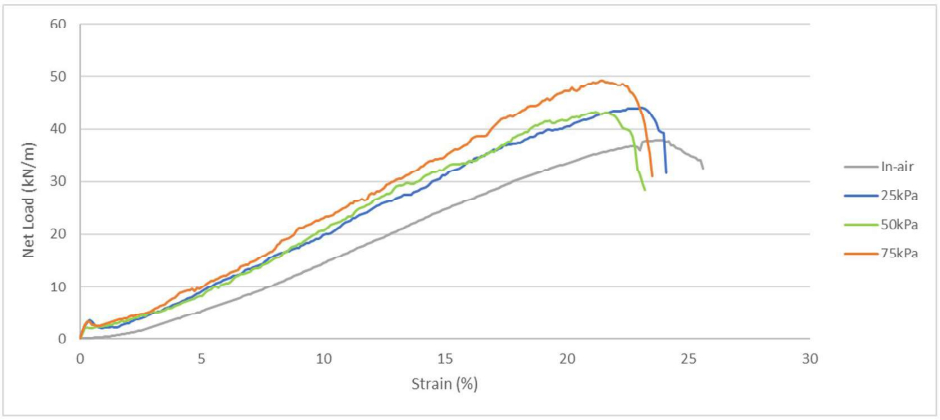


Figure 4.52. Results of tests on woven geotextile in gravel.

The effects of confinement on woven geotextile in gravel are mostly same with the one in sand. They mostly cause the same change in the material structure, but in different magnitudes. Gravel specific reasons of the change in load-strain behaviour are also explained below.

According to the in-soil test results in Figure 4.52 confinement increases the stiffness and strength of woven geotextile. When compared to the nonwoven geotextile, the influence on woven geotextile is smaller due to its lower compressibility. Lower compressibility of the woven geotextile (tighter structure) partially allows the confinement to change the internal structure of the specimen. In addition to the change of internal structure, the influence of increased strain rate due to shortened gauge length is an-

other factor. Detailed explanation about the influence of confinement on behaviour of woven geotextile is given in Section 4.3.3 (woven geotextile in sand). Those evaluations made for sand are also valid in use of gravel.

Tests in sand determined that influence of confinement is more pronounced when it is equal or greater than 50 kPa. However, even in 25 kPa, effect of confinement is clearly visible when woven geotextile is confined in gravel. The effect of soil type will be investigated in following sections and this difference is explained in that section by comparing the results. The influence of the confinement in gravel is almost same for all pressure levels from 25 to 75 kPa, when strains smaller than 8% is considered. In larger strains, influence of the confinement increases in 75 kPa and leads to a higher ultimate tensile load.

Ultimate tensile load (T_{ult}) for the woven geotextile tested in confined condition is changed even in the smallest confinement level (25 kPa). The ultimate load (T_{ult}) are 37.9, 44.1, 43.3 and 49.3 kN/m for 0, 25, 50 and 75 kPa respectively. In all confinement levels, ultimate load increases but it becomes more visible under 75 kPa. Corresponding ultimate strain values are (ε_{ult}) 23.8%, 23.0%, 21.2% and 21.5%. Increasing T_{ult} and decreasing ε_{ult} supports the conclusion of "increasing stiffness" under in-soil conditions.

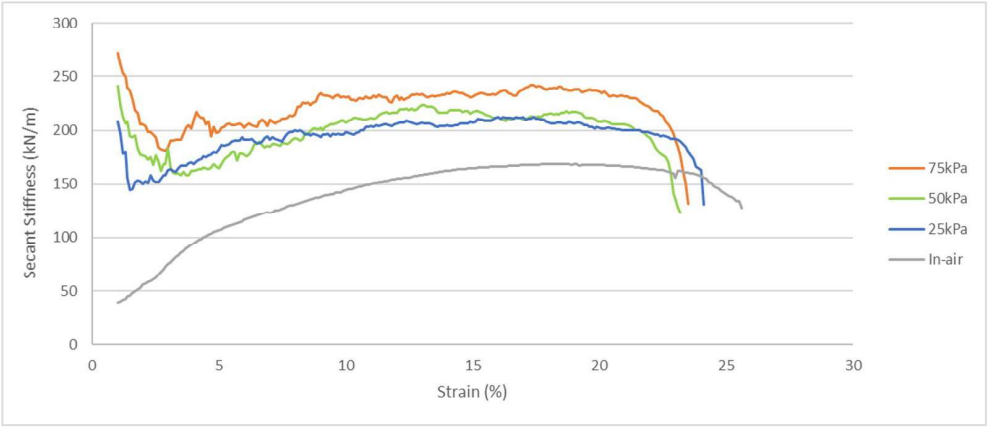


Figure 4.53. Tensile secant modulus of woven geotextile in gravel.

As depicted in Figure 4.53, there is an apparent decrease in stiffness at the beginning of the test (for in-soil tests). From the start of the test to the strains 2-4%, soil relocates and the friction behaviour changes accordingly. The displacement based on the soil relocation can also be observed at the displacement graph of loading plate, too (Figure 4.54). This means that the friction changes from static to dynamic situation following the mobilization of the soil.

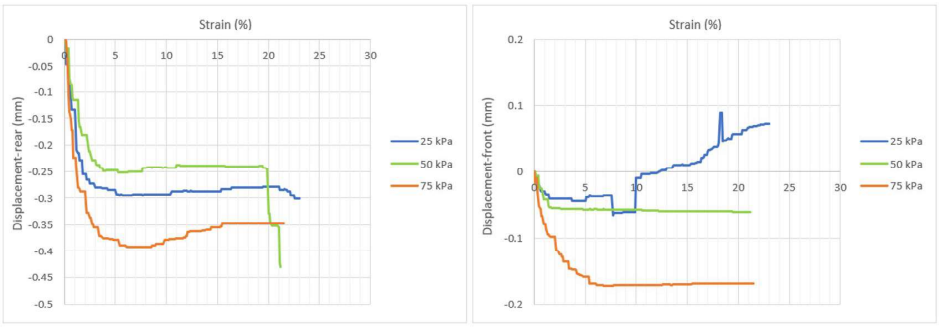


Figure 4.54. Displacement of rear and front end of loading plate with respect to strain.

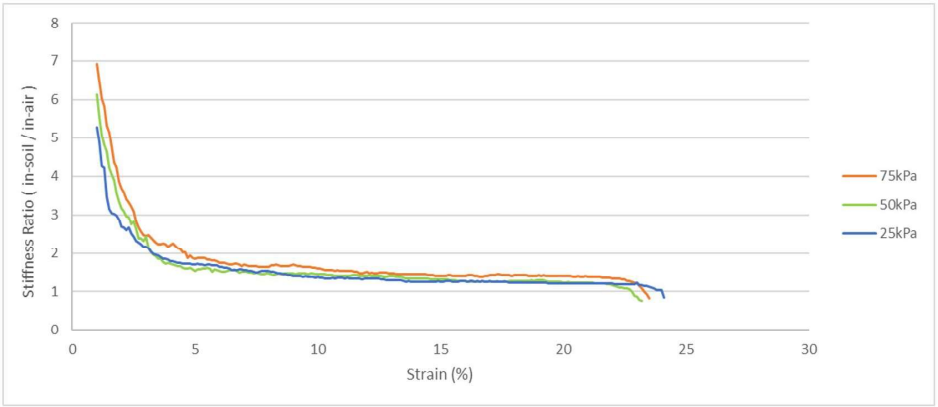


Figure 4.55. Change in tensile secant modulus with respect to unconfined (in-air) test.

The change of stiffness ratio with strain value is plotted in Figure 4.55. Stiffness ratio ($J_{sec,r}$) shows the change in stiffness in confined test with respect to the unconfined (in-air) situation. Tensile secant modulus at 5% strain ($J_{sec,5}$) increases 1.7, 1.5 and

1.9 times under 25, 50 and 75 kPa confinement pressures, respectively (1.4, 1.4 and 1.6 at 10% strain). $J_{sec,r}$ results at 5% strain in-gravel differ from the sand cases only in small pressures (25 kPa). In sand, $J_{sec,r}$ at 5% strain under 25 kPa is 1.2. The finding supports the previous finding which states that the influence of gravel is apparent even in small pressures.

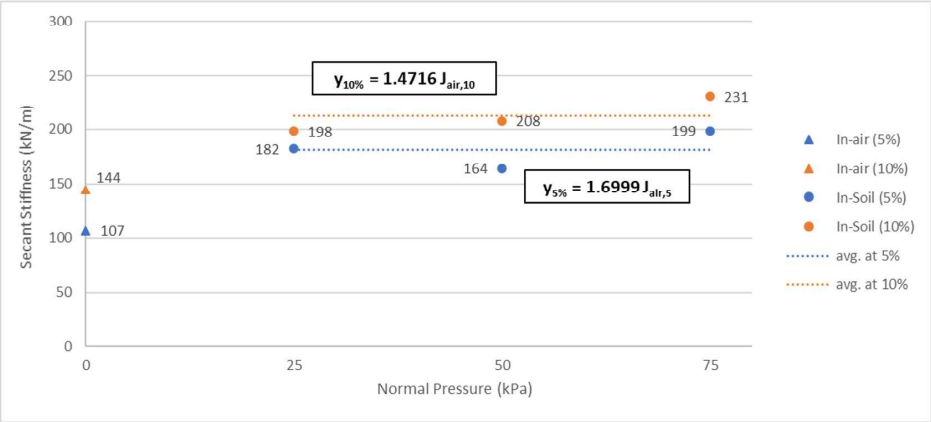


Figure 4.56. Tensile secant modulus at 5% and 10% strain for woven geotextile in gravel.

The change in tensile secant modulus at 5% and 10% strain are plotted in Figure 4.56. However, a linear regression line wouldn't be realistic due to the almost constant value of stiffness at each strain level (5% and 10% strains).

Instead of a linear regression line, the influence of confinement on secant stiffness is represented by a horizontal line and the line is defined in terms of secant stiffness values of unconfined tests ($J_{air,5}$ and $J_{air,10}$). The in-soil secant stiffness at a certain strain point (5% and 10% strain) is assumed to be constant at all confinement levels, because load-strain curves show that the increase in stiffness of the geotextile for gravel is achieved by the grab mechanism rather than the magnitude of the pressure. Therefore, it is independent from the vertical pressure (for pressures from 25 kPa to 75 kPa).

Magnitude of the horizontal line is average of in-soil secant stiffnesses for each strain level separately. As mentioned, secant stiffness at 10% strain is also investigated to interpret the results in a wider range (only for gravel cases). The mentioned relationship between in-air and in-soil stiffness values are formulated. However, performing a case specific test is suggested to be used in designs. Therefore, $J_{sec,5}$ and $J_{sec,10}$ values can be computed as

$$J_{sec,5} = 1.700 J_{air,5} \tag{4.10}$$

$$J_{sec,10} = 1.472 J_{air,10} \tag{4.11}$$

respectively.

As also observed in experiments performed in sand, stiffness increase in woven geotextile is significantly low when compared to nonwoven geotextile (due to the looser structure of nonwoven needle-punched geotextile). In addition, the woven geotextile confined in gravel is resulting in slightly higher stiffness values. The same influence of gravel is observed in nonwoven tests, too.

It can be concluded (for both geotextiles) that the geotextiles reach the upper boundary of their load-strain curve even under 25 kPa when confined in gravel. This is considered due to the mobilized grab mechanism in gravel even in low pressures, such as 25 kPa. The higher angularity of the gravel is considered the reason of the high grab potential.

4.4.4. Behaviour of (Single-Layer) Geogrid Confined in Gravel

Geogrid was tested under confined conditions as shown in Figure 4.57. The procedure explained in previous sections (sand case) is followed by using gravel. The figure proves that clamp with nonwoven cushions has proven a successful performance in terms of slippage.

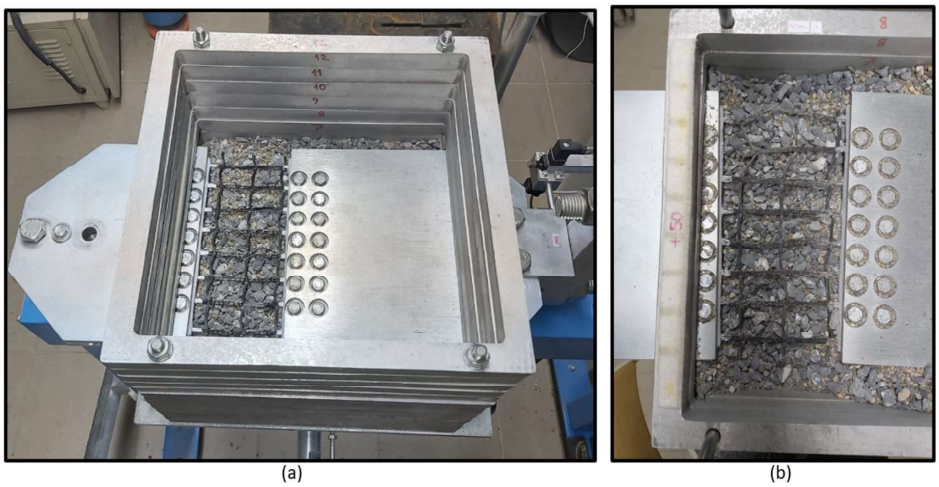


Figure 4.57. Geogrid confined in gravel (upper half of box is also filled with gravel); (a) beginning of test, (b) end of test.

Prior to the load-strain results (Figure 4.59), the displacement of the loading plate is also checked to determine any abnormal volume change of soil (Figure 4.58). In plate displacement figures, position of the plate is shown in initial position (beginning of test) and final position (at T_{ult}). Measured maximum settlements are always at the fixed clamp side (rear side) and around 0.4 mm. These findings show that vertical pressure has a minor effect on the settlement and there is no significant change in the soil volume during the test.

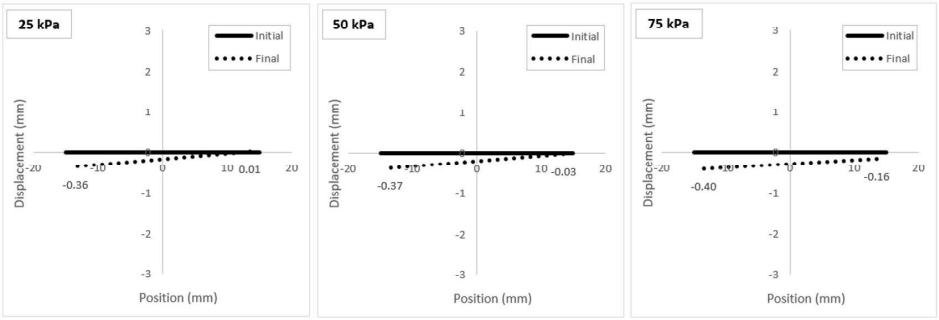


Figure 4.58. Displacement of loading plate (at T_{ult} load).

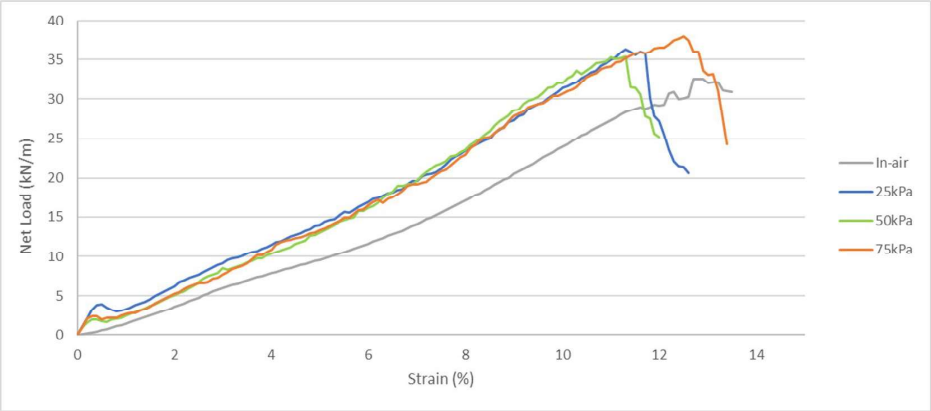


Figure 4.59. Results of tests on geogrid in gravel.

A uniaxial woven geogrid, ForTex GG 35/20 P, was used in the investigations. The geogrid is made of woven polyester fibers and PVC coated. Internal structure (inter friction of polyester fibers) controls the tensile stiffness and strength of the geogrid. Therefore, confinement influences the behaviour by changing the internal structure. Since internal structure of the geogrid is tight and stable it is less sensitive to vertical pressure when compared to nonwoven geotextile. Contrary to the results of sand group, even small confinement pressure (such as 25 kPa) has influence on tensile behaviour of geogrid. Instead of friction, this can also be explained by the grab mechanism between gravel and geogrid which is mobilized even under 25 kPa.

However, effect of confinement on change of the internal structure is limited due to the geogrid's tight structure. In other words, confinement can compress the geogrid up to a certain level. Interlocking mechanism (McGown *et al.*, 1995) between gravel and geogrid is probably another factor influencing the behaviour. Confinement and/or interlocking mechanism leads to shorter gauge length and greater strain rates. Since stiffer materials are more sensitive to strain rate (greater strain rate leads to more brittle behaviour), geogrid stiffness increases with vertical pressure.

Ultimate tensile load (T_{ult}) was increased in all confined tests with respect to the in-air experiments. Increase in T_{ult} can be pronounced for all confined levels, but it's almost equal in case of 25 and 50 kPa confinement pressures. Highest T_{ult} was

maintained under 75 kPa confinement pressure. Ultimate tensile load values are, 32.6, 36.3, 35.4 and 38.0 for 0, 25, 50 and 75 kPa confinement levels, respectively. The corresponding ultimate strain (ε_{ult}) values are 12.9%, 11.3%, 11.3% and 12.5%.

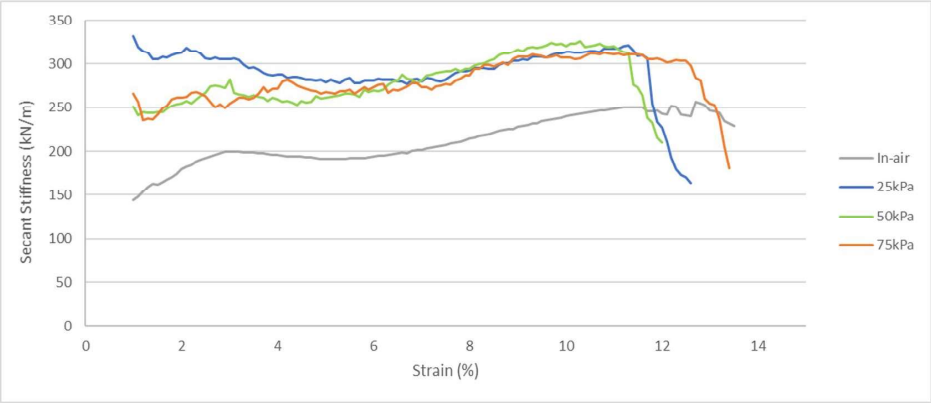


Figure 4.60. Tensile secant modulus of geogrid in gravel.

In-air samples start the test in a relatively loose state (no preloading), so the stiffness at in-air is low at the beginning of the test. This leads an ascending trend of stiffness curve up to 3% strain in Figure 4.60. At this strain level it can be considered that fibers in the geogrid ribs become aligned and start carrying the tensile load together. On the other hand, geogrid confined in gravel has more fixities than in-air case. Confinement crates extra fixity points on geogrid and reduces its gauge length. Therefore, even in small strains it can start carrying load which leads a stiffer behaviour.

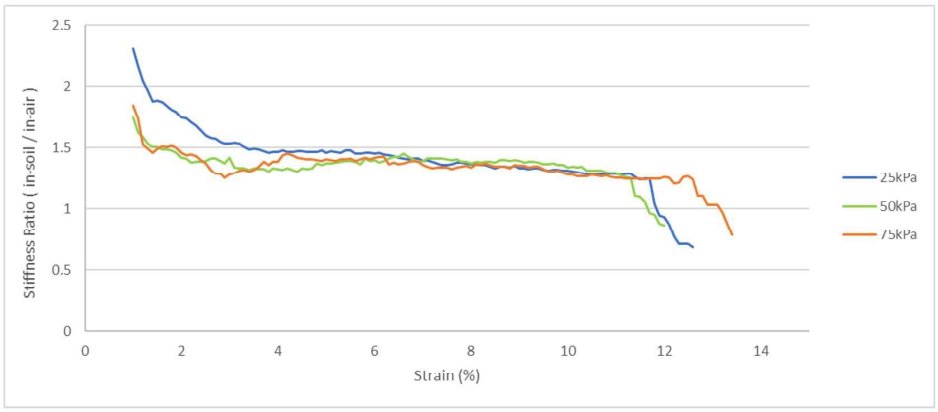


Figure 4.61. Change in tensile secant modulus with respect to unconfined (in-air) test.

The change of stiffness ratio with strain value is plotted in Figure 4.61. Stiffness ratio ($J_{sec,r}$) shows the change in stiffness in confined test with respect to the unconfined (in-air) situation. Tensile secant modulus at 5% strain ($J_{sec,5}$) increases 1.5, 1.4 and 1.4 times under 25, 50 and 75 kPa confinement pressures, respectively (1.3, 1.3 and 1.3 at 10% strain). $J_{sec,r}$ increases with respect to in-air test but almost same increment is observed for all confinement pressures from 25 to 75 kPa (1.5-1.4 times).

$J_{sec,r}$ results at 5% strain in-gravel differ from the sand cases only in small pressures (25 and 50 kPa). In sand, $J_{sec,r}$ at 5% strain is 1.0 under 25 and 50 kPa. This result supports the previous finding which states that the influence of gravel is apparent even in small pressures. While sand has no effect on the behaviour in small pressures, gravel changes the behaviour even under 25 kPa.

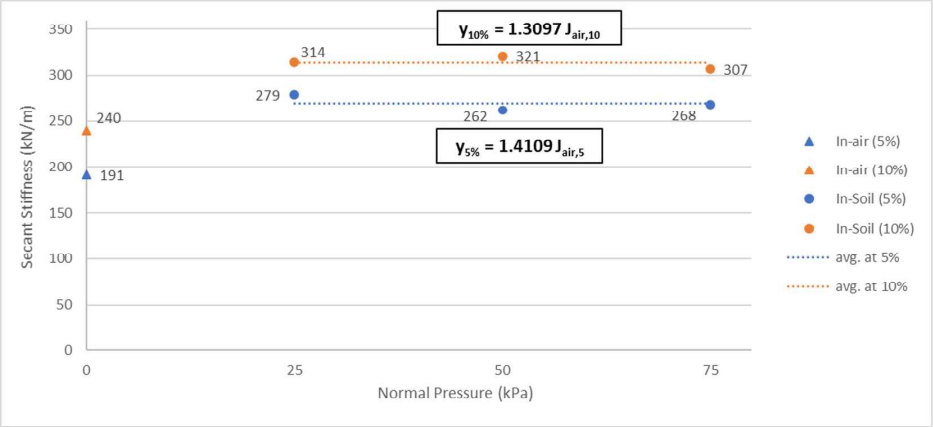


Figure 4.62. Tensile secant modulus at 5% and 10% strain for geogrid in gravel.

The change in tensile secant modulus at 5% and 10% strain are plotted in Figure 4.62. Since secant stiffness values are almost same under all confinement pressures, a linear regression line wouldn't be realistic. Instead, the influence of confinement on secant stiffness is represented by a horizontal line and the line is defined in terms of secant stiffness values of unconfined tests ($J_{air,5}$ and $J_{air,10}$). The in-soil secant stiffness at a certain strain point (5% and 10% strain) is assumed to be constant at all confinement levels, because load-strain curves show that the increase in stiffness of the geogrid for gravel is achieved by the grab mechanism rather than the magnitude of the pressure. Therefore, it is independent from the vertical pressure (for pressures from 25 kPa to 75 kPa).

Magnitude of the horizontal line is average of in-soil secant stiffnesses for each strain level separately. As mentioned, secant stiffness at 10% strain is also investigated to interpret the results in a wider range (only for gravel cases). The mentioned relationship between in-air and in-soil stiffness values are formulated but performing a case specific test is suggested to be used in designs. The consistent structure of the woven geogrid allows limited stiffness change when confined in gravel. Therefore, $J_{sec,5}$ and

$J_{sec,10}$ values can be computed as

$$J_{sec,5} = 1.411 J_{air,5} \tag{4.12}$$

$$J_{sec,10} = 1.310 J_{air,10} \tag{4.13}$$

respectively.

As also observed in experiments performed in sand, stiffness increase in geogrid is significantly low when compared to nonwoven geotextile (due to the looser structure of nonwoven needle-punched geotextile). In addition, the geogrid confined in gravel is resulting in slightly higher stiffness values (compared to sand). The same influence of gravel is observed in nonwoven and woven geotextile experiments, too.

It can be concluded for all geotextiles and geogrid used in this study that they reach the upper boundary of their load-strain curve even under 25 kPa when confined in gravel. This is considered due to the mobilized grab mechanism in gravel even in low pressures, such as 25 kPa. The higher angularity of the gravel is considered to be the reason of the high grab potential.

4.5. Effect of Soil Type on Single-Layer Tests

In previous sections, behaviour of various geosynthetics are presented and evaluated in detail. In this section, the change in behaviour is mainly evaluated with respect to the soil type used in tests. Therefore, this section only includes the brief comparison between sand and gravel single-layer test groups.

As mentioned in Section 3 - Methodology, according to USCS, Well Graded Sand (SW) and Well Graded Gravel with Sand (GW with Sand) are used in in-soil tests. In graphs below, dashed lines represent the single-layer test results conducted within gravel while continues lines represent the tests performed in sand.

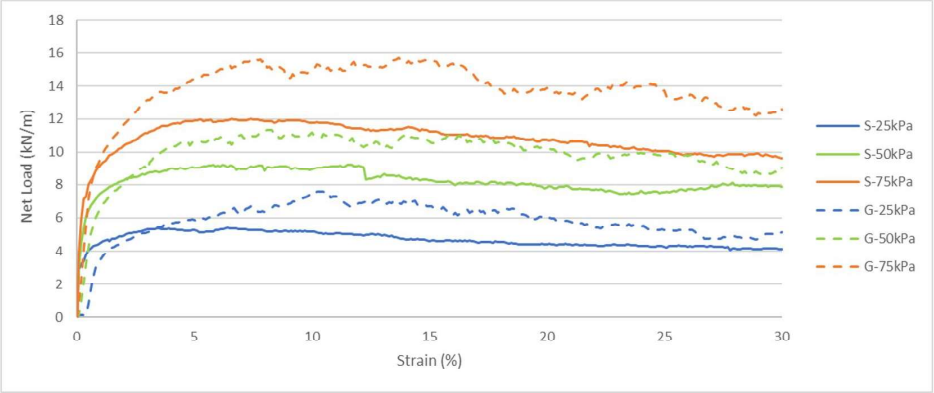


Figure 4.63. Results of clamp pull-out test in sand and gravel.

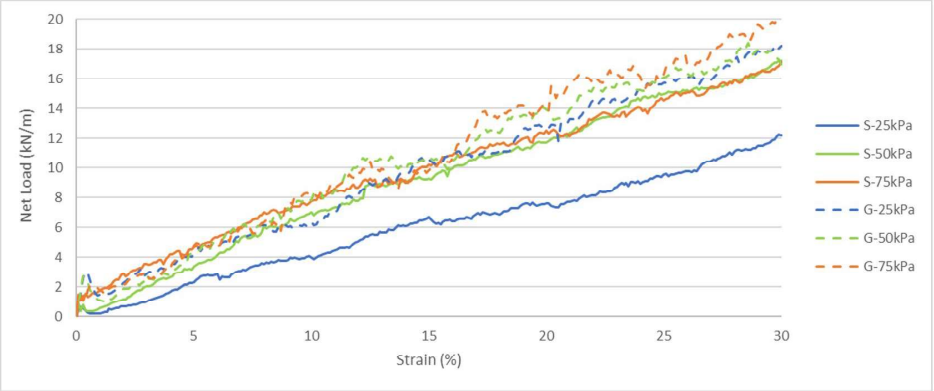


Figure 4.64. Results of tensile tests on nonwoven geotextile in sand and gravel.

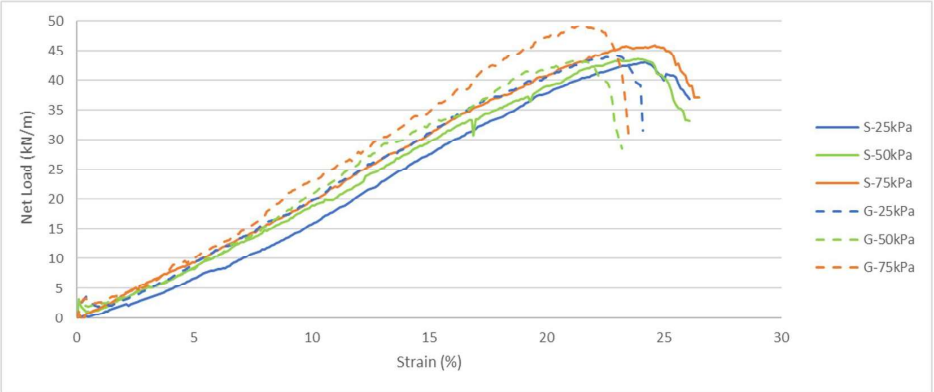


Figure 4.65. Results of tensile tests on woven geotextile in sand and gravel.

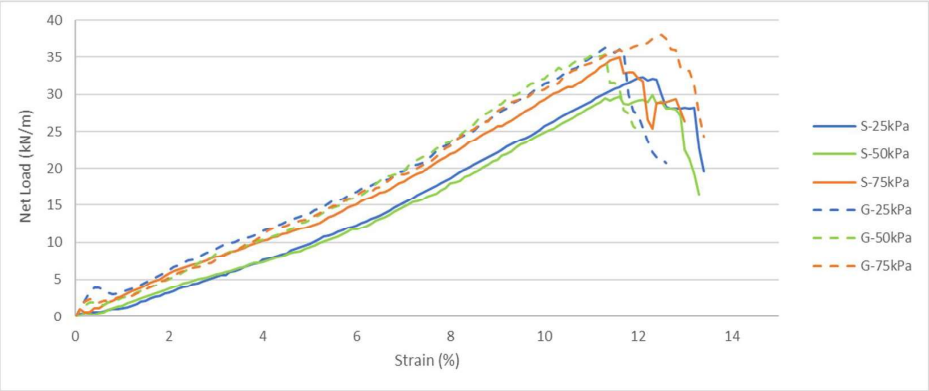


Figure 4.66. Results of tensile tests on geogrid in sand and gravel.

Figure 4.63 determines that the friction between soil and clamp is higher for gravel. This can be generalized to all geosynthetic materials. Geosynthetic wide width tensile test results indicated that behaviour of all geosynthetics is more brittle (higher stiffness) when gravel is used. In geogrids, it can also be concluded that the interlocking mechanism is more active when larger particles (gravel) are used. Based on the superior results of gravel, it is possible to conclude that particle angularity plays a significant role on the tensile behaviour of geosynthetics. In-soil geosynthetic tensile tests performed in angular soil lead higher stiffness and tensile strength unless the geosynthetic reaches the upper limit of its improvement capacity.

In general, stiffness of the geosynthetics is proportional to the confinement pressure when confined in sand. It increases with increasing pressure. Although in soil stiffness of geosynthetics are higher in gravel, it does not change with the confinement pressure. In other words, the load-strain behaviour for tests in gravel are almost same for all confinement pressure levels. Geosynthetic tested in gravel reaches its stiffest state even in the smallest confinement pressure and increasing the pressure makes no change after 25 kPa.

Results of this study also comply with the findings of Elias *et al.* (1998). Elias and co-workers stated that influence of soil on tensile behaviour of nonwoven needle-punched geotextile is more pronounced in beach sand when compared to the silty sand.

They claim that soil with larger particle size and more angular influences the tensile behaviour more.

4.6. Multi-Layer Tests in Sand

In multi-layer tests, passive reinforcements are used above and below the test sample (active reinforcement). Passive reinforcements are fixed at the rear end and free at the front end. For details of the multi-layer test method, please follow "Section 3 - Methodology". In this test set, influence of passive reinforcements on active reinforcement is investigated.

Multi-layer tests were performed under 50 kPa confinement pressure. Vertical spacing between layers are 25, 50 and 100mm. One layer of passive reinforcement is used on each side of active reinforcement. Rest of the variables (strain rate, specimen dimensions, etc.) were kept same as the single-layer tests. In graphs of this section; in-air, single-layer (under 50 kPa) and multi-layer test results are presented to be compared.

As mentioned in Section 4.3.1., friction between clamp and sand should be determined. In order to eliminate the influence of frictional loads to the test results, mentioned frictional loads between clamp and soil must be known. For this reason, clamp pull-out tests were performed to determine the clamp friction for each scenario (Figure 4.67). Dissimilar to the single-layer test, pullout tests were performed for each reinforcement separately for each vertical spacing value (25, 50 and 100 mm). Tensile load-strain curves were plotted for each pull-out test. The mentioned results are subtracted from actual test results to obtain "net tensile load-strain" curves of geosynthetics.

4.6.1. Friction Between Sand and Clamp (Clamp Pull-Out Tests), Multi-Layer Test

Some photographs from the friction tests in multi-layer case are shown in Figure 4.67. In this figure, the passive reinforcement placement and fixing them via box segments are shown. The detailed method statement is explained step by step in Section 3 – Methodology.



Figure 4.67. Clamp pull-out test in sand for multi-layer test of (a) nonwoven geotextile, (b) woven geotextile, (c) geogrid.

Clamp pull-out tests for the multi-layered case were performed under 50 kPa normal stress. Since in-soil multi-layer tests are planned to be performed under 25, 50 and 100 mm vertical spacing (s_v) values, clamp pull-out tests are also performed under same s_v values for all geosynthetic types. Load-strain results of the tests for various s_v values and geosynthetic types are given in Figure 4.71a, Figure 4.72a and Figure 4.73a.

Prior to the load-strain results, the displacement of the loading plate is also checked to determine any abnormal volume change of soil (Figure 4.68, Figure 4.69 and Figure 4.70) and the relation of displacement with the s_v value. In plate displacement figures, position of the plate is shown in initial position (beginning of test) and final position (at 30% strain). Measured maximum settlements are always at the fixed clamp side (rear side) and ranges from 0.8 to 1.2 mm. These findings show that geosynthetic type has negligible influence on the settlement of loading plate and there is no significant change in the soil volume during the test. However, there is a slight influence of s_v value to the deformations at loading plate level (top of box). It can be concluded that the passive reinforcement placed closer to the test level (clamp level) slightly reduces the deformation at distant levels (e.g. level of loading plate).

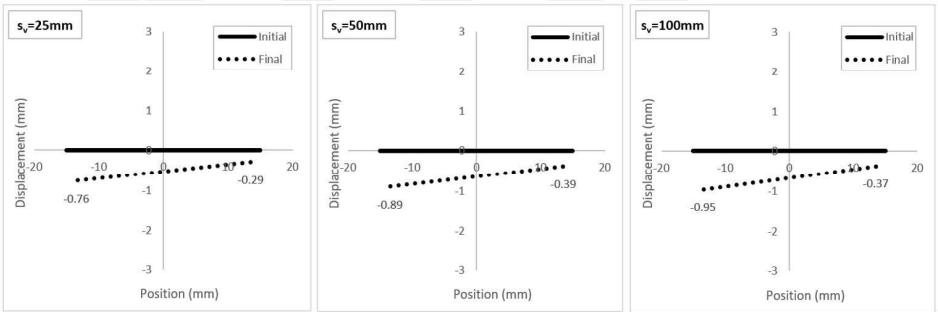


Figure 4.68. Displacement of loading plate for nonwoven geotextile (at 30% strain).

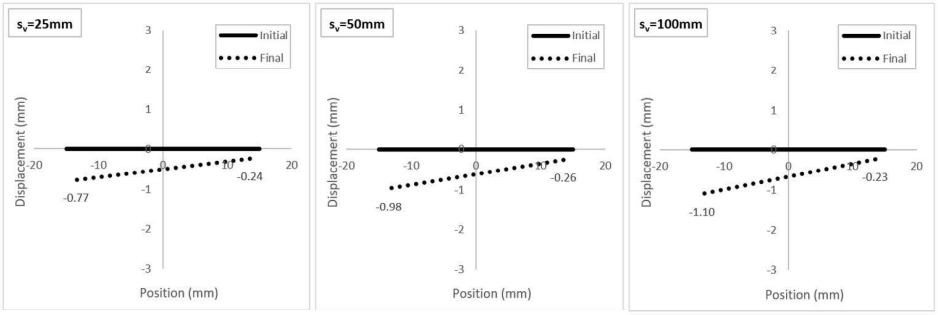


Figure 4.69. Displacement of loading plate for woven geotextile (at 30% strain).

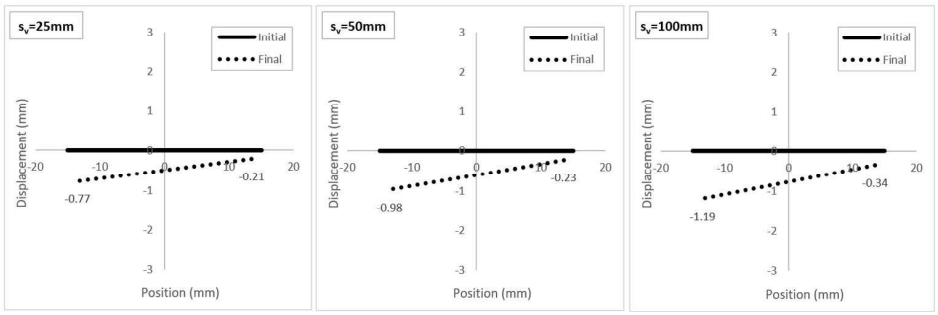


Figure 4.70. Displacement of loading plate for geogrid (at 30% strain).

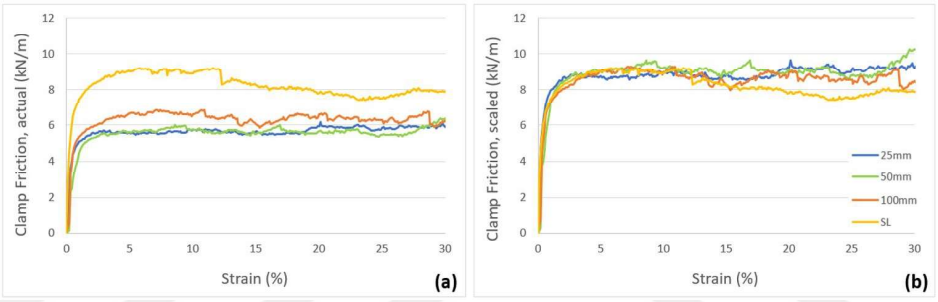


Figure 4.71. Results of clamp pull-out test in sand for nonwoven geotextile (a) actual, (b) scaled.

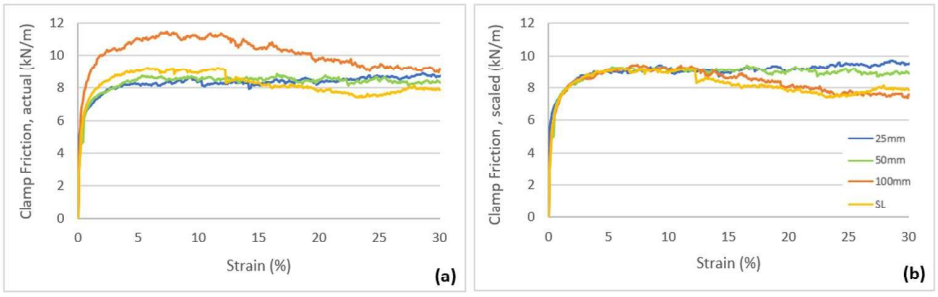


Figure 4.72. Results of clamp pull-out test in sand for woven geotextile (a) actual, (b) scaled.

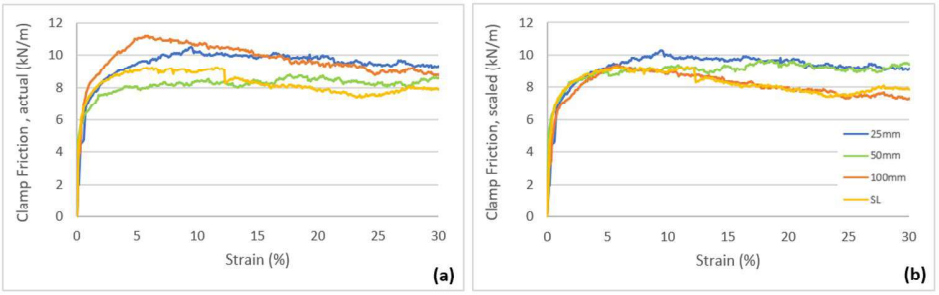


Figure 4.73. Results of clamp pull-out test in sand for geogrid (a) actual, (b) scaled.

In nonwoven geotextile, passive reinforcement reduces the frictional forces on the clamp while there is no direct relation between s_v and clamp friction for woven geotextile and geogrid (Figure Figure 4.71a, Figure 4.72a and Figure 4.73a). It can be concluded that passive reinforcement influences the pressure acting on the clamp. However, there is an apparent behaviour for all geosynthetics which shows that the frictional loads decrease in single-layer test results and s_v=100 mm results (increasing strain causes reduction in friction loads). The mentioned behaviour is more obvious when the curves of each case is scaled to the single layer situation (Figure 4.71b, Figure 4.72b and Figure 4.73b). It should be noted that scaling is only used to make the behaviour more visible, it has no physical meaning and not used in load-strain plots. The mentioned behaviour shows that passive reinforcements located close to the clamp causes a confinement effect on the clamp with the clamp's movement and this effect reduces when s_v is increased.

The clamp friction loads plotted in Figure 4.71a, Figure 4.72a and Figure 4.73a subtracted from the actual multi-layer test results (in-sand) to obtain the net load-strain curves. The influence of the passive reinforcement on the active reinforcement is investigated in following sections.

4.6.2. Behaviour of (Multi-Layer) Nonwoven Geotextile Confined in Sand

It is expected that there would be relocation of soil during the in-soil test due to the movement of the clamp and extension of the test specimen. However, it can't be

visually proved in single-layer tests (can only be hardly observed from plate displacement). Thanks to the passive reinforcement above the test specimen (in multi-layer tests), the soil relocation can be observed as deformations on the passive reinforcement located above the active reinforcement. As a result, multi-layer test method allows the researcher to observe the influence of soil relocation with respect to the distance to the test specimen.

After observations on the upper passive reinforcement, it has been proved that deformations on passive reinforcement decreases with the distance to the active reinforcement (test specimen). The maximum influence distance of the test can be considered between 50 and 100 mm (Figure 4.74). Having a passive reinforcement in influence zone digresses the results from the single-layer behaviour and it becomes closer to in-air behaviour (Figure 4.76).



Figure 4.74. Multi-layer test of nonwoven geotextile confined in sand (for 50% strain); (a) s_v=25 mm (also representative for 50 mm), (b) s_v=100 mm.

Prior to the load-strain results, the displacement of the loading plate is also checked to determine any abnormal volume change of soil (Figure 4.75). In plate displacement figures, position of the plate is shown in initial position (beginning of test) and final position (at 30% strain). Measured maximum settlements are always at

the fixed clamp side (rear side) and ranges between 1.1 and 1.3 mm (1.6 mm in single layer test, Figure 4.20). These findings show that vertical spacing has a minor effect on the settlement and there is no significant change in the soil volume during the test.

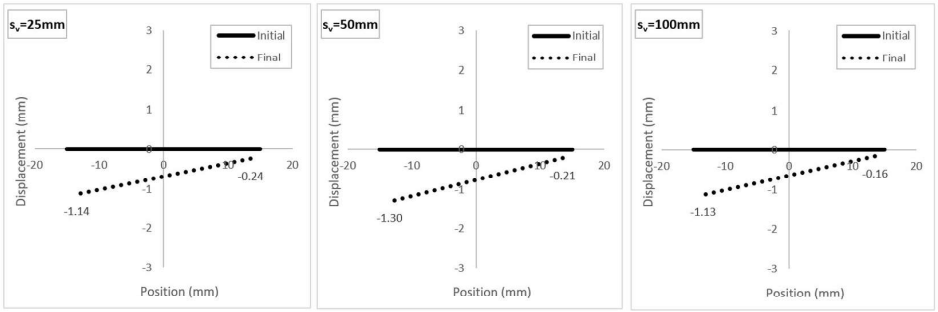


Figure 4.75. Displacement of loading plate (up to 30% strain).

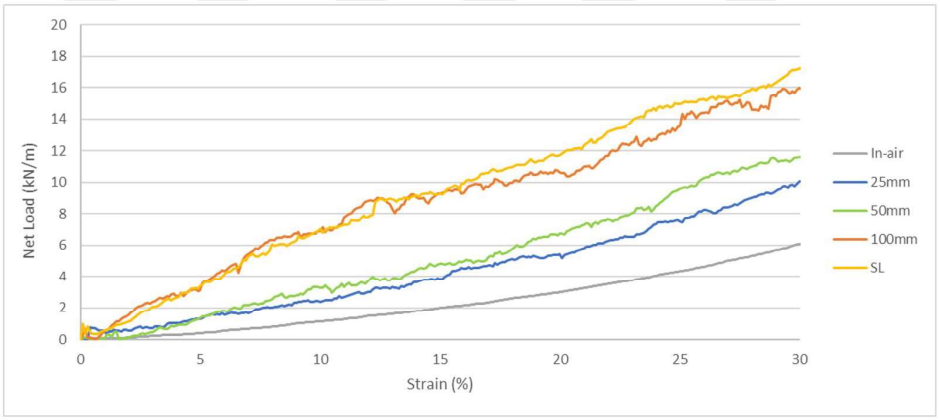


Figure 4.76. Results of multi-layer test of nonwoven geotextile in sand.

According to the Figure 4.76, passive reinforcement placed over the active reinforcement (test specimen) takes the surcharge load and reduces its effect on the test specimen. Due to the low stiffness of the nonwoven geotextile, it cannot completely take the surcharge load, so the test results differ from the in-air behaviour. The behaviour of the nonwoven test specimen is still stiffer when compared to in-air situation.

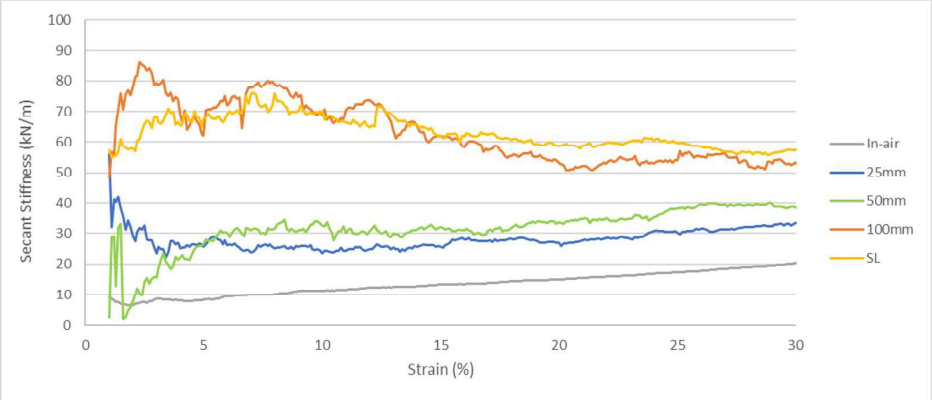


Figure 4.77. Tensile secant modulus of nonwoven geotextile in sand.

As mentioned in single-layer test results, stiffness of the needle-punched nonwoven geotextile increases with increasing strain when tested under in-air conditions. This is explained by the alignment of the individual fibers during the test.

Contrary to in-air tests, it's observed that the stiffness of the nonwoven geotextile is at its highest in the beginning of the in-soil test because the pressure and confinement reduce the strain demand of geotextile to carry the load. As also discussed in load-strain curves (Figure 4.76), Figure 4.77 shows that the behaviour of the test specimen (active reinforcement) is close to the in-air situation when vertical spacing is small, such as 25 and 50 mm (increasing stiffness with strain). On the other hand, increasing vertical spacing makes the test specimen act like it's under single-layer test conditions (decreasing stiffness with strain).

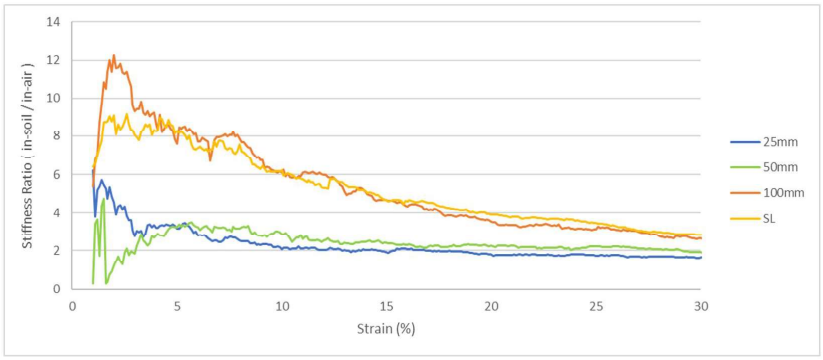


Figure 4.78. Change in tensile secant modulus with respect to unconfined (in-air) test.

The change of stiffness ratio with strain value is plotted in Figure 4.78. Stiffness ratio ($J_{sec,r}$) shows the change in stiffness in multi-layer test with respect to the unconfined in-air tests. Tensile secant modulus at 5% strain ($J_{sec,5}$) increases for every test situation when compared to in-air test.

Comparing a multi-layer test result with the single layer test result is more meaningful to determine the influence of vertical spacing. In comparison of single and multi-layer tests; $J_{sec,r}$ at 5% strain is 0.4 when vertical spacing is up to 50 mm which means reduction in stiffness with respect to single-layer test. As discussed before, having a passive reinforcement within influence zone vitiates the stiffness. $J_{sec,r}$ at 5% strain is 1.0 in case of 100 mm vertical spacing.

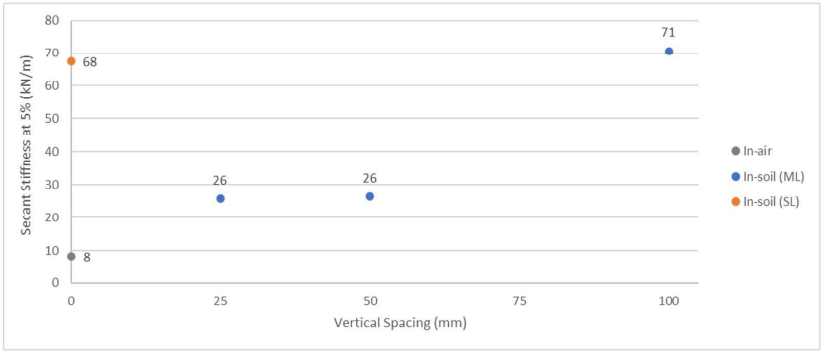


Figure 4.79. Tensile secant modulus at 5% strain for nonwoven geotextile in sand.

The change in tensile secant modulus at 5% strain is plotted in Figure 4.79. It can be concluded from the graph that a passive reinforcement in the influence zone decreases the $J_{sec,5}$. The $J_{sec,5}$ calculated in multi-layer test is 0.4 times of the one calculated in single layer test. This means that in-soil $J_{sec,5}$ decreases to almost its half when there is a passive reinforcement in the influence zone. The mentioned influence zone has been found between 50 mm and 100 mm.

4.6.3. Behaviour of (Multi-Layer) Woven Geotextile Confined in Sand

Deformation of the upper reinforcement is gradually reduced by the vertical spacing (Figure 4.80). It should be noted that deformation of upper reinforcement is based on approximately 25 mm extension of the clamp while it is 50 mm in nonwoven geotextile tests. Therefore, the deformations of nonwoven (Figure 4.74) and woven upper layer reinforcements can't be compared directly. In both cases deformed passive reinforcement carries the surcharge load thanks to the membrane effect, thus reduces the vertical pressure acting on the test specimen.

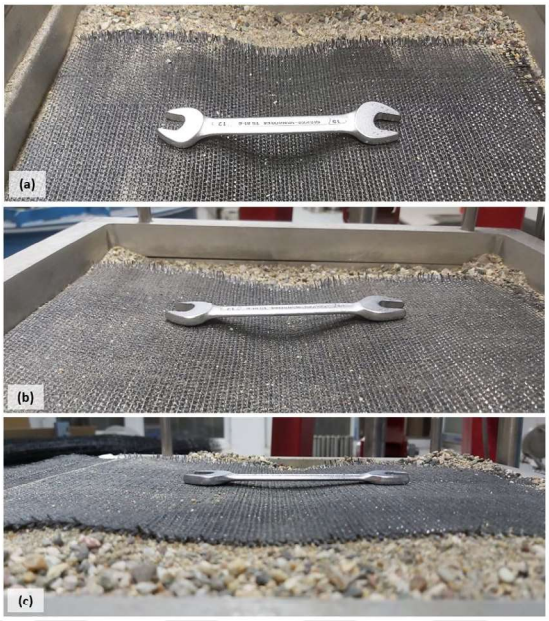


Figure 4.80. Multi-layer test of woven geotextile confined in sand (for ε_{ult} ≈26% strain); (a) s_v=25 mm, (b) s_v=50 mm, (c) s_v=100 mm.

Prior to the load-strain results, the displacement of the loading plate is also checked to determine any abnormal volume change of soil (Figure 4.81). In plate displacement figures, position of the plate is shown in initial position (beginning of test) and final position (at T_{ult} load). Measured maximum settlements are always at the fixed clamp side (rear side) and ranges from 1.0 to 1.3 mm (1.2 mm in single layer test, Figure 4.27). These findings show that vertical spacing has a minor effect on the settlement and there is no significant change in the soil volume during the test.

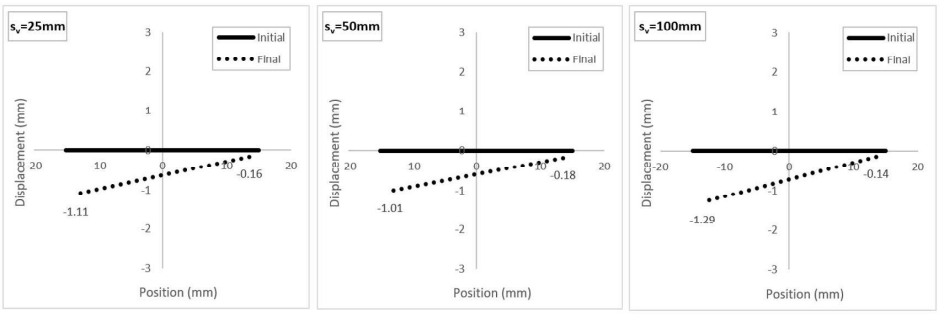


Figure 4.81. Displacement of loading plate (at T_{ult} load).

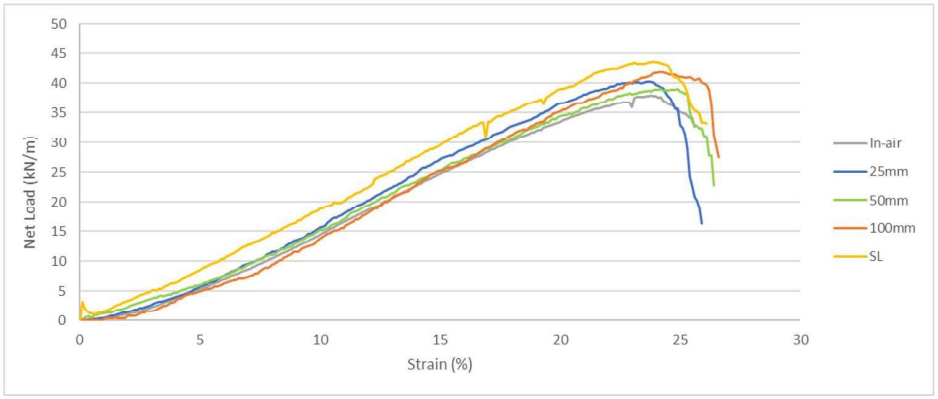


Figure 4.82. Results of multi-layer test of woven geotextile in sand.

Passive reinforcement placed over the test specimen (active reinforcement) takes the surcharge load (transfers the fixed end of reinforcement) and reduces its effect on the test specimen. Contrary to nonwoven geotextile, woven geotextile at upper layer transfers very limited load to the test specimen (due to high stiffness). Upper layer almost diminishes the effect of confinement on the test specimen and specimen acts like as it is tested under in-air conditions (Figure 4.82). The test specimen gives almost the same load-strain curve for various vertical spacing values. Since the difference is almost negligible, it can also be caused just by the deviation in specimens used in tests.

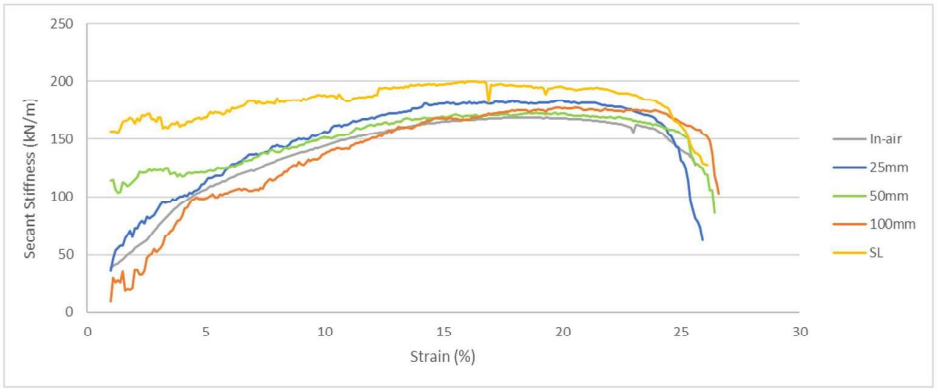


Figure 4.83. Tensile secant modulus of woven geotextile in sand.

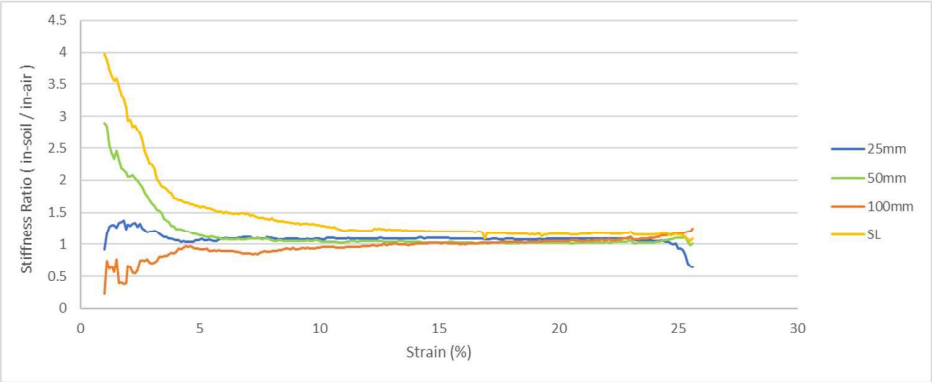


Figure 4.84. Change in tensile secant modulus with respect to unconfined (in-air) test.

The change in stiffness can be observed in both Figure 4.83 and Figure 4.84. In Figure 4.84, the stiffness ratio ($J_{sec,r}$) shows the change in stiffness in multi-layer test with respect to the unconfined in-air tests. $J_{sec,r}$ at 5% strain is almost same with in-air test when vertical spacing is 25 mm and 50 mm. However, $J_{sec,r}$ at 5% strain slightly decreases in case of 100 mm vertical spacing. The possible reasons of the mentioned reduction are explained in previous paragraph. The deviation is negligible and does not give an idea about the behaviour.

Comparing multi-layer test result with the single-layer test result is more meaningful to determine the influence of vertical spacing. In comparison of single and multi-layer tests; $J_{sec,r}$ at 5% strain is 0.7 when vertical spacing is up to 50 mm which means reduction in stiffness. $J_{sec,r}$ at 5% strain is 0.6 in case of 100 mm vertical spacing. Having a passive reinforcement within influence zone vitiates the effect of confinement on stiffness. This influence can also be observed in Figure 4.85. Woven geotextile acts like it's under unconfined conditions when there is a passive reinforcement.

The change in load-strain behaviour proves that influence zone of the woven geotextile (in sand) is greater than the one of nonwoven geotextile. The influence zone can be considered greater than 100 mm.

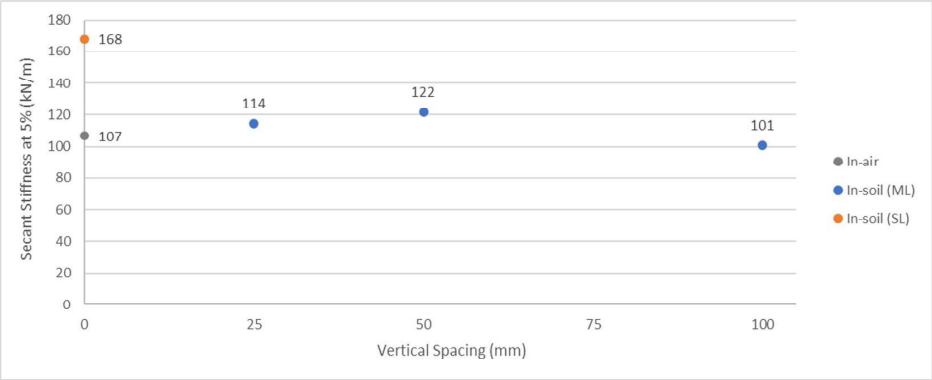


Figure 4.85. Tensile secant modulus at 5% strain for woven geotextile in sand.

4.6.4. Behaviour of (Multi-Layer) Geogrid Confined in Sand

Same procedure was applied for the multi-layer test of geogrid. An end of test photo to visualize the arrangement in the multi-layer test of geogrid is shown in Figure 4.86. As geogrid is not a continuous planar reinforcement like geotextiles, the deformations can not be observed on the upper passive reinforcement.



Figure 4.86. Multi-layer test of geogrid confined in sand (for ε_{ult} ≈12% strain), s_v=25 mm.

Prior to the load-strain results, the displacement of the loading plate is also checked to determine any abnormal volume change of soil (Figure 4.87). In plate displacement figures, position of the plate is shown in initial position (beginning of test) and final position (at T_{ult} load). Measured maximum settlements are always at the fixed clamp side (rear side) and ranges from 0.4 to 0.6 mm (0.8 mm in single layer test, Figure 4.33). These findings show that vertical spacing has a minor effect on the settlement and there is no significant change in the soil volume during the test.

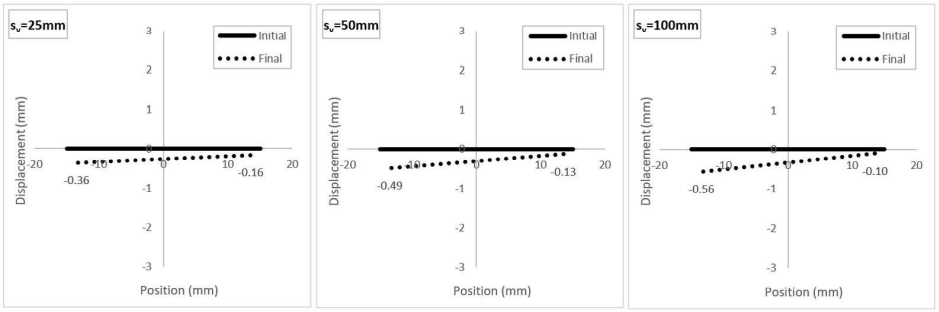


Figure 4.87. Displacement of loading plate (at T_{ult} load).

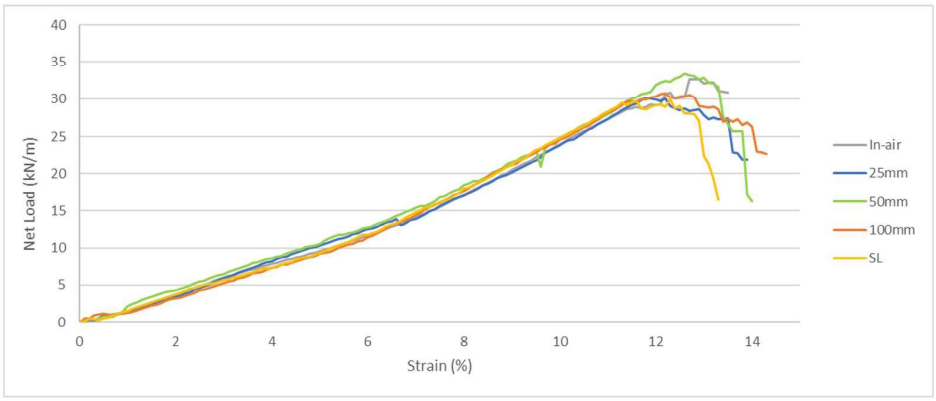


Figure 4.88. Results of multi-layer test of geogrid in sand.

Geogrid is not a continuous planar reinforcement like geotextiles. The large openings of the geogrid almost don't interrupt the particle interaction within the sand. Due to the hollow structure of the geogrid, load transfer from loading plate to the test specimen is not interrupted. Therefore, the change observed in multi-layer test of geogrid is negligible with respect to the single-layer test results (Figure 4.88 and Figure 4.89).

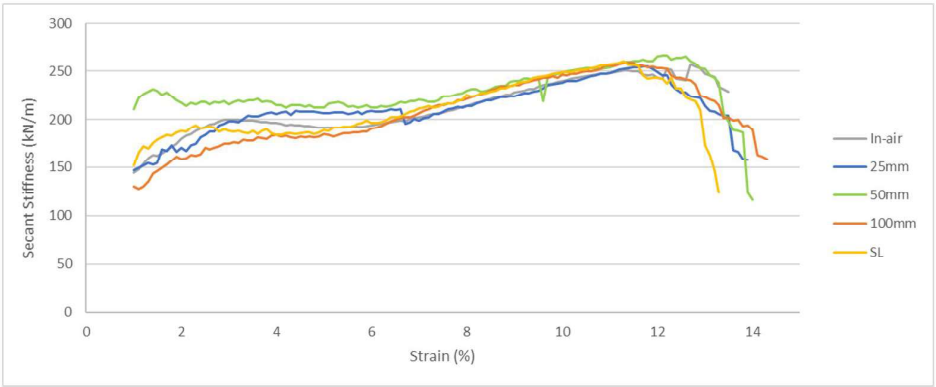


Figure 4.89. Tensile secant modulus of geogrid in sand.

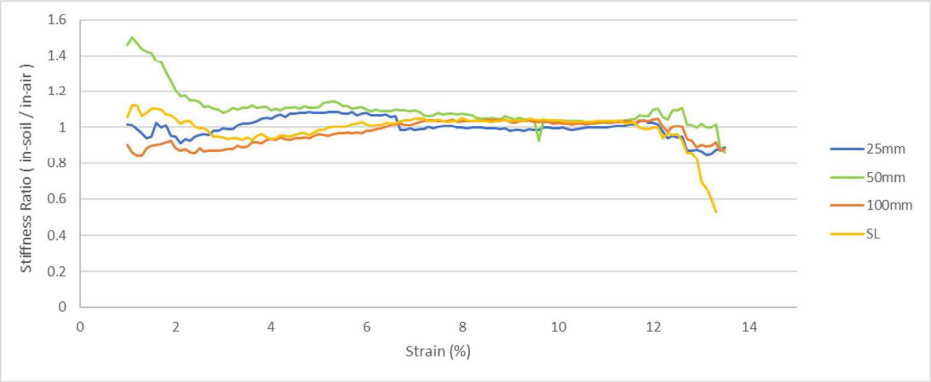


Figure 4.90. Change in tensile secant modulus with respect to unconfined (in-air) test.

The change of stiffness ratio with strain value is plotted in Figure 4.90. In single layer tests, 50 kPa has no influence on geogrid in sand. Therefore, single-layer test and in-air test results are same for this test group. Comparing multi-layer test result with the single-layer test result is more meaningful to determine the influence of vertical spacing. In comparison of single and multi-layer tests; $J_{sec,r}$ at 5% strain is 1.1 when vertical spacing is up to 50 mm which means a negligible increase in stiffness. $J_{sec,r}$ at 5% strain is 1 in case of 100 mm vertical spacing. This means that the specimen acts like it is in single-layer test when the passive reinforcements are located 100 mm away from the specimen.

There is a small difference in load-strain behaviour around 5% strain level when the vertical spacing is less than 50 mm. This can be interpreted that the close distance of passive reinforcement increases the effect of confinement and interlocking. When vertical spacing exceeds 50 mm, passive reinforcement gets out of the influence zone and the results become similar to the ones in single-layer test.

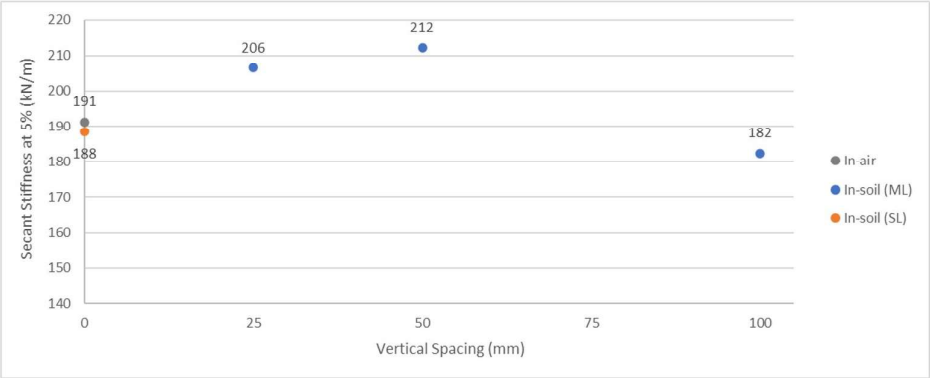


Figure 4.91. Tensile secant modulus at 5% strain for geogrid in sand.

As a general result, the influence of the passive reinforcement becomes significant for geotextiles (nonwoven and woven in this study). The passive reinforcement decreased the vertical pressure and reduced the stiffness of the geotextile. The influence of the passive reinforcement is proportional to the vertical spacing which means that there is an influence zone for each geotextile. Magnitude of influence zone for each geotextile is explained above. For geotextiles, stiffness of the passive reinforcement is another factor on the behaviour. Stiff geotextile (woven) caused a higher reduction in stiffness of the test specimen in sand.

The deviation in results observed at 5% secant stiffness doesn't explain a consistent behaviour (Figure 4.91). On the other hand, influence of passive reinforcement couldn't be observed in geogrid in sand (Figure 4.88). This has 2 reasons. First reason is the ratio of geogrid openings to the particle size of sand. Relatively large openings of geogrid (with respect to sand size) didn't interrupt the load transfer mechanism in sand. On the other hand, it's difficult to observe the changes in geogrid (in sand) under 50 kPa vertical pressure. Under the mentioned pressure, single layer results are similar with the in-air results.

4.7. Multi-Layer Tests in Gravel

In multi-layer tests, passive reinforcements are used above and below the test sample (active reinforcement). Passive reinforcements are fixed at the rear end and free at the front end. For details of the multi-layer test method, please follow "Section 3 - Methodology". In this test set, influence of passive reinforcements on active reinforcement is investigated.

Multi-layer tests were performed under 50 kPa confinement pressure. Vertical spacing between layers are 25, 50 and 100mm. One layer of passive reinforcement is used on each side of active reinforcement. Rest of the variables (strain rate, specimen dimensions, etc.) were kept same as the single-layer tests. In graphs of this section; in-air, single-layer (under 50 kPa) and multi-layer test results are presented to be compared.

As mentioned in Section 4.4.1., friction between clamp and gravel should be determined. In order to eliminate the influence of frictional loads to the test results, mentioned frictional loads between clamp and soil must be known. For this reason, clamp pull-out tests were performed to determine the clamp friction for each scenario (Figure 4.92 to Figure 4.94). Dissimilar to the single-layer test, pullout tests were performed for each reinforcement separately for each vertical spacing value (25, 50 and 100 mm). Tensile load-strain curves were plotted for each pull-out test. The mentioned results are subtracted from actual test results to obtain "net tensile load-strain" curves of geosynthetics.

4.7.1. Friction Between Gravel and Clamp (Clamp Pull-Out Tests), Multi-Layer Test

Some photographs from the friction tests in multi-layer case are shown in Figure 4.92, Figure 4.93 and Figure 4.94. In these figures, the reflection of soil replacement on passive reinforcement can be observed. These figures prove that the deformation of

passive reinforcement is more pronounced in continuous planar reinforcements.

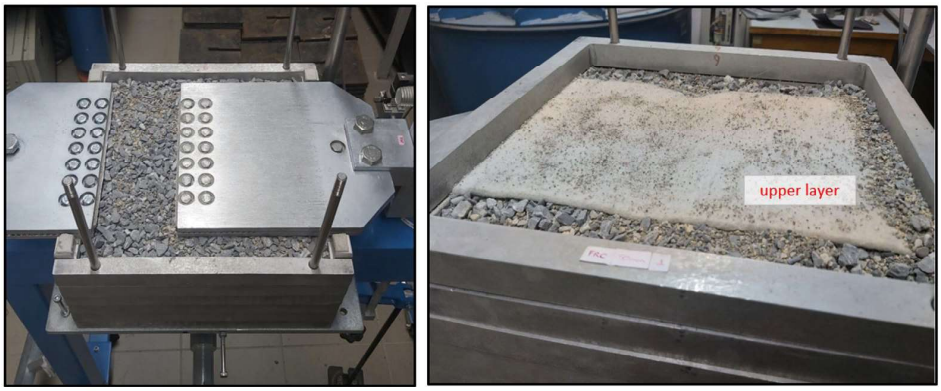


Figure 4.92. Clamp pull-out test in gravel for multi-layer test of nonwoven geotextile (s_v=50 mm and for 35% strain).



Figure 4.93. Clamp pull-out test in gravel for multi-layer test of woven geotextile (s_v=25 mm and for 35% strain).



Figure 4.94. Clamp pull-out test in gravel for multi-layer test of geogrid (s_v=25 mm and for 35% strain).

Clamp pull-out tests for the multi-layered case were performed under 50 kPa normal stress. Since in-soil multi-layer tests are planned to be performed under 25, 50 and 100 mm vertical spacing (s_v) values, clamp pull-out tests are also performed under same s_v values for all geosynthetic types. Load-strain results of the tests for various s_v values and geosynthetic types are given in Figure 4.98a, Figure 4.99a and Figure 4.100a.

Prior to the load-strain results, the displacement of the loading plate is also checked to determine any abnormal volume change of soil (Figure 4.95, Figure 4.96 and Figure 4.97) and the relation of displacement with the s_v value. In plate displacement figures, position of the plate is shown in initial position (beginning of test) and final position (at 30% strain). Measured maximum settlements are always at the fixed clamp side (rear side) and ranges from 0.2 to 0.5 mm. These findings show that geosynthetic type and s_v have negligible influence on the settlement of loading plate and there is no significant change in the soil volume during the test. However, soil type slightly changes the displacement of loading plate. Using gravel causes smaller displacements on loading plate level.

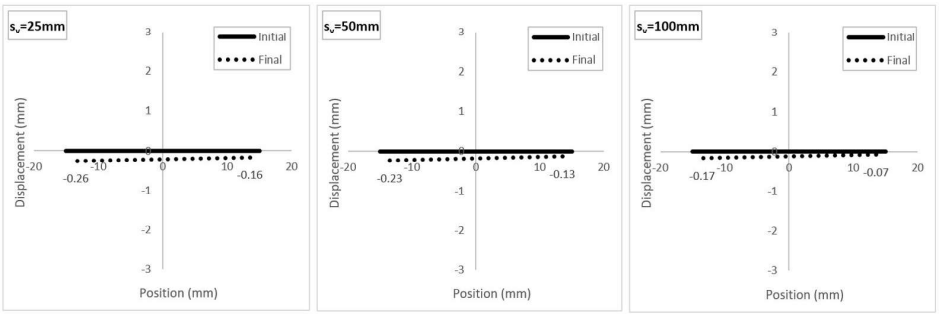


Figure 4.95. Displacement of loading plate for nonwoven geotextile (at 30% strain).

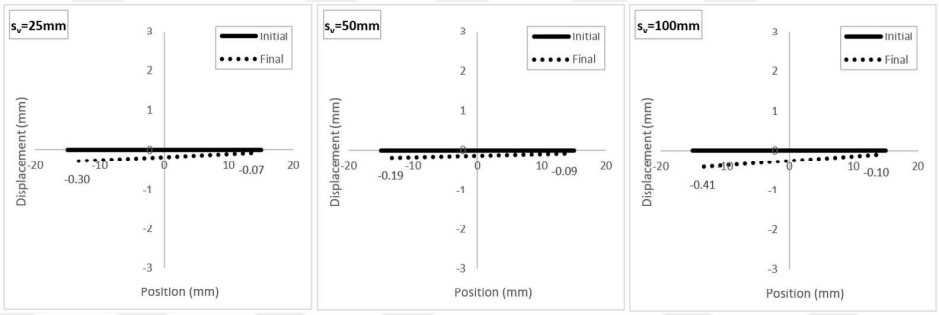


Figure 4.96. Displacement of loading plate for woven geotextile (at 30% strain).

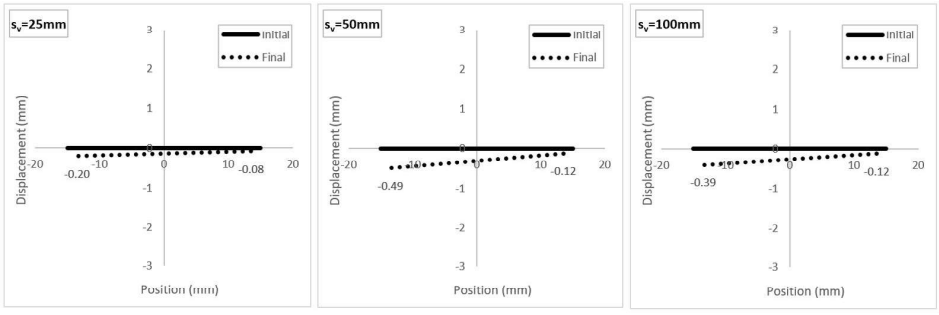


Figure 4.97. Displacement of loading plate for geogrid (at 30% strain).

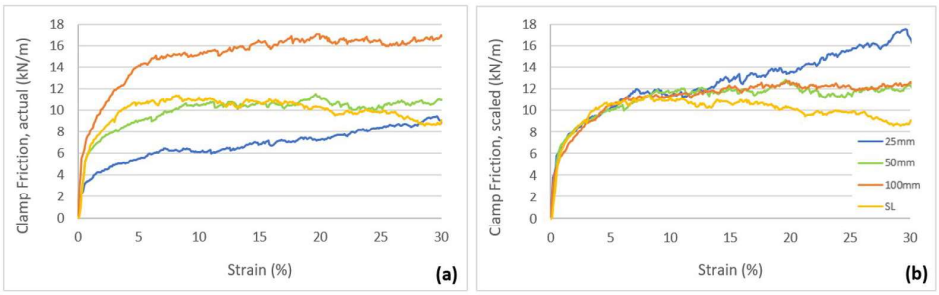


Figure 4.98. . Results of clamp pull-out test in gravel for nonwoven geotextile (a) actual, (b) scaled.

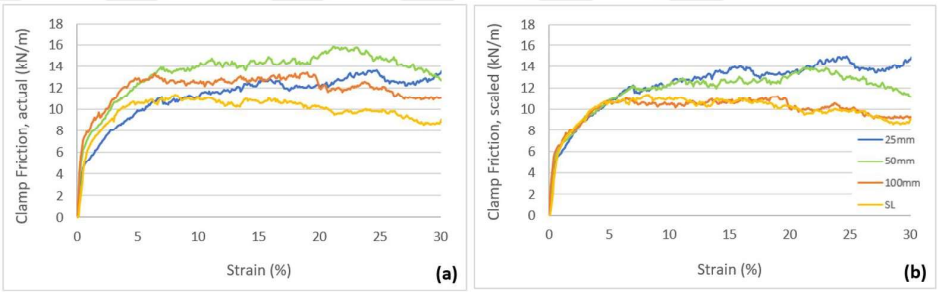


Figure 4.99. Results of clamp pull-out test in gravel for woven geotextile (a) actual, (b) scaled.

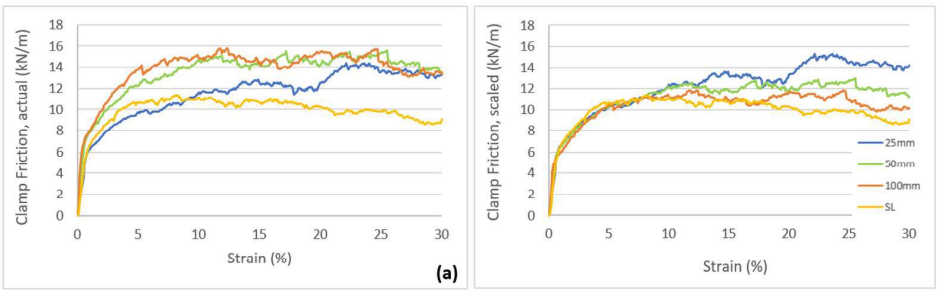


Figure 4.100. Results of clamp pull-out test in gravel for geogrid (a) actual, (b) scaled.

The pull-out performance of clamp (in gravel) in case of woven geotextile and geogrid are similar in terms of load-strain behaviour. Both woven geotextile and geogrid passive reinforcements cause an increase in clamp-gravel friction when s_v increases.

A slight decrease is observed in strains less than 10% when s_v reduces to 25 mm. This is illustrated in Figure 4.99a and Figure 4.100a. Nonwoven geotextile has the same tendency but a passive reinforcement close to the clamp caused a more dramatic reduction in load-strain behaviour when compared to relatively stiff reinforcements (woven geotextile and geogrid). This is also obvious in strains less than 10% when s_v=50 mm. This is illustrated in Figure 4.98a.

The clamp-gravel friction behaviour for all reinforcement types, there is a lower boundary of s_v. When s_v exceeds this boundary, clamp-gravel friction increases (possibly due to the confinement effect of reinforcement). This boundary can be considered 25 mm for relatively stiff reinforcements such as woven geotextile and geogrid while 50 mm for needle-punched nonwoven geotextile.

On the other hand, there is an apparent behaviour for all geosynthetics which shows that the frictional loads decrease in single-layer test results and s_v=100mm results (increasing strain causes reduction in friction loads). The mentioned behaviour is more obvious when the curves of each case is scaled to the single layer situation (Figure 4.98b, Figure 4.99b and Figure 4.100b). It should be noted that scaling is only used to make the behaviour more visible, it has no physical meaning and not used in load-strain plots. The mentioned behaviour shows that passive reinforcements located close to the clamp causes a confinement effect on the clamp with the clamp's movement and this effect reduces when s_v is increased.

The clamp friction loads plotted in Figure 4.98a, Figure 4.99a and Figure 4.100a are subtracted from the actual multi-layer test results (in-gravel) to obtain the net load-strain curves. The influence of the passive reinforcement on the active reinforcement is investigated in following sections.

4.7.2. Behaviour of (Multi-Layer) Nonwoven Geotextile Confined in Gravel

The deformation of the upper reinforcement (Figure 4.101) is smaller than the one observed in sand (Figure 4.74). Direct comparison of two figures is not realistic, so the strain difference of 15% also considered for the nonwoven geotextile. This finding is also valid for the case of woven geotextile which is given in next section. The relatively small deformation of the upper reinforcement signifies that the relocation of the soil particles is limited in gravel. Parallel to this, deformation of the soil during the test decreases when it's confined in gravel. This finding is supported by the relatively small plate displacement results (Figure 4.102).

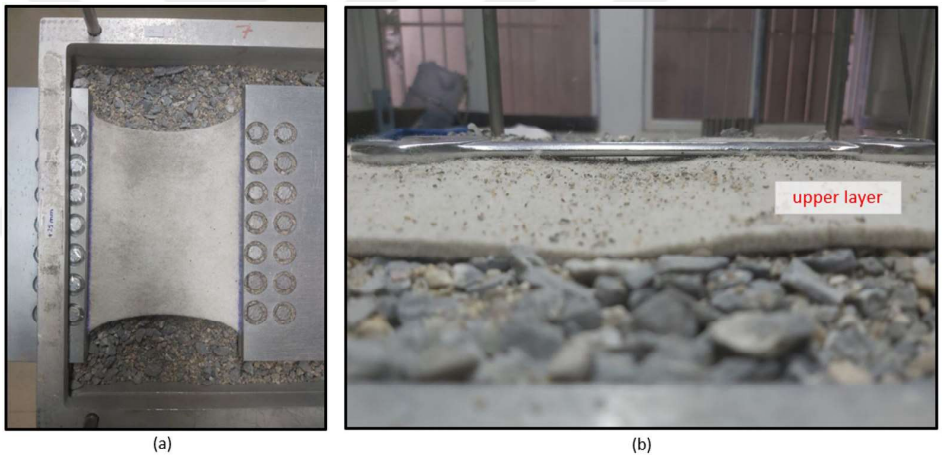


Figure 4.101. Multi-layer test (s_v=25 mm) of nonwoven geotextile confined in gravel (for 35% strain); (a) test specimen, (b) passive (upper) reinforcement (s_v=25mm).

Prior to the load-strain results, the displacement of the loading plate is also checked to determine any abnormal volume change of soil (Figure 4.102). In plate displacement figures, position of the plate is shown in initial position (beginning of test) and final position (at 30% strain). Measured maximum settlements are always at the fixed clamp side (rear side) and ranges between 0.2 and 0.3 mm (0.3 mm in single layer test, Figure 4.45). The mentioned settlement range is 1.1 to 1.3 mm for multi-layer test in sand. Both passive reinforcement deformation and plate displacement shows that the relocation of the soil is less in gravel as aforementioned in previous

paragraph.

Displacement of loading plate show that vertical spacing has a minor effect on the settlement and there is no significant change in the soil volume during the test.

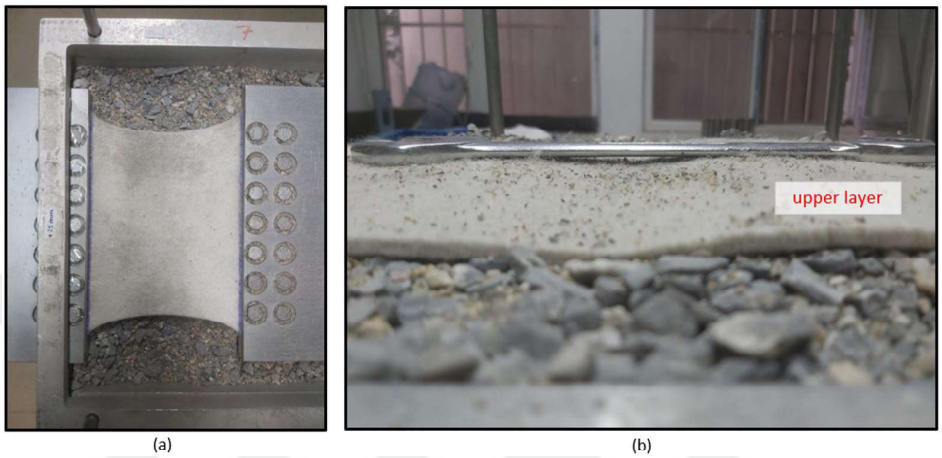


Figure 4.102. Displacement of loading plate (up to 30% strain).

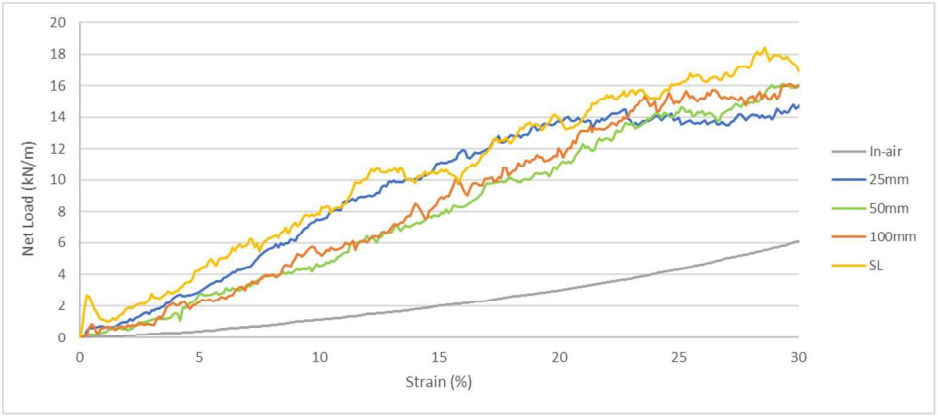


Figure 4.103. Results of multi-layer test of nonwoven geotextile in gravel.

Load-strain behaviour of the multi-layer nonwoven geotextile in gravel is given in Figure 4.103. As a result of irregular structures of nonwoven geotextile and gravel, the behaviour due to the passive reinforcements are complex to describe. The possible reason of the irregularity is the angularity and particle size of gravel. For this reason,

the uniform and predictable pressure transfer from sand to geosynthetic doesn't occur in gravel. As a result, range of results becomes wider. However, we can still conclude that passive reinforcement reduces the load-strain behaviour of nonwoven geotextile in gravel (similar to the findings in the sand).

The behaviour was expected to be closer to the single layer reinforcement with increasing vertical spacing, but stiffness doesn't increase proportional to vertical spacing (as observed in sand). This can be observed when cases of 25 mm and 50 mm are compared. Contrary to the behaviour in sand, behaviour under 25 mm is stiffer than the one in 50 mm. However, the main trend shows that, passive reinforcement has limited influence on the load-strain results of nonwoven geotextile in gravel. For all s_v values, load-strain is close to the one observed in single layer test, but slightly lower (Figure 4.103). In other words, it can be concluded that the negative effect of the passive reinforcement on the load-strain behaviour of geosynthetic is less when confined in gravel (compared to sand).

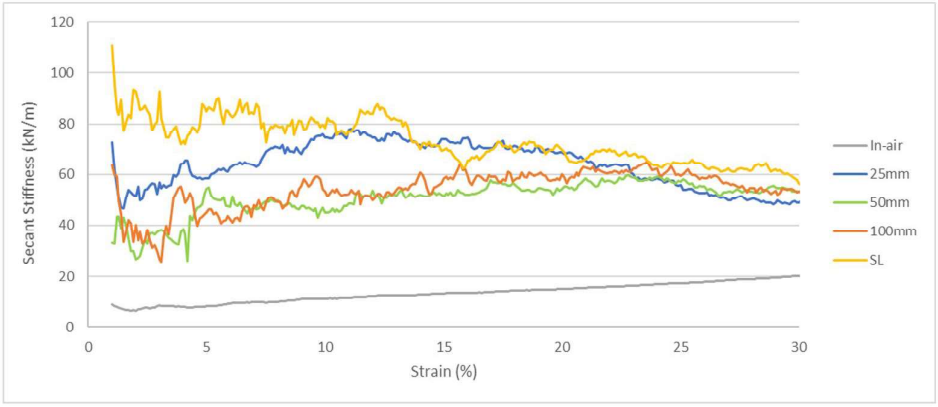


Figure 4.104. Tensile secant modulus of nonwoven geotextile in gravel.

According to the Figure 4.104, secant stiffness values at small strains for multi-layer case are smaller than the ones in single-layer situation. This can be explained by the reduction in vertical pressure due to the passive reinforcement. In the static situation and the beginning of the test, vertical pressure acting by the loading plate can't be fully transferred to the test specimen because of passive reinforcement. By

advancing the test, soil relocation increases, and the load transfer mechanism is rebuilt (after 15% strain). After the mentioned displacement of clamp, nonwoven geotextile gave almost same results for all in-soil cases. This makes passive reinforcement effective only in small strains.

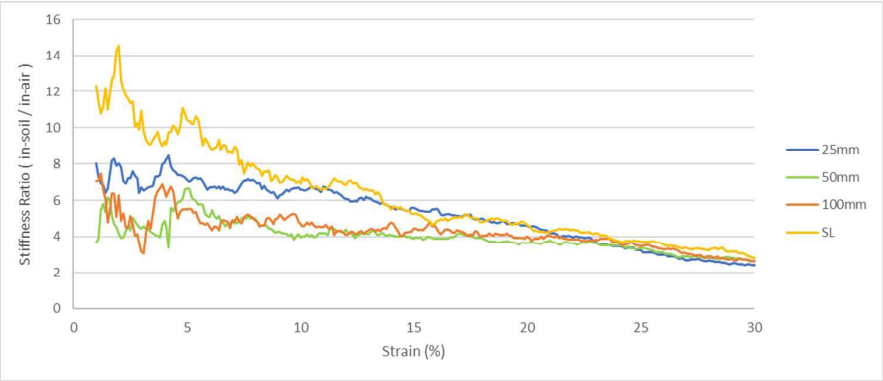


Figure 4.105. Change in tensile secant modulus with respect to unconfined (in-air) test.

The change of stiffness ratio with strain value is plotted in Figure 4.105. Stiffness ratio ($J_{sec,r}$) shows the change in stiffness in multi-layer test with respect to the unconfined in-air tests. Tensile secant modulus at 5% strain ($J_{sec,5}$) increases for every test situation when compared to in-air test.

Comparing multi-layer test result with the single layer test result is more meaningful to determine the influence of vertical spacing. In comparison of single and multi-layer tests; $J_{sec,r}$ at 5% strain is 0.6-0.7 for all vertical spacing conditions. Figure 4.105 shows that this is a local situation observed at only 5% strain. For lower strain values differentiation in secant stiffness increases. In contrast, the differentiation decreases in strains greater than 5%.

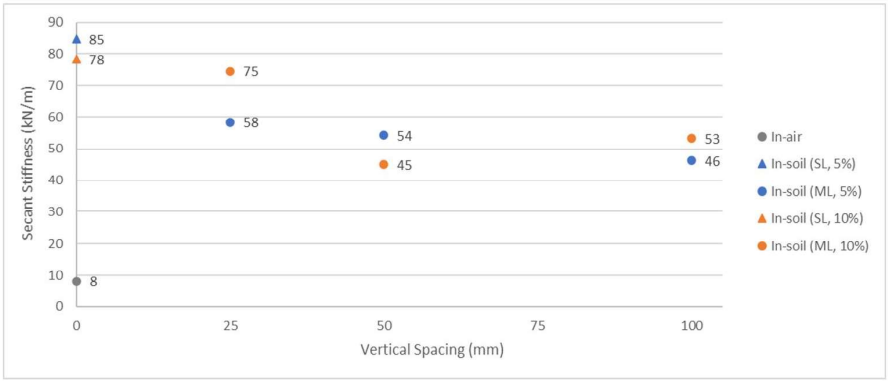


Figure 4.106. Tensile secant modulus at 5% and 10% strain for nonwoven geotextile in gravel.

Since the behaviour of nonwoven geotextile in gravel is relatively irregular, secant stiffnesses are investigated at 5% and 10% strain in Figure 4.106. When Figure 4.106 is interpreted with Figure 4.103, it can be concluded that load-strain performance decreases when passive reinforcement is used. This outcome is valid for all vertical spacing conditions.

The load-strain performance is lower than the single-layer situation for all multi-layer cases, but they are still better than the in-air performance. Among the multi-layer cases, the lowest s_v value (25 mm) leads to the best performance. The load-strain behaviour at 50 and 100 mm vertical spacings are similar and lower than the one in 25 mm. All in all, it can be concluded that there is a reducing effect of passive reinforcement but its change with vertical spacing is not well defined.

4.7.3. Behaviour of (Multi-Layer) Woven Geotextile Confined in Gravel

As stated in previous section, deformation of the upper reinforcement (for nonwoven and woven geotextiles) is low when compared to multi-layer tests in sand. Similar behaviour to nonwoven geotextile is also observed in woven geotextile, but with lower deformation. This is an expected result due to the higher stiffness of woven geotextile (Figure 4.107).

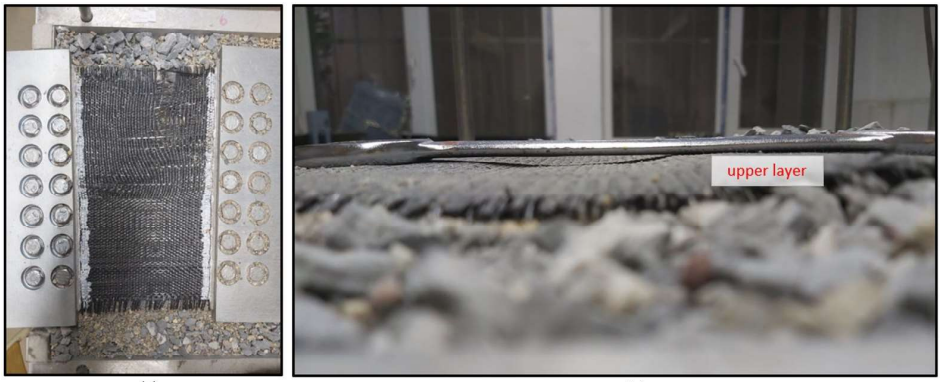


Figure 4.107. Multi-layer test of woven geotextile confined in gravel (for ε_{ult} ≈22% strain); (a) test specimen, (b)passive (upper) reinforcement (s_v=25mm).

Prior to the load-strain results, the displacement of the loading plate is also checked to determine any abnormal volume change of soil (Figure 4.108). In plate displacement figures, position of the plate is shown in initial position (beginning of test) and final position (at T_{ult} load). Contrary to previous test measured maximum settlements are not always at the fixed clamp side (rear side), but the magnitudes are negligible. Settlement of the clamp ranges between 0.1 and 0.2 mm (0.3 mm in single layer test, Figure 4.51). The mentioned settlement range is 1.0 to 1.3 mm for multi-layer test in sand. Both passive reinforcement deformation and plate displacement shows that the relocation of the soil is less in gravel as aforementioned in previous paragraph.

Displacement of loading plate show that vertical spacing has a minor effect on the settlement and there is no significant change in the soil volume during the test.

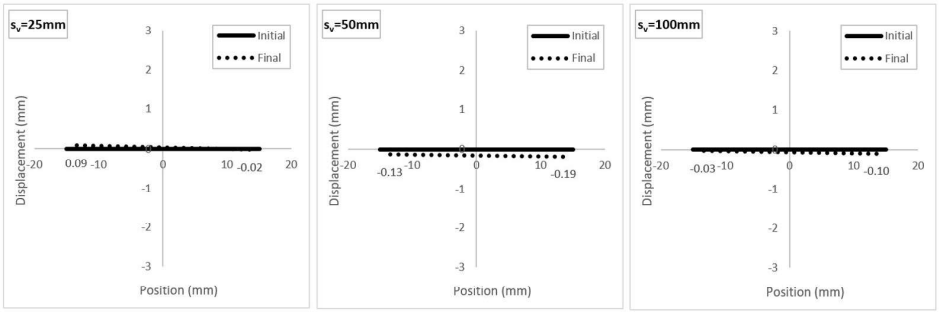


Figure 4.108. Displacement of loading plate (at T_{ult} load).

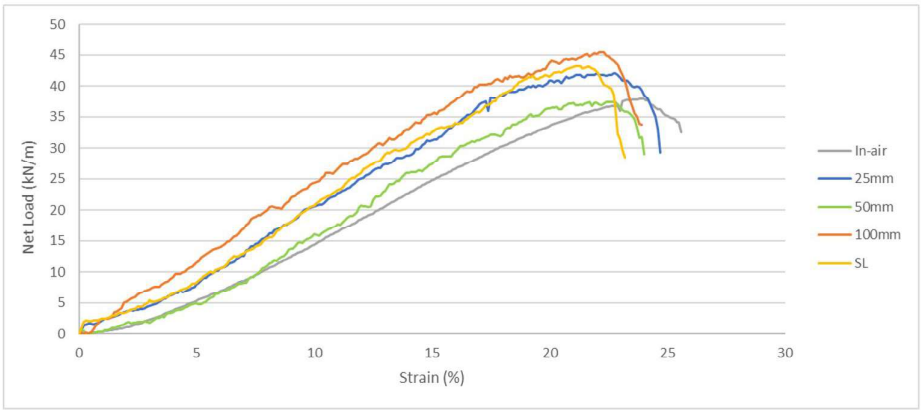


Figure 4.109. Results of multi-layer test of woven geotextile in gravel.

As depicted in Figure 4.109, the change in load-strain behaviour with vertical spacing is not linear. Load-strain behaviour is similar to single-layer test results under s_v=25 mm conditions, while it is similar to in-air behaviour under s_v=50 mm conditions. When vertical spacing reaches 100 mm, test specimen acts like a stiffer material than the specimen tested under single-layer conditions. As a result, proposing a linear relationship between s_v and load-strain behaviour becomes impossible under these circumstances. This can also be seen in terms of secant stiffness in Figure 4.110.

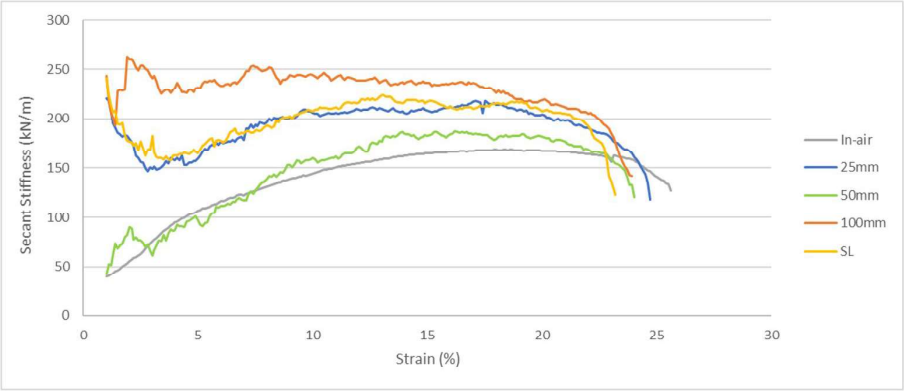


Figure 4.110. Tensile secant modulus of woven geotextile in gravel.

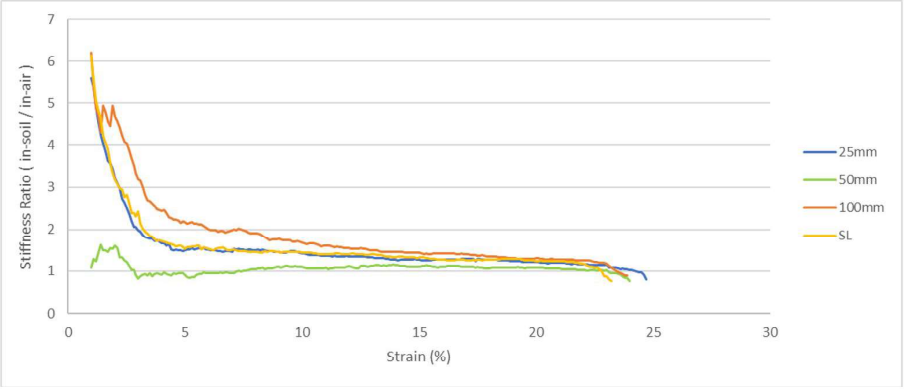


Figure 4.111. Change in tensile secant modulus with respect to unconfined (in-air) test.

The change of stiffness ratio with strain value is plotted in Figure 4.111. Stiffness ratio ($J_{sec,r}$) shows the change in stiffness in multi-layer test with respect to the unconfined in-air tests. $J_{sec,r}$ at 5% strain is almost same with in-air test when vertical spacing is 50 mm. However, Jsec,r at 5% strain reaches 2.2 in case of 100 mm and 1.5 in case of 25 mm vertical spacing.

Comparing multi-layer test results with the single layer test results is more meaningful to determine the influence of vertical spacing. In comparison of single and multi-layer tests; $J_{sec,r}$ at 5% strain is 0.6 when vertical spacing is 50 mm which means

reduction in stiffness. $J_{sec,r}$ at 5% strain is 1.4 in case of 100 mm and 1.0 in case of 25 mm vertical spacing.

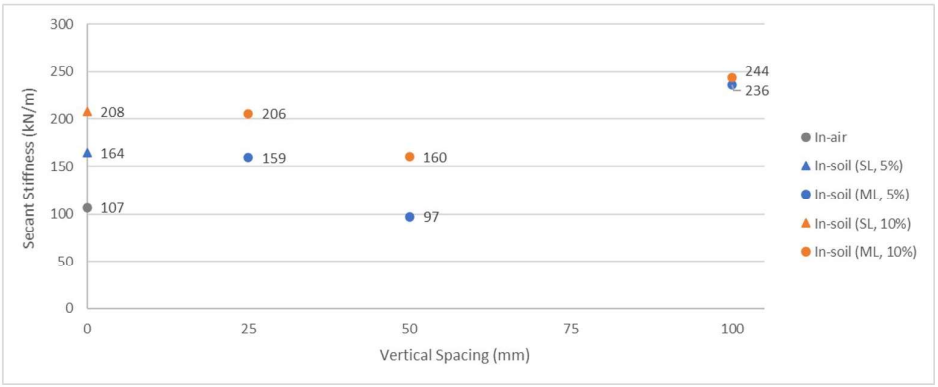


Figure 4.112. Tensile secant modulus at 5% strain for woven geotextile in gravel.

To investigate the change of secant stiffness in a wider range, change of secant stiffness at 10% strain is also included to the graph (Figure 4.112). Since the secant stiffness value represents a point in the load-strain curve, it's better to evaluate Figure 4.112 with load-strain curve (Figure 4.109). Both graphs have the same conclusion when compared to single-layer test. Load-strain behaviour does not change at s_v=25 mm, reduces at 50 mm and shows best performance at 100 mm. The behaviour does not change linearly with the vertical spacing. As a result, defining an influence distance or drawing a regression line in terms of vertical spacing becomes impossible.

4.7.4. Behaviour of (Multi-Layer) Geogrid Confined in Gravel

The end of test photograph of active and upper passive reinforcements for s_v = 25 mm are shown in Figure 4.113. Due to the hollow structure of geogrid, the deformations can't be observed on the upper passive reinforcement as it has been done in geotextiles in previous sections.

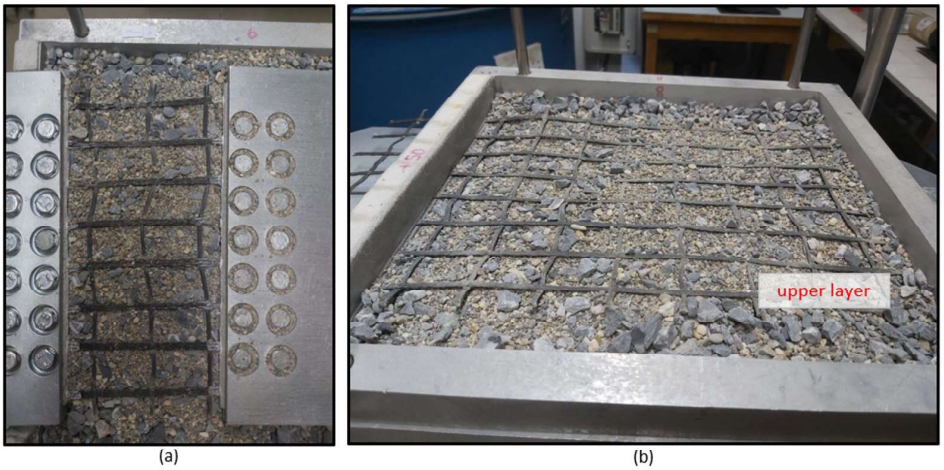


Figure 4.113. Multi-layer test of geogrid confined in gravel (for ε_{ult} ≈11% strain), s_v=25 mm.

Prior to the load-strain results, the displacement of the loading plate is also checked to determine any abnormal volume change of soil (Figure 4.114). In plate displacement figures, position of the plate is shown in initial position (beginning of test) and final position (at T_{ult} load). Measured maximum settlements are always at the fixed clamp side (rear side) and ranges between 0.2 and 0.3 mm (0.4 mm in single layer test, Figure 4.58). The mentioned settlement range is 0.4 to 0.6 mm for multi-layer test in sand. Based on passive reinforcement deformation and plate displacements, the soil relocation in case of geogrid use is less when compared to the geotextiles. Displacement of loading plate show that vertical spacing has a minor effect on the settlement and there is no significant change in the soil volume during the test.

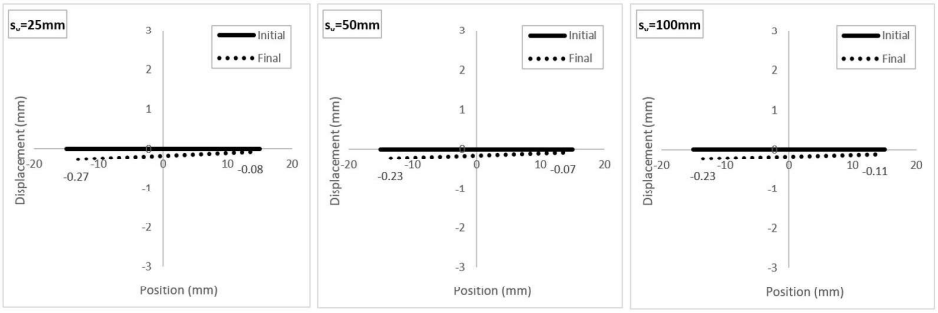


Figure 4.114. Displacement of loading plate (at T_{ult} load).

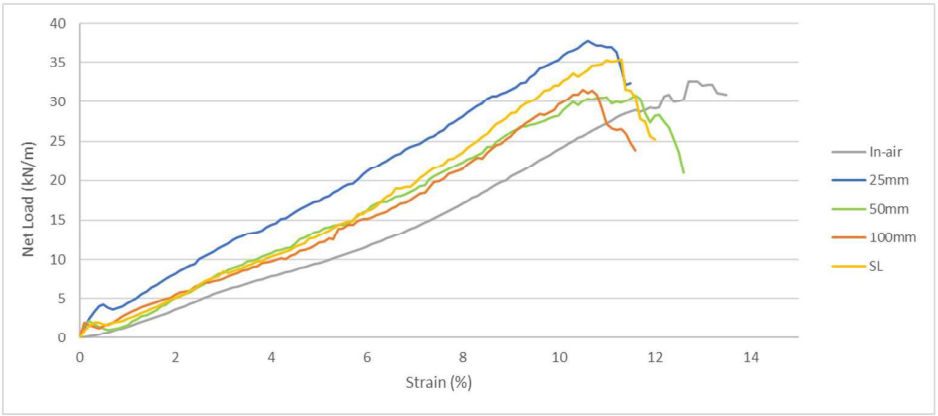


Figure 4.115. Results of multi-layer test of geogrid in gravel.

Contrary to the results observed in sand group, influence of the passive reinforcements is clearly visible when gravel is used (Figure 4.115). This can be explained by the angular shape and larger size of gravel particles (relative to the geogrid openings) which yield greater interlock strength on geogrids. However, the influence of the passive reinforcement diminishes with the distance and multi-layer test results become closer to the single-layer tests.

The effect of passive reinforcement can be observed when $s_v = 25$ mm and there is no effect of passive reinforcement at greater s_v values such as 50 mm and 100 mm. Under these circumstances the influence distance of the passive reinforcement is claimed to be 25 mm. The passive reinforcement located at 25 mm increases the stiffness

of the geogrid when compared to single-layer results. The reason of the behaviour is considered confinement effect of the passive reinforcements. By displacement of the clamp, soil particles tend to relocate and relieve, however passive reinforcements prevent the reorientation of gravels. As expected, confinement effect of the passive reinforcement disappears with the distance to the active reinforcement (s_v).

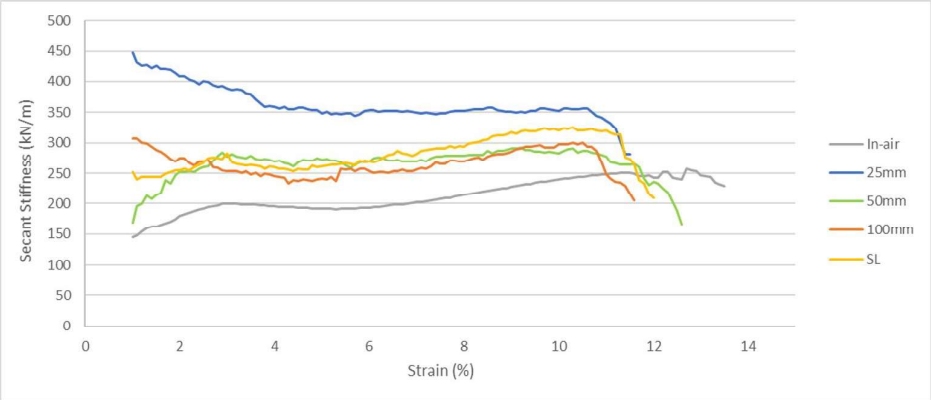


Figure 4.116. Tensile secant modulus of geogrid in gravel.

The results of load-strain behaviour can also be observed in terms of stiffness in Figure 4.116 and Figure 4.117. Thanks to the confinement effect, passive reinforcement placed close (s_v=25 mm) to the test specimen increases the secant tensile stiffness in the beginning of the test. This is due to the well-established interlocking mechanism. By the movement of the clamp and strain of the specimen, soil structure changes and influence of confinement reduces with respect to the beginning of the test (static condition).

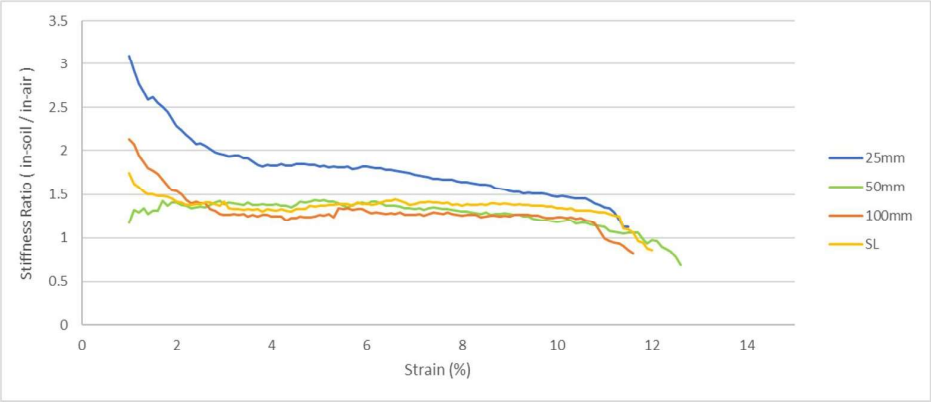


Figure 4.117. Change in tensile secant modulus with respect to unconfined (in-air) test.

As aforementioned in the general load-strain behaviour, the increase in stiffness at 5% strain level is more profound when the vertical spacing is 25 mm. The use of greater vertical distance gets the passive reinforcement out of the influence zone and the results become similar to the ones in single-layer test.

Comparing multi-layer test results with the single-layer test results is more meaningful to determine the influence of vertical spacing. In comparison of single and multi-layer tests; $J_{sec,r}$ at 5% strain are 1.04 and 0.93 when vertical spacings are 50 and 100 mm respectively. This means that the change in secant stiffness at 5% strain is negligible at 50 and 100 mm. In other words, the specimen acts like it's subjected to a single-layer test when the passive reinforcements are located 50 or 100 mm away from the specimen.

$J_{sec,r}$ at 5% strain is 1.3 when vertical spacing is 25 mm which means that multi-layer test result is 1.3 times greater than the single layer results. As a result, influence at 5% strain is worthwhile when vertical spacing is 25mm.

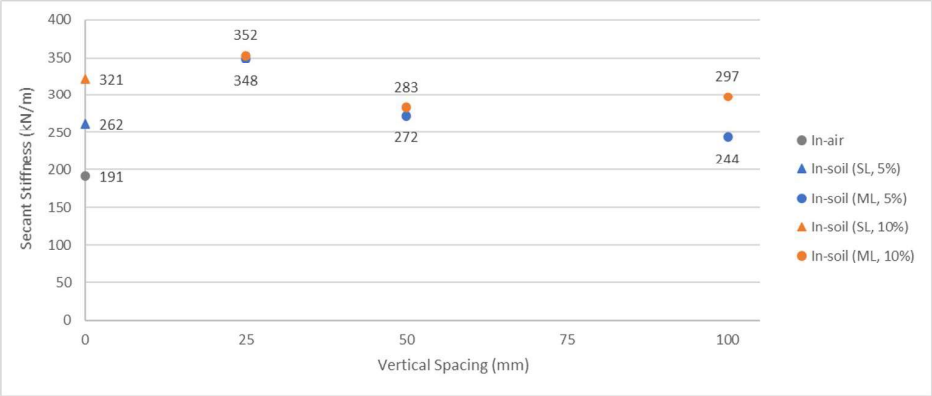


Figure 4.118. Tensile secant modulus at 5% strain for geogrid in gravel.

To investigate the change of secant stiffness in a wider range, change of secant stiffness at 10% strain is also included to the graph (Figure 4.118). Since the secant stiffness value represents a point in the load-strain curve, it's better to evaluate Figure 4.118 with load-strain curve (Figure 4.115). It can be clearly observed from both graphs that passive reinforcement located at 25 mm increases the load-strain behaviour when compared to the single-layer test. The behaviour is not influenced by the passive reinforcement when the distance exceeds 25 mm. In other words, influence distance for geogrid in gravel can be considered 25 mm.

5. CONCLUSION

In this study, an apparatus was developed to perform in-soil wide width tests on geosynthetics. The apparatus is capable of testing geosynthetics either in-air or in-soil. The purpose of the apparatus is to study the influence of soil types and vertical pressures on the tensile behaviour of reinforcement geosynthetics. The box is designed in segmental form to allow multi-layer testing. Therefore, it is also capable of investigating the effect of passive reinforcement (multi-layer test) on the test specimen. This study covers the results of 160 wide width tensile tests and their evaluation. Tests included in this study were divided into 3 main groups such as control group (in-air test), single-layer test group (in-soil) and multi-layer test group.

The vast majority of the previous studies of in-soil tensile tests were on nonwoven geotextiles. There is insufficient research on common geosynthetic reinforcements such as woven geotextile and geogrid. This study was carried out on 3 types of geosynthetics. Geosynthetics used in the study are needle-punched nonwoven geotextile, woven geotextile and woven geogrid.

Fine sand (up to 2 mm) and rubber/membrane were used in the previous studies in the literature. For a better simulation of site conditions, soils commonly used in reinforcement applications on site were included in this study. In-soil tests were performed using two types of soils. According to USCS, the soil types used in the study are classified as Well Graded Sand and Well Graded Gravel with Sand.

Control group tests (unconfined in-air tests) proved that the performance of the apparatus was satisfactory, because the in-air wide width test results of geosynthetics comply with the ones given in the respective technical specifications of the manufacturers. The in-air tests also showed that clamp design could hold the specimen tight without a slippage and without damaging it.

The proposed apparatus is superior to the ones in previous studies because of its versatility. Thanks to the large box design, coarser soils can also be used as confinement material. On the other hand, segmental form of the box enables each segment to be used as a clamp for passive reinforcements. Therefore, in-soil multi-layer tests can be performed. The vertical pressure is applied as dead weight in the proposed apparatus. Applying vertical pressure as dead weight makes the apparatus more stable and practical in terms of maintenance. Finally, in the proposed apparatus test specimens can be held within the soil throughout the test. This aspect becomes crucial for in-soil tests.

Vertical pressures of 25, 50 and 75 kPa were applied to the in-soil single layer tests and the results were compared with the in-air test group. In-soil multi-layer tests were performed under 50 kPa vertical pressure. The variable in multi-layer tests was the vertical spacing of passive reinforcement (distance to the test specimen). The mentioned vertical spacing (s_v) values investigated in the study are 25, 50 and 100 mm. All tests were performed at a constant strain rate of 2% strain/min. Load-strain plots were drawn up to 30% strain or rupture of the reinforcement. The mentioned in-soil tests were performed in sand and gravel medium, and results are summarized below.

Needle-punched nonwoven geotextile consists of randomly entangled fibers. This manufacturing process makes the nonwoven geotextile very loose when compared to other geosynthetic products. As a result of this structure, nonwoven geotextile's stiffness is very low in the in-air tests. This behaviour prevents nonwoven geotextile to be considered as reinforcement in design.

However, in-soil single-layer test results showed that the stiffness improves when nonwoven geotextile is tested under vertical pressures. The improvement is at its highest in small strains and reduces with strain due to the degradation in soil structure. The improvement was observed both in sand and gravel test groups. While the improvement is proportional to the vertical pressure in sand, it directly reaches its upper limit when confined in gravel. This shows that the soil property (particle shape, size,

and gradation) is important on the behaviour of nonwoven geotextile.

It can be speculated that the increase in stiffness can be as a result of the following: *i*) The increase in the confinement increases the friction between individual fibers, *ii*) intrusion of the fine particles in-between geotextile fibers limits the fiber stretching and causes an increase in stiffness, *iii*) when a rupture of individual fiber occurs, the ruptured fiber still can carry a stress because it may be held fixed between individual soil particles. This leads to a more progressive failure and increased stiffness. *iv*) the interface friction between geotextile and soil. Due to this interface friction, specimen is subjected to the soil resistance which causes higher tensile loads in the specimen compared to the in-air tests. To sum up, the effect of stiffness increase is caused by the change in the loose structure of nonwoven geotextile and the friction between geotextile and soil.

The change of secant stiffness of nonwoven geotextile at 5% strain ($J_{sec,5}$) is found to be proportional to vertical pressure (σ_n) or sand. However, secant stiffness of nonwoven geotextile at 5% strain ($J_{sec,5}$) in gravel does not depend on the vertical pressure, for vertical pressures of 25, 50 and 75 kPa. This is a clear indication that the mechanisms between nonwoven geotextile and sand or gravel are of different nature. When compared to in-air test, under 75 kPa increase of $J_{sec,5}$ reaches 11.5 times in sand and 11.8 times in gravel.

Using passive reinforcement in sand reduced the stiffness of nonwoven geotextile but never reached the in-air results. In sand, increasing the vertical spacing (s_v) makes the behaviour close to the single-layer test results. The change in behaviour is also valid when gravel is used but the influence of passive reinforcement on the test specimen is lower and more irregular. The change in behaviour is caused by the different stress transfer mechanisms in soil. In sand, the vertical pressure is uniformly applied on the specimen while grab mechanism is also effective in gravel. As stated above, behaviour in sand depends on the level of vertical pressure while the influence of gravel is apparent even in small pressures and does not change proportional to pressure.

In single-layer test results, woven geotextile showed a similar behaviour to the nonwoven geotextile. Woven geotextile is made of aligned filaments in warp (machine direction) and weft (cross-machine direction) directions. This makes the woven geotextile more stable than nonwoven geotextile. Since the woven geotextile is stiffer than nonwoven geotextile, the change in load-strain behaviour was expected to be lower compared to nonwoven geotextiles. On the other hand, the interface friction between geotextile and soil can also be considered for woven geotextiles an important contributor to the stiffness increase.

Similar to the nonwoven geotextile, the change of secant stiffness of woven geotextile at 5% strain ($J_{sec,5}$) is proportional to the vertical pressure (σ_n) for sand. However, describing a linear relationship with respect to the pressure is not realistic in gravel. When compared to in-air test, under 75 kPa increase of $J_{sec,5}$ reaches 1.7 times in sand and 1.9 times in gravel. Though these increases are not as impressive as the ones in nonwoven geotextile, it is still a significant increase in stiffness and will certainly effect the behavior of the reinforced system.

Furthermore, ultimate load (T_{ult}) and corresponding strain (ε_{ult}) of woven geotextile were also influenced by the confinement. T_{ult} was increased under confinement in all cases. The range of increment on T_{ult} was 14-21% in sand and 16-30% in gravel. According to these results, confinement also increases the ultimate load of the woven geotextile in addition to the increase in stiffness. ε_{ult} values were almost same in sand but slightly lower in gravel with respect to in-air test.

Multi-layer test of woven geotextile in sand gave almost similar behaviour with nonwoven geotextile. Using passive reinforcement in sand reduced stiffness of woven geotextile and almost reached the in-air results. However, a slight increase in T_{ult} was still observed in the results. In both nonwoven and woven geotextiles in sand, upper passive reinforcement is carrying the vertical pressure and interrupts the pressure transfer to test specimen. Contrary to behaviour in sand, test specimen's behaviour differs from in-air results when passive reinforcement was placed in gravel. The possible

reason of an improved load-strain behaviour in gravel is changing confinement effect due to the location of passive reinforcement. Unfortunately, the change in behaviour is irregular and not proportional to s_v. The apparatus is insufficient to have further interpretations in results of multi-layer woven geotextile tests in gravel.

In single-layer test results in sand, load-strain behaviour of geogrid was only changed when vertical pressure exceeds 50 kPa. The improvement was observed under all vertical pressures from 25 to 75 kPa when confined in gravel. Again, gravel showed a greater performance in improving the stiffness.

The geogrid used in the study is made of polyester fibers coated by PVC. Therefore, internal structure (fiber friction) may change with confinement but very limited when compared with nonwoven geotextile. Interlocking mechanism (McGown et al., 1995) between soil and geogrid is probably another factor influencing the behaviour. Test specimen has an actual gauge length of 100 mm. However, confinement and/or interlocking mechanism may create restraint points along the specimen which act like fictive clamps. This behaviour yields to practically shorter sample length during the tests, consequently greater strain rates. Since stiffer materials are more sensitive to strain rate (greater strain rate leads to more brittle behaviour), geogrid stiffness increases with vertical pressure.

Similar to the nonwoven and woven geotextile, the change of secant stiffness of geogrid at 5% strain ($J_{sec,5}$) is proportional to vertical pressure (σ_n) for sand. However, the relation is relatively less accurate. However, describing a linear relationship with respect to the pressure is not realistic in gravel. When compared to in-air test, under 75 kPa increase of of $J_{sec,5}$ reaches 1.3 times in sand and 1.4 times in gravel.

Moreover, ultimate load (T_{ult}) and corresponding strain (ε_{ult}) of geogrid were also influenced by the confinement. T_{ult} was slightly increased under confinement greater than 50 kPa in sand and under all confinement levels in gravel. The range of increment on T_{ult} was 0-7% in sand and 9-17% in gravel. According to these results, confinement

also increases the ultimate load of the geogrid in addition to the increase in stiffness. ε_{ult} values were almost same in sand but slightly lower in gravel with respect to in-air test.

The influence of passive reinforcement couldn't be observed in multi-layer test of geogrid in sand. The ratio of geogrid opening size to the sand size was high to interact or change the pressure acting on the test specimen. Therefore, result of all vertical spacing situation gave the same result with the single layer test.

In gravel, locating the passive reinforcement close to the test specimen improved the load-strain behaviour of geogrid. It can be speculated that the presence of another geogrid reinforcement in the near vicinity is increasing the interaction capacity of gravel particles and geogrid by providing an increased horizontal confinement. However, the effect diminishes when s_v exceeds 25 mm. This means that when passive reinforcement is located further than 25 mm, test specimen acts like it's in the single-layer conditions.

REFERENCES

Allen, T.M., B.R., Christopher and R.D., Holtz, 1992, *Performance of a 41 Foot High Geotextile Wall*, WA-RD 257.1, Washington, USA.

Andrawes, K.Z., A., McGown and M.H., Kabir, 1984, "Uniaxial Strength Testing of Woven and Nonwoven Geotextiles", *Geotextiles and Geomembranes*, Vol. 1, pp. 41-56.

Balakrishnan, S., 2016, *Studies on the Performance of Geosynthetic Reinforced Soil Walls with Marginal Backfills*, Ph.D Dissertation Report, Indian Institute of Technology, Bombay.

Balakrishnan, S. and B.V.S., Viswanadham, 2017, "Evaluation of Tensile Load-Strain Characteristics of Geogrids through In-Soil Tensile Tests", *Geotextiles and Geomembranes*, Vol. 45, No. 1, pp. 35-44.

Ballegeer, J.P. and J.T.H. Wu, 1993, "Intrinsic Confined and Unconfined Load-Deformation Properties of Geotextiles", *In: Geosynthetic Soil Reinforcement Testing Procedures*, S.C. Jonathan Cheng, Philadelphia, U.S.A., pp. 16-31.

Bell, J., 1982, "Development of Test Methods by ASTM", *In: Second International Conference on Geotextiles*, Las Vegas, U.S.A., Industrial Fabrics Association International, Minneapolis, Vol. 2, pp. 331-333.

Berg, R.R., B.R., Christopher and N.C., Samtani, 2009, *Design of Mechanically Stabilized Earth Walls and Reinforced Soil Slopes - Volume I*, FHWA-NHI-10-024, Washington (DC).

Boyle, S.R., M., Gallagher and R.D., Holtz, 1996, "Influence of Strain Rate, Specimen Length and Confinement on Measured Geotextile Properties", *Geosynthetics International*, Vol. 3, No. 2, pp. 205-225.

Das, B.M., 2011, *Geotechnical Engineering Handbook*, J. Ross Publishing, Florida.

El-Fermaoui, A. and E., Nowatzki, 1982, "Effect of Confining Pressure on Performance of Geotextiles in Soils", *In: Second International Conference on Geotextiles*, Vol. 3, Industrial Fabrics Association International, Minnesota, Las Vegas, U.S.A..

Elias V., 2000, *Corrosion/Degradation of Soil Reinforcements for Mechanically Stabilized Earth Walls and Reinforced Soil Slopes*, FHWA-NHI-00-044, Washington (DC).

Elias V., Z., Yuan, R.H., Swan Jr. and R. C. Bachus, 1998, *Development of Protocols for Confined Extension/Creep Testing of Geosynthetics for Highway Applications*, FHWA-RD-97-143, Virginia.

Fahmy, R.F.W., 1982, *The Prediction and Measurement of the Behaviour of Soil-Geotextile Model Systems Acting in Plane Strain*, PhD Thesis, Strathclyde University, Glasgow.

International Organization for Standardization (ISO), 10319, 2015, "Geotextiles – Wide-width ensile test", International Organization for Standardization, Geneva, Switzerland.

Kokkalis, A. and N., Papacharisis, 1989, "A Simple Laboratory Method to Estimate the In-Soil Behaviour of Geotextiles", *Geotextiles and Geomembranes*, Vol. 8, No. 2, pp. 147-157.

Leshchinsky, D. and D.A., Field, 1987, "In-Soil Load, Elongation, Tensile Strength and Interface Friction of Nonwoven Geotextiles", *Proceedings of Geosynthetics'87*, New Orleans, USA, Vol. 1, pp. 238-249.

Ling, H.I., D., Leshchinsky and F., Tatsuoka, 1997, "Stress-Confinement Effect of Nonwoven Geotextile on Design of Reinforced Soil Retaining Wall", *Soils and Foundatios*, Vol. 37, No. 4, pp. 121-126.

Ling, H.I., J.T.H., Wu and F., Tatsuoka, 1992, "Short-Term Strength and Deformation Characteristics of Geotextiles under Typical Operational Conditions", *Geotextiles and Geomembranes*, Vol. 11, No. 2, pp. 185-219.

Ling, H. I., J.T.H., Wu, F., Tatsuoka, T., Sato and J. Nishimura, 1990, "Strength and Deformation Characteristics of A Nonwoven Geotextile Under Soil Confinement Conditions", *In: 25th Japan National Conference on Soil Mechanics and Foundation Engineering*, Okayama, Japan.

McGown, A. and K.Z., Andrawes, 1982, "An Approach to Laboratory Testing of Geotextiles", *Quarterly Journal of Engineering Geology*, Vol. 15, pp. 177-185.

McGown, A., I., Yogarajah, K.Z., Andrawes and M.A., Saad, 1995, "Strain Behaviour of Polymeric Geogrids Subjected to Sustained and Repeated Loading in Air and in Soil", *Geosynthetics International*, Vol. 2, No. 1, pp. 341-355.

McGown, A., K.Z., Andrawes, M.H., Kabir, 1982, "Load-Extension Testing of Geotextiles Confined In-Soil", *In: Second International Conference on Geotextiles*, Vol. 3, pp. 1-6 1982.

Mendes, M.J.A., E.M., Palmeira, E., Matheus, 2007, "Some Factors Affecting the In-Soil Load Strain Behaviour of Virgin and Damaged Nonwoven Geotextiles", *Geosynthetics International*, Vol. 14, No. 1, pp. 39-50.

Morsy, A.M., J.G., Zornberg, D., Leshchinsky, J., Han, 2019, "Soil-Reinforcement Interaction: Effect of Reinforcement Spacing and Normal Stress", *Journal of Geotechnical and Geoenvironmental Engineering*, Vol. 145, No. 12, pp. 39-50.

Murray, R.T. and A., McGown, 1982, "The Selection of Testing Procedures for the Specification of Geotextiles", *In: Second International Conference on Geotextiles*, Vol. 2, pp. 1-6 1982.

Resl, S., 1990, "Soil-Reinforcing Mechanisms of Nonwoven Geotextiles", *Proceedings Of*

The Fourth International Conference On Geotextiles, Geomembranes And Related Products, Vol. 1, pp. 93-96.

Shrestha, S.C. and J.R., Bell, 1982, "A Wide Strip Tensile Test of Geotextiles", *In: Second International Conference on Geotextiles*, Vol. 3, pp. 1-6.

Springman, S., M., Bolton, J., Sharma, S., Balachandran, 1992, "Modelling and Instrumentation of A Geotextile in the Geotechnical Centrifuge", *In: Proceedings of International Symposium on Earth Reinforcement Practice*, pp. 167-172.

The American Society for Testing Materials (ASTM) D2487-11, 2011, "Standard Practice for Classification of Soils for Engineering Purposes (Unified Soil Classification System)", *American Society for Testing and Materials, West Conshohocken*, Pennsylvania, USA.

The American Society for Testing Materials (ASTM) D 4253-14, 2014, "Standard Test Methods for Maximum Index Density and Unit Weight of Soils Using a Vibratory Table", *American Society for Testing and Materials*, West Conshohocken, Pennsylvania, USA.

The American Society for Testing Materials (ASTM) D 4254-14, 2014, "Standard Test Methods for Minimum Index Density and Unit Weight of Soils and Calculation of Relative Density", *American Society for Testing and Materials*, West Conshohocken, Pennsylvania, USA.

The American Society for Testing Materials (ASTM) D 4595, 2011, "Standard Test Method for Tensile Properties of Geotextiles by the Wide-width Strip Method", *ASTM International*, West Conshohocken, Pennsylvania, USA.

The American Society for Testing Materials (ASTM) D 6637, 2015, "Standard Test Method for Determining Tensile Properties of Geogrids by the Single or Multi-rib Tensile Method", *ASTM International*, West Conshohocken, Pennsylvania, USA.

The American Society for Testing Materials (ASTM) D 854-14, 2014, "Standard Test Methods for Specific Gravity of Soil Solids by Water Pycnometer", *American Society for Testing and Materials*, West Conshohocken, Pennsylvania, USA.

Wang, A., B., Zhang and L., Lu, 1990, "Research of Influence of Test Conditions on the Tensile Strength of Geotextile", *Proceedings of the Fourth International Conference on Geotextiles, Geomembranes and Related Products*, Vol. 2, pp. 782.

Wang, Y., 2001, "A Method for Tensile Test of Geotextiles with Confining Pressure", *Journal of Industrial Textiles*, Vol. 30, No. 4, pp. 289-302.

Wilson-Fahmy, R.F., R.M. ,Koerner, and J.A., Fleck, 1993, *Unconfined and Confined Wide Width Tension Testing of Geosynthetics*, Geosynthetic Soil Reinforcement Testing Procedures, ASTM STP 1190, S.C. Jonathan Cheng, Ed., American Society for Testing and Materials, Philadelphia.

Won, M.S. and Y.S., Kim, 20072, "Internal Deformation Behaviour of Geosynthetic Reinforced Soil Walls", *Geotextiles and Geomembranes*, Vol. 25, No. 1, pp. 10-2.

Wu, J.T.H., 1991, "Measuring Inherent Load-Extension Properties of Geotextiles for Design of Reinforced Structures", *Geotechnical Testing Journal*, Vol. 14, No 2, pp. 157-165.

Zheng, J. and R.D., Hryciw, 2015, "Traditional Soil Particle Sphericity, Roundness and Surface Roughness by Computational Geometry", *Géotechnique*, Vol. 65, No. 6, pp. 494-506.

APPENDIX A: RAW RESULTS OF THE TESTS

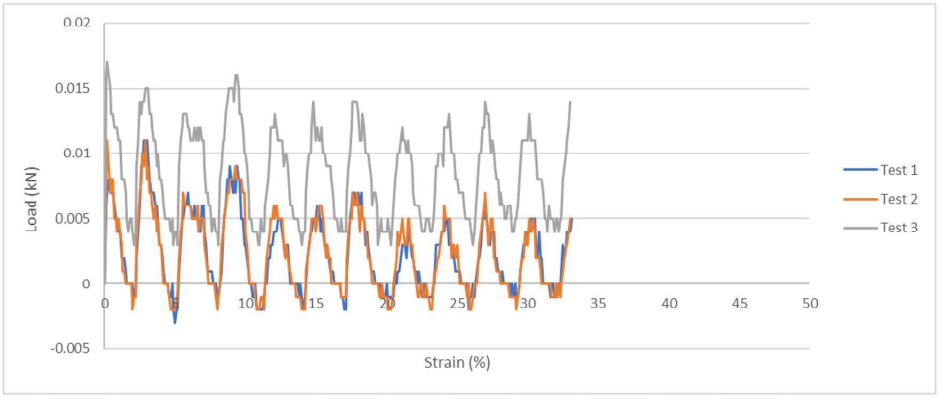


Figure A.1. Noise of the apparatus.

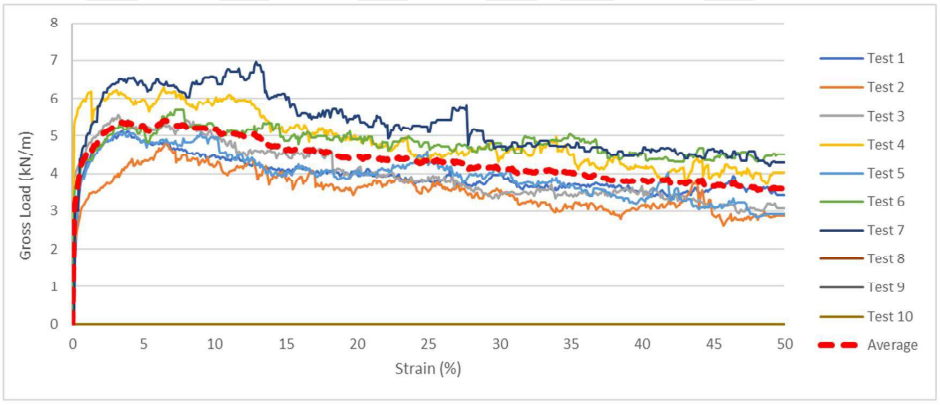


Figure A.2. Clamp pull-out tests in sand (single-layer, 25 kPa).

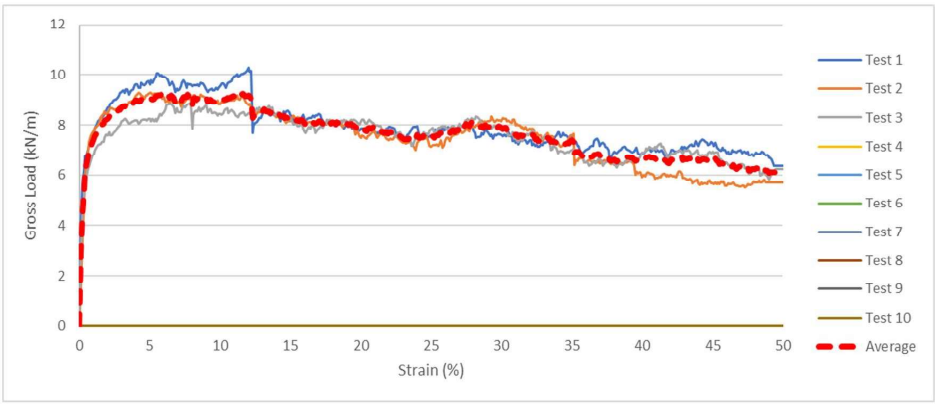


Figure A.3. Clamp pull-out tests in sand (single-layer, 50 kPa).

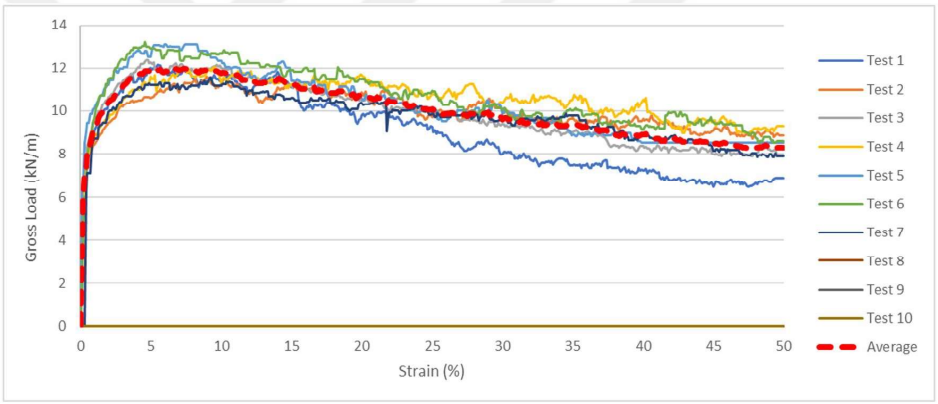


Figure A.4. Clamp pull-out tests in sand (single-layer, 75 kPa).

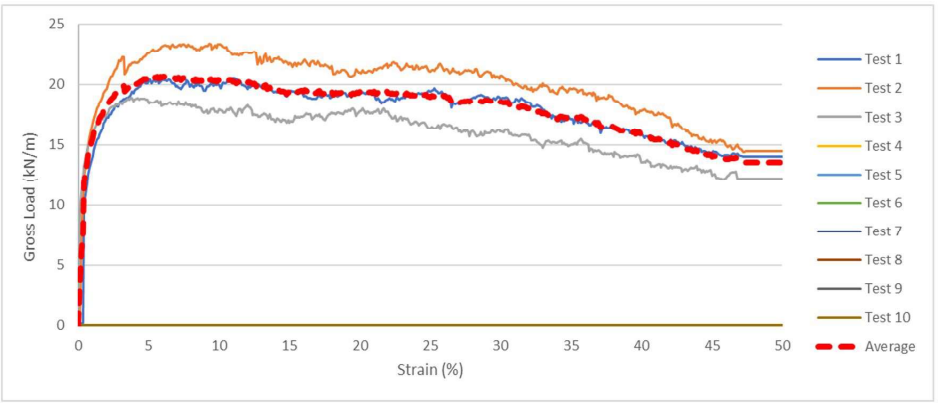


Figure A.5. Clamp pull-out tests in sand (single-layer, 125 kPa).

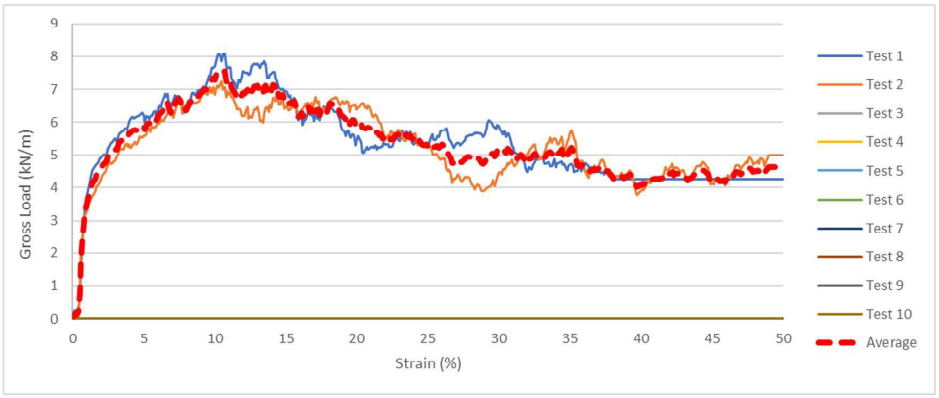


Figure A.6. Clamp pull-out tests in gravel (single-layer, 25 kPa).

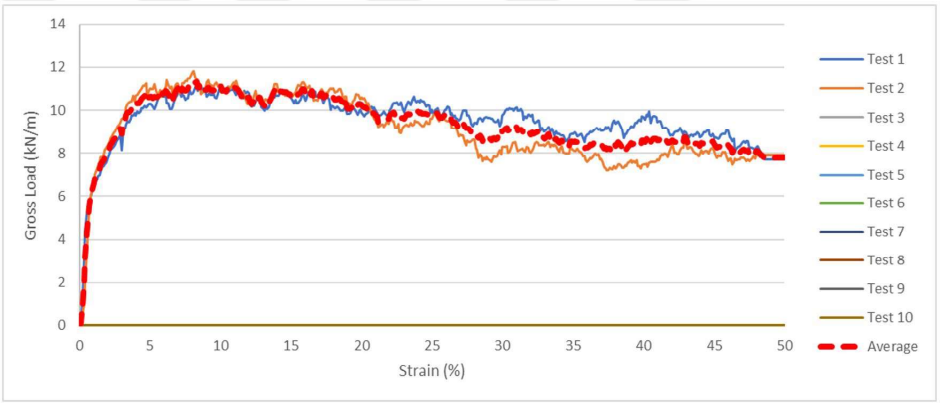


Figure A.7. Clamp pull-out tests in gravel (single-layer, 50 kPa).

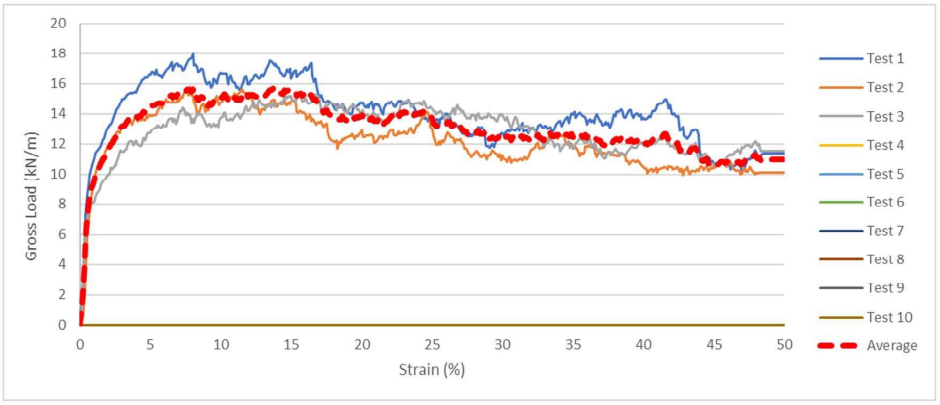


Figure A.8. Clamp pull-out tests in gravel (single-layer, 75 kPa).

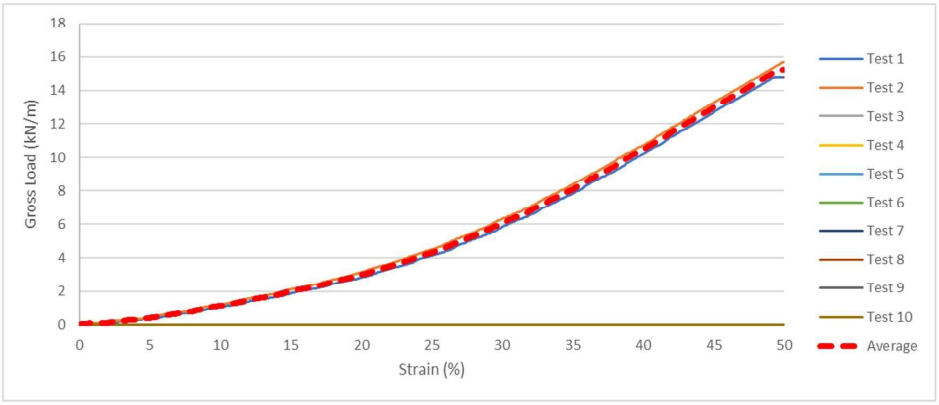


Figure A.9. In-air tests of NWGT.

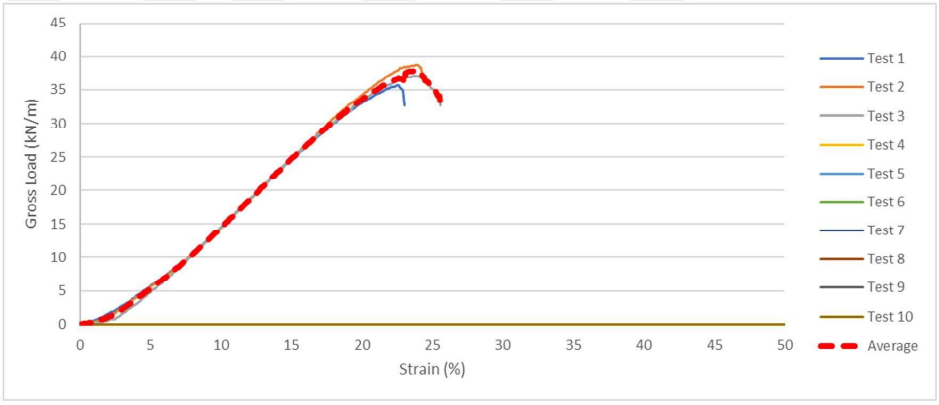


Figure A.10. In-air tests of WGTX.

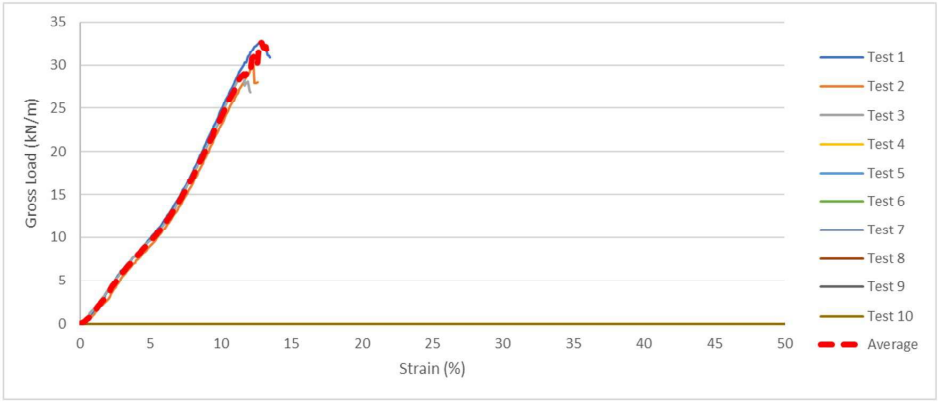


Figure A.11. In-air tests of WOGD.

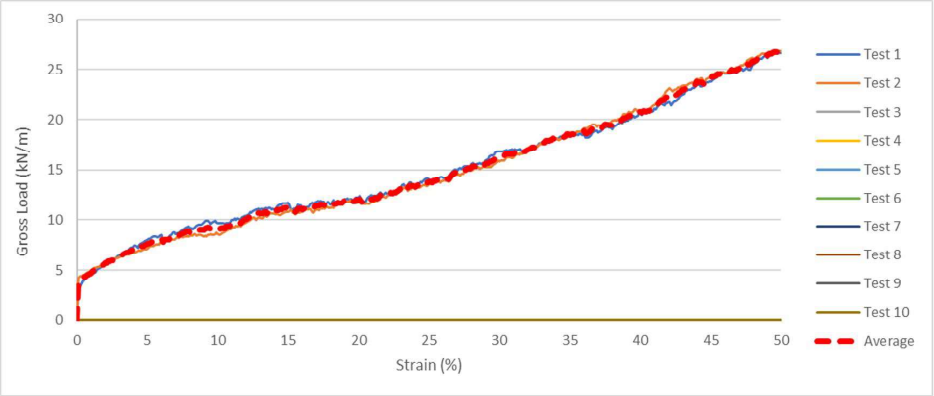


Figure A.12. Single-layer NWGT in sand (25 kPa).

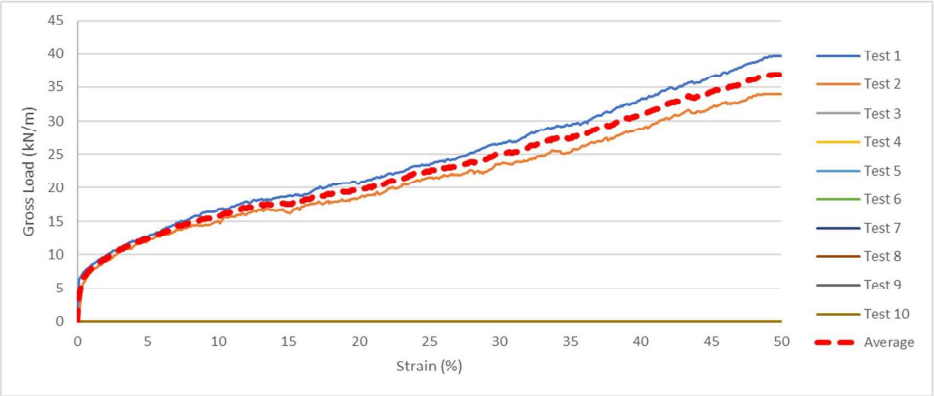


Figure A.13. Single-layer NWGT in sand (50 kPa).

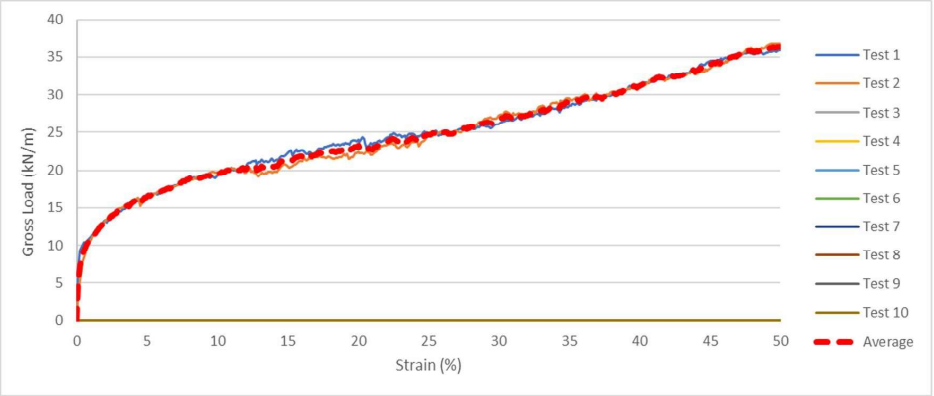


Figure A.14. Single-layer NWGT in sand (75 kPa).

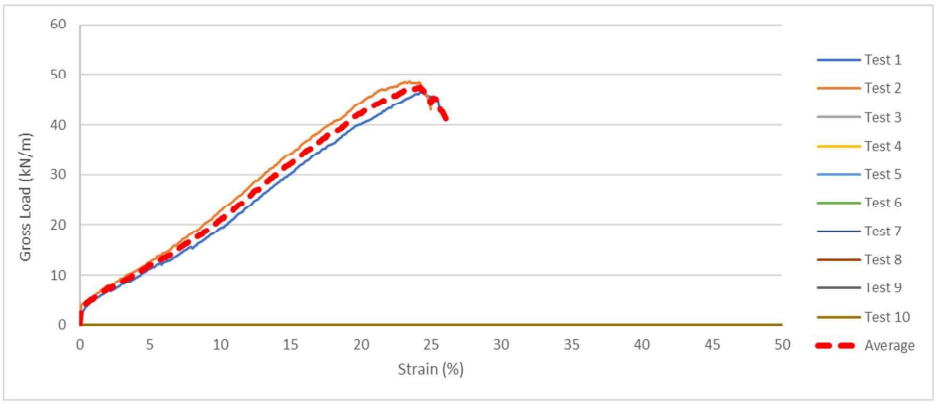


Figure A.15. Single-layer WGTX in sand (25 kPa).

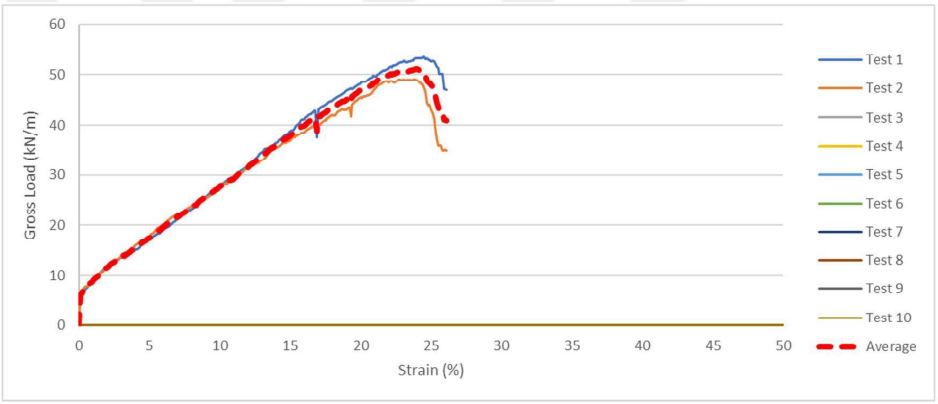


Figure A.16. Single-layer WGTX in sand (50 kPa).

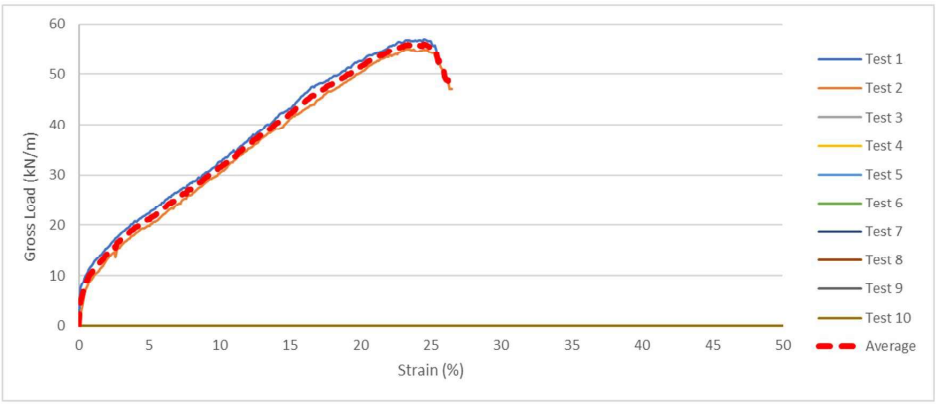


Figure A.17. Single-layer WGTX in sand (75 kPa).

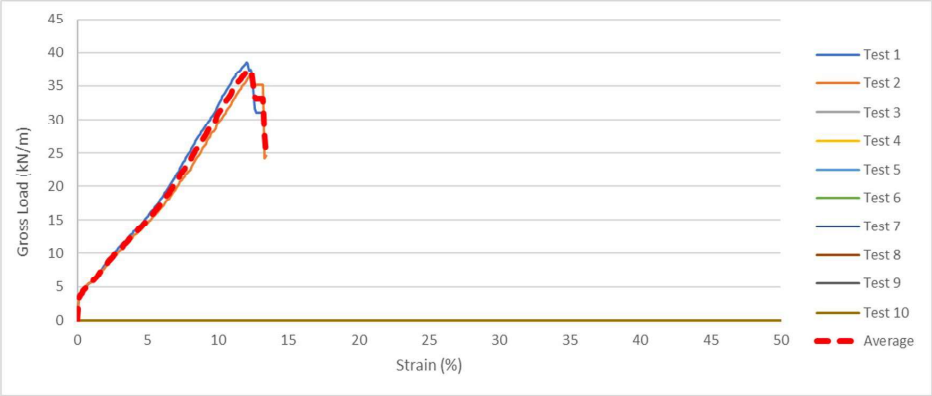


Figure A.18. Single-layer WOGD in sand (25 kPa).

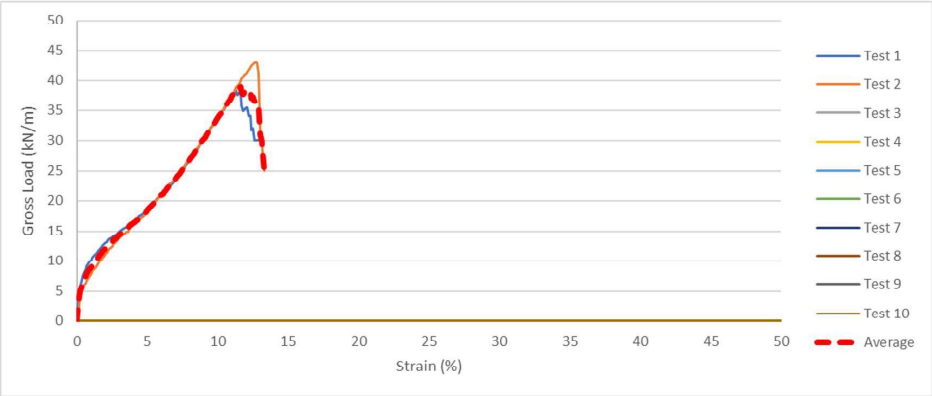


Figure A.19. Single-layer WOGD in sand (50 kPa).

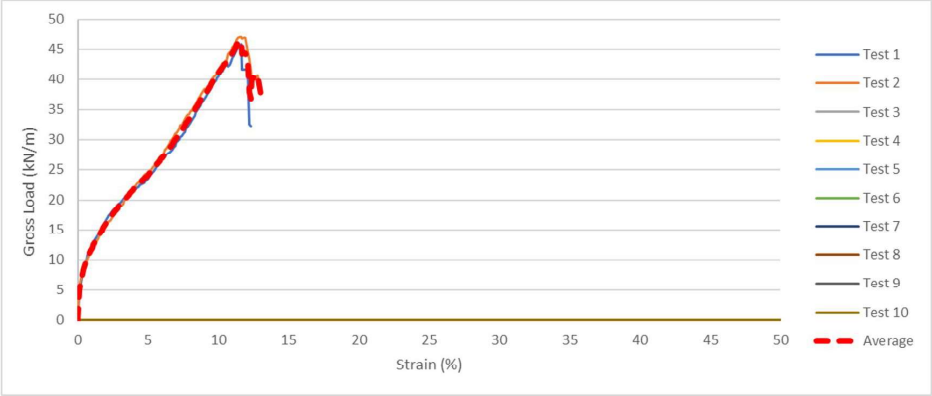


Figure A.20. Single-layer WOGD in sand (75 kPa).

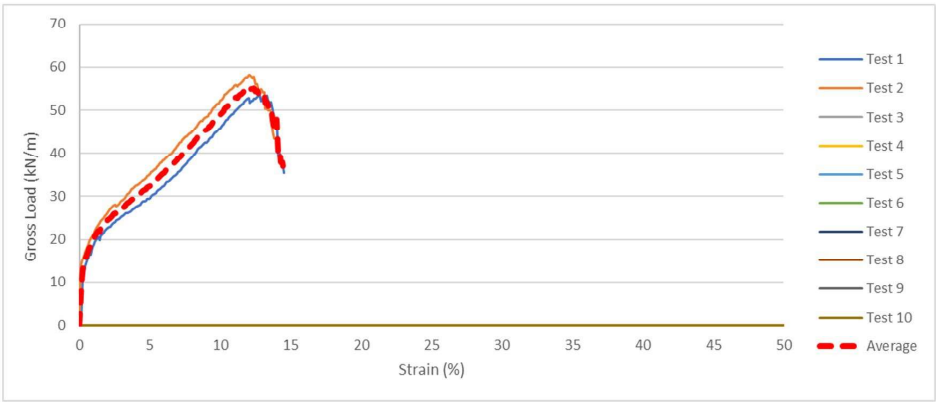


Figure A.21. Single-layer WOGD in sand (125 kPa).

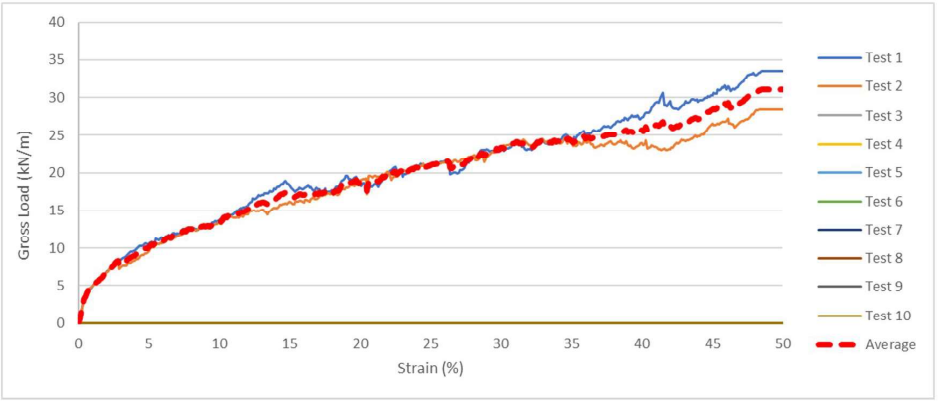


Figure A.22. Single-layer NWGT in gravel (25 kPa).

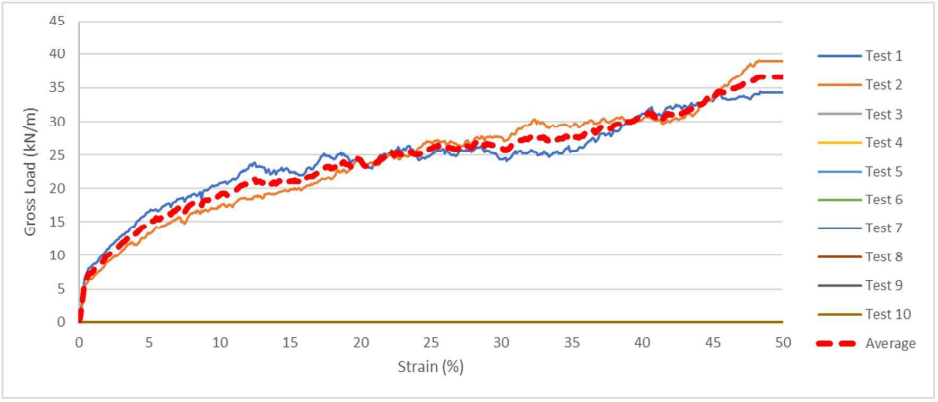


Figure A.23. Single-layer NWGT in gravel (50 kPa).

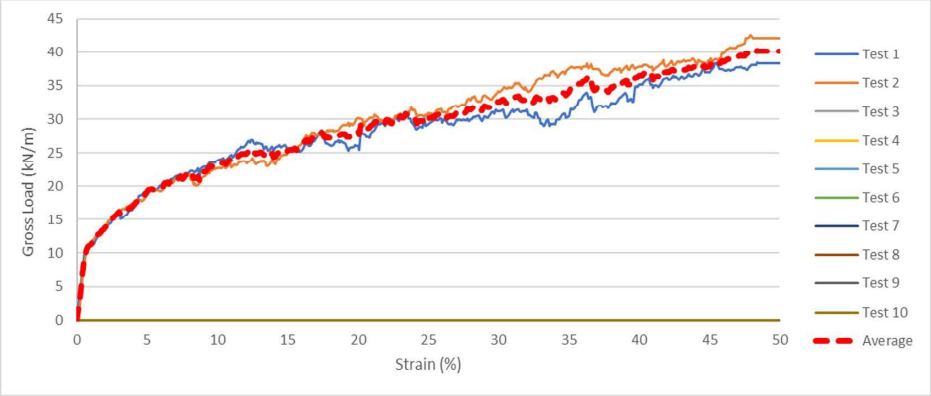


Figure A.24. Single-layer NWGT in gravel (75 kPa).

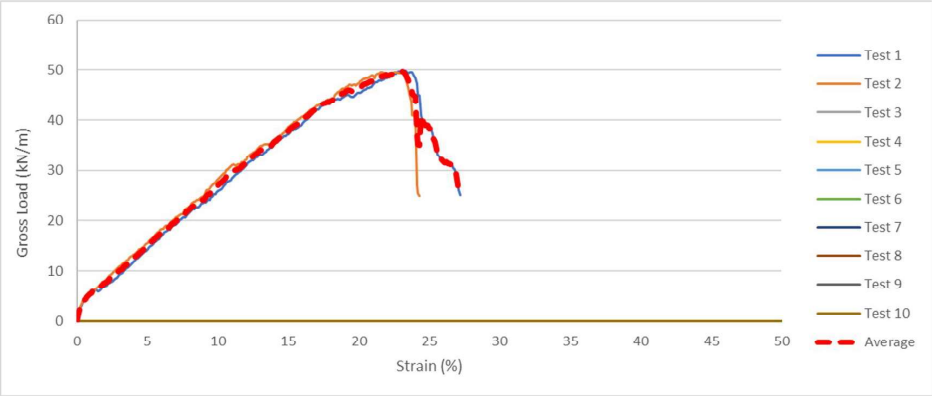


Figure A.25. Single-layer WGTX in gravel (25 kPa).

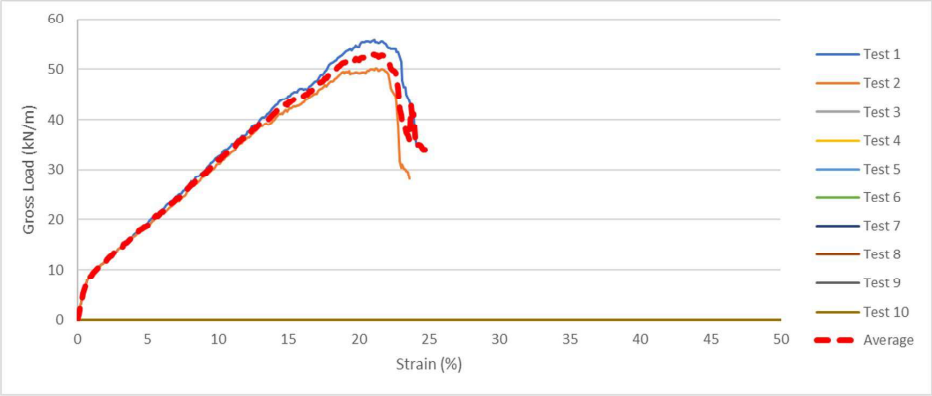


Figure A.26. Single-layer WGTX in gravel (50 kPa).

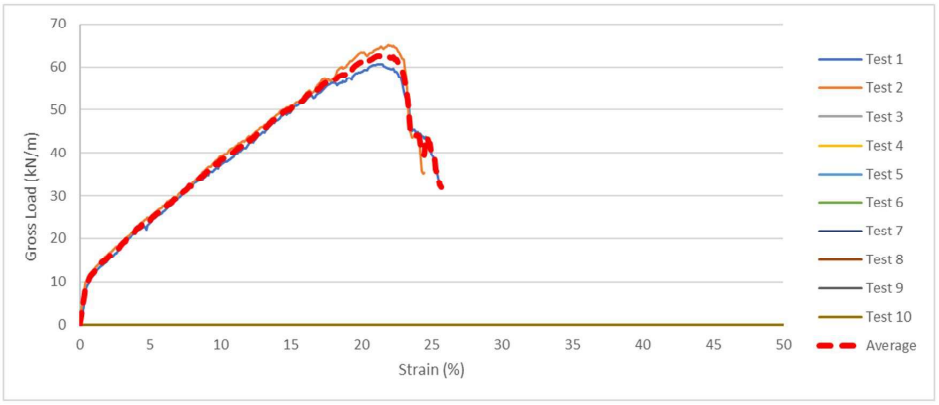


Figure A.27. Single-layer WGTX in gravel (75 kPa).

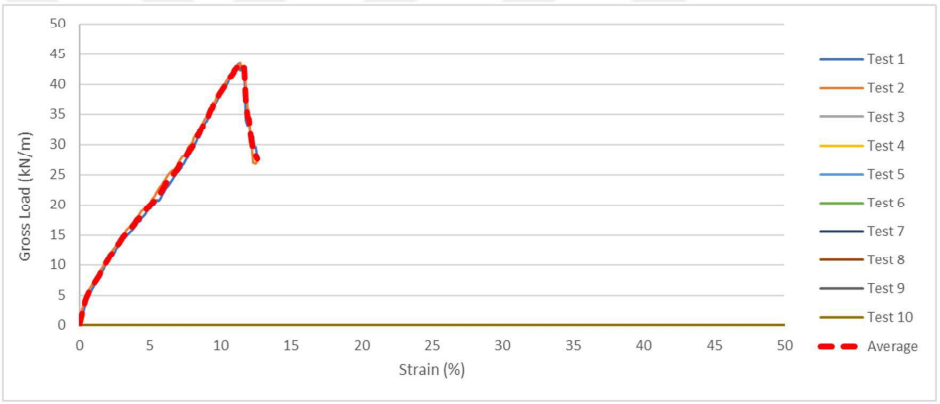


Figure A.28. Single-layer WOGD in gravel (25 kPa).

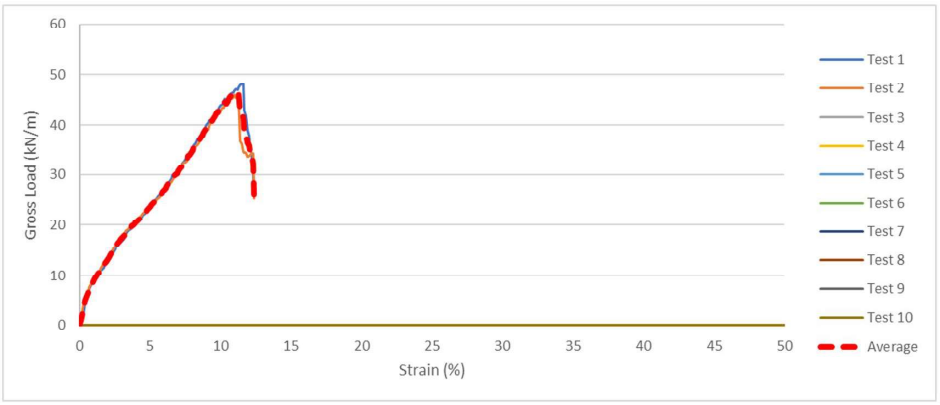


Figure A.29. Single-layer WOGD in gravel (50 kPa).

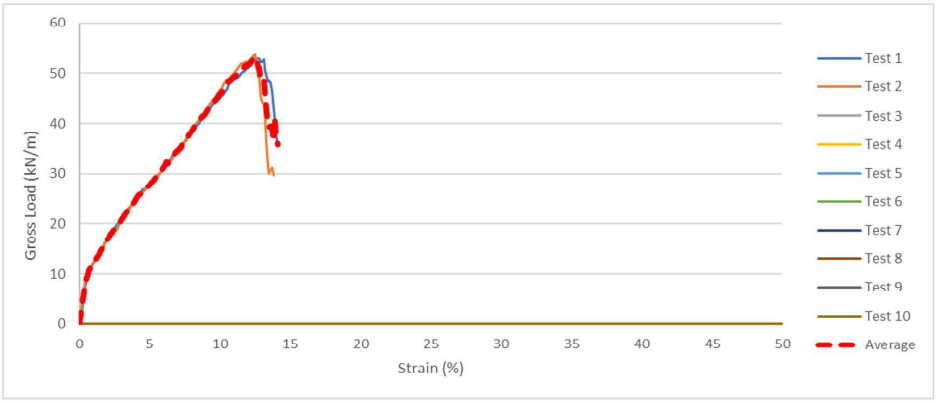


Figure A.30. Single-layer WOGD in gravel (75 kPa).

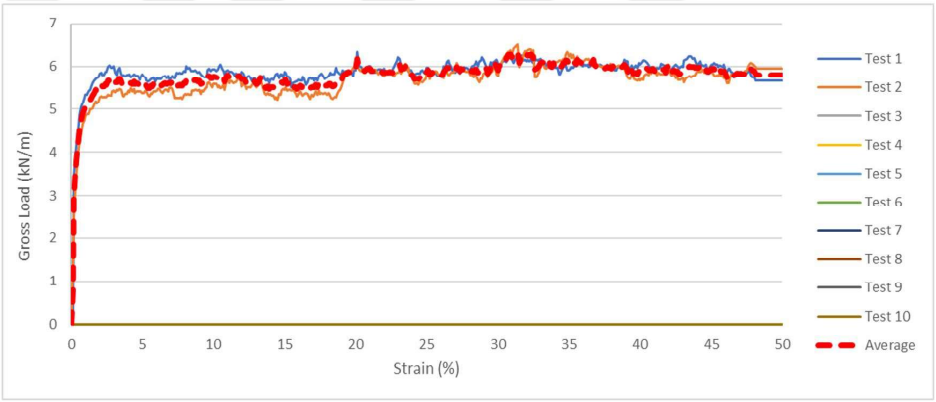


Figure A.31. Clamp pull-out tests in sand (multi-layer, NWGT, 25 mm).

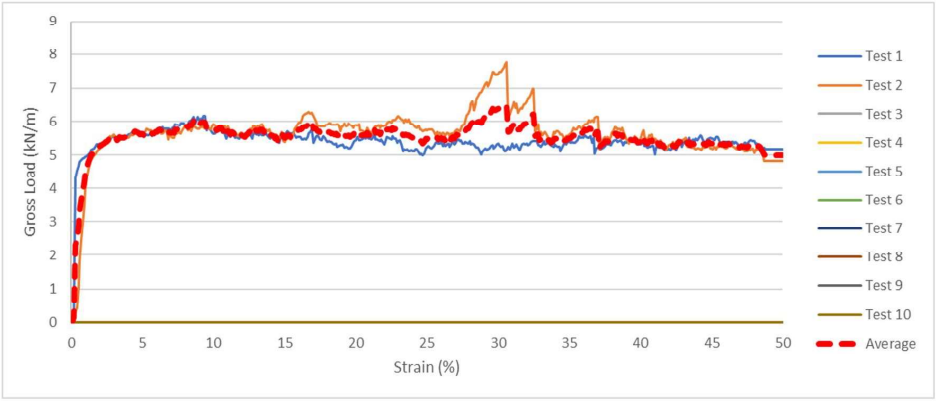


Figure A.32. Clamp pull-out tests in sand (multi-layer, NWGT, 50 mm).

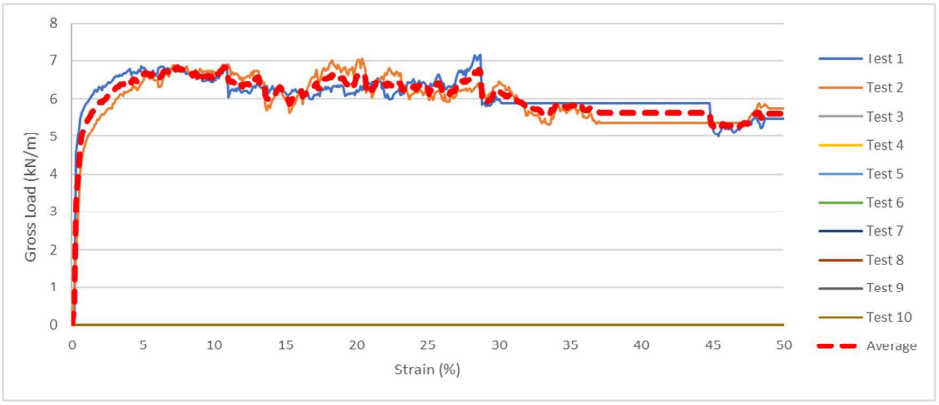


Figure A.33. Clamp pull-out tests in sand (multi-layer, NWGT, 100 mm).

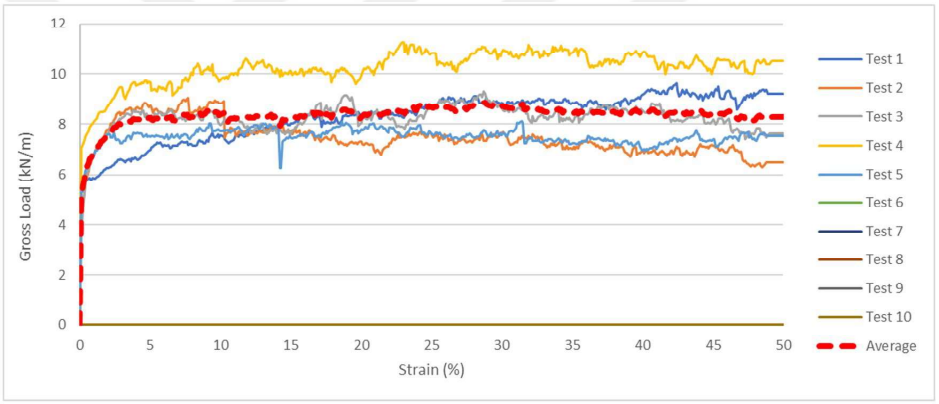


Figure A.34. Clamp pull-out tests in sand (multi-layer, WGTX, 25 mm).

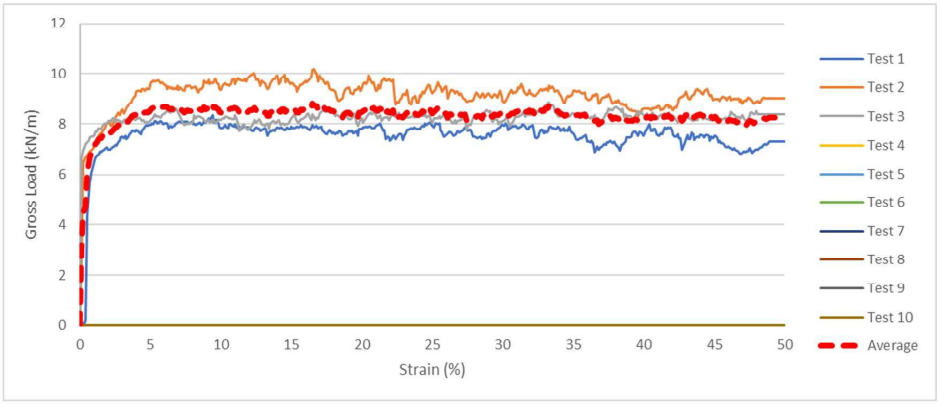


Figure A.35. Clamp pull-out tests in sand (multi-layer, WGTX, 50 mm).

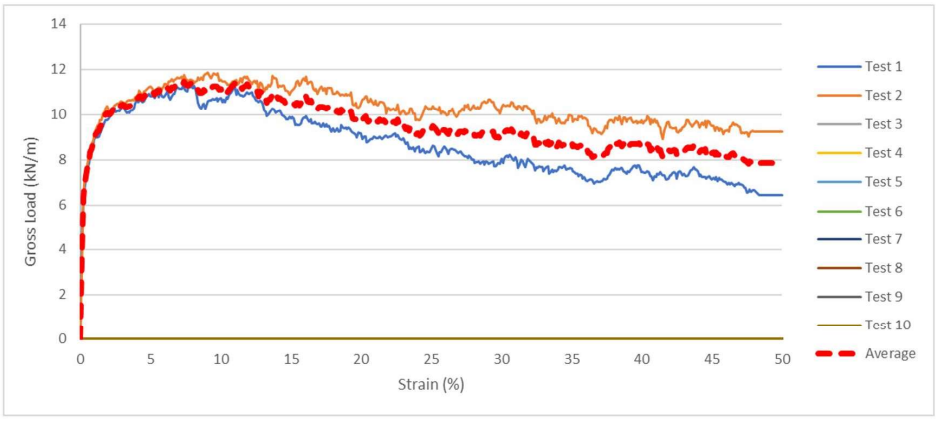


Figure A.36. Clamp pull-out tests in sand (multi-layer, WGTX, 100 mm).

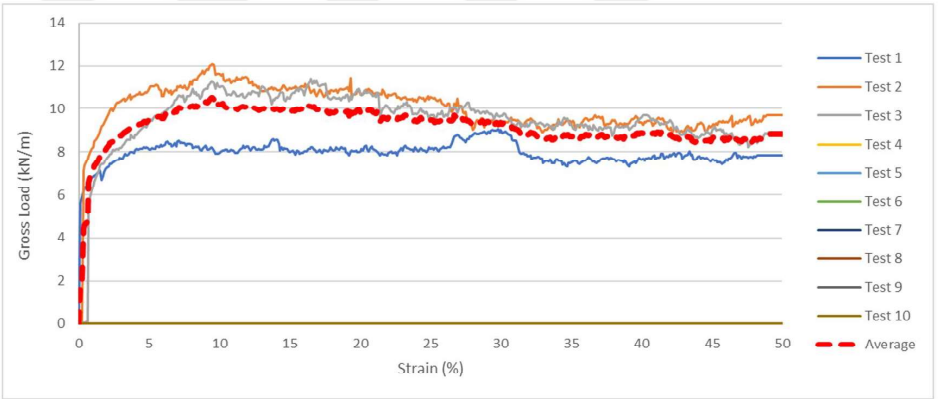


Figure A.37. Clamp pull-out tests in sand (multi-layer, WOGD, 25 mm).

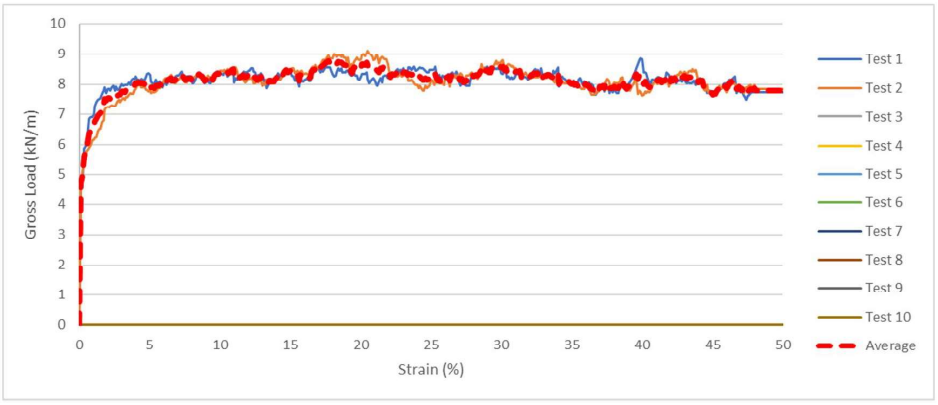


Figure A.38. Clamp pull-out tests in sand (multi-layer, WOGD, 50 mm).

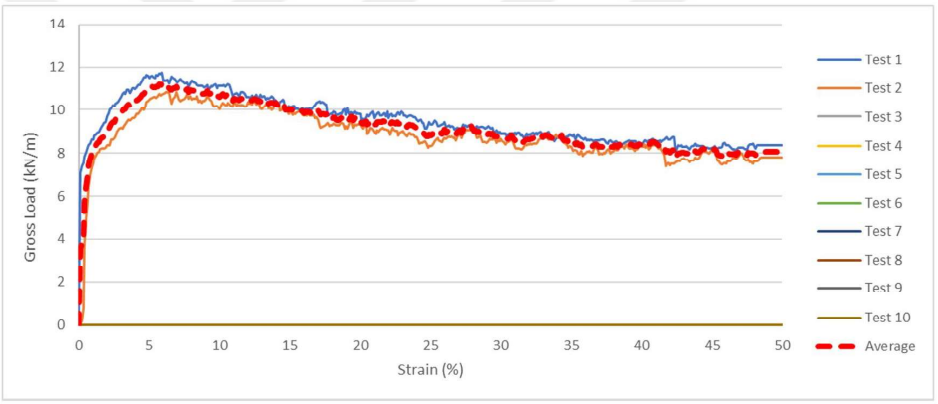


Figure A.39. Clamp pull-out tests in sand (multi-layer, WOGD, 100 mm).

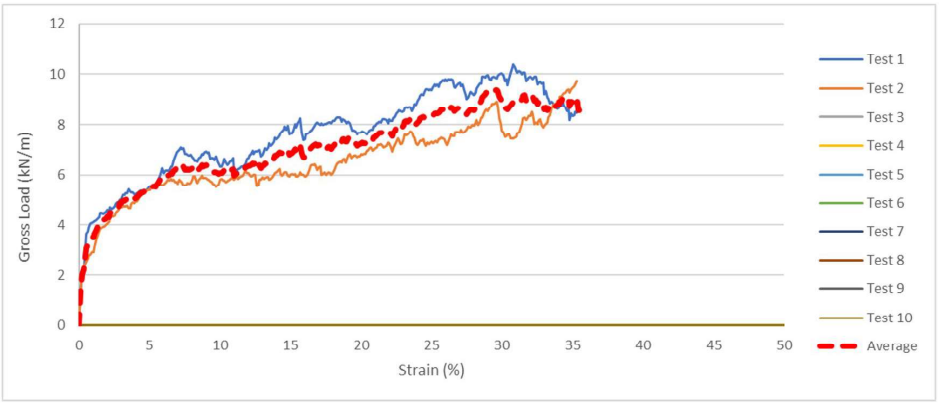


Figure A.40. Clamp pull-out tests in gravel (multi-layer, NWGT, 25 mm).

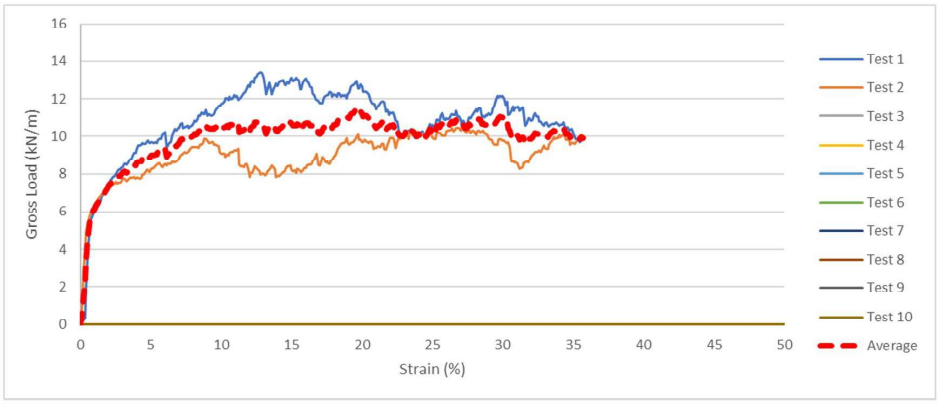


Figure A.41. Clamp pull-out tests in gravel (multi-layer, NWGT, 50 mm).

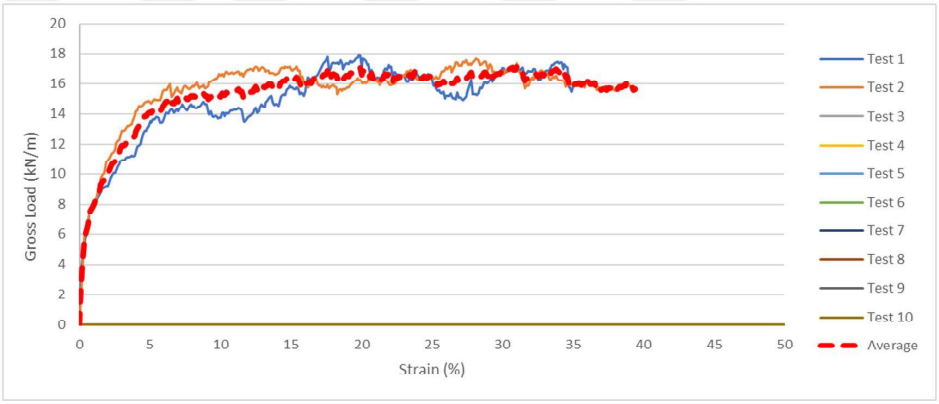


Figure A.42. Clamp pull-out tests in gravel (multi-layer, NWGT, 100 mm).

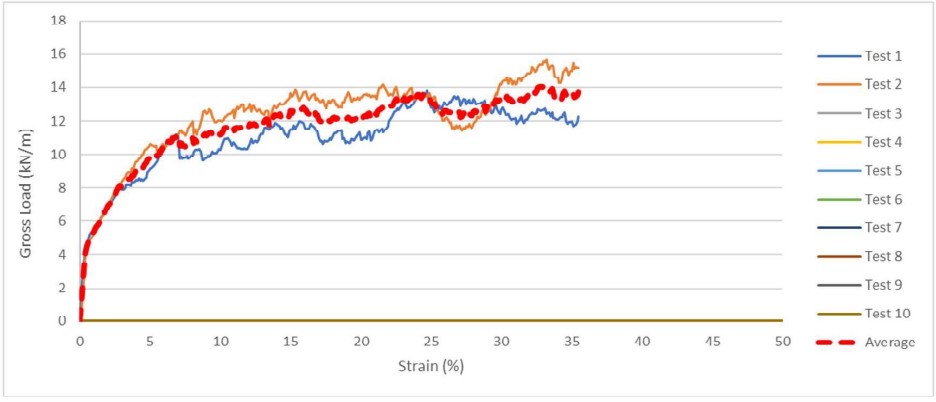


Figure A.43. Clamp pull-out tests in gravel (multi-layer, WGTX, 25 mm).

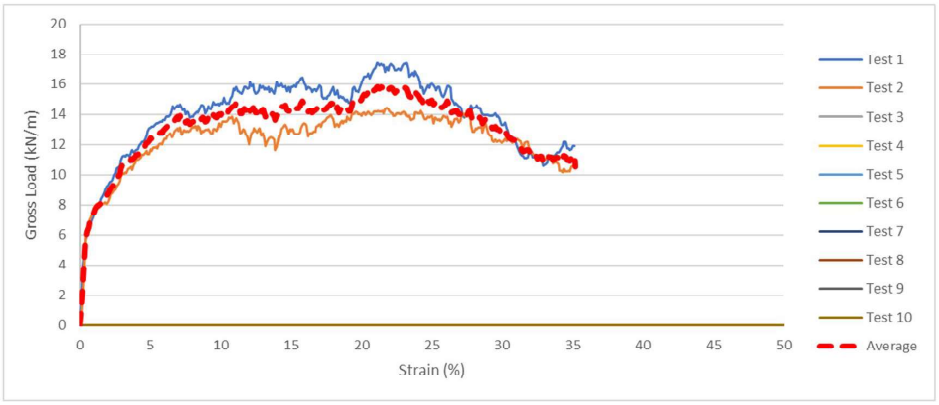


Figure A.44. Clamp pull-out tests in gravel (multi-layer, WGTX, 50 mm).

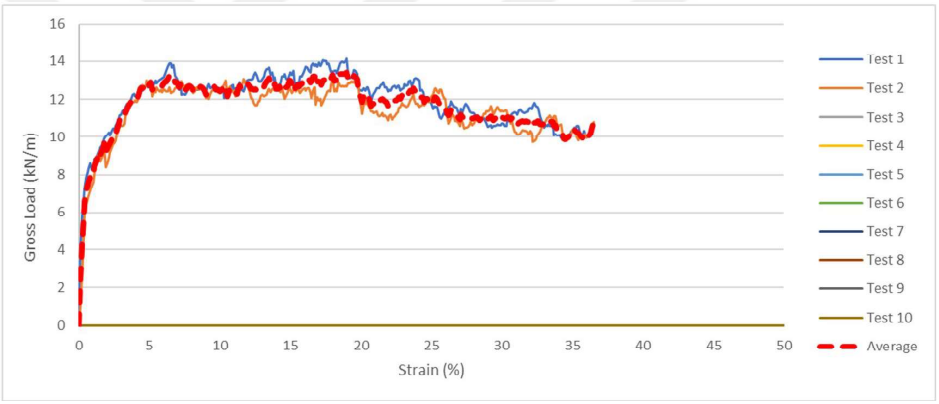


Figure A.45. Clamp pull-out tests in gravel (multi-layer, WGTX, 100 mm).

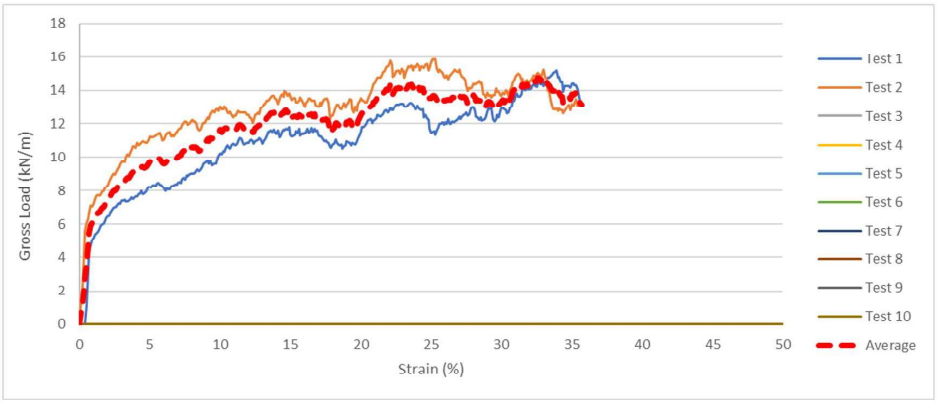


Figure A.46. Clamp pull-out tests in gravel (multi-layer, WOGD, 25 mm).

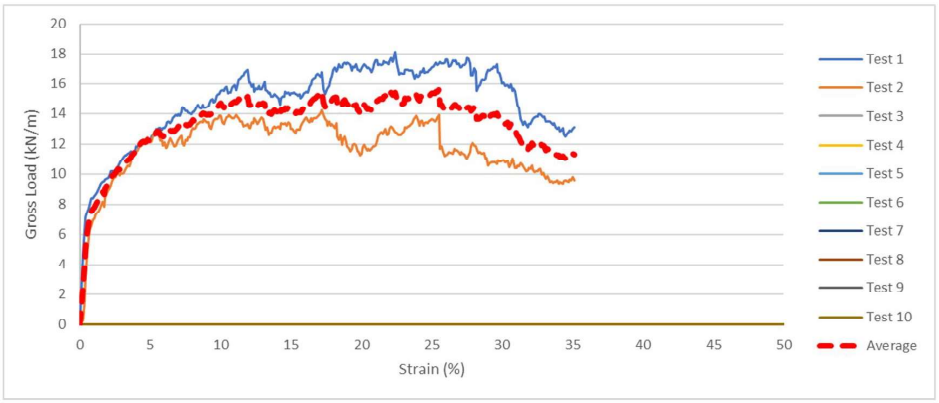


Figure A.47. Clamp pull-out tests in gravel (multi-layer, WOGD, 50 mm).

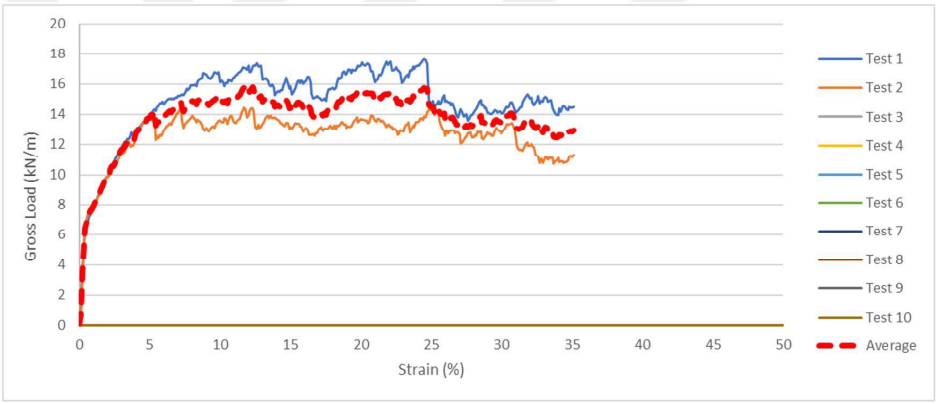


Figure A.48. Clamp pull-out tests in gravel (multi-layer, WOGD, 100 mm).

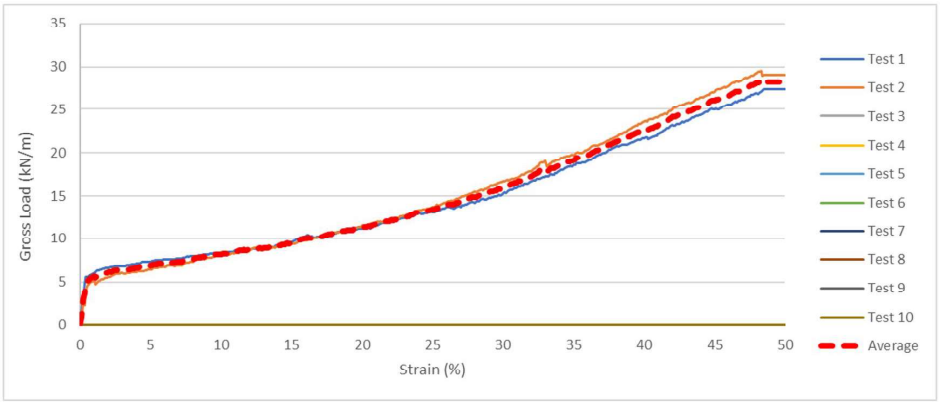


Figure A.49. Multi-layer NWGT in sand (25 mm).

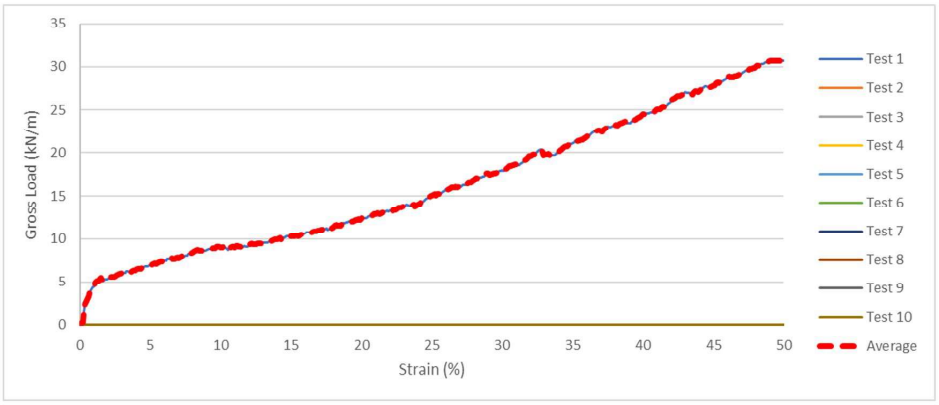


Figure A.50. Multi-layer NWGT in sand (50 mm).

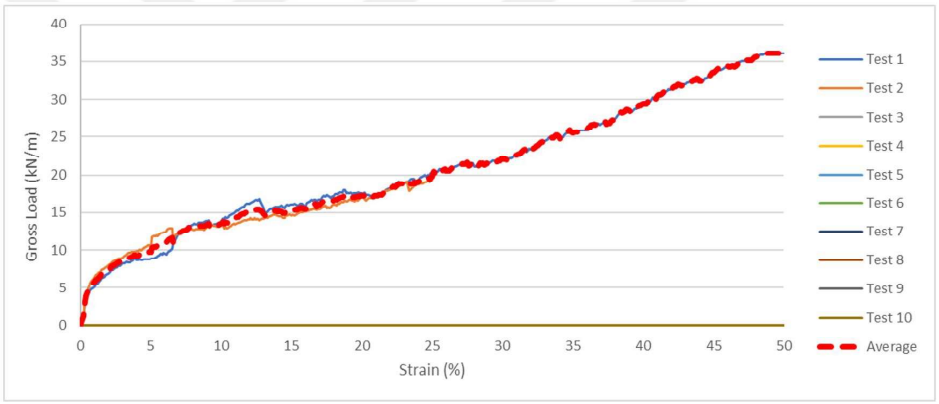


Figure A.51. Multi-layer NWGT in sand (100 mm).

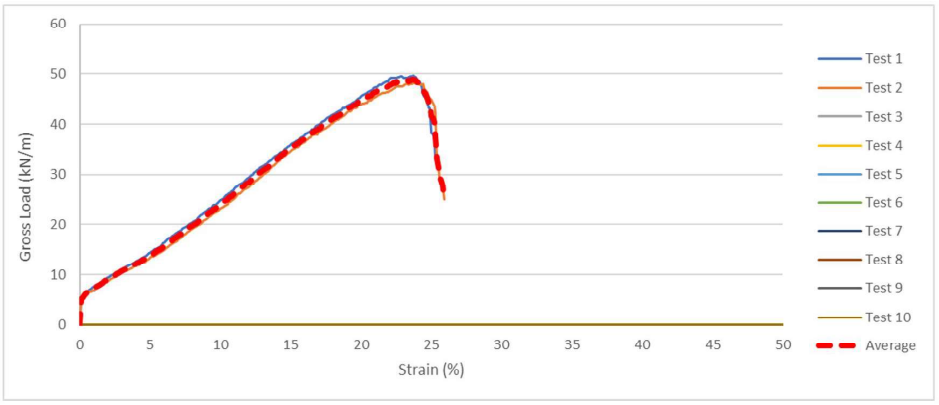


Figure A.52. Multi-layer WGTX in sand (25 mm).

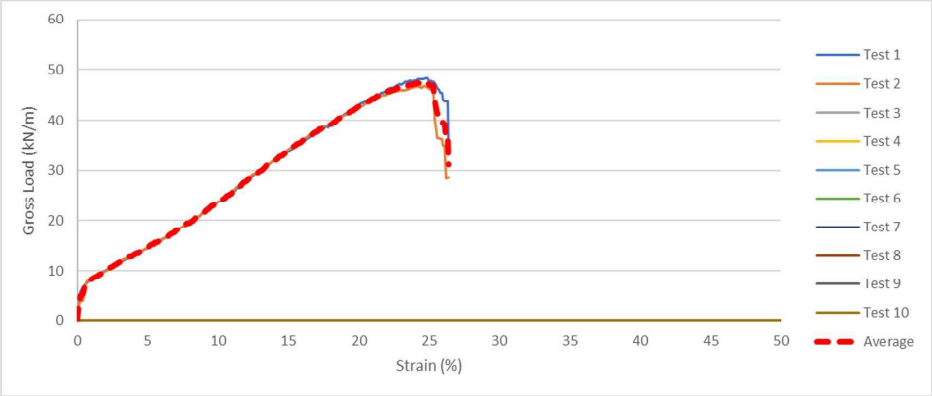


Figure A.53. Multi-layer WGTX in sand (50 mm).

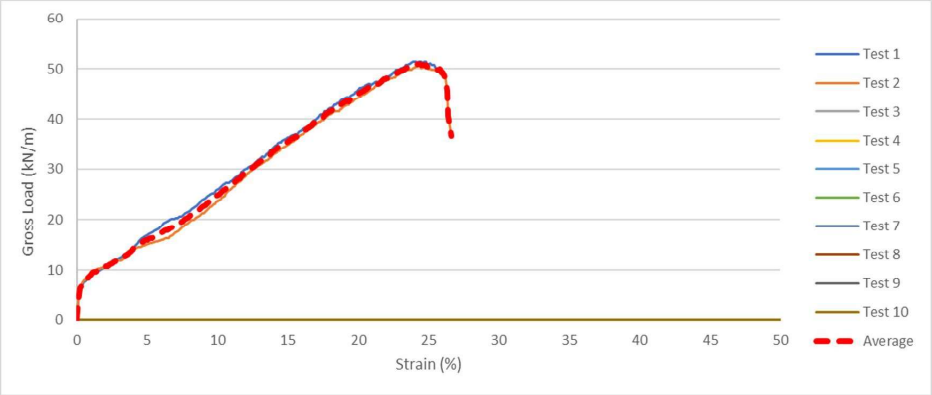


Figure A.54. Multi-layer WGTX in sand (100 mm).

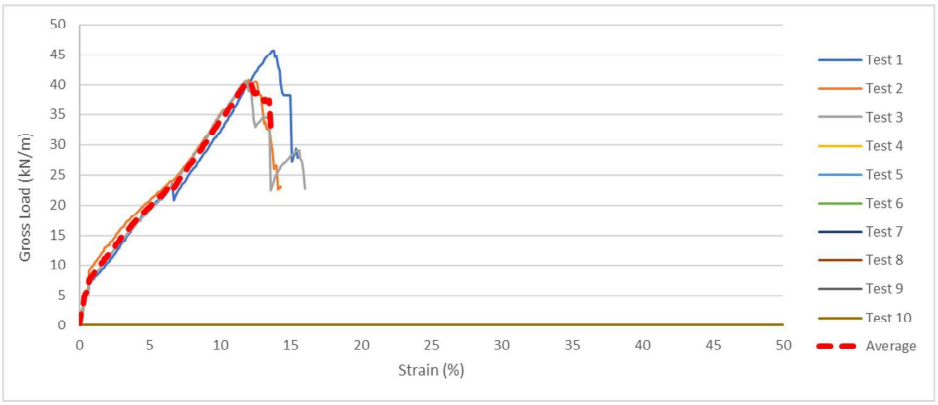


Figure A.55. Multi-layer WOGD in sand (25 mm).

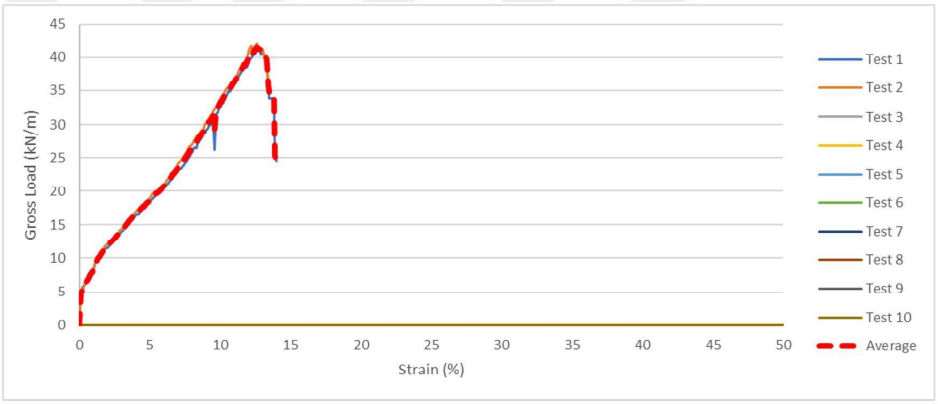


Figure A.56. Multi-layer WOGD in sand (50 mm).

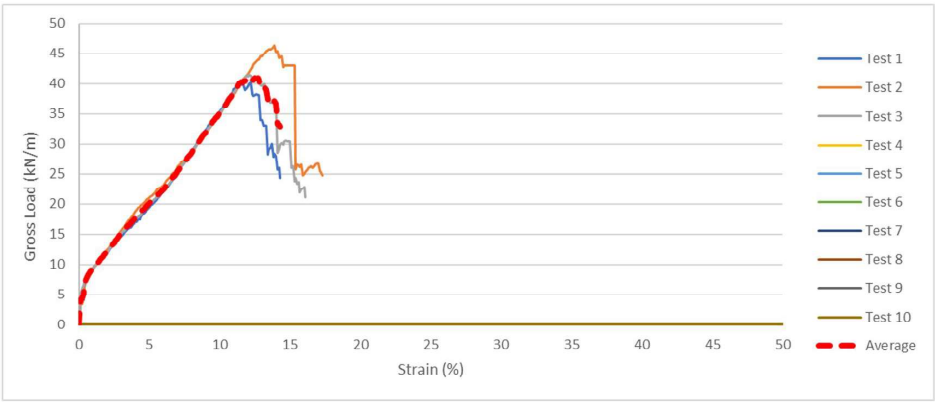


Figure A.57. Multi-layer WOGD in sand (100 mm).

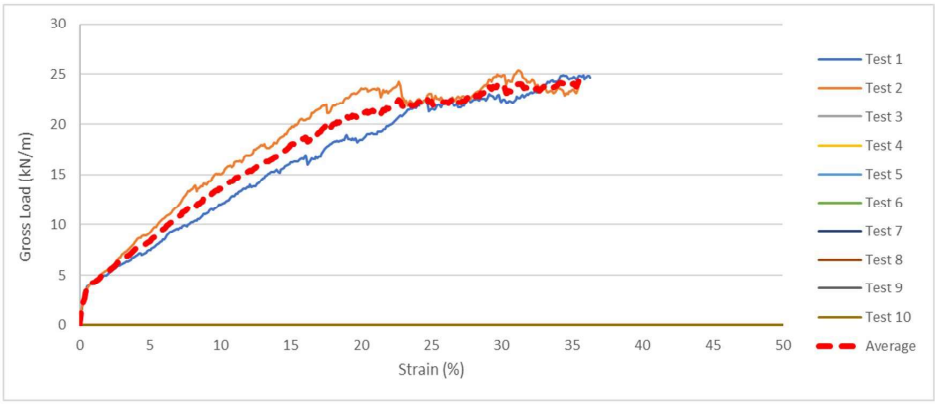


Figure A.58. Multi-layer NWGT in gravel (25 mm).

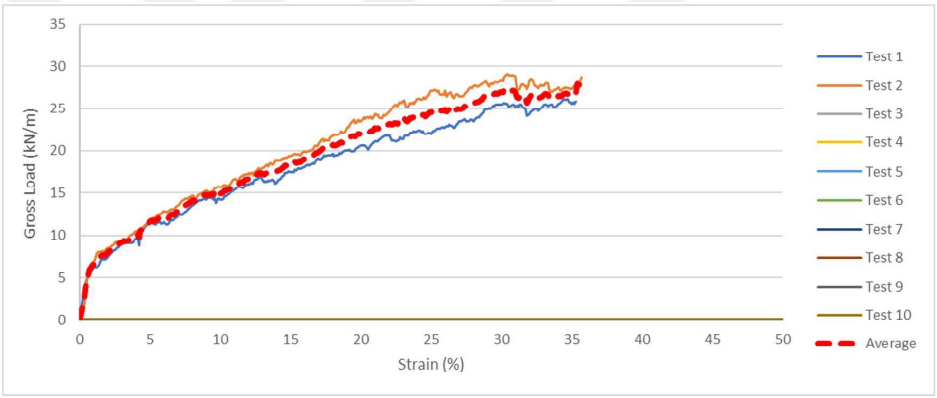


Figure A.59. Multi-layer NWGT in gravel (50 mm).

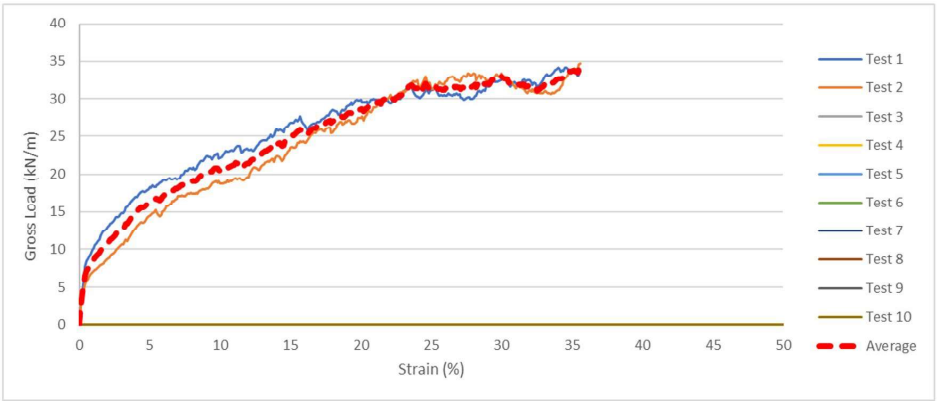


Figure A.60. Multi-layer NWGT in gravel (100 mm).

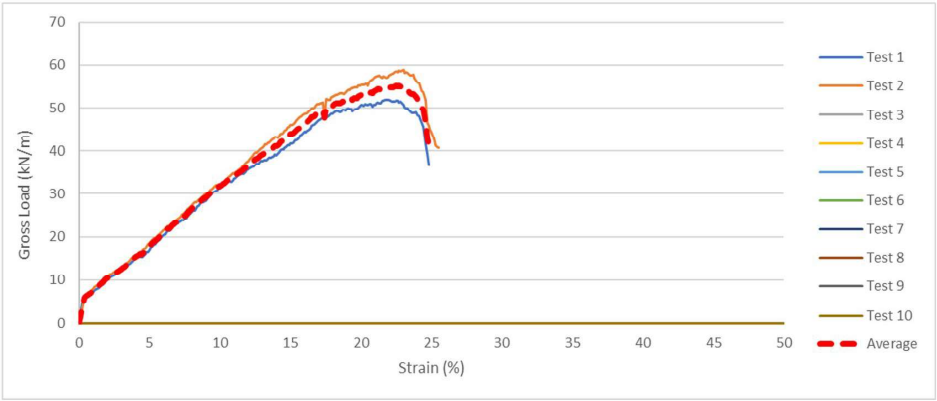


Figure A.61. Multi-layer WGTX in gravel (25 mm).

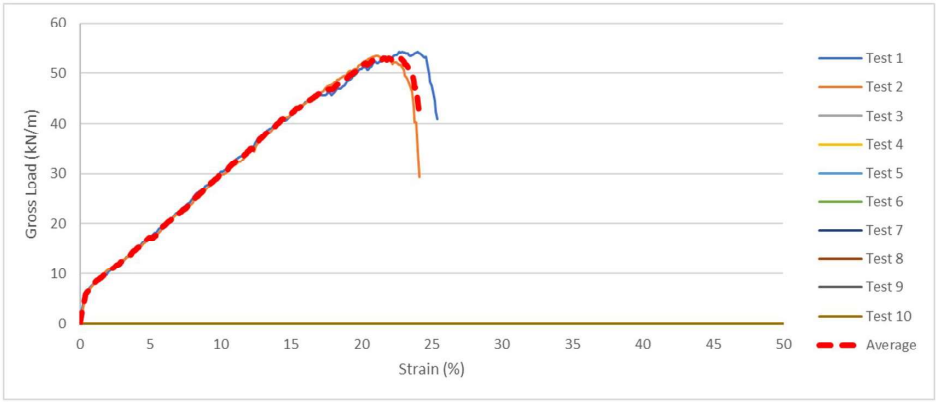


Figure A.62. Multi-layer WGTX in gravel (50 mm).

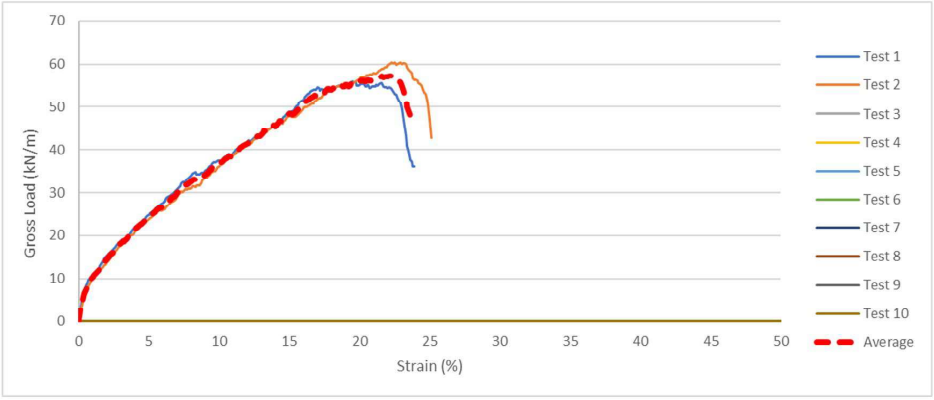


Figure A.63. Multi-layer WGTX in gravel (100 mm).

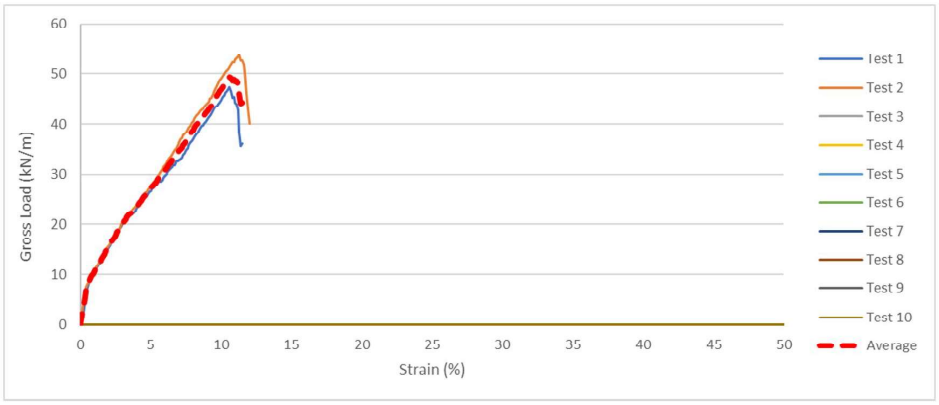


Figure A.64. Multi-layer WOGD in gravel (25 mm).

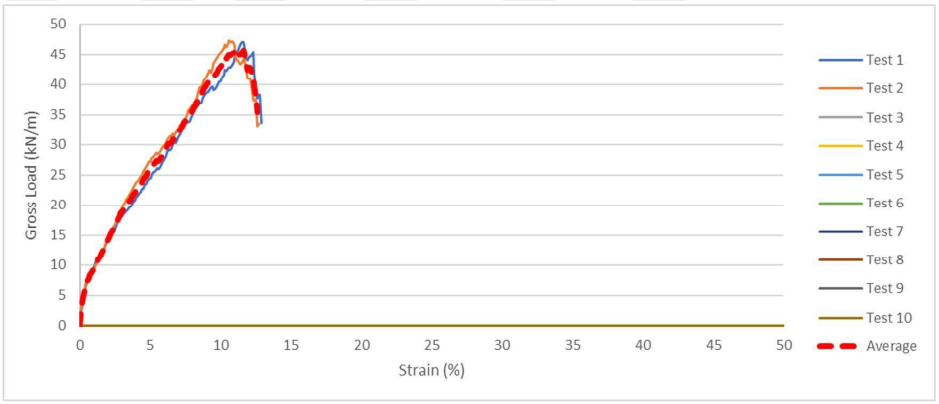


Figure A.65. Multi-layer WOGD in gravel (50 mm).

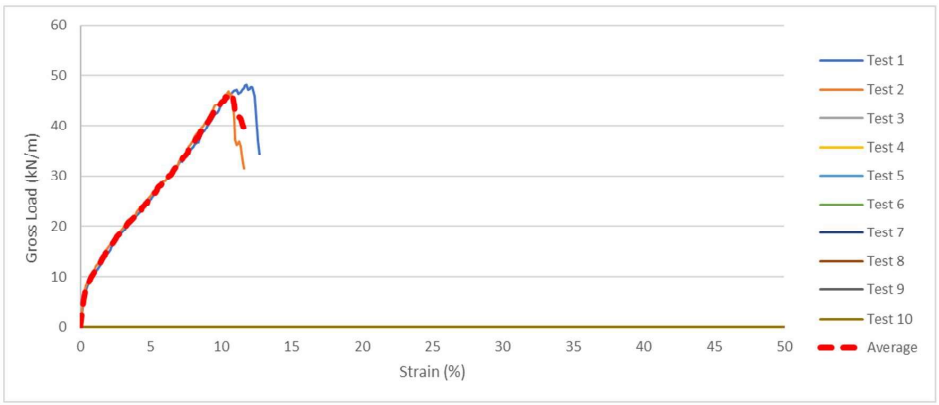


Figure A.66. Multi-layer WOGD in gravel (100 mm).

APPENDIX B: EVALUATION OF STIFFNESS INCREASE IN FINITE ELEMENT ANALYSES

The test box has been modeled and test has been simulated by performing finite element analyses (FEM). FEM is not capable of modelling the internal structure of reinforcements and soils (orientation of fibers/filaments/grains, hollow form of geogrid, etc.). Therefore, the stiffness increase (under surcharge) due to the changes in internal structure of reinforcements cannot be observed in FEM. However, FEM can provide results to understand how the behavior of the soil will change with pressure and hence the interaction between soil and reinforcement.

Among the materials used in this study, both nonwoven and woven geotextiles have suitable form (continuous and sheet-like form) to be modeled in plane-strain conditions of FEM and sand provides sufficiently uniform pressure distribution to be modeled in FEM, as well. As a result, using FEM analyses for geotextiles in sand can provide the most realistic simulation.

For this reason, in-air (a dummy soil was defined for in-air conditions) and in-soil single-layer tests of nonwoven and woven geotextiles have been analyzed by using FEM and results are compared with laboratory results. In FEM analyses, 5 mm displacement (5% strain) has been applied to the geotextile specimen and the secant stiffness at 5% strain (J_{sec5}) values were calculated. The material properties used in the models are shown in Table B.1. The geometry of models are shown in Figure B.1.

Table B.1. Materials used in FEM model.

Material	Material Model	Parameters
SW	Mohr Coulomb (Drained)	γ=16.61 kN/m^3, E=33 MPa, Φ'=42.5^o, c=1 kPa, ν=0.3, e_0=0.56
Dummy Soil	Mohr Coulomb (Drained)	γ=0.001 kN/m^3, E=1 MPa, Φ'=1^o, c=1 kPa, ν=0.3, e_0=0.50
NWGT	Linear Elastic	T=0.407 kN/m at 5% $\rightarrow$ EA=8.15 kN/m
WGTX	Linear Elastic	T=5.345 kN/m at 5% $\rightarrow$ EA=106.90 kN/m
Steel plate (t=2cm)	Linear Elastic	EA=4000 MN/m, EI=133.33 kNm^2/m, w=1.172 kN/m/m for γ=78.6 kN/m^3, ν=0.2
Interface Element	-	R=0.90 (between NWGT and sand) R=0.50 (between WGTX and sand) R=0.46 (between sand and box)

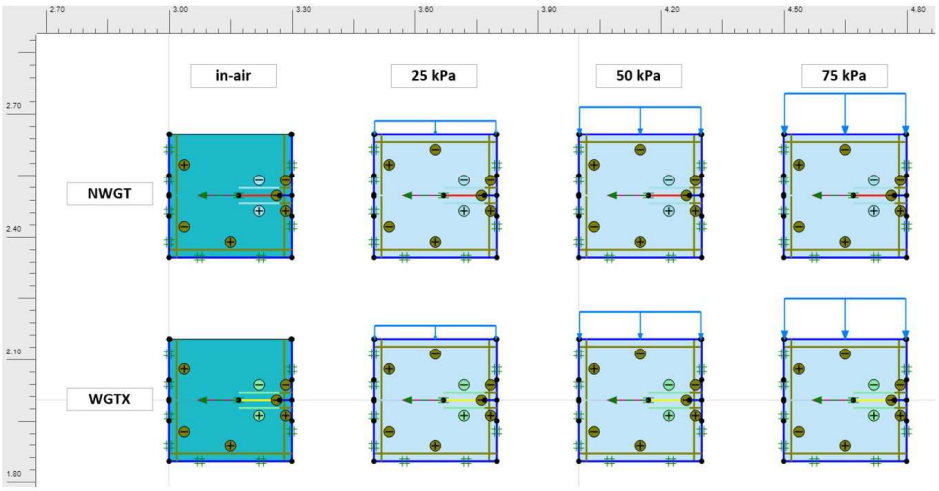


Figure B.1. Model geometry in FEM.

FEM analyses provided the axial loads on the geotextiles corresponding to 5 mm of displacement. Then, J_{sec5} values of geotextiles were recalculated using the strain and calculated tensile stress from the FEM analyses. These J_{sec5} values were compared with

the J_{sec5} results of laboratory tests. The graphs for nonwoven geotextile and woven geotextile are plotted in Figure B.2 and Figure B.3.

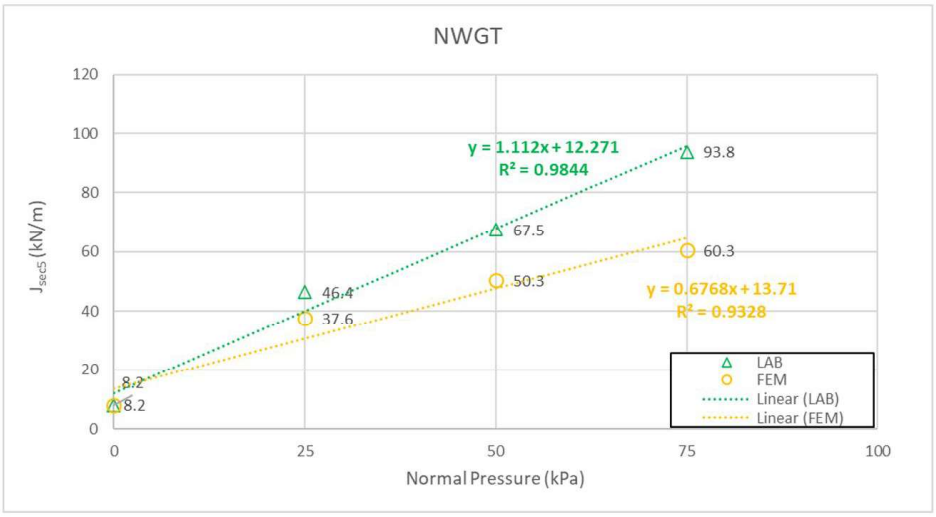


Figure B.2. Change of Jsec5 of NWGT with pressure for laboratory and FEM tests.

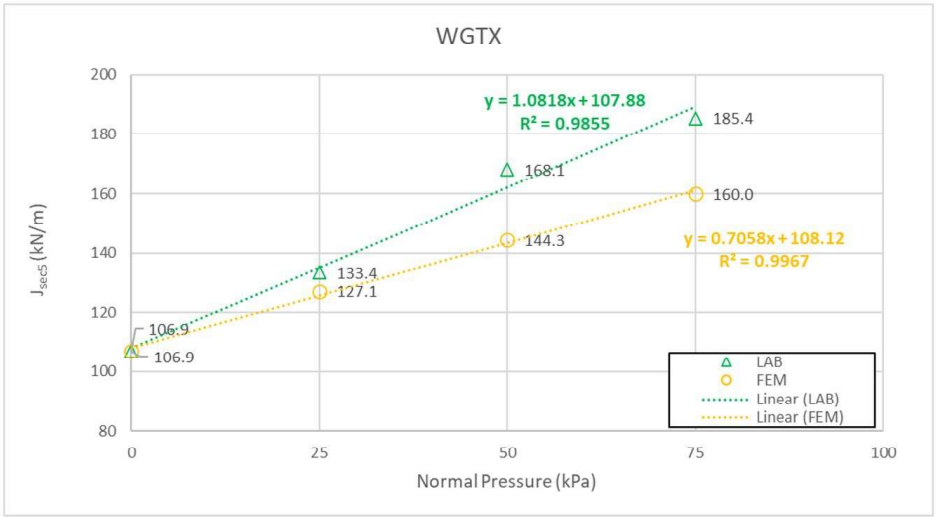


Figure B.3. Change of Jsec5 of WGTX with pressure for laboratory and FEM tests.

In FEM models, initial J_{sec5} (the stiffness value entered in material properties) values are taken from the in-air test results of the laboratory which are 8.15 and 106.90 kN/m for NWGT and WGTX, respectively. Figure B.2 and Figure B.3 show that the stiffness increases in FEM model when the test is performed under confined

conditions. This finding supports the laboratory results on stiffness increase. However, the J_{sec5} increase in FEM model is less than the one observed in laboratory tests. As aforementioned, FEM cannot model the internal structure of geotextiles. Based on this, the difference of J_{sec5} increase between laboratory and FEM results can be considered the inherent stiffness increase of the geotextile itself due to the applied pressure on them.

To estimate the inherent stiffness increase (inherent $J_{sec5,r}$), more FEM models were analyzed. The initial J_{sec5} (8.15 and 106.90 kN/m) for each pressure case is increased in FEM model to make FEM results the same as laboratory results. The so determined modified FEM (Mod. FEM) values are shown in Figure B.4. The inherent $J_{sec5,r}$ values (after Mod. FEM models) are plotted in Figure B.5. As can be seen from Figure B.5, which is showing the determined inherent $J_{sec5,r}$ results, it can be concluded that the $J_{sec5,r}$ increases with increasing pressure. It can be seen that under a pressure of 75 kPa the inherent $J_{sec5,r}$ increases by 2.45 times for the nonwoven and 1.24 times for the woven geotextile. This increase in stiffness can be considered to be caused by solely the change in the internal structure of the geotextiles.

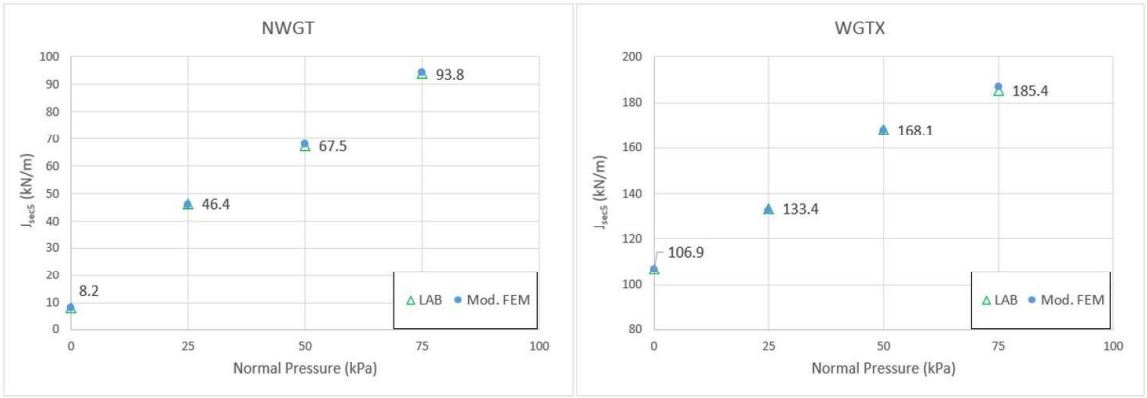


Figure B.4. Modified FEM models to reach laboratory results.

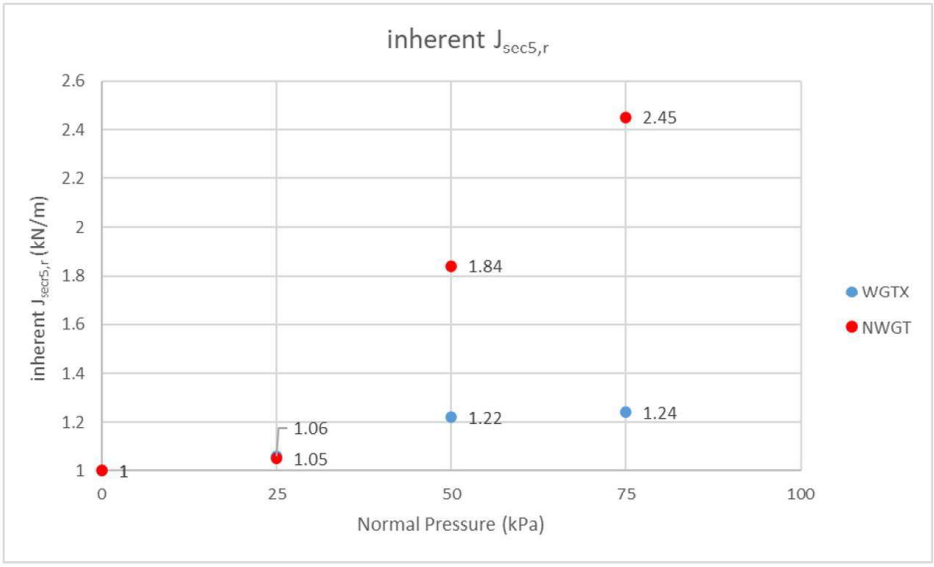


Figure B.5. Inherent $J_{sec5,r}$.

As explained before the geogrid cannot be modeled properly using a FEM and therefore no such analyses have been conducted for geogrids.